IFT

Instituto de Física Teórica
Universidade Estadual Paulista

Thesis IFT–006/17

Chiral and Flavor Symmetries in Holographic QCD: Pion Excited States, Strong Couplings of Charmed Mesons and Inverse Magnetic Catalysis

Carlisson Miller Cantanhede Pereira

Supervisor

Dr. Gastão Inácio Krein

August 2017

Agradecimentos

Durante todos os anos de doutorado, vivi uma experiência incrível, repleta de aprendizados e amizades cultivadas. Olhando para trás, posso recordar dos caminhos e desafios que passei, desde a vida díficil no Maranhão até os problemas mais recentes, e confesso que me supreendo que cheguei até aqui, ao final de um doutorado em Física. Apesar da vida familiar difícil, esta mesma me ensinou a olhar pra frente e ser determinado em meus objetivos e, com certeza, essa conclusão de mais uma etapa da minha vida foi fruto dessa grande lição.

Essa tese é dedicada principalmente aos meus pais, Antônio Pedro Pereira e Marta Célia Braga Cantanhede que, sem formação escolar suficiente para ter uma condição de vida melhor, tiveram garra e determinação e foram capazes de darem uma boa educação para meu irmão e para mim, mesmo quando nossas situações financeiras eram precárias. Toda a luta dos meus pais em garantir o básico para que eu estudasse e ainda fosse uma pessoa honrada é um dos exemplos que levo sempre comigo e me faz seguir em frente. Somado a eles, acrescento minha avó que, como lavradora, nos ensinou o valor de se conquistar as coisas.

Também sou grato as greves dos professores durante meu ensino médio; através delas, tive a oportunidade de frequentar as bibliotecas municipais e desenvolver meu interesse pela Física. E claro, aos bons professores do meu ensino médio, que viram em mim interesse e me presentearam com meu primeiro livro de Física.

Mas, definitivamente, foi na Universidade Federal do Maranhão que decidi meu rumo. E, neste caso, conheci dois professores que traçaram meu destino, os professores Drs. Manoel Messias e Rodolfo Casana. Se hoje sou capaz de aprender alguma coisa em Física, eu devo isso a eles, pois eles transformaram aquele estudante inexperiente em um Físico. Estes professores, com suas visões apuradas em identificar alunos interessados, se preocupavam em me ajudar e me ajudaram em diversas situações. Sou muito grato a eles por todas as oportunidades e, sem dúvida, essa tese é reflexo do bom trabalho deles.

Nesta parte, eu aproveito para agradecer aos diversos amigos que contribuíram direta ou indiretamente para o meu doutorado, entre eles posso citar os amigos do IFT: Renato, Pablo, Ernany, Guilherme, Fernando, Paulo, Natália, Ana, Henrique, Patrice, Stefano, George, Daniel e tantos outros. Também menciono aqueles fora do IFT como o Wagner e o Taciano, que dividiram todo esse tempo residência comigo e se tornaram bons amigos. Ainda nesse estágio final, conheci uma pessoa muito importante para a mim, Rosane Rocha, que com todo seu carinho tornou esses últimos meses menos penosos e mais divertidos.

Também agradeço enormemente ao Professor Dr. Jorge Noronha da USP que me apresentou, pela primeira vez, a correspondência holográfica e esteve presente em muitas discussões durante esses anos. Sua gentileza em compartilhar seus conhecimentos somaram muito para atingir a formação que tenho hoje. Outro professor importante na minha formação foi o Professor Dr. Nick Evans da University of Southampton (UK) que, sem hesitar, aceitou meu convite para um doutorado sanduíche e me deu a oportunidade de expandir meus conhecimentos na área e, como resultado, ele é parte desta tese.

Por fim, e mais importante, quero agradecer a dois personagens que, de fato, fizeram essa tese realmente acontecer, o Professor Dr. Gastão Krein e o Dr. Alfonso Bayona. Tenho enorme agradecimento ao Prof. Gastão por ter me aceitado como seu aluno de doutorado e confiado em trabalharmos neste tema. Além de ter compartilhado comigo seus conhecimentos em QCD e física hadrônica, ele confiou e me deixou livre para colaborar com outros grupos de pesquisa. Se hoje sei fazer alguma pesquisa em Física foi, sem dúvida, graças as suas dicas e referências, que aprecio muito. E tudo isso foi complementado pelo Dr. Alfonso Bayona, que veio ao IFT no momento certo e desde então atuou como um excelente co-orientador para mim. Ele teve a paciência de me ensinar detalhamente o que é holografia, deu diversas dicas de como fazer pesquisa, me apresentou a comunidade científica da área e sempre que precisei dele, ele esteve disposto em trabalhar e ensinar coisas. Por isso, serei eternamente grato a eles.

Este trabalho contou com apoio da Coordenação de Aperfeiçoamento de Pessoal de Nível Superior (**CAPES**).

Esta tese é resultado de três trabalhos científicos publicados na Physical Review D:

- Strong couplings and form factors of charmed mesons in holographic QCD - **Phys.Rev. D96 (2017) no.1, 014017**
- Inverse Magnetic Catalysis in Bottom-Up Holographic QCD - **Phys.Rev. D94 (2016) no.7, 074034**
- Decay constants of the pion and its excitations in holographic QCD - **Phys.Rev. D91 (2015) 065024**

Resumo

Existem poucas dúvidas de que a QCD seja a teoria correta das interações fortes. As dificuldades em resolver a teoria em baixas energias no regime fortemente acoplado e não perturbativo tem deixado sem respostas muitas questões importantes, tais como a natureza do confinamento e o mecanismo de hadronização. Diversos métodos têm sido usados para estudar suas propriedades e consequências a baixas energias. Esses métodos incluem a QCD na rede, as equações de Dyson-Schwinger, a teoria de perturbação chiral e os modelos de quarks. Recentemente, a dualidade gauge/gravidade tem fornecido uma nova maneira de acessar o regime fortemente acoplado de uma teoria de calibre via uma teoria de gravidade dual, em especial da QCD através de modelos holográficos. Tais modelos são usualmente denominados modelos holográficos para a QCD, ou apenas modelos AdS/QCD. Nesta tese investigamos importantes problemas de interesse atual em física hadrônica envolvendo as quebras das simetrias chiral e de sabor usando modelos holográficos para a QCD. Estes problemas são: (1) o desaparecimento das constantes de decaimento leptônicas dos estados excitados do pion no limite quiral; (2) os efeitos da quebra de simetria de sabor no acoplamentos do méson ρ aos mésons charmosos D and D^* e seus fatores de forma eletromagnéticos; (3) os efeitos de um campo magnético e da temperatura sobre o condensado quiral, sinalizando uma catálise magnética inversa.

Palavras Chaves: Cromodinâmica Quântica, Quarks e Glúons, Simetria Quiral, Simetria de Sabor, Catálise Magnética Inversa, Dualidade Calibre/Gravidade, Holografia

Áreas do conhecimento: Teoria de Partículas e Campos, Física Hadrônica, Física Nuclear.

Abstract

There is little doubt that QCD is the correct theory for the strong interactions. The difficulties in solving the theory at low energies in the strongly interacting, non-perturbative regime have left unanswered many important questions, such as the nature of confinement and the mechanism of hadronization. Several approaches have been used to study its properties and consequences at low energies. These include lattice QCD, Dyson-Schwinger equations, chiral perturbation theory and quark models. More recently, the gauge/gravity duality has provided a new way to access the strongly coupled regime of a gauge theory via a dual gravity theory, in special of QCD through holographic models. Such models are usually named as holographic QCD models, or just AdS/QCD models. In this thesis, we investigate three problems of contemporary interest in hadronic physics involving the chiral and flavor symmetries holographic QCD models. These problems are: (1) the vanishing of the leptonic decay constants of the excited states of the pion in the chiral limit; (2) the effects of the flavor symmetry breaking on the strong couplings of the ρ meson to the charmed D and D^* mesons and the their electromagnetic form factors; (3) the effects of a magnetic field and temperature on the chiral condensate, signalizing inverse magnetic catalysis.

Keywords: Quantum Chromodynamics, Quarks and Gluons, Chiral Symmetry, Flavor Symmetry, Inverse Magnetic Catalysis, Gauge/Gravity duality, Holography

Research areas: Theory of Particles and Fields, Hadron Physics, Nuclear Physics.

Contents

1 Introduction

Quantum Chromodynamics (QCD) is at present universally accepted as the theory of the strong interaction. The strong interaction is responsible for the bulk of the visible matter in the universe. This matter is contained in atomic nuclei. The fundamental degrees of freedom in the theory are the quarks and gluons that carry color charges. But quarks and gluons are not observed in isolation, they are permanently confined in the interior of the hadrons. Hadrons are strongly interacting subatomic particles; the most well known hadrons are the proton, neutron, and the pion. The existing hadrons are classified into baryons and mesons. Baryons have half-integer spin, and mesons have integer spin. Up today, six types (or flavors) of quarks are known: the up (u) and down (d) quarks, which exist in ordinary matter which is composed of protons and neutrons, and the strange (s), charm (c), bottom (b), and top (t) quarks, which are produced in high energy particle collisions, they are much heavier than the u and d quarks and decay quickly. At high energies, QCD is very well understood, it correctly describes strongly interacting matter under the extreme conditions reached in high energy particle collisions, where quarks and gluons are probed at short relative distances. Our knowledge of the theory under such conditions is due to a property known as asymptotic freedom [1, 2]. This property asserts that the quark-gluon interaction becomes weak at high energies, or at small relative distances. It allows the use of systematic and well-controlled weak-coupling expansions developed in quantum field theory. However, not much is known on how precisely quarks and gluons become permanently confined in the interior of hadrons. This feature is known as the confinement of the color charge, which means that the interaction becomes stronger as quarks and gluons try to separate. Here, new theoretical methods that go beyond weak-coupling expansions are required. At this energy regime, another prominent QCD phenomenon is present: dynamical chiral symmetry breaking (DCSB), which is responsible for more than 98% of the visible mass in the universe. The Higgs particle gives masses to the quarks, but these masses alone explain less than 5% of the masses of the protons and neutrons. The rest of the masses is explained as coming from the strong quark-gluon interactions that lead to dynamical chiral symmetry breaking.

One interesting new development in the last decades has been the discovery of the AdS/CFT correspondence, or gauge/gravity duality [3, 4, 5] (see Ref. [6] for a review), which relates quantum gauge field theories in d dimensions to theories of quantum gravity in $(d+1)$ or higher dimensions. In particular, in the limit that the QFT is strongly coupled with a large number of gauge degrees of freedom, the corresponding quantum gravity theory is a classical theory of gravity. Thus, problems in strongly coupled QFT's can be mapped to problems in higher dimensional classical theories of gravity which may pose an easier challenge. Models based on gauge/gravity duality have been applied to investigate nonperturbative low-energy observables of phenomenological interest in QCD, especially in hadron physics. In particular, interesting holographic models incorporating features of DCSB and its explicit breaking by quark masses have been introduced to study pion [7, 8] and kaon [9] physics, including their electromagnetic form factor. The spectrum of scalar glueballs have been studied in this new approach utilizing a different class of models [10]. Light baryons have also been studied in the gauge/gravity duality through their identification with Skyrmions in the AdS space [11]. Finally, it is worth mentioning that applications of the gauge/gravity have been employed to study problems in condensed matter physics [12]. Thus, the exploration and integration of different areas of physics has been a especially attractive feature of the gauge/gravity duality.

In this thesis we study three problems of current interest in hadron physics using the framework based on the gauge/gravity duality. The first problem is related to the phenomenon of DCSB. QCD predicts that the leptonic decay constants of the excited states of the pion vanish in the chiral limit when chiral symmetry is dynamically broken [13]. Although chiral symmetry is not an exact symmetry in the real world, as the masses of the u and d quarks are not zero, their masses are much smaller than the typical strong interaction scale (Λ_{QCD}, to be defined in the coming chapter) so that it is natural to expect that the leptonic decay constants of the excited states of the pion are very much suppressed in nature. The essential point behind the suppression of the decay constants, as we shall discuss in this thesis, is the dynamical breaking of chiral symmetry in QCD and the (pseudo) Goldstone boson nature of the ground-state pion. The second problem we tackle in this thesis is related to the consequences of the breaking of flavor symmetry due to the quark masses on strong hadron coupling constants. This issue is of great contemporary interest in connection with the interactions of the heavy-light charmed D mesons with light hadrons and atomic nuclei [14, 15, 16]. Of particular interest in this thesis are the effects of SU(4) flavor symmetry breaking on effective meson couplings due to the different values of the current quark masses in the QCD Lagrangian. This issue has been discussed in the context of different approaches and models, which include the constituent quark model [17, 18], QCD sum rules [19], Dyson-Schwinger equations [20, 21], and lattice QCD [22]. Finally, we study of QCD in the presence of an external magnetic field. It has recently attracted much attention because of its phenomenological relevance and of many interesting theoretical features as a possibility of new phases in the QCD phase diagram [23] and more recently its influence on the dynamics of the chiral condensate [24], known as the inverse magnetic catalysis (IMC).

The thesis is organized as follows. In chapter 2 we briefly review some important aspects of QCD. We discuss its origins, passing by the phenomenology of hadrons that led to the establishment of the quark model. We discuss its similarities and differences with quantum electrodinamics (QED). Furthermore, we present the QCD Lagrangian, discuss its symmetries and present the relevance of its intrinsic scale, Λ_{QCD}. We also discuss in more detail the chiral physics from the QCD Lagrangian and how it affects the hadronic spectrum. Moreover, we discuss the phenomenon of quark-gluon confinement phenomenon and introduce the Wilson loop, a quantity relevant for discussing color confinement in the context of pure-gauge theories.

Chapter 3 contains the general holographic framework used in the thesis. We present arguments to motivate the duality by a geometrization of the renormalization group, in which the AdS space emerges naturally. The holographic dictionary is explained, which is very important to make connection with the QFT of interest. The connection with physical observables in the QFT, done via correlation functions, is described in this chapter, as well as the holographic prescription to evaluate such correlation functions. To illustrate this prescription, we will apply it to a scalar field theory. The inclusion of the thermal effects in the duality is also discussed. We conclude the chapter discussing briefly the real origin of this duality, through of the Dp brane dynamics, which makes clear the limit of applicability of the duality that is used in the present context. We also discuss briefly how to include flavor degrees of freedom in the duality.

In chapter 4, we start discussing briefly the two main approaches commonly used to study QCD via the gauge/gravity duality: the top/down and bottom-up approaches. Then, we present the background which satisfies a confinement criterium, the hard wall background. We introduce the bottom-up holographic QCD model used in this thesis and show how the model incorporates DCSB. By exploring the action of the model up to second order, we show how to evaluate vacuum expectation values of operators of interest, to obtain a 4d effective action for mesons and their leptonic decay constants. Finally, we end the chapter exploring the action up to third order to obtain the couplings for 2 pseudoscalar and vector mesons and for the 3 vector mesons.

Chapters 5 and 6 contain our results using the bottom-up holographic QCD model to study, respectively, the vanishing of the leptonic decay constants for the excited states of the pion and the effects of SU(4) flavor symmetry breaking on three-meson couplings. In chapter 5, we start identifying the pion in the model and obtain the pionic excitation spectrum. We show explicitly that the model reproduces the partially conserved axial current (PCAC) and Gell-Mann-Oakes-Renner (GOR) relationship. In the numerical part, we show that our results are in complete agreement with the QCD prediction. In chapter 6, we extend the bottom-up holographic QCD model to include four flavors. The mesons in the $SU(4)$ flavor representation are identified and we explore the action up to third order to evaluate the strong coupling constants. Also, the electromagnetic (EM) form factors are defined using a generalized vector meson dominance (GVMD) freamework. We present how the $SU(4)$ flavor symmetry breaking numerically impacts the values of three-meson couplings. We also present results for the EM form factors for the pseudoscalar and vector mesons, comparing them with experimental and lattice results.

In chapter 7 we apply the gauge/gravity duality at finite temperature and in presence of an external magnetic field. We introduce a different model, the dynamic holographic QCD model, which is also a bottom-up approach. We start reviewing the D3/D7 brane configuration and show how the model generates a chiral condensate dynamically. We incorporate the effects of temperature in the model to reproduce a second order chiral phase transition. An external magnetic field is included in the model. We show that the model gives inverse magnetic catalysis (IMC), in that the critical temperature for chiral restoration decreases with magnetic field. We also show that the chiral condensate presents a nonmonotonic behavior. Both effects are similar to what is observed the lattice QCD simulations.

Finally, our conclusions are presented in chapter 8.

2 Introduction to QCD

For a long time, it has been assumed that some observed elementary particles are not elementary at all. For example, in Ref [25], it was suggested that the pion is composed by a nucleon and an antinucleon. The discovery of kaons and hyperons in the 1950s, led to models in which such particles were taken as fundamental objects and others as composite objects. A good description for this scenario was achieved by the model proposed by Sakata [26], in which the proton, the neutron and the Λ-hyperon were taken as fundamental particles. In this model, the states p, n, Λ served as basis to build the scheme of unitary symmetry $SU(3)$ and conducted to the classification of the pseudoscalar and vector mesons, although it had some problems in the description of baryons. Some years later, another model appeared, the Eightfold Way, proposed independently by Gell-Mann [27] and Neeman [28]. It is based in the classification of hadrons via an $SU(3)$-group and the great advantage of that model is that the mesons and the baryons could be described simultaneously by the model. A great success of the model was the experimental verification of its prediction of the Ω^- hyperon, confirming the validity of this symmetry.

Initially, the theoretical ideas on the internal structure for the hadrons arose in the papers of Gell-Mann [29] and Zweig [30]. They showed that the $SU(3)$ octet symmetry can be understood on the basis of a fundamental triplet of some "hypothetical" particles, named by Gell-Mann as quarks [1] that carry fractional electric charges. Such particles had specific quantum numbers to be consistent with the hadrons known at the time; they are presented in Table 2.1.

As said, initially the quarks were considered as mathematical objects in the understanding of hadrons, but years later it became clear that, in fact, hadrons should be considered as bound systems of quarks. In this picture, the mesons would consist of a quark-antiquark pair and the baryons known at that time would consist of three quarks

$$M = \bar{q}q, \quad B = qqq. \tag{2.1}$$

[1] In that time, Gell-Mann was uncertain on the term he intended to coin, until he found the word quark in James Joyce's book Finnegans Wake

flavour	charge	isospin	strangeness	baryon charge
u	$2/3$	$I = 1/2,\ I_3 = 1/2$	0	$1/3$
d	$-1/3$	$I = 1/2,\ I_3 = -1/2$	0	$1/3$
s	$-1/3$	$I = 0$	-1	$1/3$

Table 2.1: Quantum numbers of the quarks in the Eightfold Way

Despite the great success of the quark model, countless attempts to find these particles (quarks) as free and with such fractional electric charges failed, see [31]. This impossibility in which quarks cannot be seen as experimentally free particles is the hypothesis of quark confinement. Differently to hadrons, quarks have a new quantum number, the “color” [32, 33], and it was established that just colourless particles could be observed as free particles.

In 1969, another great step was given in the understanding of the quark structure of hadrons: the introduction of the parton hypothesis [34]. In the deep inelastic scattering (DIS) experiments, an energetic lepton interacts with the target hadron via exchange of a virtual photon and, by analyzing the cross section, the parton structure of hadrons can be observed. The experimental observations also revealed that interacting partons are particles that carry the same quantum numbers of quarks predicted by Gell-Mann’s model. In particular, the proton would consist of three valence quarks. In addition, in the two experiments H1 and ZEUS at the HERA laboratory, detailed investigations in the momentum distributions of the proton revealed that quark-partons carry about half of the momentum of the fast proton and the remaining half of this momentum would be carried by a new neutral particle inside the proton, they are now known to be the gluons. The HERMES experiment at HERA laboratory has conducted extensive and detailed studies of the gluon contribution to the proton spin. It is important to point out that the gluons were theoretically predicted in the mid-1970s. Their properties can be also investigated through other processes as: Drell-Yan pair ($\mu^+\mu^-$) production in hadron collisions, hadron production with large p_T, hard hadron jets and, in particular, e^+e^- annihilation.

Nowadays it is well understood that the quarks of the Eightfold Way (u, d and s) are not the only existing quarks. In fact, from experimental verification, three new species of quarks or flavors, were discovered: the c-quark, the b-quark and the t-quark. The masses of the Eightfold Way quarks are considerably smaller than of those new quarks. Therefore, when dealing with processes with small momentum transfers (soft processes) involving light hadrons we can focus our attention on the light quarks which realize the lowest representation of the $SU(3)_{flavor}$ group.

The current understanding of hadrons as bound states of quarks is based on quantum chromodynamics (QCD), the underlying theory of strong interactions, which is a non-Abelian gauge theory [35]. Quantum electrodynamics (QED) is characterized by the presence of electrically charged fermions (electrons) and neutral photons and has as basic processes the emission and absorption of photons by electrons, as illustrated in Fig. 2.1a. In QCD, on the other hand, each quark has a color charge and, from experimental observation, quarks appear in three color charges, each quark can transform into another by emitting or absorbing one of the 8 possible colored gluons. As the gluons carry color charge, in addition to quarks emmiting/absorbing gluons as in Fig. (2.1b), gluon-gluon interactions like in Fig. (2.1c) and Fig. (2.1d). The latter processes make the theory more complicated compared to QED.

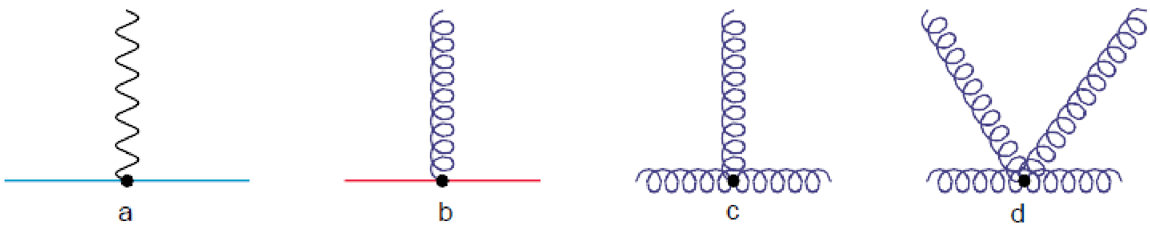

Figure 2.1: QED interaction vertex (a): an electron emits/absorbs a photon; QCD interaction vertices: gluon emission/absorbsion by a quark (b) or by a gluon (c) and gluon-gluon interactions (d)

One of the great differences between QED and QCD comes from interactions showed in (c) and (d) which affect the behavior of the effective charge. In fact, at low energies, the QCD effective charge increases significantly and nonperturbative physics takes place. On the other hand, at high energies, the effective charge decreases significantly, signalizing that the theory is asymptotically free [1, 2]. This makes possible the use of perturbation theory. Perturbative QCD (pQCD) is a very powerful theoretical framework that allows to study QCD analytically and generates all the results obtained in the parton model and, in addition, predicts possible deviations from it. For a detailed analysis about the pQCD calculations and their comparisons with results from experimental data, the reader is directed to Refs. [36, 37, 38].

In soft processes, when there is growth of the effective charge, perturbative methods, based on an expansion in the coupling strength, cannot be applied and a study from first principles employing analytical methods based on quark and gluon degrees of freedom becomes extremely difficult. But, despite of this, some progress has been made using the Dyson-Schwinger equations of QCD [39]. The theoretical difficulties in the study of hadron physics from first principles also motivated the construction of effective models such as chiral effective theories [40, 41], heavy quark effective theories (HQET) [42, 43], non-relativistic QCD (NRQCD) [44], and soft-collinear effective theory (SCET) [45]. A powerful first-principles numerical method to study QCD is the formulation of the theory on lattice (Lattice QCD). Lattice QCD has been used for computations of static or low energy quantities involving a few hadrons, like masses or near threshold form factors. It is also a powerful technique for examining the thermal behaviour of QCD. More recently, a different class of models, based on the gauge/gravity duality [46, 47, 48, 49], has raised great interest in the exploration of nonperturbative aspects of QCD. We will discuss this at length in the next sections.

In the nonperturbative regime of QCD, its properties are dominated by two emergent phenomena: confinement, namely, the theory's elementary degrees of freedom (quarks and gluons) cannot be isolated, and dynamical chiral symmetry breaking (DCSB), which is a remarkably effective mass generating mechanism, responsible for the mass of more than 98% of visible matter in the Universe. We will discuss these phenomena shortly ahead.

2.1 QCD Lagrangian

The combination of the successes of the quark and parton models motivated the adoption of Yang Mills theory with the color symmetry elevated to a $SU(3)_c$ local symmetry group. The QCD Lagrangian is written as

$$\mathcal{L} = \sum_{flavors} \bar{\psi}_i^f (i\gamma^\mu \mathcal{D}_\mu - M)_{ij} \psi_j^f - \frac{1}{4} F^{\mu\nu,a} F^a_{\mu\nu}. \tag{2.2}$$

Before describing the components of this Lagrangian, it is important to explain the notation employed

- The greek indices ($\mu,\ \nu, \ldots$) are Lorentz indices.
- f represents the flavor index.
- $i,\ j,\ k$ in the quark fields ψ are colors indices in the fundamental representation ($i,\ j,\ k = 1, 2, 3$).
- $a,\ b,\ c$ in the gluon fields A^a_μ are colors indices in the adjoint representation ($a,\ b,\ c = 1, 2, ..., 8$).

In the Lagrangian (2.2), M is quark mass matrix and the covariant derivative is defined as

$$(\mathcal{D}_\mu)_{ij} = \partial_\mu \delta_{ij} + ig(t^a)_{ij} A^a_\mu. \tag{2.3}$$

Here, g is the coupling constant, t^a are the generators of $SU(3)$ and they define the so-called structure constants through of the commutation relations

$$\left[t^a, t^b\right] = if^{abc}t^c. \tag{2.4}$$

It is possible to demonstrate that these structure constants satisfy the following Jacobi identity

$$f_{abe}f_{ecd} + f_{cbe}f_{aed} + f_{dbe}f_{ace} = 0. \tag{2.5}$$

In the fundamental representation, these matrices are Gell-mann matrices, given by

$$t^1 = \frac{1}{2}\begin{pmatrix} 0 & 1 & 0 \\ 1 & 0 & 0 \\ 0 & 0 & 0 \end{pmatrix}, \quad t^2 = \frac{1}{2}\begin{pmatrix} 0 & -i & 0 \\ i & 0 & 0 \\ 0 & 0 & 0 \end{pmatrix}, \quad t^3 = \frac{1}{2}\begin{pmatrix} 1 & 0 & 0 \\ 0 & -1 & 0 \\ 0 & 0 & 0 \end{pmatrix}, \tag{2.6}$$

$$\tag{2.7}$$

$$t^4 = \frac{1}{2}\begin{pmatrix} 0 & 0 & 1 \\ 0 & 0 & 0 \\ 1 & 0 & 0 \end{pmatrix}, \quad t^5 = \frac{1}{2}\begin{pmatrix} 0 & 0 & -i \\ 0 & 0 & 0 \\ i & 0 & 0 \end{pmatrix}, \quad t^6 = \frac{1}{2}\begin{pmatrix} 0 & 0 & 0 \\ 0 & 0 & 1 \\ 0 & 1 & 0 \end{pmatrix}, \tag{2.8}$$

$$\tag{2.9}$$

$$t^7 = \frac{1}{2}\begin{pmatrix} 0 & 0 & 0 \\ 0 & 0 & -i \\ 0 & i & 0 \end{pmatrix}, \quad t^8 = \frac{1}{\sqrt{12}}\begin{pmatrix} 1 & 0 & 0 \\ 0 & 1 & 0 \\ 0 & 0 & -2 \end{pmatrix}, \tag{2.10}$$

$$\tag{2.11}$$

and are normalized as

$$\mathrm{Tr}\left(t^a t^b\right) = \frac{1}{2}\delta^{ab}. \tag{2.12}$$

The covariant derivative in Eq. (2.3), implies in the quark-gluon interaction term

$$\mathcal{L}_{int} = -g\bar{\psi}_i A^\mu_a (t^a)_{ij}\gamma_\mu \psi_j. \tag{2.13}$$

Therefore, quarks interact with gluons in a way similar to electrons interacting with photons. A new feature here is that the quark can change its color charge from i to j by emitting or absorbing a gluon, coupling through an $SU(3)_c$ generator $(t^a)_{ij}$, as shown in Fig. 2.2.

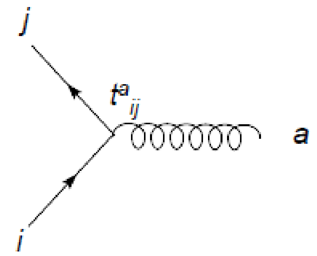

Figure 2.2: The color of a quark can change from i to j by a gluon of color a, coupled through the $SU(3)$ generator $(t^a)_{ij}$.

In the term that refers to gluon dynamics (gauge term) in (2.2), the tensor strength $F^a_{\mu\nu}$ is given by

$$F^a_{\mu\nu} = \partial_\mu A^a_\nu - \partial_\nu A^a_\mu - g f^{abc} A^b_\mu A^c_\nu. \tag{2.14}$$

Note that, apart from the standard partial derivative terms in $F^{\mu\nu a} F^a_{\mu\nu}$, there are non-linear terms $(A^b_\mu A^c_\nu)^2$ and $\partial_\mu A^a_\nu A^{\mu b} A^{\nu c}$. Therefore, the eight gluons do not come in as a simple repetition of the photon in QED theory, they have three and four-gluon self-interactions. We depicted such interaction terms schematically in Fig. 2.1.

As a gauge invariant theory, the Lagrangian (2.2) is invariant under local symmetry transformations

$$\psi \rightarrow U(x)\psi, \tag{2.15}$$

$$A^a_\mu t^a \rightarrow U(x) A^a_\mu t^a U^\dagger(x) + i g^{-1} (\partial_\mu U(x)) U^\dagger(x) \tag{2.16}$$

where $U(x)$ is an element of $SU(3)_c$.

It is well known that a renormalization procedure shows that the strong coupling in QCD, in fact, runs with the energy or momentum involved in a process. Namely, for large values of a typical momentum transfer Q in, e.g. a scattering process, one has that

$$\alpha_s(Q^2) = \frac{1}{b_0 \ln(Q^2/\Lambda^2_{QCD})}, \quad b_0 = \frac{1}{6\pi}(11N_c - 2N_f), \tag{2.17}$$

at the one-loop level. This procedure introduces in the theory a dimensionful parameter Λ_{QCD}, which represents the scale at which the coupling constant becomes large and the physics becomes nonperturbative. Therefore, Λ_{QCD} sets the scale for strong interaction physics. In a particular renormalization scheme ($\overline{\mathrm{MS}}$-sheme) [50], it is found that $\Lambda_{QCD} \sim 250$ MeV, for three flavors. This scale is widely responsible to sets the mass scale for the proton and neutron masses, and hence, the mass scale of the baryonic mass in the Universe.

In the same way as the coupling constant runs, so do the quark masses, i.e. they depend on the renormalization scale. Because quarks are confined, there is no true quark mass pole, as in QED, for example. A quark mass pole is well defined only in the context of perturbation theory. When one quotes a value of a quark mass, this value refers to a particular renormalization scheme.

As we have mentioned before, the nonperturbative QCD physics is dominated by chiral dynamics and confinement. Both topics will be discussed in the next sections.

2.1.1 Chiral Dynamics

In the above paragraph, we have briefly discussed the strong interaction scale Λ_{QCD} through the running of the QCD coupling. Now we can clarify the notion of light and heavy quarks. Briefly speaking, light quarks are the ones with masses much smaller than Λ_{QCD}, and heavy quarks with masses much larger than Λ_{QCD}. Clearly, from Table 2.2, the up and down quarks are qualified as light quarks, whereas the charm, bottom, and top as heavy quarks. The strange quark is more subtle, it appears neither light nor heavy. In some cases, it can be regarded as light, in others, as heavy.

Quark flavor	up	down	strange	charm	bottom	top
Masses	1.5-4 MeV	4-8 MeV	100 MeV	1.25 GeV	4.25 GeV	175 GeV

Table 2.2: Quark masses in the $\overline{\mathrm{MS}}$ renormalization scheme at a scale of $\mu = 2GeV$.

For our purposes in this section, we focus on the light quarks, which are the most relevant to the real world. To understand the physics related with such quarks, it is convenient to consider a theoretical limit in which their masses are exactly zero, known as *chiral limit*. This limit is a good approximation as a starting point to discuss the physics of the real world.

In the chiral limit, the spin of the quark can either be in the direction of motion, which we call a right-handed quark and denote its field by ψ_R, or in the opposite direction of the motion, we call it a left-handed quark, with the corresponding field denoted by ψ_L. In this way, each flavor can be arranged as

$$\psi = \begin{pmatrix} \psi_L \\ \psi_R \end{pmatrix}, \quad \psi_{R,L} = \frac{1 \pm \gamma_5}{2}\psi. \tag{2.18}$$

The QCD Lagrangian in Eq. (2.2) can, therefore, be written as

$$\mathcal{L} = \sum_{flavors} \bar{\psi}^f_{L,i}(i\gamma^\mu \mathcal{D}_\mu)_{ij}\psi^f_{L,j} + \bar{\psi}^f_{R,i}(i\gamma^\mu \mathcal{D}_\mu)_{ij}\psi^f_{R,j} - \frac{1}{4}F^{\mu\nu,a}F^a_{\mu\nu}, \tag{2.19}$$

and, as consequence, it presents the following symmetry

$$\psi_L \to \psi'_L = U_L\psi_L, \quad \psi_R \to \psi'_R = U_R\psi_R, \tag{2.20}$$

where $U_{L,R}$ are $N_f \times N_f$ unitary matrices [2]. This symmetry is commonly known as *Chiral Symmetry* and the group of chiral transformations is denoted by $U(N_f)_L \times U(N_f)_R$.

Since $U(N_f) = U(1) \times SU(N_f)$, we have two $U(1)$ symmetries, one for the left part $U_L(1) = e^{i\alpha_L}$ and another for the right part $U_R(1) = e^{i\alpha_R}$. From now on, we focus on the two $SU(N_f)$ symmetries, the $U(1)$ parts, one related to baryon number and the other to axial symmetry (which is anomalous), will not be discussed here. According to Noether's theorem, the $SU(N_f)_L \times SU(N_f)_R$ chiral symmetry leads to the the following conserved currents

$$J^a_{L\mu} = \bar{\psi}_L\gamma_\mu t^a\psi_L, \quad J^a_{R\mu} = \bar{\psi}_R\gamma_\mu t^a\psi_R. \tag{2.21}$$

For a better physical interpretation, we construct vector and axial vector currents from the linear combinations

$$J^{a,\mu}_V = J^{a,\mu}_R + J^{a,\mu}_L = \bar{\psi}\gamma^\mu t^a\psi, \quad J^{a,\mu}_A = J^{a,\mu}_R - J^{a,\mu}_L = \bar{\psi}\gamma_\mu\gamma_5 t^a\psi. \tag{2.22}$$

We can find the charges Q_a and Q_{a5} associated with these currents by integrating the temporal part of the above currents. It is straightforward to check that the charges obey the following algebra

$$[Q_a, Q_b] = if_{abc}Q_c; \quad [Q_{a5}, Q_b] = if_{abc}Q_{c5}; \quad [Q_{a5}, Q_{b5}] = if_{abc}Q_c. \tag{2.23}$$

Note that, the above relations show that the operators Q_a form a subgroup of the chiral symmetry group, it is known as flavor group. This can be better understood separating the vector and axial parts of $SU(N_f)_L \times SU(N_f)_R$ group. Thus, using (2.22), we have the following vector and axial transformations

$$\psi \to \psi' = U_V\psi, \quad \psi \to \psi' = U_A\psi, \tag{2.24}$$

where $U_{V,A}$ are unitary matrices of the chiral group denoted by $SU(N_f)_V \times SU(N_f)_A$. In this form, the $SU(N_f)_V$ refers to the vector part and flavor group and $SU(N_f)_A$ refers to the axial part [3]

[2] In the present case, we are considering the chiral limit of N_f flavors in order to obtain a general description.

[3] The $SU(N_f)_A$ is not a real group, because two axial transformations do not lead to another axial transformation.

For $N_f = 2$, the flavor group is known as isospin group and states are labeled by the total isospin I and its third component I_3. A classical example of the realization of the isospin group is the proximity of the proton and neutron masses, which have $I = 1/2$ and can be represented as

$$p = \Big|I = \frac{1}{2}, I_3 = \frac{1}{2}\rangle, \quad n = \Big|I = \frac{1}{2}, I_3 = -\frac{1}{2}\rangle. \tag{2.25}$$

As an example of a multiplet with $I = 1$ we have the three pions

$$\pi^+ = \Big|I = 1, I_3 = 1\rangle, \quad \pi^0 = \Big|I = 1, I_3 = 0\rangle, \quad \pi^- = \Big|I = 1, I_3 = -1\rangle, \tag{2.26}$$

all having nearly identical masses. This shows that the isospin is a very good approximate symmetry in the light hadron spectrum. However, the hadron spectrum does not presents the complete $SU(2)_V \times SU(2)_A$ symmetry. This can be seen as follows: let $|h, +\rangle$ be a hadron eigenstate of the QCD massless Hamiltonian H^0_{QCD} with eigenvalue M_h,

$$H^0_{QCD}|h, +\rangle = M_h|h, +\rangle. \tag{2.27}$$

In the Hilbert space, the Q_a and Q_{a5} charges act as generators of the transformation; given as

$$U_V = e^{i\alpha^a_V Q^a}, \quad U_A = e^{i\alpha^a_A Q^{5a}}. \tag{2.28}$$

The $SU(2)_V \times SU(2)_A$ symmetry implies that

$$[H^0_{QCD}, Q^a] = [H^0_{QCD}, Q^{5a}] = 0. \tag{2.29}$$

Acting with the U_A operator on the left of Eq. (2.27) and using the above commutation relation, we obtain in the same way:

$$H^0_{QCD} U_A|h, +\rangle = M_h U_A|h, +\rangle. \tag{2.30}$$

As the axial transformation changes the parity of the state, we obtain

$$H^0_{QCD}|h, -\rangle = M_h|h, -\rangle \quad \text{with} \quad |h, -\rangle = U_A|h, +\rangle. \tag{2.31}$$

This fact would imply in the existence of degenerate parity doublets in the hadron spectrum. For example, the spectra of vector ($J^P = 1^-$) and axial-vector ($J^P = 1^+$) mesonic excitations should be identical. But, this is not realized in the hadron spectrum, signalizing that chiral symmetry is broken. This can be understood using $|h, +\rangle = \hat{P}^+_h|0\rangle$, where $\hat{P}^+_h$ is the operator that creates a hadron h with positive parity. Then, we have (for an infinitesimal)

$$U_A|h, +\rangle = U_A \hat{P}^+_h U^\dagger_A U_A|0\rangle = \hat{P}^-_h e^{i\alpha^a_A Q^{5a}}|0\rangle \simeq |h, -\rangle + i\alpha^a_A \hat{P}^-_h Q^{5a}|0\rangle + \dots \tag{2.32}$$

Then, if the vacuum is not annihilated by Q^{5a}, the previous arguments no longer apply and the particles with different parities will have different masses, as in the case of hadron spectrum. This shows that chiral symmetry is dynamically broken by the QCD vacuum.

The dynamical chiral symmetry breaking means that the QCD vacuum contains a population of quark anti-quark pairs, which are represented by the nonzero values of vacuum expectation values

$$\langle 0|\bar{\psi}\psi|0\rangle = \langle 0|\bar{\psi}_u\psi_u|0\rangle = \langle 0|\bar{\psi}_d\psi_d|0\rangle = \langle 0|\bar{\psi}_s\psi_s|0\rangle. \tag{2.33}$$

This operator has a precise definition in terms of the full quark propagator, as

$$\langle 0|\bar{\psi}(x)\psi(x)|0\rangle = -i\mathrm{Tr}\lim_{y\to x_+} S_F(x-y), \quad S_F(x-y) = -i\langle 0|\mathcal{T}\psi(x)\bar{\psi}(y)|0\rangle. \tag{2.34}$$

This is known as the chiral condensate, or quark condensate. It is often used as an order parameter for the dynamical chiral symmetry breaking.

In summary, one has that the vacuum expectation value $\langle\bar{\psi}\psi\rangle$ is nonzero, i.e. there are quark condensates in the QCD vacuum. Thus, in QCD, one has that

$$Q_a|0\rangle = 0, \quad Q_{a5}|0\rangle \neq 0. \tag{2.35}$$

However, according to Goldstone's theorem, this leads to the existence of three massless spin-0 pseudoscalar bosons. They are pseudoscalars because Q_{a5} has odd parity.

Clearly, in the real world there are no such massless pseudoscalars. But, there are pions. The pion masses are indeed much smaller than a typical hadron mass, about 140 MeV. The pions are called pseudo-Goldstone bosons because the chiral symmetry is not exact. It is slightly broken by the finite up and down quark masses, which appear in the symmetry breaking term in the Lagrangian (2.2)

$$\mathcal{L}_M = -\bar{\psi}M\psi = -m_u\bar{u}u - m_d\bar{d}d. \tag{2.36}$$

If we consider three flavors, the u, d, s quarks, we have now eight axial charges, hence, there should be eight massless spin-0 pseudoscalar bosons. But, as before, because of the symmetry breaking due to quark masses, we have the pseudo-Goldstone bosons: pions $(\pi^\pm, \pi^0)$, kaons $(K^\pm, K^0, \bar{K}^0)$ and the η meson.

2.1.1.1 Pion leptonic decay constant, PCAC and Gell-Mann-Oakes-Renner relation (GOR)

Let us first consider the weak decay of the pion, illustrated in Fig. 2.3. This process is well described using Fermi's theory, where the weak interaction Hamiltonian involves a current-current part, where the currents are a sum of axial and vector components

$$\mathcal{H}_{wk} = \frac{iG_{wk}}{\sqrt{2}}(J^{\mu}_{V+} + J^{\mu}_{A+}) \sum_l \bar{l}\gamma_\mu(1+\gamma_5)\nu_l + h.c, \tag{2.37}$$

where l runs over the fields of the three charged leptons e, μ and τ; ν_l runs over the fields of the associated neutrinos and $J^{\mu}_{V\pm}$ and $J^{\mu}_{A\pm}$ are the charge changing currents

$$J^{\mu}_{V\pm} = J^{\mu}_{V_1} \pm J^{\mu}_{V_2} \quad , \quad J^{\mu}_{A\pm} = J^{\mu}_{A_1} \pm J^{\mu}_{A_2}. \tag{2.38}$$

A good review on this subject is found in Ref. [51]. As discussed in this reference, the constant

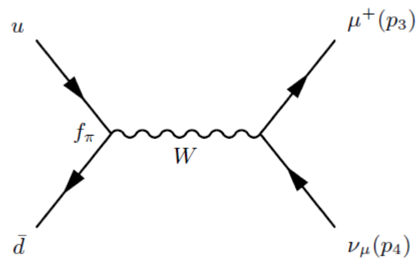

Figure 2.3: Weak decay charged pion.

G_{wk} can be determined using beta-decay transitions, like $\pi \to \pi^0 + e^+\nu_e$. Due to parity, the matrix element $\langle 0|J^{a,\mu}_A|\pi\rangle$ controls completely the weak decay of the pion. Also, because of the vector nature of the current, this matrix element is proportional to the pion momentum. Using the fact that the pion is spinless, we have then

$$\langle 0|J^{a,\mu}_A(x)|\pi^b(p)\rangle = if_\pi p_\mu \delta^{ab} e^{-ip\cdot x}, \tag{2.39}$$

and the proportionality constant, f_π, is the leptonic decay constant. Experimentally, its value is $f_\pi = 93$ MeV.

Now, let us take the divergence of Eq. (2.39):

$$\langle 0|\partial_\mu J^{a,\mu}_A(x)|\pi^b(p)\rangle = f_\pi m_\pi^2 \delta^{ab} e^{-ip\cdot x}, \tag{2.40}$$

with $q^2 = q^\mu q_\mu = m_\pi^2$. The above equation gives an interesting piece of insight: the axial current could be carried by a pion field:

$$J^{a,\mu}_A(x) = f_\pi \partial^\mu \Phi^a(x), \tag{2.41}$$

that means the divergence of the axial-vector current is related with the pion field $\Phi(x)$ (up to a constant).

This can be better understood by looking at the expression of the axial-vector current in Eq. (2.22). In fact, taking the divergence of this current we find

$$\partial_\mu J_A^{a,\mu} = i\bar{\psi}\{M, t^a\}\gamma_5\psi. \tag{2.42}$$

Even if all quark masses are equal, there remains a non-zero contribution proportional to the quark mass

$$\partial_\mu J_A^{a,\mu} = 2im\bar{\psi}t^a\gamma_5\psi = 2mP^a, \tag{2.43}$$

where P^a is a pseudoscalar density corresponding to the pseudoscalar mesons. This is the famous PCAC (partially conserved axialvector current) relation: the divergence of the axial-vector current is a pseudoscalar current. This equation will become useful later.

Next, if we consider the equal time commutation relation $[Q_a^A, P^b] = -1/2i\delta_{ab}\bar{\psi}\psi$, we have for the pion case ($a = b = 1$)

$$[Q_1^A, P^1] = -\frac{i}{2}(\bar{\psi}_u\psi_u + \bar{\psi}_d\psi_d), \tag{2.44}$$

for which the vacuum expectation value suggests that $Q_1^A|0\rangle \neq 0$, consistent with nonzero values for the quark condensate, $\langle\bar{\psi}\psi\rangle \neq 0$.

This strongly confirms the Y. Nambu's suggestion that the vacuum is not invariant under chiral transformation. Moreover, using the PCAC relation in Eq. (2.43), we have

$$[Q_1^A, \partial_\mu J_A^{1,\mu}] = -\frac{i}{2}(m_u + m_d)\langle\bar{\psi}_u\psi_u + \bar{\psi}_d\psi_d\rangle. \tag{2.45}$$

Next, inserting a complete set of pion states

$$\int \frac{d^3p}{2E_p(2\pi)^3}|\pi_a(p)\rangle\langle\pi_a(p)| = 1, \tag{2.46}$$

and using Eq. (2.40) with the definition

$$\langle 0|Q_a^A(t=0)|\pi_b(p)\rangle = i\delta_{ab}f_\pi E_p(2\pi)^3\delta^3(\vec{p}), \tag{2.47}$$

one finds the GOR relation

$$2m_\pi^2 f_\pi^2 = -(m_u + m_d)\langle\bar{\psi}_u\psi_u + \bar{\psi}_d\psi_d\rangle + \mathcal{O}(m_{u,d}^2). \tag{2.48}$$

From this, one sees that the GOR relation establishes a clear connection between quark degrees of freedom and mesonic properties, like the pion mass and its decay constant.

2.1.2 Confinement

As we discussed in the introduction, another important feature of QCD at low energies is the color confinement in that isolated quarks cannot be found in nature. As mentioned in the Introduction, color confinement of QCD is a theoretical hypothesis which is consistent with experimental observations. A conclusive proof from first principles QCD still remains a big challenge for theoretical physicists.

In order to make clear this, let us suppose that we have a color singlet state, as a quark-antiquark pair, and try to break it by pulling them apart. As a result, the interaction between them becomes stronger as the distance between them becomes larger. This is very similar to what happens in a spring. Indeed, in a spring the potential energy increases when we stretch it. And, if we stretch it beyond of the elastic limit, it breaks into two pieces. In the quark-antiquark pair case, if we pull them beyond of a limiting distance, a new quark anti-quark pair is generated due to enormous quantity of energy produced. As a consequence, one cannot have quarks as free particles.

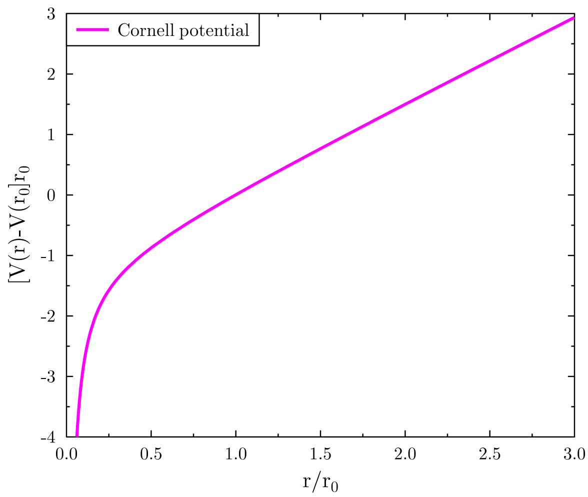

Figure 2.4: Potential energy between a pair of a heavy quark-antiquark pair when the existence of light quarks are ignored [52].

It is important to mention that the above discussion is to some extent a speculation. For a more complete understanding of this, we need to make precise calculations in QCD at small energy scales, when the QCD coupling gets strong. The best way we know to solve QCD in this regime is to perform numerical simulations on a finite space-time lattice. In this way, it is possible to find the potential energy between a quark anti-quark pair when there are no dynamical quarks; this approximation is named a quenched approximation. The simulations show that this potential does increase linearly beyond the distance of a few fermis, as shown in Fig. 2.4. Of course, this is not relevant for the real world, because one cannot neglect light quarks. Some authors [53], however, believe that understanding confinement in QCD necessarily requires understanding confinement in pure-gauge Yang-Mills theory.

The behavior of some gauge invariant observables can signalize if a given gauge system (with no light quarks) is, or is not, confining. These are the Wilson loop, the Polyakov loop, the 't Hooft loop, and the vortex free energy. In this thesis, the relevant one will be the Wilson loop.

2.1.2.1 Wilson loop

Considering an $SU(N)$ gauge theory and two space-time points x^μ and $x^\mu + \epsilon^\mu$, where ϵ^μ is infinitesimal, we define the following *Wilson link*

$$W(x+\epsilon, x) = \exp\Big[i\epsilon^\mu A_\mu(x)\Big], \tag{2.49}$$

where $A_\mu(x)$ is in the adjoint representation of the $SU(N)$ group, hence it is an $N \times N$ matrix-valued traceless hermitian gauge field. Expanding the Wilson link, we have

$$W(x+\epsilon, x) = I + i\epsilon^\mu A_\mu(x) + \mathcal{O}(\epsilon^2). \tag{2.50}$$

Now, let us examine the behavior of the Wilson link under a gauge transformation. Using the gauge transformation of $A_\mu(x)$ given in Eq. (2.16), we find

$$W(x+\epsilon, x) \to I + i\epsilon^\mu U(x) A_\mu(x) U^\dagger(x) - \epsilon^\mu U(x)\partial_\mu U^\dagger(x). \tag{2.51}$$

Since $UU^\dagger = 1$, we have $-U(x)\partial_\mu U^\dagger(x) = +\partial_\mu U(x) U^\dagger(x)$ and we can rewrite the above equation as

$$W(x+\epsilon, x) \to \Big[(I + \epsilon^\mu \partial_\mu) U(x)\Big] U^\dagger(x) + i\epsilon^\mu U(x) A_\mu(x) U^\dagger(x). \tag{2.52}$$

The first term can be also rewritten as

$$(I + \epsilon^\mu \partial_\mu) U(x) = U(x+\epsilon) + \mathcal{O}(\epsilon^2). \tag{2.53}$$

In the second term, we can replace $U(x)$ by $U(x+\epsilon)$ when we neglect $\mathcal{O}(\epsilon^2)$ terms. Then, we get

$$W(x+\epsilon, x) \to U(x+\epsilon)\Big(I + i\epsilon^\mu A_\mu(x)\Big) U^\dagger(x), \tag{2.54}$$

which is equivalent to

$$W(x+\epsilon,x) \to U(x+\epsilon)W(x+\epsilon,x)U^\dagger(x). \tag{2.55}$$

Now, let us consider a finite Wilson link. This is specified by a starting point x and n sequential infinitesimal displacement ϵ_j. The ordered set of ϵ's defines a path P through space-time that starts at x and ends at $y = x + \epsilon_1 + \ldots + \epsilon_n$. Then, one can define the *Wilson line* given by

$$W_P(y,x) = W(y, x+\epsilon_n)\ldots W(x+\epsilon_1+\epsilon_2, x+\epsilon_1)W(x+\epsilon_1,x), \tag{2.56}$$

and this expression is equivalent to

$$W_P(y,x) = \int_P \exp\Big[idx^\mu A_\mu(x)\Big]. \tag{2.57}$$

Using Eq. (2.55) and the unitarity property of $U(x)$, we see that, under a gauge transformation, the Wilson line transforms as

$$W_P(y,x) \to U(y)W_P(y,x)U^\dagger(x). \tag{2.58}$$

Now if we consider a path that returns to its starting point, forming a closed and oriented curve C in space-time, we can define the *Wilson loop* as the trace of the Wilson line for this path

$$W(C) = \mathrm{Tr} W_P(x,x), \tag{2.59}$$

whose expression is given as

$$W(C) = \oint_C \exp\Big[idx^\mu A_\mu(x)\Big]. \tag{2.60}$$

Using Eq. (2.58), we see that the Wilson loop is gauge invariant,

$$W(C) \to W(C). \tag{2.61}$$

Then, the path integral for the Wilson loop expectation value is written as

$$\langle W_C\rangle = \frac{1}{Z}\int \mathcal{D}U e^{-\beta S}\mathrm{Tr} P\exp\Big(i\oint_C dx_\mu A^\mu\Big). \tag{2.62}$$

Now, let us consider a quark-antiquark pair at a (spatial) distance R, at $t=0$. We take the quark masses to infinity and let them evolve for a large time T, as illustrated in Fig. 2.5 . To describe this system we consider a theory that consists of an $SU(N)$ lattice gauge field, with spacing a, coupled to a quark field in color group representation r. The action is given by

$$S = \beta\sum_p \Big(1 - \frac{1}{N}\mathrm{Re}\ \mathrm{Tr}[U(p)]\Big) + S_{matter}, \tag{2.63}$$

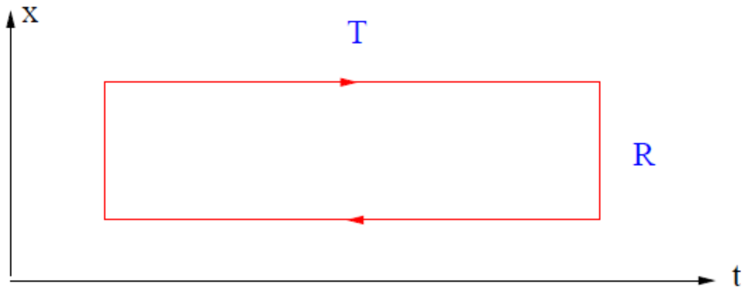

Figure 2.5: Retangular Wilson loop.

where $U(p)$ is the plaquette variable, given by

$$U(p) = \exp\Big(ia^2 F_{\mu\nu}F_{\mu\nu} + \mathcal{O}(a^3)\Big), \tag{2.64}$$

and the matter action is

$$S_{matter} = -\frac{1}{2}\sum_{x,\mu=\pm 1}^{\pm 4}\Big[\bar{\psi}(x)(\alpha+\gamma_\mu)U_\mu^{(r)}(x)\psi(x+\mu)\Big] + \sum_x (m_q+4\alpha)\bar{\psi}(x)\psi(x), \tag{2.65}$$

where $\gamma_{-\mu} = -\gamma_\mu$, $0 \le \alpha \le 1$, and $U_\mu^{(r)}(x)$ denotes the link variable in group representation r, with $U_{-\mu}(x) = U_\mu^\dagger(x-\mu)$.

Now, let Q be an operator which creates a color-singlet two-particle state, with separation R:

$$Q(t) = \bar{\psi}(0,t)\Big[\Gamma\prod_{n=0}^{R-1} U_i^{(r)}(ni,t)\Big]\psi(Ri,t), \tag{2.66}$$

where Γ is some 4×4 matrix, constructed from Dirac γ matrices. One can evaluate the term $\langle Q^\dagger(T)Q^\dagger(0)\rangle$ by using the path integral formulation. The quark fields can be integrated out and the leading contribution at large m_q is obtained by bringing down from the action a set of terms $\psi(\alpha+\gamma_4)U\psi$; some details can be found in [54]. After some effort, one obtains

$$\begin{aligned}\langle Q^\dagger(T)Q(0)\rangle &= \frac{1}{Z}\int \mathcal{D}U\mathcal{D}\psi\mathcal{D}\bar{\psi}Q^\dagger(T)Q(0)e^{-S} \\ &\sim C(m_q+4\alpha)^{-2T}\frac{1}{Z_U}\int \mathcal{D}U\chi_r[U(R,T)]e^{-S_U},\end{aligned} \tag{2.67}$$

where $\chi_r[g]$ is the group character (trace) of group element g in representation r, C is a constant arising from a trace over spinor indices and $U(R,T)$ is the path-ordered product of links along the rectangular contour with opposite sides of lengths R separated by time T. In the continuum limit, this gives

$$W(C) = P\exp\Big[\oint_C dx^\mu A_\mu(x)\Big]. \tag{2.68}$$

Therefore, the integration in Eq. (2.67) is precisely the Wilson loop. One can them write this same equation as

$$\langle Q^\dagger(T)Q(0)\rangle \sim C(m_q+4\alpha)^{-2T}\langle W_C(R,T)\rangle. \tag{2.69}$$

On the other hand, using the usual rules of quantum mechanics in imaginary time the correlator in Eq. (2.67) can also be written as

$$\begin{aligned}\langle Q^\dagger(T)Q(0)\rangle &= \frac{\sum_{n,m}\langle 0|Q^\dagger(T)|n\rangle\langle n|e^{-HT}|m\rangle\langle m|Q(0)|0\rangle}{\langle 0|e^{-HT}|0\rangle} \\ &= \sum_n |c_n|^2 e^{-(V(R)+\Delta E_n)T}, \quad \Delta E_n = E_n - V(R).\end{aligned} \tag{2.70}$$

The lowest energy eigenstate has energy $E_0 = V(R)$ by definition, which is referred to as the static quark potential. The higher energy eigenstates are denoted by their excess energies ΔE_n. Considering T sufficiently large, the higher-energy terms in the sum are then sufficiently suppressed. Now, by comparing the above relation with that in Eq. (2.69), we have

$$\sum_n |c_n|^2 e^{-(V(R)+\Delta E_n)T} \sim C(m_q+4\alpha)^{-2T}\langle W_C(R,T)\rangle. \tag{2.71}$$

Subtracting the $\ln(m_q+4\alpha)$, which is independent of R and therefore irrelevant for our purposes, we have

$$V(R) = -\lim_{T\to\infty} \ln\Big[\frac{\langle W_C(R,T+1)\rangle}{\langle W_C(R,T)\rangle}\Big], \tag{2.72}$$

or in a more simplified way

$$\langle W(C)\rangle \sim e^{-TV(R)} \quad , \quad T\to\infty, \tag{2.73}$$

where $V(R)$ will be referred from now on as the static quark potential. Again, this is the potential for massive color charged sources. Using this criterium, the confinement problem is to show that $V(R)$ has the asymptotic behavior

$$V(R) \sim \sigma R. \tag{2.74}$$

Thus, the string tension σ can serve as an order parameter for the confined phase, in which $\sigma \neq 0$ for all color charge sources.

We finish this chapter pointing out that we have assumed the absence of light matter fields which could, through pair creation, screen the charge of the massive sources. We also point out that it is not easy to construct a model incorporating both features dynamically, dynamical chiral symmetry breaking and quark-gluon confinement. But, many efforts have been made in the last years using different approaches. We mention a few examples: Dyson-Schwinger equations [55], Hamiltonian model involving constituents quarks [56], phenomenological models [57, 58], the Polyakov and Nambu-Jona-Lasinio (NJL) models [59, 60], Quark-Meson (QM) models [61, 62, 63] as well as their extensions with nonlocal interactions [64].

An interesting approach to deal with QCD in the strong coupling limit is to explore the theory in the Large-N_c limit. In the beginning of the 1970's, 't Hooft suggested [65] that the theory is simplified when the number of colors N_c is very large. In this case, the expansion parameter would be $1/N_c$, and the expectation is that one could study QCD in the limit $N_c \to \infty$ and then perform an expansion in $1/N_c$.

In particular, a new approach based on gauge/gravity duality has been used to incorporate these two properties of nonperturbative QCD to calculate quantities in strongly coupled theories like quantum chromodynamics at low energies.

3 Gauge/Gravity duality

As we mentioned in the introduction of this thesis, the gauge/gravity duality relates the strongly coupled physics of a system to a classical dynamics of gravity in one higher dimension. Originally, the formulation of the duality proposed by Maldacena [3] related a four-dimensional conformal field theory (CFT) to a geometry of an Anti-de-Sitter (AdS) space in five dimensions, hence it was named as AdS/CFT duality. The original papers show that the AdS/CFT duality was inspired in the studies of solitonic solutions, the Dp branes, in string theories, where the gauge field theories have been realized on hypersurfaces embedded in a higher dimensional space which contains gravity.

Since then, the study of the duality has been extended and applied to investigate very different problems, as: the analysis of the strong coupling dynamics of QCD, especially in the study of relativistic heavy ion collisions [66], the physics of black holes [67] and also in different problems in condensed matter physics (holographic superconductors, quantum phase transitions, cold atoms, . . .) [12]. This extended version of the AdS/CFT duality is named as Gauge/Gravity duality or holographic duality. In the present chapter, we will discuss the Gauge/Gravity duality in more details. It is organized as follows: in section 3.1, we present a motivation of the duality using a geometrization of a simple renormalization group; in section 3.2, we introduce the important holographic dictionary to clarify the duality; in section 3.3, we show how to evaluate correlations functions via the duality and use the holographic dictionary; in section 3.4, we apply the correspondence for the scalar field case, with the aim of gaining some insight; in section 3.5, we show how to include temperature effects in the duality and how this affects the background; and, finally, in section 3.6, we show briefly the origin of this duality and discuss how to include flavors in the duality, which is relevant for our purposes in this thesis.

3.1 Motivation

We start this part motivating the gauge/gravity duality via the Kadanoff-Wilson renormalization group approach within a geometrical perspective. For instance, let us consider a non-gravitational system on a lattice whose spacing is a and the Hamiltonian is given by

$$H = \sum_i J_i(x,a)\mathcal{O}^i(x,a), \tag{3.1}$$

where x denotes the different lattice sites and i labels the different operators $\mathcal{O}_i$ and $J_i(x,a)$ are the sources (currents) of the respective operators at the point x on the lattice. Notice that we have also included a second argument in J^i and $\mathcal{O}^i$ to make clear they correspond to a lattice spacing a. It is well known in renormalization group approach that we "coarse grain" the lattice by increasing the lattice spacing a and then by replacing multiple sites by a single site with the average value of the lattice variables. In this process, the Hamiltonian structure keeps the form of Eq. (3.1) but each current and operator will acquire a different weight. In this way, for each step of coarse graining, the currents $J_i(x,a)$ change. For example, supposing that we double the lattice spacing in each step, then we would get a succession of currents like:

$$J_i(x,a) \to J_i(x,2a) \to J_i(x,4a) \to \dots. \tag{3.2}$$

In this way, the currents J_i acquire a dependence on the the lattice spacing. We can compute this evolution in the currents, writing them as $J_i(x,u)$, where $u = (a, 2a, 4a, \dots)$ represents the length scale at which we probe the system. The evolution of the currents with the scale determines the so-called β-function for each operator, given by

$$u\frac{\partial}{\partial u}J_i(x,u) = \beta_i(J_i(x,u),u). \tag{3.3}$$

At weak coupling regime, the β_i's can be determined in perturbation theory. But, at strong coupling nonperturbative methods must be considered.

At strong coupling, the AdS/CFT idea is to consider the length scale u as an extra spatial dimension. In this picture, the succession of lattices at different values of u are considered as slices of a new higher-dimensional space. Moreover, the currents $J_i(x,u)$ are considered as fields living in the space labeled by the usual four dimensions plus the extra dimension u. We can then write

$$J_i(x,u) = \phi_i(x,u). \tag{3.4}$$

Then, all dynamics of the fields ϕ_i will be governed by some action in five dimensions. Indeed, the AdS/CFT duality states that the dynamics of these fields is determined by some gravity theory (i.e. by some metric) that needs to be found. Therefore, one can naively consider the holographic duality as a kind of geometrization of the renormalization group of a given quantum field theory, and the microscopic currents of the quantum field theory in the UV regime are identified with the values of the bulk fields at the boundary of the extra-dimensional space. Thus, one can state that the quantum field theory lives on the boundary of the higher-dimensional space as illustrated in Fig. 3.1.

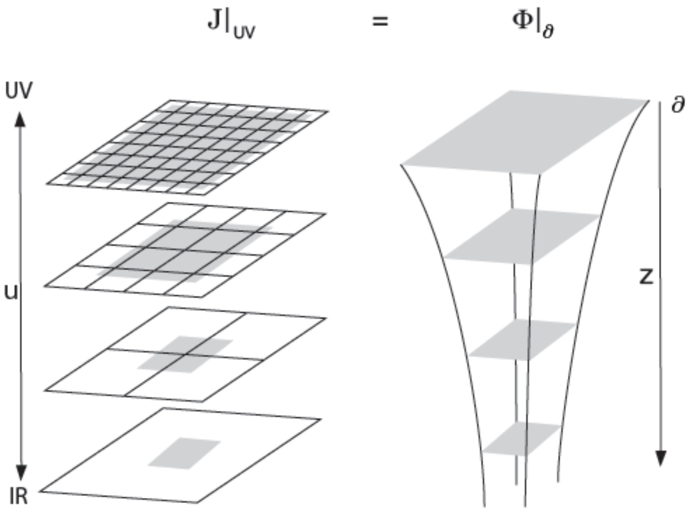

Figure 3.1: On the left we illustrate the Kadanoff-Wilson renormalization of a lattice system. In the AdS/CFT correspondence the lattices at different scales are considered as the layers of the higher dimensional space represented on the right of the figure.

This way, the fields ϕ_i of the dual gravity theory must have the same tensor structure of the corresponding dual operator $\mathcal{O}^i$ of quantum field theory, in such a way that the product $\phi_i \mathcal{O}^i$ is a scalar. In this way, a scalar field will be dual to a scalar operator, a vector field A_μ will be dual to a vector operator J^μ and a spin two field $g_{\mu\nu}$ will be dual to a second order tensor $T_{\mu\nu}$ operator and that is naturally identified with the energy-momentum tensor $T_{\mu\nu}$ of the quantum field theory.

Another characteristic raised by the holographic duality is the matching of the degrees of freedom on both sides of the correspondence. In order to explain this point, let us consider a quantum field theory in a d-dimensional space-time. The number of degrees of freedom of the system is measured by the entropy, which is an extensive quantity. Thus, if R_{d-1} is a $(d-1)$-dimensional spatial region, at fixed time, its entropy is proportional to its volume in $d-1$ dimensions. It is written as

$$S_{QFT} \propto \text{Vol}(R_{d-1}). \tag{3.5}$$

On the other hand, on the gravity side, as we have seen, the theory lives in a $(d+1)$-dimensional space-time. An important question that we could ask is if such a higher dimensional theory can contain the same information as its lower dimensional dual. The key element to answer this question is the fact that entropy in quantum gravity is a subextensive quantity [68]. Indeed, in a gravitational theory, the entropy in a volume is bounded by the entropy of a black hole that fits inside the volume. In this way, according to the so-called holographic principle, the entropy is proportional to the surface of the black hole horizon (and not to the volume enclosed by the horizon). In formal terms, the black hole entropy is given by the Bekenstein-Hawking formula, as follows

$$S_{BH} = \frac{A_H}{4G_N}, \tag{3.6}$$

where A_H is the correspondent area of the event horizon and G_N is the Newton constant. In order to apply it for our purposes, let R_d be a spatial region in the $(d+1)$-dimension space-time where the gravity theory lives and, at fixed time, the region R_d is bounded by a $(d-1)$-dimensional manifold $R_{d-1} = \partial R_d$. Then, according to Eq. (3.6), the gravitational entropy associated with R_d scales as

$$S_{BH} \propto \mathrm{Area}(\partial R_d) \propto \mathrm{Vol}(R_{d-1}), \tag{3.7}$$

which agrees with the QFT behavior in Eq. (3.5).

3.1.1 The Anti-de Sitter space

Once motivated the duality from a naive point of view, the challenge is to find the correct geometry corresponding to the specific quantum field theory. In general, this task consists in a very hard problem. However, if the quantum field theory is located at a fixed point of the renormalization group flow, it means that its β-function vanishes and it becomes a conformal field theory (CFT), and the corresponding metric can be easily found. Indeed, considering a quantum field theory in d space-time dimensions, the most general metric in $(d+1)$-dimensions with Poincaré invariance in d-dimensions is

$$ds^2 = \Omega^2(z)(-dt^2 + d\vec{x}^2 + dz^2), \tag{3.8}$$

where z is the coordinate of the extra dimension: we use $\vec{x} = (x^1, \dots, x^{d-1})$ and $\Omega(z)$ is a function to be determined. Note that using the comparison with the RG, the z coordinate is clearly related to the energy scale as $z = u^{-1}$. In this way, as the quantum field theory is conformal invariant, ds^2 must be invariant under the transformation, as follows

$$(t, \vec{x}) \to \lambda(t, \vec{x}), \quad z \to \lambda z. \tag{3.9}$$

Then, by imposing the invariance of the metric in Eq. (3.8) under the transformation given in Eq. (3.9), we obtain that the function $\Omega(z)$ must transform as

$$\Omega(z) \rightarrow \lambda^{-1}\Omega(z), \tag{3.10}$$

which fixes $\Omega(z)$ to be

$$\Omega(z) = \frac{L}{z}, \tag{3.11}$$

where L is a constant, which we will conveniently refer to it as the Anti-de Sitter radius. Thus, by replacing the above function into the metric in Eq. (3.8) we arrive at the following form for ds^2

$$ds^2 = \frac{L^2}{z^2}(-dt^2 + d\vec{x}^2 + dz^2), \tag{3.12}$$

which is the line element of the AdS_{d+1} space in $(d+1)$-dimensions, that we will denote by AdS_{d+1} space-time. Notice that for each fixed value of z, this metric becomes a Minkowski space-time. Usually, the boundary of the AdS space-time is referred to be located at $z = 0$. Notice still that this metric is singular at $z = 0$. This happens because this coordinate system is not appropriated to write this metric and the singularity disappears changing the coordinate system. Despite of this, we will keep this coordinate system due to its simplicity, but this means that it will be necessary to introduce a regularization procedure in order to define physical quantities in the AdS_{d+1} boundary.

It is worth to remember that the AdS space-time itself arises as solution of the equation of motion of a gravity action of the type

$$I = \frac{1}{16\pi G_N}\int d^{d+1}x\sqrt{|g|}[-2\Lambda + R + c_2R^2 + c_3R^3], \tag{3.13}$$

with G_N being the Newton constant, the c_i are constants, $g = \det(g_{\mu\nu})$, $R = g^{\mu\nu}R_{\mu\nu}$ the Ricci scalar and Λ is a cosmological constant. In particular, in the case $c_2 = c_3 = \ldots = 0$, the action (3.13) becomes the Einstein-Hilbert (EH) action of general relativity with a cosmological constant. In this case the equations of motion are just the Einstein equations

$$R_{\mu\nu} - \frac{1}{2}g_{\mu\nu}R = -\Lambda g_{\mu\nu}. \tag{3.14}$$

We can still use some algebraic manipulations and find the following expression for the scalar curvature

$$R = g^{\mu\nu}R_{\mu\nu} = -\frac{d(d+1)}{L^2}. \tag{3.15}$$

In this thesis, we will be mostly interested in gauge theories in $3+1$ dimensions, which corresponds to set $d = 4$ in our formulas. Thus, the dual geometry found above for this case is AdS_5. This was precisely the system studied in [3] by Maldacena, who conjectured that the dual QFT is the super Yang-Mills theory with four supersymmetries ($\mathcal{N} = 4$ SYM).

3.1.2 Matching the degrees of freedom

Once identified the AdS space-time as the dual of a conformal field theory, we can now evaluate and compare explicitly the degrees of freedom of the both sides of the duality, using the previous arguments in terms of entropy. So, let us consider first the QFT side. We located this system in a spatial box of size R, which acts as an IR cutoff, and we introduce a lattice spacing a which regulates the UV region. In d space-time dimensions, the system has R^{d-1}/a^{d-1} cells. In CFT, there is an important concept, the central charge, that appears in the commutator of two components of the stress-energy tensor and essentially counts the number of degrees of freedom in the theory.

If the CFT considered is a $SU(N)$ gauge field theory, the gauge fields are $N \times N$ matrices living in the adjoint representation of this group. Therefore, in the limit large of N, the theory contains N^2 independent components. Thus, in the $SU(N)$ CFT's, the central charge scales as $c_{SU(N)} \sim N^2$. In this way, the entropy of the CFT scales as

$$S_{CFT} \sim \frac{R^{d-1}}{a^{d-1}} c_{SU(N)} \sim \frac{R^{d-1}}{a^{d-1}} N^2 \tag{3.16}$$

Next, we count the number of degrees of freedom from the AdS side, N_{dof}^{AdS}. As we have seen before, the gravitational entropy is bounded by the black hole entropy, given in Eq. (3.7), and written as

$$S_{grav.} = \frac{A_\partial}{4G_N}, \tag{3.17}$$

where, in the AdS case, A_∂ is the area of the region at the boundary $z \equiv \epsilon \to 0$ of AdS$_{d+1}$, at fixed time. Then, we evaluate A_∂ by integrating the volume element corresponding to the metric, as

$$A_\partial = \int_{\mathbb{R}^{d-1}, z\equiv\epsilon} d^{d-1}x\sqrt{g} = \Big(\frac{L}{\epsilon}\Big)^{d-1} \int_{\mathbb{R}^{d-1}} d^{d-1}x. \tag{3.18}$$

The last integral is the volume of $\mathbb{R}^{d-1}$ and it is infinite. As done in the CFT side, we regulate it by enclosing the system in a box of size R and we get

$$\int_{\mathbb{R}^{d-1}} d^{d-1}x = R^{d-1}. \tag{3.19}$$

Thus, the area of the A_∂ is given by

$$A_\partial = \Big(\frac{RL}{\epsilon}\Big)^{d-1}, \tag{3.20}$$

and, the entropy in Eq. (3.17) can be written as

$$S_{grav.} = \frac{1}{4G_N}\Big(\frac{RL}{\epsilon}\Big)^{d-1}. \tag{3.21}$$

In addition, Newton's constant is directly related to the Planck length l_P, which is a measure of the quantum fluctuations of the space-time; the relation is

$$G_N = (l_P)^{d-1}. \tag{3.22}$$

Then, Eq. (3.21) becomes

$$S_{grav.} = \frac{1}{4}\Big(\frac{R}{\epsilon}\Big)^{d-1}\Big(\frac{L}{l_P}\Big)^{d-1}. \tag{3.23}$$

In general terms, as the number of degrees of freedom of the gravity theory is proportional to gravitational entropy, $S_{grav.} \sim N_{dof}^{grav.}$, the duality establishes a matching between the degrees of freedom of both sides by identifying the gravitational entropy (3.23) with the CFT entropy (3.16), leading to

$$\Big(\frac{L}{l_P}\Big)^{d-1} \sim N^2. \tag{3.24}$$

Notice that, in the limit $L \gg l_P$, we have ignored the quantum fluctuations of the space-time and gravity becomes classical, leading to the AdS space-time. This classical gravity limit implies that the degrees of freedom of the dual gauge field theory must be large, making it a large-N gauge field theory. In this way, we conclude that the classical gravity theory is reliable if

$$\text{classical gravity - AdS} \rightarrow \Big(\frac{L}{l_P}\Big)^{d-1} \sim N^2 \gg 1, \tag{3.25}$$

The action of our gravity theory in the AdS$_{d+1}$ space of radius L contains a factor L^{d-1}/G_N and, when the coefficient multiplying such action is large, the dual gravity theory is (semi)classical. In this case the path integral is dominated by a saddle point.

3.2 The holographic dictionary

As discussed before, in the duality, the sources of a gauge field theory living in the boundary theory act as fields evolving in the gravitational bulk. In general terms, there is a field in the bulk for each operator that we can write in the boundary theory. So, a lot of fields. However, in most of the cases, we will be only interested in a few boundary operators of the gauge field theory and, correspondingly, a few bulk fields. Such a mapping between operators (sources) and fields in the bulk is usually known as *holographic dictionary.*

As seen previously, a simplest example maps the source for a scalar operator $\mathcal{O}(x)$ in the boundary to a scalar field $\phi(x,z)$ in the bulk :

$$\phi(x,z) \longleftrightarrow \mathcal{O}(x). \tag{3.26}$$

We will explore this in more details soon where we will show that the mass of the bulk scalar maps into the dimension of the boundary operator. But first, let us also think about fields of more general spin. As we mentioned in the motivation of the duality, we can find the fields in the bulk corresponding to the bulk operators by just considering their tensor structures. In this way, fermionic fields in the bulk are mapped into fermionic operators in the boundary; vector fields in the bulk are mapped into vector operators in the boundary and so on. One of the most important example is a bulk massless gauge field $A_m(x,z)$; it maps into a conserved current J_μ in the boundary as

$$A_m(x,z) \longleftrightarrow J_\mu. \tag{3.27}$$

It is not hard to show that gauge symmetry in the bulk leads to conservation law of the boundary current, $\partial_\mu J^\mu = 0$. [1] This will be discussed in detail in this thesis soon.

We conclude this part recalling a very important points. Any theory involving gravity necessarily has a bulk metric g_{AB}, and holographically, it is dual to the energy-momentum tensor in the boundary

$$g_{AB} \longleftrightarrow T_{\mu\nu}, \tag{3.28}$$

where, diffeomorphism invariance in the bulk ensures the conservation of the energy and momentum currents, $\partial_\mu T^{\mu\nu} = 0$.

3.3 Correlation functions

Once explained the holographic dictionary, next we want to understand how to extract information about the strongly coupled gauge theory in d-dimensions using the correspondence described here. In order to do this, let us consider the following correlation functions of local operators in the QFT

$$\langle \mathcal{O}(x_1)\mathcal{O}(x_2)\ldots\mathcal{O}(x_n)\rangle. \tag{3.29}$$

[1] Here we have that the m vector index in the bulk runs over one more value than the boundary μ index. This does not cause a problem with the dictionary because you can always use gauge invariance to set $A_z = 0$.

In a gauge field theory, such correlators can be calculated using a generating function, which is obtained by perturbing the lagrangian by a source term as

$$\mathcal{L} \to \mathcal{L} + J(x)\mathcal{O}(x) = \mathcal{L} + \mathcal{L}_J, \tag{3.30}$$

with the generating functional written as

$$Z_{QFT}[J] = \left\langle \exp[\int \mathcal{L}_J] \right\rangle = e^{W_{QFT}[J]}, \tag{3.31}$$

where $W_{QFT}[J]$ is the generating functional of the connected Green's functions. The connected correlators are obtained from the functional derivatives of $\ln Z_{QFT}[J]$, or just $W_{QFT}[J]$ as

$$\left\langle \prod_{i=1} \mathcal{O}(x_i) \right\rangle = \prod_{i=1} \frac{\delta}{\delta J(x_i)} \ln Z_{QFT}[J]\Big|_{J=0} = \prod_{i=1} \frac{\delta}{\delta J(x_i)} W_{QFT}[J]\Big|_{J=0}. \tag{3.32}$$

Our main task here is clarify how to incorporate this prescription on the gravity side. In this context, Gubser, Klebanov, Polyakov and Witten [4, 5] have discovered the right procedure to evaluate correlation functions of a field theory via its dual gravity theory, the GKPW prescription. Those authors have followed the ideas obtained in the context of string theory where the open strings are sources for closed strings. In this way, following the holographic dictionary, the QFT is thought to live on the AdS boundary and on the gravitational side the source is restricted to this boundary. Then, the sources will act as boundary conditions for its corresponding fields propagating in the bulk gravity theory. In general, these fields can present some divergences at the boundary and, because of this, a regularization procedure must be considered, as we will show explicitly.

In a precise form, the GKPW prescription is the mathematical "backbone" of AdS/CFT correspondence and it identifies the partition function of a QFT in the presence of a source $J(x)$ with the partition function of a bulk gravitational theory where the asymptotically Anti-de Sitter boundary value of the fields ϕ are matched with the sources $J(x)$. This identification is written as

$$Z_{QFT}[J(x)] = Z_{str}[\phi_0(x)] = \int \mathcal{D}\phi e^{-S_{str}[\phi(x,z)]|_{\phi_0(x)}}. \tag{3.33}$$

In general, the right-hand side of this equation is very difficult to compute, but it simplifies dramatically in the classical gravity limit (3.25). In this limit, the string theory path integral is dominated by the saddle point approximation, that contains the classical gravity theory. So, we have

$$Z_{QFT}[J(x)] = Z_{str}[\phi_0(x)] \sim e^{-S_{grav}[\phi(x,z)]}|_{\phi \to \phi_0(x)}, \quad N \gg 1. \tag{3.34}$$

The duality conjecture asserts that this classical gravity action (3.34) is precisely related to the generating functional for a connected Green's function in Eq. (3.32) as

$$W_{QFT}[J] = -S_{grav}[\phi(x,z)]|_{\phi\to\phi_0(x)}. \tag{3.35}$$

Therefore, the correlation functions of the QFT can now be evaluated as

$$\langle\mathcal{O}(x_1)...\mathcal{O}(x_n)\rangle = \frac{\delta^{(n)}S_{grav}[\phi_0]}{\delta\phi_0(x_i)...\delta\phi_0(x_n)}\Big|_{\phi_0=0}. \tag{3.36}$$

In most of the cases, the on-shell action (S_{grav}) needs to be renormalized as it typically suffers from infinite volume (i.e. IR) divergences due to the integration region near the boundary of AdS. Such divergences are dual to UV divergences in the gauge field theory, which is consistent with the idea that, the duality is also a UV/IR duality. The procedure to eliminate these divergences on the gravity side is well understood and named as 'holographic renormalization'. A good review on this topic is found in Ref. [69].

3.4 Massive scalar field in AdS space

In order to study the consistency of the duality, let us consider for simplicity a scalar field ϕ with mass m^2 in the background of an AdS$_{d+1}$ space-time with classical action given by

$$I_\phi = -\frac{1}{2}\int d^{d+1}x\sqrt{|g|}\Big((\partial_n\phi)^2 + m^2\phi^2\Big). \tag{3.37}$$

The equation of motion derived from this action is

$$\frac{1}{\sqrt{|g|}}\partial_n(\sqrt{|g|}\partial^n\phi) - m^2\phi = 0, \tag{3.38}$$

and using the metric (3.12), this equation explicitly becomes

$$z^{d+1}\partial_z(z^{1-d}\partial_z\phi) + z^2\partial_\mu\partial^\mu\phi - m^2\phi = 0. \tag{3.39}$$

Now, due to translational invariance in 4d, let us perform the Fourier transform of ϕ in the x^μ coordinates

$$\phi(x,z) = \int\frac{d^dk}{(2\pi)^d}e^{ikx}\varphi_k(z). \tag{3.40}$$

Then, the equation of motion (3.39) becomes

$$z^{d+1}\partial_z(z^{1-d}\partial_z\varphi_k) - k^2z^2\varphi_k - m^2\varphi_k = 0. \tag{3.41}$$

Let us focus on the region near to the boundary $z \approx 0$. Therefore, taking the limit $z \to 0$ in the Eq. (3.41) we find the solution

$$\varphi_k(z) \to \phi_0(k) z^{d-\Delta} + \phi_1(k) z^{\Delta}, \tag{3.42}$$

where Δ is given by

$$\Delta = \frac{d}{2} + \sqrt{\frac{d^2}{4} + m^2}. \tag{3.43}$$

In particular, the powers $d - \Delta$ and Δ in Eq. (3.42) are roots of the equation $m^2 = \Delta(\Delta - d)$. Now, by performing the inverse Fourier transform, we can write for (3.42) an expansion near the boundary in position space

$$\phi(x, z) = \phi_0(x) z^{d-\Delta} + \phi_1(x) z^{\Delta}, \quad z \to 0. \tag{3.44}$$

We highlight here that, the first solution $z^{d-\Delta}$ is the normalizable solution as it leads to finite action (3.37). On the other hand, the second solution, z^{Δ}, is the non-normalizable solution, as it leads to a divergent action. Notice still that, $d - \Delta$ and Δ are real as long as $m^2 \geq -d^2/4$. This bound, known as *Breitenlohner-Freedman* (BF) bound [70], states that a small negative m^2 does not lead to an instability in AdS$_{d+1}$ as it would in a flat space instead, the would be instability is lifted by the harmonic potential generated by the AdS$_{d+1}$ curvature.

If the BF bound is satisfied, we have as consequence that $d - \Delta \leq \Delta$. Then, the term behaving as z^{Δ} in Eq. (3.44) is the dominant one as $z \to 0$. So, let us take the boundary as $z \approx 0$ and neglect the subdominant term, for now. We have

$$\phi(x, z = \epsilon) \sim \epsilon^{d-\Delta} \phi_0(x). \tag{3.45}$$

Notice that, as $d - \Delta$ is negative if $m^2 > 0$, the leading term is typically divergent as we approach the boundary at $z = \epsilon \to 0$. In order to identify correctly the QFT source $J(x)$ with the boundary value of the field $\phi(x, z)$, we need to remove the divergences of the latter. We will simply do it by extracting the divergent multiplicative factor from (3.45), i.e. the QFT source $J(x)$ is identified with $\phi_0(x)$. Equivalently, we define

$$J(x) = \phi_0(x) = \lim_{z \to 0} z^{-(d-\Delta)} \phi(x, z). \tag{3.46}$$

Clearly, with such a definition, $J(x)$ is always finite. Conversely, at leading order, we can write $\phi(x, z) = z^{d-\Delta} J(x)$.

In order to interpret the meaning of Δ, let us focus at the boundary action. Remember that as the current $J(x)$ couples with the operator $\mathcal{O}(x)$, the action at the boundary is given by

$$I_{bdy} \sim \int d^d x \sqrt{|\gamma_\epsilon|}\phi(x,\epsilon)\mathcal{O}(x,\epsilon), \tag{3.47}$$

where $\gamma_\epsilon = (L/\epsilon)^{2d}$ is the determinant of the induced metric at the $z = \epsilon$ boundary. Then, using Eq. (3.46), we have $\phi(x,\epsilon) = \epsilon^{d-\Delta}J(x)$ and using it in the expansion for I_{bdy}, we get

$$I_{bdy} \sim L^d \int d^d x J(x)\epsilon^{-\Delta}\mathcal{O}(x,\epsilon). \tag{3.48}$$

In order to make I_{bdy} finite and independent of ϵ as $\epsilon \to 0$ we must require

$$\mathcal{O}(x,\epsilon) = \epsilon^{\Delta}\mathcal{O}(x), \tag{3.49}$$

which means that the operator also scales with Δ. In order words, passing from $z = 0$ to $z = \epsilon$ means a scale transformation in the QFT in lower dimension. Thus, Δ must be interpreted as the mass scaling dimension of the dual operator $\mathcal{O}$. Similarly, from the relation $\phi(x,\epsilon) = \epsilon^{d-\Delta}J(x)$, it follows that $d - \Delta$ is the mass scaling dimension of the source $J(x)$.

3.4.1 One-point function

The first correlation function we can find for the scalar field in AdS$_{d+1}$ space-time is the 1-point function. In addition, it is also interesting to compute the one-point function of an operator $\mathcal{O}$ in the presence of the source ϕ_0, given by

$$\langle \mathcal{O}(x)\rangle_{\phi_0} = \frac{\delta S_{grav}[\phi]}{\delta \phi_0(x)}. \tag{3.50}$$

In other words, $\langle \mathcal{O}(x)\rangle$ is understood as being the response of the operator to the source ϕ_0. Taking into account the relation between ϕ and ϕ_0, given in Eq. (3.46), we get

$$\langle \mathcal{O}(x)\rangle_{\phi_0} = \lim_{z\to 0} z^{d-\Delta}\frac{\delta S_{grav}[\phi]}{\delta \phi(x,z)}. \tag{3.51}$$

We can compute in a closed form the functional derivative of the classical on-shell action with respect to $\phi(x,z)$. In fact, the action S_{grav} be represented as

$$S_{grav} = \int_{AdS} dz d^d x \mathcal{L}[\phi, \partial\phi], \tag{3.52}$$

with AdS being a $(d+1)$-dimensional manifold whose boundary is located at $z = 0$. Under a general change $\phi \to \phi + \delta\phi$, the classical action S_{grav} changes as

$$\delta S_{grav} = \int_{\mathcal{A}\lceil\mathcal{S}} dz d^d x \Big[\frac{\partial \mathcal{L}}{\partial \phi}\delta\phi + \frac{\partial \mathcal{L}}{\partial(\partial_m \phi)}\delta(\partial_m\phi)\Big]. \tag{3.53}$$

Now using, in the above equation, the condition $\delta(\partial_m\phi) = \partial_m(\delta\phi)$ and next integrating by parts and finally using the Euler-Lagrange equations, we find that

$$\delta S_{grav} = \int_{\mathcal{M}} dz d^d x \partial_m (\Pi^m(x,z)\delta\phi), \quad \Pi^m(x,z) = \frac{\partial\mathcal{L}}{\partial(\partial_m\phi)}, \tag{3.54}$$

where $\Pi^m(x,z)$ is the generalized conjugate momentum to $\phi(x,z)$. As the boundary is located at $z = \epsilon \to 0$, we can write

$$\delta S_{grav} = \int_\epsilon^\infty dz \int d^d x \partial_z (\Pi^z(x,z)\delta\phi) = -\int_{\partial\mathcal{M}} d^d x \Pi^z(x,\epsilon)\delta\phi(x,\epsilon). \tag{3.55}$$

Thus, from this, it follows that

$$\frac{\delta S_{grav}}{\delta\phi(x,\epsilon)} = \Pi^z(x,\epsilon) = -\frac{\partial\mathcal{L}}{\partial(\partial_z\phi)}. \tag{3.56}$$

In this way, the one-point function in Eq. (3.51) is rewritten as

$$\langle\mathcal{O}(x)\rangle_{\phi_0} = \lim_{z\to 0} z^{d-\Delta}\Pi^z(x,z). \tag{3.57}$$

Using the Lagrangian written in Eq. (3.37) and the asymptotic behavior in (3.44) we find that the one-point function (3.57) is

$$\langle\mathcal{O}(x)\rangle_{\phi_0} = \phi_1(x). \tag{3.58}$$

And, then, returning to Eq. (3.44), the field near to the boundary of the scalar field takes the form

$$\phi(x,z) = J(x)\ z^{d-\Delta} + \langle\mathcal{O}(x)\rangle_J\ z^{\Delta}, \quad z \to 0. \tag{3.59}$$

3.4.2 Linear response

A small space and time perturbation in a equilibrium state of a certain physical system consists the basis of the linear response theory. The one point function with a source can be written in the path integral representation as

$$\langle\mathcal{O}(x)\rangle_J = \int \mathcal{D}\phi\mathcal{O}(x)e^{-S_E+\int d^d y J(y)\mathcal{O}(y)}. \tag{3.60}$$

Expanding the exponent in this expression in a power series of the source J and just keeping the terms up to linear order, we have

$$\langle\mathcal{O}(x)\rangle_J = \langle\mathcal{O}(x)\rangle_{J=0} + \int d^d y \langle\mathcal{O}(x)\mathcal{O}(y)\rangle J(y) + \dots. \tag{3.61}$$

Defining the two-point function $G(x-y)$ as

$$G(x-y) = \langle \mathcal{O}(x)\mathcal{O}(y) \rangle, \tag{3.62}$$

the Eq. (3.61), can be rewritten as

$$\langle \mathcal{O}(x) \rangle_J = \langle \mathcal{O}(x) \rangle_{J=0} + \int d^d y G(x-y) J(y) + \dots. \tag{3.63}$$

We consider observables such that $\langle \mathcal{O}(x) \rangle_{\phi=0}$ is zero. Notice that, this vanishing can always be achieved subtracting the vacuum expectation value (VEV) without source in Eq. (3.63). In this way, the fluctuations of the observable can be measured by $\langle \mathcal{O}(x) \rangle_J$. So, the linear response is written as

$$\langle \mathcal{O}(x) \rangle_J = \int d^d y G(x-y) J(y). \tag{3.64}$$

Going to momentum space, this expression is rewritten as

$$\langle \mathcal{O}(k) \rangle_J = G(k) J(k), \tag{3.65}$$

and we can rewrite the two-point function in momentum space as

$$G(k) = \frac{\langle \mathcal{O}(k) \rangle_J}{J(k)}. \tag{3.66}$$

In the framework of the AdS/CFT correspondence, we have obtained $\langle \mathcal{O}(k) \rangle_J$ in (3.57), the two-point function in momentum space is then:

$$G(k) = \lim_{z \to 0} z^{d-\Delta} \frac{\Pi^z(k,z)}{\phi_0(k)}. \tag{3.67}$$

To exemplify our description, let us consider a spatially constant electric field $E^i(\omega)$, oscillating with frequency ω, and acting on a system whose response is the charge current $J^i(\omega)$. At first order, this is described by Ohm's law

$$J^i(\omega) = \sigma^{ij}(\omega) E_j(\omega). \tag{3.68}$$

where $\sigma^{ij}(\omega)$ is the conductivity tensor for alternating currents. In the language of the previous subsections, we consider an external vector potential $A_\mu(x)$, which plays the role of $\phi(x)$, and a conserved current $J^i(x)$, which corresponds to the operator $\mathcal{O}(x)$. In the temporal gauge ($A_t = 0$), the electric field E_k is simply given by $E_k = -\partial_t A_k$. Using the following Fourier decomposition $A_k \sim e^{-i\omega t}$, the electric field becomes $E_k = i\omega A_k$. Now, by comparing Ohm's law (3.68) with (3.66), we obtain a simple expression for the electric conductivity tensor of alternating currents

$$\sigma^{ij}(\omega) = \frac{G^{ij}(k)}{i\omega}. \tag{3.69}$$

In our context, $G^{ij}(k)$ are the components of the retarded correlator of currents in Fourier space. Notice that the spatial momentum q is set to zero.

Our analysis can be easily extended for the fields with higher order spins. Indeed, the relation (3.43) and the near-boundary behaviour (3.44) also apply to a bulk spin-one and spin-two fields. In general terms, in the case of a bulk p-form, the dimension Δ of the dual operator is the largest root of the equation

$$m^2 = (\Delta - p)(\Delta + p - d), \tag{3.70}$$

and the behavior of the fields near to the boundary becomes

$$\phi_{\mu_1 \ldots \mu_p}(x, z) \approx A_{\mu_1 \ldots \mu_p} z^{d-p-\Delta} + B_{\mu_1 \ldots \mu_p} z^{\Delta - p}, \quad z \to 0. \tag{3.71}$$

In summary, we have seen that the AdS space-time corresponds to the solution dual to the vacuum of a CFT. But, the gauge/gravity duality we have presented here also can be used to study theories with no scale invariance, like QCD. In fact, QCD is not a conformal theory and a direct consequence is that the dual background is no longer AdS space-time, instead, it is a different space-time that is just AdS in the UV regime (near to the boundary). All the efforts will be to find a correct metric in the IR regime.

3.5 Finite temperature in Gauge/Gravity duality

Let us next show how to incorporate finite temperature in the gauge/gravity duality. We start recalling that, the partition function in statistical mechanics in the canonical ensemble is given by

$$Z = \mathrm{Tr}\ \mathrm{e}^{-\beta \mathrm{H}} \tag{3.72}$$

where, H is the hamiltonian operator, β related with the temperature by $\beta = 1/T$, we have take the Boltzmann constant $k_B = 1$. The thermal average of an operator $\mathcal{O}$ at the temperature T is

$$\mathcal{O}_T = \frac{\mathrm{Tr}\Big[\mathcal{O}\ \mathrm{e}^{-\beta \mathrm{H}}\Big]}{Z}. \tag{3.73}$$

Using the path integral approach, the average $\mathcal{O}_T$ is written as

$$\mathcal{O}_T = \frac{1}{Z} \int [\mathcal{D}\psi] \langle \psi(x) | \mathcal{O}\ e^{-\beta H} | \psi(x) \rangle, \tag{3.74}$$

where $|\psi(x)\rangle$ is the state corresponding to the operator $\hat{\psi}(x)$, given by

$$\hat{\psi}(x) |\psi(x)\rangle = \psi(x) |\psi(x)\rangle. \tag{3.75}$$

The trace in (3.74) is taken the same initial and final state $|\psi(x)\rangle$ in the evaluation of the expectation value. Still, note that the hamiltonian operator represents a time evolution and, using this, we can rewrite (3.74) as

$$\mathcal{O}_T = \frac{1}{Z}\int [\mathcal{D}\psi]\langle\psi(x,t)|\mathcal{O}|\psi(x,t+i/T)\rangle. \tag{3.76}$$

It is well known that, thermal correlation functions are evaluated considering an imaginary time evolution and by imposing periodic boundary conditions for bosons and antiperiodic boundary conditions for fermions. Therefore, the Euclidean time t_E is periodic, as $t_E \to t_E + \frac{i}{T}$. Thus, the compactification of Euclidean time is equivalent to having $T \neq 0$.

Next, we will show how the temperature of the field theory is related with the Hawking temperature of a black hole [71]. For simplicity, we will assume an Euclidean metric :

$$ds^2 = g(z)\Big[f(z)dt_E^2 + d\vec{x}^2\Big] + h(z)dz^2, \tag{3.77}$$

where we assume that the functions $f(z)$ and $h(z)$ are null at $z = z_h$, which is the location of the horizon, and that $g(z_h) \neq 0$. Then, for $z \approx z_h$, we have

$$f(z) \approx f'(z_h)(z - z_h) \quad , \quad h(z) \approx h'(z_h)(z - z_h). \tag{3.78}$$

For the $g(z)$ function, we just take $g(z) = g(z_h)$. Then, the Euclidian metric near to the horizon can be rewritten as

$$ds^2 \approx g(z_h)\Big[f'(z_h)(z - z_h)dt_E^2 + d\vec{x}^2\Big] + \frac{1}{h'(z_h)}\frac{dz^2}{z - z_h}. \tag{3.79}$$

In order to write the metric in an elegant way, let us define two new coordinates: a radial ρ and an angular θ, as

$$\frac{1}{h'(z_h)}\frac{dz^2}{z - z_h} = d\rho^2 \quad , \quad g(z_h)f'(z_h)(z - z_h)dt_E^2 = \rho^2 d\theta^2, \tag{3.80}$$

which corresponds to defining θ as

$$\theta = \frac{1}{2}\sqrt{g(z_h)f'(z_h)h'(z_h)}\,t_E. \tag{3.81}$$

In these new coordinates, Eq. (3.79) becomes

$$ds^2 \approx g(z_h)d\vec{x}^2 + d\rho^2 + \rho^2 d\theta^2, \tag{3.82}$$

where the two last parts have the metric of a plane. The event horizon is now located at $\rho = 0$ and in order to avoid problems with any curvature singularity in this point, the θ variable must be a periodic coordinate with period 2π. In order to find a relation between the value of T and the event horizon of the black hole, first notice that the periodicity under $\theta \to \theta + 2\pi$ is equivalent to periodicity under $t_E \to t_E + 1/T$, therefore:

$$\frac{1}{T} = \frac{4\pi}{\sqrt{g(z_h)f'(z_h)h'(z_h)}}. \tag{3.83}$$

where T has the same form of the Hawking temperature [71]. As a simple application, we use the AdS_{d+1} black hole case. Its metric is

$$ds^2 = \frac{L^2}{z^2}\Big[f(z)dt_E^2 + d\vec{x}^2 + \frac{dz^2}{f(z)}\Big], \tag{3.84}$$

where $f(z)$ has the following function

$$f(z) = 1 - \frac{z^d}{z_h^d} \tag{3.85}$$

with z_h located the event horizon. By comparing with the general form of metric in (3.77), the other functions in Eq. (3.84) are given by

$$g(z) = \frac{L^2}{z^2} \quad , \quad h(z) = \frac{z^2}{L^2}f(z). \tag{3.86}$$

In this case, the derivatives of $f'(z)$ and $h'(z)$ at the horizon are

$$f'(z_h) = -\frac{d}{z_h} \quad , \quad h'(z_h) = -\frac{dz_h}{L^2}. \tag{3.87}$$

And, as a consequence, using (3.83), the temperature becomes

$$T = \frac{d}{4\pi z_h}. \tag{3.88}$$

This relation will be very useful in chapter 7 where we will study the Inverse Magnetic Catalysis (IMC) via dynamic holographic QCD. Surprisingly, not only the temperature, but also all the thermodynamical properties of the black hole, turn out to be the same as those of the dual gauge theory. For example, in Ref. [72] the authors have performed a simple but important calculation, namely that of the entropy density of large N $\mathcal{N} = 4$ SYM at strong coupling.

As we have mentioned previously, all the holographic description made so far, starting from QFT and getting a gravity theory, is commonly named as bottom-up approach. We will discuss briefly in the following, the origin of this approach: the AdS/CFT correspondence.

3.6 AdS/CFT correspondence

Let us first review some important aspects in the description of the duality. We start pointing out the concept of strings. Inspired in the point particle in special relativity, we can make a classical description of a relativistic string as follows. The motion of a particle in space-time describes a curve, the so-called worldline, and it can be represented by a function $x^\mu = x^\mu(\sigma)$, where σ is the worldline coordinate and it parameterizes the path of the particle. This is shown in Fig. 3.2 This

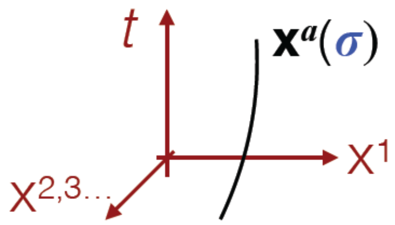

Figure 3.2: Worldline of a point particles

way, its action of the particle is proportional to the integral of the line element along the trajectory in space-time, with the coefficient being given by the mass m of the particle

$$S = -m \int ds = -m \int \sqrt{g_{ab} dx^a dx^b}. \tag{3.89}$$

Next, we consider a relativistic string, which is a one-dimensional object moving in space-time. Its motion will span a surface, the so-called worldsheet, as shown in Fig. 3.3. By analogy with the particle action (3.89), the action for the relativistic string, known as the Nambu-Goto action, is given by

$$S_{str} = -T_{str} \int d^2\sigma \sqrt{\det g_{\alpha\beta}}, \tag{3.90}$$

where T_{str} is the tension of the string, given by

$$T_{str} = \frac{1}{2\pi\alpha'} \quad , \quad \alpha' = l_s^2 \quad \text{(fundamental length scale)}, \tag{3.91}$$

and g_{ab} is the induced metric on the worldsheet defined by $g_{\alpha\beta} = \partial_\alpha x^a \partial_\beta x^b g_{ab}$.

Its important to mention that in string theories one has open and closed strings, depending on the boundary conditions. Standard methods of quantum mechanics can be used in the quantization of the strings. For the open strings case, their spectrum present a set of massless particles of spin one. For our purposes, the important fact arises when looking at the spectrum of closed strings: in general terms, the closed string spectrum contains states with a finite number of massless

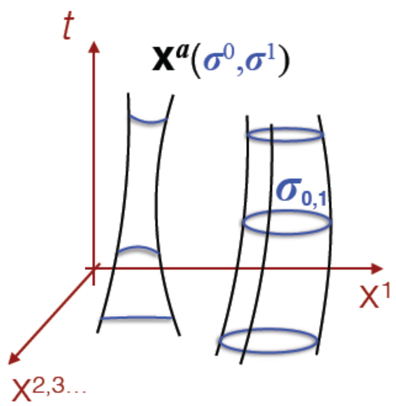

Figure 3.3: Worldsheet of a one-dimensional object (string)

modes (graviton) and an infinite tower of massive modes with masses of order $m_s = l_s^{-1} = \alpha'^{-1/2}$. Thus, at low energies $E \ll m_s$, all the possible higher order corrections come in powers of $\alpha' E^2$ from integrating out the massive string modes.

This perturbative regime of strings is tractable, but the theory also has a non-perturbative sector and it plays a crucial role in the formulation of the correspondence. In such a regime, solitonic solutions take place and change the physics of the strings. These solitonic solutions are known as Dp-branes and are extended objects in $p+1$ directions (p spatial + time), where open strings can end [73]. Also, the Dp-branes are also dynamical structures that can move and get excited. We can write an action for its dynamics, known as Dirac-Born-Infeld (DBI) action. In fact, for a single brane, the action takes the form

$$S_{DBI} = -T_{Dp} \int d^{p+1}x e^{-\Phi} \sqrt{-\det(g_{ab} + 2\pi l_s^2 F_{ab})} + \text{fermions}, \tag{3.92}$$

with T_{Dp} being the tension of the Dp-brane, which in terms of the string coupling constant g_s and the string length l_s, is given by

$$T_{Dp} = \frac{1}{(2\pi)^p g_s l_s^{p+1}}. \tag{3.93}$$

Finally, the dilation field Φ, in Eq. (3.92), is directly related to the string coupling constant as $e^\Phi \sim g_s$. Notice still that $T_{Dp} \sim g_s^{-1}$, which confirms the idea of the Dp-branes being non-perturbative objects in string theory.

In the case of a single Dp-brane, the massless spectrum which represents excitations along the brane is composed by an Abelian gauge field $A_\mu(x)$ ($\mu = 0, \ldots, p$) and a massless spectrum which represents excitations transverse to the brane is composed by $9-p$ scalar fields $\phi^i(x)$ ($i = 1, \ldots, 9-p$). Clearly, there are also all the superpartners. Therefore, in this non-perturbative sector, we have closed and open strings (which end in the Dp-brane) in a flat background. They, of course, interact with each other, as illustrated in the Fig. 3.4

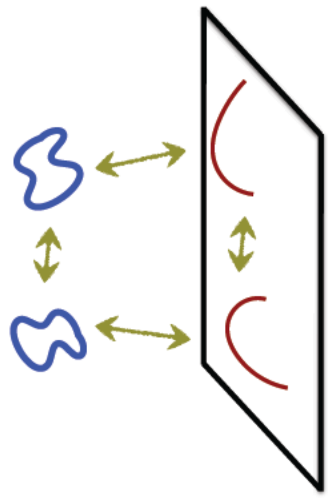

Figure 3.4: Interactions between open-open, closed-closed and open-closed strings

Now, let us move on and consider a stack of N_c Dp-branes located in 10 dimensional space-time [2]. Now, in this new context, there are now open strings stretching between different branes and in total we have $N_c \times N_c$ types of open strings, depending on which brane their endpoints lie. Those strings stretching between different branes lead to massive vector fields with masses of the order of $m \sim r/l_s$. However, when the N_c branes are coincident ($r \to 0$), all the vector fields become massless [see Fig. 3.5] and, as consequence, we get $N_c \times N_c$ massless gauge fields A^μ and $N_c \times N_c$ massless X^i scalar fields which transform in the adjoint representation of $U(N_c)$, which can be decomposed into $U(N_c) = U(1) \times SU(N_c)$. As a conclusion of this discussion, we see that a stack of N_c Dp-branes realizes an $SU(N_c)$ gauge theory in $p+1$ dimensions.

The dynamics of this full system is composed by the brane action (S_{DBI}), associated with the excitations of open strings, the bulk action (S_{bulk}), associated with the excitations closed strings, and the interaction action ($S_{int.}$), associated with the interaction between open and closed strings:

$$S = S_{DBI} + S_{bulk} + S_{int.}. \tag{3.94}$$

As all the forms of matter gravitate, and the D-branes are no exception, they can deform the space-time in which they are embedded. Using the equations of supergravity [74] we can find explicitly the metric produced by the presence of N_c Dp-branes. As we want to make connection with QCD,

[2]We use N_c to make conection with QCD latter and the branes can be named as “color” branes

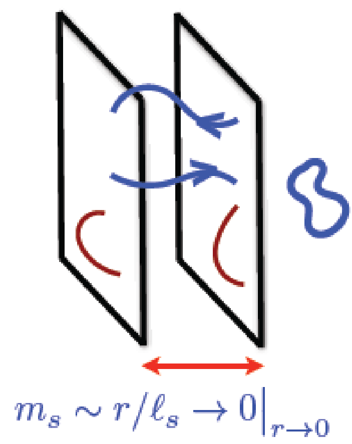

Figure 3.5: Strings stretching between two D-branes.

we set $p = 3$, and this way, the D3-branes in type IIB theory lead to Horowitz metric

$$ds^2 = H^{-1/2}(-dt^2 + dx_1^2 + dx_2^2 + dx_3^2) + H^{1/2}(dr^2 + r^2 d\Omega_5^2), \tag{3.95}$$

where t, x_1, x_2, x_3 are coordinates along the branes, and the radial coordinate $r^2 = y_1^2 + \ldots + y_6^2$, with $y_1, \ldots, y_6$, are the transverse coordinates to D3-branes. The function $H(r)$ is given by

$$H(r) = 1 + \frac{R^4}{r^4} \quad , \quad \frac{R^4}{l_s^4} = 4\pi g_s N_c. \tag{3.96}$$

An important regime is the limit of large-N_c, when the open and closed strings are decoupled from each other and are noninteracting: $S_{int.} \to 0$. But the couplings like open-open strings and closed-closed strings remain. Note that the gravitational effects of the D3-branes are controlled by the factor $g_s N_c$. In the limit $g_s N_c \ll 1$, the radius characterizing such effect becomes small in string units and, hence, the closed strings feel a space-time everywhere except very close to the hyperplane where the D3-branes are located. In this regime, a description from the closed string perspective is intractable.

On the other hand, at low energies of string theory ($l_s \to 0$), by expanding the DBI action (3.92) and keeping just the quadratic terms in F_{ab} and $\partial_a X^i$ we obtain

$$S_{DBI}^{(2)} = \int d^4x \mathrm{Tr}\Big(- \frac{1}{4\pi g_s} F_{ab}F^{ab} - \sum_i \frac{1}{2} D_a X^i D^a X^i + \pi g_s \sum_{ij} [X^i, X^j] \Big) + \mathcal{O}(l_s), \tag{3.97}$$

where, for simplicity, we have written just the bosonic part. This is precisely the $\mathcal{N} = 4$ super-Yang-Mills theory when we set

$$g_{YM}^2 = (2\pi) g_s. \tag{3.98}$$

So, its known the Yang-Mills coupling is the t'Hooft constant $\lambda = g^2_{YM} N_c$ and it controls the loop expansion of the theory. The limit considered here ($g_s N_c \ll 1$) can be reinterpreted easily as $\lambda \ll 1$. Thus, for this case, the dynamic of the system at low energies is reduced to

$$S \approx S_{SUSY} + S_{\text{IIB } string\ in\ M_{10}}. \tag{3.99}$$

In the opposite limit ($\lambda \gg 1$), the situation reverts, the open string description becomes intractable, since one would need to deal with strongly coupled open strings. So, we have closed strings moving in this curved space, Fig. 3.6

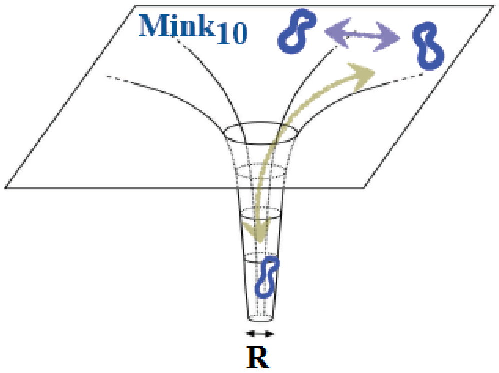

Figure 3.6: Excitations of the system in the closed string description.

As said before, the parameter R is thus understood as the length scale characteristic of the range of the gravitational effects of large N_c D3-branes. For $r \gg R$, the metric is asymptotically Minkowski where closed strings live. For $r \ll R$, in the other limit, so-called near-horizon limit $r \ll R$, the metric element (3.95) becomes

$$ds^2 = ds^2_{AdS_5} + R^2 d\Omega_5^2, \tag{3.100}$$

where the AdS$_5$ space-time is

$$ds^2_{AdS_5} = \frac{r^2}{R^2}(-dt^2 + dx_1^2 dx_2^2 + dx_3^2) + \frac{R^2}{r^2} dr^2, \tag{3.101}$$

is exactly the metric element in (3.12) of a five-dimensional Anti-de Sitter space-time written in terms of $r = R^2/z$. As final conclusion of this part, one has that in the strong gravity region the ten-dimensional metric factorizes into AdS$_5 \times S^5$, where closed strings live. Then, for this case, the dynamics of the system at low energies is reduced to

$$S \approx S_{\text{SUGRA } AdS_5 \times S^5} + S_{\text{IIB string in } M_{10}}, \tag{3.102}$$

where SUGRA means the supergravity action.

In this context, Maldacena conjectured that these two descriptions are equivalents. In the low-energy limits, such a conjecture leads to

$$\{\mathcal{N}=4\ SU(N_c)\ \text{SUSY theory}\} \approx \{S_{\text{SUGRA}\ AdS_5\times S^5}\}. \tag{3.103}$$

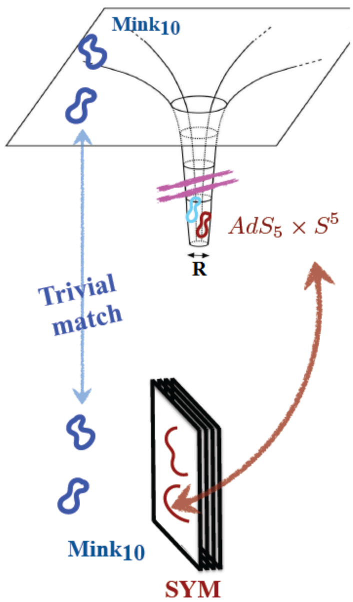

Figure 3.7: Correspondence.

We finish this section clarifying the validity limit of the duality. Firstly, remembering that Newton's constant G in ten-dimensional can be rescaled as $G \sim l_p^8$, with l_p being the Planck length and, secondly, as also the Newton's constant is defined as $16\pi G = (2\pi)^7 g_s^2 l_s^8$, we have

$$\frac{l_p^8}{R^8} \propto \frac{1}{N_c^2}, \qquad \frac{l_s^4}{R^4} \propto \frac{1}{\lambda}, \tag{3.104}$$

where we have omitted purely numerical factors. Thus, the limit considered to get the descriptions of the N_c D3 branes is read now as

$$N_c \gg 1, \quad \lambda \gg 1, \tag{3.105}$$

namely, we can neglect the quantum gravitational fluctuations and the stringy effects.

3.6.1 Adding Flavors in AdS/CFT correspondence

In the correspondence briefly presented here we have obtained an $\mathcal{N}=4$ SUSY which describes supersymmetric gluons in the adjoint representation of $SU(3)$. But, we know that QCD is not supersymmetric and it has quarks transforming in the fundamental representation of the $SU(3)$ color gauge group. In order to add matter degrees of freedom in the fundamental representation, and to prepare us to construct holographic models more closely related to QCD, we must extend the AdS/CFT correspondence. The simplest way to do this is in the limit in which the number of quark flavors is much smaller than the number of colours, i.e. when $N_f \ll N_c$. In such a case, the inclusion of N_f favors in the gauge field theory corresponds to the inclusion of N_f Dp-brane probes in the $\mathrm{AdS}_5 \times S^5$ geometry sourced by the D3-branes [75]. One of the characteristics of these flavor branes is to extend into at least one of the six extra dimensions perpendicular to the D3-branes, denoted here as $y_1, \ldots, y_6$ (3.8). This makes the flavor branes to extend in the radial direction r of AdS_5, with r defined by $r^2 = y_1^2 + \ldots + y_6^2$. Otherwise, the flavor degrees of freedom would only be present for one particular energy scale.

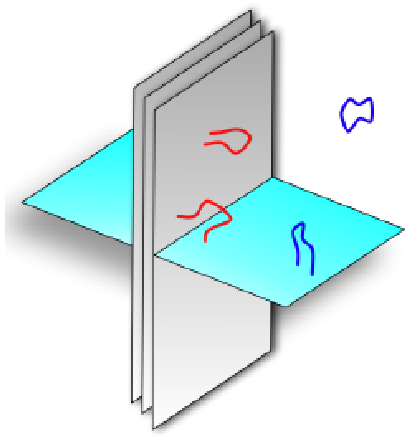

Figure 3.8: Excitations of the system in the open string description

Before closing this chapter, let us make clear an important conceptual point. It is well known that, in the 't Hooft limit ($N_c \to \infty$ with N_f fixed), all the dynamics is completely dominated by the gluons, and, therefore, the quarks can be completely ignored. One might well wonder what is the interest of introducing fundamental degrees of freedom in a large-N_c theory. A direct answer for this is to think in the large-N_c limit *a la* Veneziano limit, in which N_f/N_c is kept small but still finite [3]. So, from QFT side, any observable can be expanded in powers of $1/N_c^2$ and N_f/N_c and this limit is rigorously obtained from the dual description in terms of N_f Dp-branes probes in $\mathrm{AdS}_5 \times S^5$. The leading order contribution of Dp-brane will give us the leading order contribution

[3]Note that, the Veneziano limit is richer than the 't Hooft limit, since setting $N_f = 0$ one recovers the 't Hooft limit.

of the fundamental matter, of relative order N_f/N_c.

So far, we do not have specified the value of p yet and neither the precise nature of the flavor degrees of freedom in the gauge theory. Since we wish to consider stable Dp-branes in type IIB string theory, we must set $p = 1, 3, 7, ...$, otherwise, the solutions are unstable. In chapter 7, we will focus in the $D3/D7$ configuration and studying their consequences.

4 The Holographic QCD model

Holographic QCD aims to study the strongly coupled regime of QCD using AdS/CFT (or more generally the gauge/gravity correspondence) to get an analytical model for the structure of hadrons and their interactions [76, 77]. Before specifying the model relevant for this thesis, we will explain shortly how the gauge/gravity duality can be applied to QCD.

In the previous chapter, we have considered N_c D3-branes that are piled up on top of each other. As we have discussed, there are $N_c \times N_c$ species of open strings that provide massless excitations and, in this way, piled-up D3-branes can support non-Abelian $SU(N_c)$ gauge theories. From the QCD point of view, this part can build the gluon part of QCD. After this, we have introduced a different kind of Dp-brane, which is put perpendicular to the original piled-up D3-brane, then there appears a new kind of open string that bridges the original piled-up N_c Dp-brane and the new Dp-brane. As mentioned, that open strings led to massive fermions in the fundamental representation of $SU(N_c)$ gauge group. Therefore, we can think of this as the quark degrees of freedom, as quarks are in the fundamental representation of the gluon gauge group. This is the essential point of holographic QCD.

We also have discussed another point of view of the brane configurations: we replace the piled-up N_c D3-branes by a background ten-dimensional curved geometry. This provides the AdS geometry, which corresponds to a strong coupling limit ($\lambda \gg 1$) of the gluonic theory. Therefore, a N_f probe flavor Dp-brane in this AdS geometry corresponds to a gluonic theory with N_f flavor quarks. This is the big hope of holography: a complicated strongly coupled theory of gluons and a quark, which is mapped into a rather simple flavor Dp-brane theory in AdS geometry. This is holographic QCD. Many different models of holographic QCD can be constructed, describing different theories corresponding to different physical situations/processes, depending of the type, number and configuration of D-branes.

Recall that, we have discussed that the correspondence is valid in the two limits, namely large N_c and large λ, when we can approximate string theory as a gravity theory. Clearly, these limits led to some crucial differences between holographic QCD and true QCD/nuclear physics. In fact, in QCD we have $N_c = 3$ while in holographic QCD any quantities are computed at the leading order of the $1/N_c$ expansion at $N_c = \infty$. This led us to conclude that the holographic methods to describe QCD are better reliable in quantities which are independent on the values of N_c. Besides, we highlight that, depending on the physical quantities of interest, one can choose a specific holographic model among many. In general terms, holographic QCD models can be constructed via two approaches:

- **Top down approach**: In this approach, we start choosing an adequate configuration of Dp-brane in order to get as close as possible to realistic QCD. A very well known one is the D3/D7 model [78], where the quark flavors are included by N_f D7 branes. This model has been very useful in the understanding of the correspondence, once the simplicity of the metric makes it possible to obtain many results analytically. Another important setup has been obtained using a background sourced by D4-brane and by introducing a flavor D6-brane. It exhibits an interesting phase diagram, but unfortunately it is unable to contain chiral fermions [79]. But, undoubtly, the most closely related to QCD is the famous Sakai-Sugimoto [80, 81] holographic QCD model, where they introduced the Yang-Mills fields via massless open string fluctuations of a stack of N_c D4 branes, the flavor fields through fermionic open string fluctuations between D4 branes, and a pair of N_f D8-branes and $\bar{D}$8-branes. This model is nonsupersymmetric and describes $SU(N_c)$ Yang-Mills theory and gives a geometrical point of view about chiral symmetry breaking.

- **Bottom-Up approach**: In this approach, an holographic QCD model is built by looking at the phenomenology of hadrons in QCD. One identifies the relevant operators to describe the physics we are interested in and they act as fields in the geometry that, in turn, is modified to reproduce hadron phenomenology [7, 8]. The Kaluza-Klien modes of five dimensional fields with quantum numbers of QCD states are identified with the hadronic resonances. In chapter 2, we mentioned that there are two emergent phenomena in nonperturbative QCD: the dynamical chiral symmetry breaking and color confinement. A good Bottom-Up Holographic QCD model should take into account both phenomena. This approach will be followed in this thesis and all these details will be clear.

In section 4.2 we discuss briefly the criterium that the background should satisfy in order to be confining. In section 4.3 we present a five dimensional action and discuss how dynamical chiral symmetry breaking (DCSB) is implemented in the model. We also study the vacuum structure of the model and show how a chiral condensate is identified, as well as, the bare quark mass. As will be discussed, they are input parameters in this model. We also make explicit some algebraic manipulations in the expansion of the action up to third order in the fields and some definitions. In section 4.4 we focus on the action to second order in the fields and investigate its properties. Using the holographic dictionary, we find the holographic currents and discuss their conservation. We use the Kaluza-Klein (KK) expansion to find the 4d off-shell action and this process will led to normalization conditions and equations of motion for the normalized modes of the fields. We also use the KK expansion to find a holographic prescription for the decay constant for mesons. Finally, in section 4.5, we investigate the action in third order in the fields manipulating it in order to find a convenient form to use the KK expansion. We use symmetry properties to find correct couplings that will be useful for the hadronic process in the subsequent chapter.

4.1 Bottom-Up approach

As we have seen, the bottom-up approach aims to construct a five dimensional action based in the mapping of the operators in QCD into fields living in the five dimension space-time. In this sense, the gluon sector is mapped into to fluctuations of space-time and the flavor sector is mapped into to fields living in this background. The backreaction simulates the interaction of quarks and gluons. This is illustrated in the Fig. 4.1.

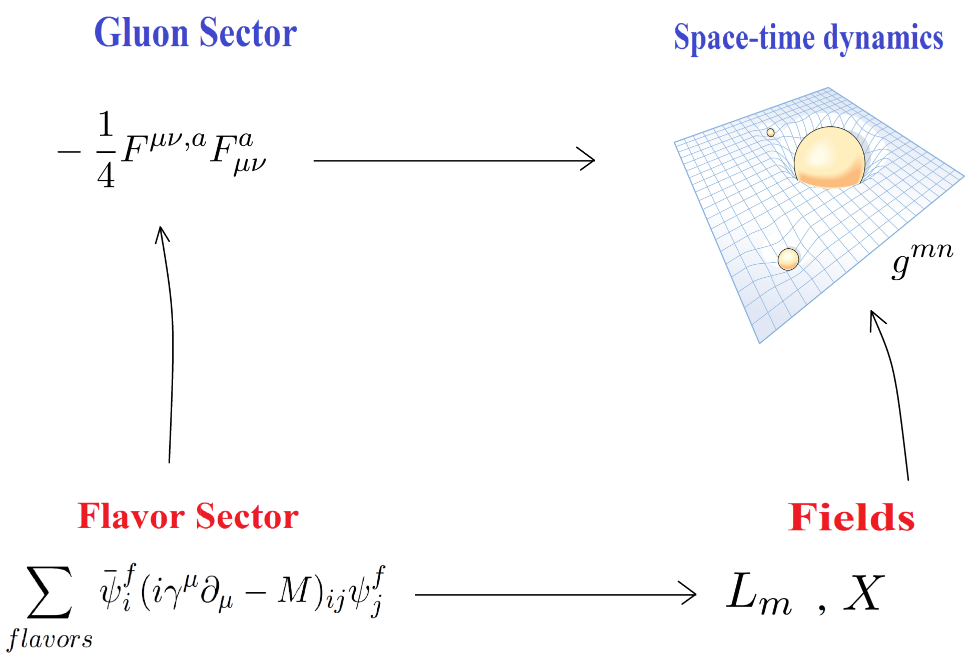

Figure 4.1: Representation of the duality

The full five dimensional action that describes the system is written as

$$S = S_g + \frac{N_f}{N_c} S_f, \tag{4.1}$$

where S_g is the gravity action that describes the gluon dynamics and S_f is the action that describes the flavor dynamics.

Using the holographic dictionary conjecture, the operators of the gluon sector are given as follows

$$\begin{array}{llll} 4D : \mathcal{O}(x^\mu) & & 5D : \phi(x^\mu, z) & \\ T^{\mu\nu} & \to & g^{mn}(x,z) & \langle T^\mu_\mu \rangle = \dfrac{\beta(g_s)}{2g_s} \mathrm{Tr} F^2 \\ \mathrm{Tr}F^2 & \to & \Phi(x,z) & \end{array}$$

This way, the action for pure gluon sector, known as dilaton-gravity action, is

$$S_g = \frac{1}{16\pi G_5} \int d^5x \sqrt{|g|} e^{-2\Phi} (R + 4\partial_M \Phi \partial^M \Phi - V(\Phi)),$$

where the Φ is the dilaton field. The action for the flavor sector S_f will be explored in section 4.3.

In the limit $N_f/N_c \ll 1$, there is no backreaction of the flavor action under background and, this way, the dynamic of the two actions are decoupled.

The general metric in five dimensions can be written as

$$ds^2 = G_{00}(z)dt^2 + G_{\vec{x}\vec{x}}(z)d\vec{x}^2 + G_{zz}(z)dz^2, \tag{4.2}$$

where the coefficients G_{00}, $G_{\vec{x}\vec{x}}(z)$ and $G_{zz}(z)$ are determined by solving the dilaton-gravity equation. A specific case occurs when $\Phi = 0$. In this case, the solution is the AdS$_5$ space-time, whose metric element is

$$ds^2 = \frac{L^2}{z^2}(dt^2 - d\vec{x}^2 - dz^2), \quad V(\Phi) = -\frac{12}{L^2},$$

where $0 < z < \infty$. Now, we will show that the background must satisfy a criterium to be confining.

4.2 Holographic description of quark-antiquark potential

In chapter 2, we have introduced the Wilson loop and discussed its relation to the potential between a quark and an antiquark. As we saw, it is a excellent quantity to investigate confinement in pure-gauge QCD. Holographically, the Wilson loop can be represented by a string moving in AdS space-time. Following the standard gauge/gravity prescription in a strongly coupled theory, that has a gravity dual, the vacuum expectation value of a static Wilson loop $W(C)$ is represented by the generating functional Z_{str} of a static string moving in the bulk of the dual space [82]. In a semi-classical gravity approximation we have that

$$\langle W(C)\rangle = Z_{str} \sim e^{-S_{str}}, \quad g_s \to 0,\ \lambda \to \infty, \tag{4.3}$$

where S_{str} is the classical Nambu-Goto action, given in (3.90), that we rewrite as

$$S_{str} = \frac{1}{2\pi\alpha'} \int d\sigma d\tau \sqrt{G_{\mu\nu}\partial_a X^\mu \partial_b X^\nu}. \tag{4.4}$$

By comparing the holographic prescription (4.3) with the usual definition for the Wilson loop in terms of the quark anti-quark potential, given in (2.73), we have that

$$V_{\bar{q}q} = \lim_{T\to\infty} \frac{S_{str}}{T}. \tag{4.5}$$

A detailed and systematic analysis of static strings described by Wilson loops was presented in [83]. The authors assumed a following general form for the metric

$$ds^2 = G_{00}(z)dt^2 + G_{\vec{x}\vec{x}}(z)d\vec{x}^2 + G_{zz}(z)dz^2, \tag{4.6}$$

where $\vec{x}$ denotes the usual spatial boundary coordinates while z is the radial direction. Choosing the world sheet coordinates $\sigma = x$ and $\sigma = t$ and assuming translation invariance along t, the string action with endpoints fixed at $x = \pm L/2$ reduces to the form

$$S_{str} = \frac{T}{2\pi\alpha'} \int_{-L/2}^{L/2} dx \sqrt{M(z(x))(z(x))^2 + V(z(x))}, \tag{4.7}$$

where we have defined

$$M(z) = G_{00}G_{zz}, \quad V(z) = G_{00}G_{\vec{x}\vec{x}}. \tag{4.8}$$

The profile $z(x)$ of the string can be determined by considering expression (4.7) as representing an “action integral” for the evolution in coordinate x. Its corresponding Lagrangian density is

$$\mathcal{L}(z, z') = \frac{1}{2\pi\alpha'} \sqrt{M(z)z'^2 + V(z)}, \tag{4.9}$$

from which, the conjugate momentum is

$$p = \frac{\partial \mathcal{L}}{\partial z'} = \frac{1}{2\pi\alpha'} \frac{M(z)z'}{\sqrt{M(z)z'^2 + V(z)}}. \tag{4.10}$$

Therefore, the Hamiltonian density is given by

$$\mathcal{H}(z, p) = pz' - \mathcal{L}(z, z'(z, p)) = -\frac{1}{2\pi\alpha'} \frac{V(z)}{\sqrt{M(z)z'^2 + V(z)}} = -\frac{1}{(2\pi\alpha')^2} \frac{V(z)}{\mathcal{L}}. \tag{4.11}$$

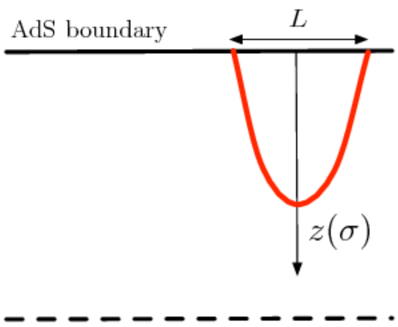

Figure 4.2: Representation of a string moving in AdS space-time and connecting a quark and an antiquark.

Note that, for evolution in x, this quantity is a constant of motion and it can be conveniently evaluated at the maximum value of coordinate z: $z_* = z(0)$ with $z'(0) = 0$. This leads to

$$\mathcal{H}(z,0) = -\frac{1}{2\pi\alpha'}V(z_*), \tag{4.12}$$

that is also valid for $\mathcal{H}(z,p)$, once it is a constant of motion. It is then straightforward to express the Lagrangian density as

$$\mathcal{L} = \frac{V(z)}{2\pi\alpha'\sqrt{V(z_*)}}, \tag{4.13}$$

and then to obtain the differential equation for the string profile

$$\frac{dz}{dx} = \pm\frac{\sqrt{V(z)}}{\sqrt{M(z)}}\frac{\sqrt{V(z)-V(z_*)}}{\sqrt{V(z_*)}}. \tag{4.14}$$

In this way, using the expression for the Lagrangian in (4.13) and (4.14), the string action (4.7) is written as

$$S_{str} = \frac{T}{\pi\alpha'}\int_0^{z_*} dz \frac{\sqrt{M(z)}}{\sqrt{V(z)}}\frac{V(z)}{\sqrt{V(z)-V(z_*)}}. \tag{4.15}$$

Now, we are able to compare this result, obtained from a holographic perspective, with the usual definition for the quark-antiquark potential in (2.73). So, using (4.5), we obtain

$$V_{\bar{q}q} = \frac{1}{\pi\alpha'}\int_0^{z_*} dz \frac{\sqrt{M(z)}}{\sqrt{V(z)}}\frac{V(z)}{\sqrt{V(z)-V(z_*)}}. \tag{4.16}$$

We can still express this potential in terms of the distance between the quark and antiquark. In fact, the distance L can be written as

$$L = \int dx = \int \left(\frac{dz}{dx}\right)^{-1} dz = 2\int \frac{\sqrt{M(z)}}{\sqrt{V(z)}}\frac{\sqrt{V(z_*)}}{\sqrt{V(z)-V(z_*)}}, \tag{4.17}$$

and we rewrite the quark-antiquark potential (4.16) as

$$V_{\bar{q}q} = \frac{\sqrt{V(z_*)}}{2\pi\alpha'}L + \frac{1}{\pi\alpha'}\int_0^{z_*} dz \frac{\sqrt{M(z)}}{\sqrt{V(z)}} \frac{V(z) - V(z_*)}{\sqrt{V(z) - V(z_*)}}. \tag{4.18}$$

As observed by the authors in [83], in general, this expression is singular, but it can be regularized by the subtraction of the quark masses, given as

$$m_q = \frac{1}{2\pi\alpha'}\int_0^{\infty} dz \sqrt{M(z)}. \tag{4.19}$$

Then, the regularized quark anti-quark potential, $V_{\bar{q}q}^{reg} = V_{\bar{q}q} - m_q$ is

$$V_{\bar{q}q}^{reg} = \frac{\sqrt{V(z_*)}}{2\pi\alpha'}L + \frac{1}{\pi\alpha'}\int_0^{z_*} dz \frac{\sqrt{M(z)}}{\sqrt{V(z)}} \frac{V(z) - V(z_*)}{\sqrt{V(z) - V(z_*)}} - \frac{1}{2\pi\alpha'}\int_0^{\infty} dz \sqrt{M(z)}. \tag{4.20}$$

The above expression has an interesting form because the first term shows an explicit linear dependence in the quark-antiquark distance, L. It might still there be an implicit L dependence in the second and third terms given above.

In order to simplify our expressions and to make easier our discussion, let us rewrite the second and third terms in (4.20) as

$$K(z_*) = \frac{1}{\pi\alpha'}\int_0^{z_*} dz \frac{\sqrt{M(z)}}{\sqrt{V(z)}} \frac{V(z) - V(z_*)}{\sqrt{V(z) - V(z_*)}} - \frac{1}{2\pi\alpha'}\int_0^{\infty} dz \sqrt{M(z)}. \tag{4.21}$$

Again, the authors [83] have discussed in details the behavior of the function $V_{\bar{q}q}^{reg}$ using the coordinate $s = z^{-1}$, instead of z. They have concluded that if $V(s)$ has a minimum, or $M(s)$ diverges at $s = s_*$, $z = z_*$ (in our case), *linear confinement* occurs if and only if $V(s_*) > 0$, and the corresponding string tension is $V(s_*)$. They also have proved that, in the confining case, the correction with the linear potential, the $K(s_*)$ function, is either a negative power of the separation, or exponentially small. And when there is no confinement, the potential found is asymptotically a negative power of the separation, L.

Note that, all information about confinement involves the background metric. For example, in the pure AdS_5 case, the metric elements are $G_{00}(s) = G_{\vec{x}\vec{x}}(s) = s^2$ and $G_{ss}(s) = s^{-2}$. Therefore, we obtain the following functions

$$M(s) = G_{00}G_{uu} = 1, \quad V(s) = G_{00}G_{\vec{x}\vec{x}} = s^4. \tag{4.22}$$

It is obvious that the $V(s)$ function has a minimum at $s_* = 0$ and this leads to $V(s_*) = 0$. So, the linear term in (4.16) vanishes, revealing that the pure AdS_5 is non confining. The same authors in [83] have found the sub-leading terms and showed that they behaves like

$$V_{\bar{q}q}^{reg} \sim L^{-1} + \mathcal{O}(L^{-7/4}). \tag{4.23}$$

The simplest way to obtain a confining background is to cut off the background at a value $s_* = s_0$, so that, the minimum is now at $s = s_0$, and we have $V(s_0) > 0$. This ensures that the linear term in (4.20) is non zero and makes the background confining.

Returning to the z coordinate, we just conclude that the cut-off is $z = z_0$, and the metric element becomes

$$ds^2 = \frac{1}{z^2}(dz^2 + dt^2 + d\vec{x}^2), \qquad 0 < z < z_0. \tag{4.24}$$

This approach to obtain the confinement is commonly known as Hard Wall approach. In the next chapters, we will consider this background.

4.3 DCSB implementation in holographic QCD

DCSB was first implemented in holographic QCD in Refs. [7, 8]. Here we will follow the conventions and notation of Ref. [7]. We start pointing out that the holographic dictionary maps each 4d field theory operator $\mathcal{O}(x)$ to a 5d field $\phi(x,z)$ living in the AdS$_5$ space. In the case of QCD, the relevant operators for describing DCSB are the left and right handed currents $J^a_{L\mu} = \bar{q}_L\gamma_\mu t^a q_L$, $J^a_{R\mu} = \bar{q}_R\gamma_\mu t^a q_R$, corresponding to the $SU(N_f)_L \times SU(N_f)_R$ chiral flavor symmetry and the quark bilinear operator $\bar{q}_R q_L$ is related to DCSB. In the gravitational side, these 4d operators will correspond to 5d gauge fields $L^a_m(x,z)$, $R^a_m(x,z)$ and a 5d bifundamental scalar field $X(x,z)$, both living in a AdS$_5$ slice described by Eq. (4.24). Its worth to mention that, there is an infinite amount of operators in QCD and, hence, also an infinite number of bulk fields in the AdS$_5$ space. The most relevant ones for the purposes in this thesis in the meson sector are those three introduced above. So, we will neglect all other fields.

The authors in [4, 5] have found that the mass of a p-form in 5d AdS space-time is related to the dimension Δ of the dual 4d operator via the relation $m^2 = (\Delta - p)(\Delta + p - 4)$. In this way, we have that the gauge fields $L^a_m(x,z)$, $R^a_m(x,z)$ are massless, whereas the scalar field $X(x,z)$ has dimension of negative mass squared $m^2 = -3$. These facts are summarized in Table (4.1).

Based on these facts, the authors in [7] have proposed a 5d action to describe the chiral properties of meson and their interactions. It can be written as

$$S = \int d^5x\sqrt{|g|}\,\mathrm{Tr}\Big[(D^m X)^\dagger (D_m X) + 3|X|^2 - \frac{1}{4g_5^2}\left(L^{mn}L_{mn} + R^{mn}R_{mn}\right)\Big], \tag{4.25}$$

where have been defined

$$D_m X = \partial_m X - iL_m X + iXR_m, \quad L_{mn} = \partial_m L_n - \partial_n L_m - i\left[L_m, L_n\right], \tag{4.26}$$

4D: $\mathcal{O}(x^\mu)$	5D: $\phi(x^\mu, z)$	p	Δ	m^2
$\bar{q}_L \gamma_\mu t^a q_L$	$L^a_m(x,z)$	1	3	0
$\bar{q}_R \gamma_\mu t^a q_R$	$R^a_m(x,z)$	1	3	0
$\bar{q}_R q_L$	$\frac{2}{z} X(x,z)$	0	3	-3

Table 4.1: 4d-5d correspondence and masses of bulk fields.

$$R_{mn} = \partial_m R_n - \partial_n R_m - i\left[R_m, R_n\right]. \tag{4.27}$$

The action (4.25) includes the N_f gauge fields L_m and R_m, corresponding to the left and right-handed flavor currents $J^a_{L,\mu}$ and $J^a_{R,\mu}$ in QCD, and the bifundamental scalar X, dual to the quark bilinear operator $\bar{q}_R q_L$, and all the dynamics of the 5-d fields L_m, R_m and X is described by this action.

In a chiral world, i.e. if all quark masses are zero, the action (4.25) has $SU(N_f)_L \times SU(N_f)_R$ chiral symmetry, i.e. it is invariant under

$$X \to X' = U_L X U_R^\dagger \tag{4.28}$$

as well as

$$L_m \to L'_m = U_L L_m U_L^\dagger + i(\partial_m U_L)U_L^\dagger, \quad R_m \to R'_m = U_R R_m U_R^\dagger + i(\partial_m U_R)U_R^\dagger \tag{4.29}$$

where $U_L, U_R \in SU(N_f)_L, SU(N_f)_R$. However, since quarks have masses to begin with, the chiral symmetry is only an approximate one, thus giving the pseudoscalar mesons a mass, which are then referred to as pseudo-Goldstone bosons, as the pions and kaons.

4.3.1 Vacuum Structure of the Model

The vacuum structure of the model is found turning off all the L_m, R_m and π, remaining only the field X_0. Thus, the action (4.25) becomes

$$S = \int d^5x \sqrt{|g|}\, \mathrm{Tr}\left[\partial^z X_0 \partial_z X_0 + 3X_0^2\right] = \int d^5x \frac{1}{z^5}\, \mathrm{Tr}\left[-z^2(\partial_z X_0)^2 + 3X_0^2\right]. \tag{4.30}$$

We use the trace property for the bilinear operator

$$\mathrm{Tr}(A^\dagger A) = \sum_{i=1}^{N_f} \sum_{j=1}^{N_f} |a_{ij}|^2, \tag{4.31}$$

so that the action (4.30) can be written as

$$S = \sum_{i,j=1}^{N_f} \int d^5x \left(-\frac{1}{z^3}(\partial_z X_{0ij})^2 + 3\frac{1}{z^5} X_{0ij}^2 \right). \tag{4.32}$$

Taking the variation of S with respect to X_{0ij} and remembering that the individual components X_{0ij} are independent, we have

$$\partial_z \left(\frac{1}{z^3} \partial_z X_{0ij} \right) + 3\frac{1}{z^5} X_{0ij} = 0. \tag{4.33}$$

The general solution to this homogeneous linear second order ordinary differential equation is given by the polynomial equation

$$v_{ij}(z) = 2X_{0ij} = A_{ij}z + B_{ij}z^3. \tag{4.34}$$

Comparing this solution with that of a scalar field in AdS space-time, given in (3.59), and remembering that the boundary has $d = 4$, we conclude that the operator dimension should be $\Delta = 3$. Then, the A_{ij} corresponds to a source with dimension 1 and B_{ij} to its correspondent vacuum expectation value with dimension 3. Since X_0 is dual to the operator $\bar{q}_R q_L$, the coefficients A_{ij} have the interpretation of the quark mass M_{ij}, responsible for the explicit breaking of chiral symmetry and B_{ij} the correspondent VEV, that also can be obtained by

$$\Sigma_{ij} = -\frac{d \ln Z_{QFT}}{dM_{ij}} = \frac{dS}{dM_{ij}}, \tag{4.35}$$

with the interpretation of being the chiral condensate, which is responsible for the dynamical chiral symmetry breaking, and it is the natural chiral order parameter [8]

Note that, the hard wall AdS/QCD model presented here shows that the chiral condensate is exactly the coefficient B_{ij}, i.e, $\Sigma_{ij} = B_{ij}$. In other words, the model proposed is unable to give an chiral condensate as function of the quark mass, as expected from QCD. Because of this, we will treat the chiral condensate, as well as the quark mass, as input parameter. Then, one gets

$$v_{ij}(z) = M_{ij}z + \Sigma_{ij}z^3, \tag{4.36}$$

A particular normalization scheme for the scalar VEV is implemented in [84]. The normalization scheme arises from the fact that when coupling an operator $\mathcal{O}$ to a source ϕ^0 one always has the freedom to redefine $\mathcal{O} \to \zeta\mathcal{O}$ and $\phi^0 \to \phi^0/\zeta$, keeping the coupling term $\mathcal{O}\phi^0$ unchanged. In the case of $v(z)$, we have

$$v_{ij}(z) = \zeta M_{ij}z + \frac{1}{\zeta}\Sigma_{ij}z^3. \tag{4.37}$$

The authors fixed the rescaling parameter ζ[1] by matching the two-point correlation function of the scalar field between the QCD result at large Euclidean momentum, k^2, and that calculated from the gravity dual, obtaining

$$\zeta = \frac{\sqrt{N_c}}{2\pi}. \tag{4.38}$$

We have discussed in the introduction of this chapter that QCD holographic is valid in the limit $N_c \to \infty$. Here we will consider, as an approximation, the following value for number of colors $N_c = 3$, which is true for QCD.

4.3.2 The Flutuations around the vacuum

To investigate the consequences of DCSB on meson properties, we consider perturbations around the background fields in Eq. (4.37). First of all, it is convenient to rewrite the fluctuations gauge invariants, L_m and R_m in terms of vector and axial vector fields, as follows

$$L_m = V_m + A_m, \quad R_m = V_m - A_m. \tag{4.39}$$

With this, the last two terms in the action (4.25) are rewritten as

$$\mathrm{Tr}\left(L^{mn}L_{mn} + R^{mn}R_{mn}\right) = 2\mathrm{Tr}\left(V^{mn}V_{mn} + A^{mn}A_{mn}\right), \tag{4.40}$$

where we have defined

$$V_{mn} = v_{mn} - i\left([V_m, V_n] + [A_m, A_n]\right), \quad A_{mn} = a_{mn} - i\left([V_m, A_n] + [A_m, V_n]\right), \tag{4.41}$$

$$v_{mn} = \partial_m V_n - \partial_n V_m, \quad a_{mn} = \partial_m A_n - \partial_n A_m\,. \tag{4.42}$$

Next, we expand the action up to third order in the gauge fields, since we are interested in the mesonic spectrum, described by the second order terms, and also in the three meson vertices, studied in the next chapter, when the third order terms are relevant. The expansion is straightforward and we obtain

$$\begin{aligned}\mathrm{Tr}\left(L^{mn}L_{mn} + R^{mn}R_{mn}\right) &= v_a^{mn}v_{mn}^a + a_a^{mn}a_{mn}^a \\ &+ 2f^{abc}\Big[v_a^{mn}\left(V_m^b V_n^c + A_m^b A_n^c\right) + a_a^{mn}\left(V_m^b A_n^c + A_m^b V_n^c\right)\Big] \\ &+ \mathcal{O}(V^4, V^2A^2, A^4),\end{aligned} \tag{4.43}$$

[1] The scaling parameter will ensure that the values of M_{ij} and Σ_{ij} correspond to quark masses and condensates in QCD.

where the structure constants f^{abc} of the Lie algebra of the $SU(N_f)$ group are defined in (2.4). On the other hand, the covariant derivative $D_m X$, defined in (4.26), can be rewritten as

$$D_m X = \partial_m X - i[V_m, X] - i\{A_m, X\} = \tilde{D}_m X - i\{A_m, X\}\,. \tag{4.44}$$

A nice property of this way of writing the covariant derivative is that the operator $\tilde{D}_m O$ does not change the hermiticity of O whereas $-i\{A_m, O\}$ inverts it. This property is useful because it will help us to eliminate many terms and make our calculations shorter.

The bifundamental field X is decomposed into the real part X_0 and a pseudoscalar fluctuation π in the following form [9]:

$$X = e^{i\pi} X_0\, e^{i\pi}. \tag{4.45}$$

The expansion of X in powers of π takes the form

$$X = X_0 + i\{\pi, X_0\} - \frac{1}{2}\{\pi, \{\pi, X_0\}\} - \frac{i}{6}\{\pi, \{\pi, \{\pi, X_0\}\}\} + \mathcal{O}(\pi^4)\,. \tag{4.46}$$

Interestingly, the even (odd) terms of the expansion are hermitian (anti-hermitian). Then it is convenient, for our calculations, to decompose X into hermitian and anti-hermitian parts : $X = X_H + X_A$, where X_H and X_A have the following expansions

$$\begin{aligned} X_H &= X_0 - \frac{1}{2}\{\pi, \{\pi, X_0\}\} + \mathcal{O}(\pi^4)\,, \\ X_A &= i\{\pi, X_0\} - \frac{i}{6}\{\pi, \{\pi, \{\pi, X_0\}\}\} + \mathcal{O}(\pi^5)\,. \end{aligned} \tag{4.47}$$

In the same way, the covariant derivative $D_m X$ can also be decomposed into hermitian and anti-hermitian parts

$$D_m X = (D_m X)_H + (D_m X)_A\,, \tag{4.48}$$

where we used the following definition

$$(D_m X)_H = \tilde{D}_m X_H - i\{A_m, X_A\}, \quad (D_m X)_A = \tilde{D}_m X_A - i\{A_m, X_H\}\,. \tag{4.49}$$

Using this decomposition we can rewrite the first term in (4.25) as

$$\begin{aligned} \mathrm{Tr}\Big[(D^m X)^\dagger (D_m X)\Big] &= \mathrm{Tr}\Big[(D^m X)^H (D_m X)_H - (D^m X)^A (D_m X)_A\Big] \\ &= \mathrm{Tr}\Big[(\tilde{D}^m X_H)(\tilde{D}_m X_H) - (\tilde{D}^m X_A)(\tilde{D}_m X_A) + 2i\{A^m, X_H\}(\tilde{D}_m X_A) \\ &- 2i\{A^m, X_A\}(\tilde{D}_m X_H) + \{A^m, X_H\}\{A_m, X_H\} \\ &- \{A^m, X_A\}\{A_m, X_A\}\Big]\,, \end{aligned} \tag{4.50}$$

where we have used the properties of hermiticity of the operator $\tilde{D}_m$. Expanding up to quartic order in π and A_m, we find (see Appendix 9 for more details about the calculation)

$$\begin{aligned}
\mathrm{Tr}\Big[(D^m X)^\dagger (D_m X)\Big] &= \mathrm{Tr}\Big[\tilde{D}^m X_0 \tilde{D}_m X_0 + \{\tilde{D}^m \pi, X_0\}\{\tilde{D}_m \pi, X_0\} + [\tilde{D}^m \pi, \pi][\tilde{D}_m X_0, X_0] \\
&- 2\{A^m, X_0\}\{\tilde{D}_m \pi, X_0\} - 2[A^m, \pi][\tilde{D}_m X_0, X_0] + \{A^m, X_0\}\{A_m, X_0\}\Big] \\
&+ \mathcal{O}(\pi^4) + \mathcal{O}(A\pi^3) + \mathcal{O}(A^2\pi^2), \qquad (4.51)
\end{aligned}$$

where we have used the following trace identity

$$\mathrm{Tr}(\{A, B\}\{C, D\}) = \mathrm{Tr}(\{B, C\}\{A, D\}) - \mathrm{Tr}([A, C], [B, D])\,. \qquad (4.52)$$

Reorganizing the terms in (4.51), we obtain

$$\begin{aligned}
\mathrm{Tr}\Big[(D^m X)^\dagger (D_m X)\Big] &= \mathrm{Tr}\Big[\tilde{D}^m X_0 \tilde{D}_m X_0 + \{\tilde{D}^m \pi - A^m, X_0\}\{\tilde{D}_m \pi - A_m, X_0\} \\
&+ [\tilde{D}_m X_0, X_0][\tilde{D}^m \pi - 2A^m, \pi]\Big] + \mathcal{O}(\pi^4, A\pi^3, A^2\pi^2). \qquad (4.53)
\end{aligned}$$

Now, using the definition of $\tilde{D}_m$ given in (4.44) and the property $[\partial_m X_0, X_0] = 0$, arising from the fact that X_0 is diagonal, we have

$$\begin{aligned}
\mathrm{Tr}\Big[(D^m X)^\dagger (D_m X)\Big] &= \mathrm{Tr}\Big[\partial^m X_0 \partial_m X_0 - [V^m, X_0][V_m, X_0] + \{\partial^m \pi - A^m, X_0\}\{\partial_m \pi - A_m, X_0\} \\
&- 2i\{[V^m, \pi], X_0\}\{\partial_m \pi - A_m, X_0\} - i[[V_m, X_0], X_0][\partial^m \pi - 2A^m, \pi]\Big] \\
&+ \mathcal{O}(\pi^4, A\pi^3, A^2\pi^2, V^2\pi^2)\,. \qquad (4.54)
\end{aligned}$$

In the above expression, we just kept terms up to the third order, relevant for this thesis. Expanding the fields in terms of the $SU(N_f)$ generators T^a and remembering that X_0 is diagonal ($X_0^i\,\delta^{ij}$ with $i = (1, .., N_f)$) we can write the first and second terms in the action (4.25) as

$$\begin{aligned}
\mathrm{Tr}\Big[(D^m X)^\dagger (D_m X) + 3|X|^2\Big] &= (\partial^m X_0^i)\,(\partial_m X_0^i) + 3X_0^i X_0^i + \frac{(M_V^a)^2}{2} V_a^m V_m^a \\
&+ \frac{M_A^{ab}}{2}(\partial^m \pi^a - A^{m,a})(\partial_m \pi_b - A_{m,b}) \\
&+ M_A^{ae} f^{ebc}\,(\partial_m \pi^a - A_m^a) V^{m,b} \pi^c \\
&- \frac{(M_V^b)^2}{2} f^{abc}\,(\partial_m \pi^a - 2A_m^a) V^{m,b} \pi^c \\
&+ \mathcal{O}(\pi^4, A\pi^3, A^2\pi^2, V^2\pi^2)\,, \qquad (4.55)
\end{aligned}$$

where M_V^a and M_A^{ab} are defined by the traces

$$\mathrm{Tr}([T^a, X_0][T^b, X_0]) = -\frac{(M_V^a)^2}{2}\delta^{ab}, \quad \mathrm{Tr}(\{T^a, X_0\}\{T^b, X_0\}) = \frac{M_A^{ab}}{2}\,. \qquad (4.56)$$

We highlight that the authors in [9] used a different definition to express these cubic terms; they used the following quantities

$$g^{abc} = -2i\mathrm{Tr}(\{T^a, X_0\}[T^b, \{T^c, X_0\}]), \quad h^{abc} = -2i\mathrm{Tr}([T^b, X_0]\{T^a, \{T^c, X_0\}\})\,. \qquad (4.57)$$

These are related to our terms through of the identities

$$g^{abc} - h^{cba} = M_A^{ae} f^{ebc}, \quad h^{abc} - h^{cba} = (M_V^b)^2 f^{abc} \,. \tag{4.58}$$

Now, collecting the results from (4.43) and (4.55), the original action (4.25), up to the third order, takes the following form

$$S = S_0 + S_2 + S_3 + \ldots \,, \tag{4.59}$$

where

$$\begin{aligned} S_2 &= \int d^5x \sqrt{|g|} \Big\{ -\frac{1}{4g_5^2} v_a^{mn} v_{mn}^a + \frac{(M_V^a)^2}{2} V_a^m V_m^a - \frac{1}{4g_5^2} a_a^{mn} a_{mn}^a \\ &+ \frac{M_A^{ab}}{2} (\partial^m \pi^a - A^{m,a})(\partial_m \pi_b - A_{m,b}) \Big\} \,, \end{aligned} \tag{4.60}$$

$$\begin{aligned} S_3 &= \int d^5x \sqrt{|g|} \Big\{ -\frac{1}{2g_5^2} f^{abc} v_a^{mn} \left(V_m^b V_n^c + A_m^b A_n^c \right) - \frac{1}{g_5^2} f^{abc} a_a^{mn} V_m^b A_n^c \\ &- \frac{(M_V^b)^2}{2} f^{abc} (\partial_m \pi^a - 2A_m^a) V^{m,b} \pi^c + M_A^{ae} f^{ebc} (\partial_m \pi^a - A_m^a) V^{m,b} \pi^c \Big\} \,, \end{aligned} \tag{4.61}$$

and S_0 is exactly the action for X_0 given in (4.30), confirming the consistency of the procedure. We recall that the expression for the action up to the third order obtained here is valid for the $SU(N_f)$ group for any N_f.

Next, we will discuss in more detail the properties that come from the action up to second and third orders.

4.4 Exploring the Action up to second order

We start this section exploring the symmetries involved in the kinetic term (4.60). Clearly, we identify that the axial fields present the following symmetry

$$A_m^a \to A_m^a - \partial_m \lambda_A^a, \quad \pi^a \to \pi^a - \lambda_A^a, \tag{4.62}$$

that will be useful in the process of obtaining an effective 4d action. In the vector part, the mass term M_V^a doesn't allow a gauge symmetry. But, in the case in which we have $M_V^a = 0$, this sector presents the symmetry

$$V_m^a \to V_m^a - \partial_m \lambda_V^a \quad . \tag{4.63}$$

This will be made more clear when we write the holographic currents and their conservations described below.

4.4.1 Field equations and Holographic currents

Our next step is to determine the equations of motions that describe the dynamics of the fields and also we present a way to extract directly the vacuum expectation values of the operators, named here as holographic currents. Firstly, let us write the kinetic action (4.60) as $S_2 = \int d^5x \mathcal{L}_2$. Its variation takes the following form

$$\begin{aligned}\delta S_2 &= \int d^5x \left[\left(\frac{\partial \mathcal{L}_2}{\partial V^a_\ell} - \partial_m P^{m\ell}_{V,a} \right) \delta V^a_\ell + \left(\frac{\partial \mathcal{L}_2}{\partial A^a_\ell} - \partial_m P^{m\ell}_{A,a} \right) \delta A^a_\ell + \left(\frac{\partial \mathcal{L}_2}{\partial \pi^a} - \partial_m P^{m}_{\pi,a} \right) \delta \pi^a \right] \\ &+ \int d^5x \, \partial_m \left(P^{m\ell}_{V,a} \, \delta V^a_\ell + P^{m\ell}_{A,a} \, \delta A^a_\ell + P^{m}_{\pi,a} \, \delta \pi^a \right) , \end{aligned} \tag{4.64}$$

where $P^{m\ell}_{V,a}$ and $P^{m\ell}_{A,a}$ are the conjugate momenta to the vector fields V^a_ℓ, A^a_ℓ and $P^m_{\pi,a}$ is the conjugate momenta of the pseudoscalar π^a. Their expressions are obtained using Eq. (4.60):

$$\begin{aligned} P^{m\ell}_{V,a} &= \frac{\partial \mathcal{L}_2}{\partial(\partial_m V^a_\ell)} = -\frac{1}{g_5^2} \sqrt{|g|} \, v^{m\ell}_a \, , \\ P^{m\ell}_{A,a} &= \frac{\partial \mathcal{L}_2}{\partial(\partial_m A^a_\ell)} = -\frac{1}{g_5^2} \sqrt{|g|} \, a^{m\ell}_a \, , \\ P^{m}_{\pi,a} &= \frac{\partial \mathcal{L}_2}{\partial(\partial_m \pi^a)} = M^{ab}_A \sqrt{|g|} \, (\partial^m \pi_b - A^m_b) \, , \end{aligned} \tag{4.65}$$

Still, using Eq. (4.60), we find the derivatives of $\mathcal{L}_2$ with respect to the fields

$$\begin{aligned} \frac{\partial \mathcal{L}_2}{\partial V^a_\ell} &= (M^a_V)^2 \sqrt{|g|} V^\ell_a \, , \\ \frac{\partial \mathcal{L}_2}{\partial A^a_\ell} &= -M^{ab}_A \sqrt{|g|} \left(\partial^\ell \pi^b - A^{\ell,b} \right) \, , \\ \frac{\partial \mathcal{L}_2}{\partial \pi^a} &= 0 \, . \end{aligned} \tag{4.66}$$

Imposing the stationarity condition $\delta S_2 = 0$, we find from the first three terms in Eq. (4.64) the field equations

$$\begin{aligned} &\partial_m \left[\sqrt{|g|} v^{mn}_a \right] + g_5^2 (M^a_V)^2 \sqrt{|g|} \, V^n_a = 0 \, , \\ &\partial_m \left[\sqrt{|g|} a^{mn}_a \right] - g_5^2 M^{ab}_A \sqrt{|g|} \, (\partial^n \pi_b - A^n_b) = 0 \, , \\ &\partial_m \left[M^{ab}_A \sqrt{|g|} \, (\partial^m \pi_b - A^m_b) \right] = 0 \, . \end{aligned} \tag{4.67}$$

Through these equations we can find the mass spectrum of the vector, axial-vector and pseudoscalar mesons by solving them in momentum space with the appropriate boundary conditions, as has been done in [9], where the authors have used the Green function method. Here, instead, we will choose a different method based on the Kaluza-Klein expansion (see the Appendix 9) in order to rewrite the equations of motion in terms of the holographic coordinate z. The main reason to use this method is because it allows us to extract a 4d off-shell action for the mesons.

Now, let us move on and obtain the vacuum expectation value for the 4d operators, the holographic currents. The surface term in (4.64) has a nonvanishing contribution

$$\delta S_2^{\text{Bdy}} = \int d^4x \Big(P^{z\mu}_{V,a}\, \delta V^a_\mu + P^{z\mu}_{A,a}\, \delta A^a_\mu + P^z_{\pi,a}\, \delta\pi^a \Big)^{z=z_0}_{z=\epsilon}. \tag{4.68}$$

The terms at $z = z_0$ vanish under the following conditions

$$\partial_z V^a_\mu|_{z=z_0} = \partial_z A^a_\mu|_{z=z_0} = \partial_z \pi^a|_{z=z_0} = A_z|_{z=z_0} = V_z|_{z=z_0} = 0, \tag{4.69}$$

that are chosen since they are consistent with the gauge transformations (4.62, 4.63), for $\partial_z\lambda = 0$. So, the three terms in (4.68) that form a surface term, whose nonvanishing contribution, can be written as

$$\delta S_2^{\text{Bdy}} = -\int d^4x \left[\langle J^{\hat\mu}_{V,a}\rangle \left(\delta V^a_{\hat\mu}\right)_{z=\epsilon} + \langle J^{\hat\mu}_{A,a}\rangle \left(\delta A^a_{\hat\mu}\right)_{z=\epsilon} + \langle J_{\pi,a}\rangle \left(\delta\pi^a\right)_{z=\epsilon} \right], \tag{4.70}$$

where

$$\langle J^{\hat\mu}_{V,a}(x)\rangle = P^{z\mu}_{V,a}|_{z=\epsilon} = -\frac{1}{g_5^2}\left(\sqrt{|g|}v^{z\mu}_a\right)_{z=\epsilon}, \tag{4.71}$$

$$\langle J^{\hat\mu}_{A,a}(x)\rangle = P^{z\mu}_{A,a}|_{z=\epsilon} = -\frac{1}{g_5^2}\left(\sqrt{|g|}a^{z\mu}_a\right)_{z=\epsilon}, \tag{4.72}$$

$$\langle J_{\pi,a}(x)\rangle = P^{z}_{\pi,a}|_{z=\epsilon} = \left[\sqrt{|g|}M_A^{ab}\left(\partial^z\pi_b - A^z_b\right)\right]_{z=\epsilon} = \partial_{\hat\mu}\langle J^{\hat\mu}_{A,a}(x)\rangle. \tag{4.73}$$

Here we have used the holographic prescription that the bulk fields act on the boundary as a current of the gauge field theory. These holographic currents are identified with the vacuum expectation values of the 4d vector (4.71), axial (4.72) and pseudoscalar (4.73) current operators in Minkowski space-time, respectively. From (4.67) and (4.71), we have that $\partial_{\hat\mu}\langle J^{\hat\mu}_{V,a}(x)\rangle \neq 0$ when $(M_V^a)^2 \neq 0$, i.e. the vector current is not conserved for those cases. We will briefly discuss the consequence of this relation in the sector of scalar mesons. Also, we note that, taking the divergence of the axial holographic current in (4.72) and using the second equation in (4.67), we compare with (4.73) and obtain $\partial_{\hat\mu}\langle J^{\hat\mu}_{A,a}(x)\rangle = \langle J_{\pi,a}(x)\rangle$, i.e, the divergence of the axial current is the pseudoscalar current. We will discuss this relation in more detail in the next chapter and will show how it leads to partial conservation of the axial current (PCAC).

4.4.2 The 4d effective action

Now, we will show how to obtain the action in four dimensions in order to describe the mesonic spectrum in the Hard Wall model. To obtain this, we use the metric (4.24), so that the kinetic action (4.60) takes the form

$$\begin{aligned} S_2 &= \int d^4x \int \frac{dz}{z} \Big\{ -\frac{1}{4g_5^2}\left[(v^a_{\hat\mu\hat\nu})^2 - 2(v^a_{z\hat\mu})^2 \right] + \frac{(M_V^a)^2}{2z^2}\left[(V^a_{\hat\mu})^2 - (V^a_z)^2 \right] \\ &- \frac{1}{4g_5^2}\left[(a^a_{\hat\mu\hat\nu})^2 - 2(a^a_{z\hat\mu})^2 \right] + \frac{M_A^{ab}}{2z^2}\Big[(\partial^{\hat\mu}\pi^a - A^{\hat\mu,a})(\partial_{\hat\mu}\pi^b - A^b_{\hat\mu}) \\ &- (\partial_z\pi^a - A^a_z)(\partial_z\pi^b - A^b_z) \Big] \Big\}. \end{aligned} \tag{4.74}$$

The vector and axial-vector fields $V^a_{\hat\mu}$, $A^a_{\hat\mu}$ can be decomposed into transverse and longitudinal parts, i.e.

$$V^a_{\hat\mu} = V^{\perp,a}_{\hat\mu} + \partial_{\hat\mu}\xi^a, \quad A^a_{\hat\mu} = A^{\perp,a}_{\hat\mu} + \partial_{\hat\mu}\phi^a\,, \tag{4.75}$$

where $\partial_{\hat\mu}V^{\perp,a}_{\hat\mu} = \partial_{\hat\mu}A^{\perp,a}_{\hat\mu} = 0$. Using the gauge symmetry (4.62), we can set

$$A^a_{\hat\mu} \;\to\; A^{\perp,a}_{\hat\mu}, \quad A^a_z \to -\partial_z\phi^a, \quad \pi^a \to \pi^a - \phi^a\,. \tag{4.76}$$

We point out that we have chosen a different gauge that was used by the authors in [9]. In addition, we also introduce the fields $\tilde\pi^a$ and $\tilde\phi^a$ through the relations

$$V^a_z = -\partial_z\tilde\pi^a, \quad \tilde\phi^a = \xi^a + \tilde\pi^a\,. \tag{4.77}$$

Now, using the expressions (4.75), (4.76) and (4.77), the action (4.74) takes the form

$$\begin{aligned} S_2 &= \int d^4x \int \frac{dz}{z} \Big\{ -\frac{1}{4g_5^2}\Big[(v^{\perp,a}_{\hat\mu\nu})^2 - 2(\partial_z V^{\perp,a}_{\hat\mu})^2 - 2(\partial_z\partial_{\hat\mu}\tilde\phi^a)^2 \Big] \\ &+ \frac{(M_V^a)^2}{2z^2}\Big[(V^{\perp,a}_{\hat\mu})^2 + (\partial_{\hat\mu}\tilde\pi^a - \partial_{\hat\mu}\tilde\phi^a)^2 - (\partial_z\tilde\pi^a)^2 \Big] \\ &- \frac{1}{4g_5^2}\Big[(a^{\perp,a}_{\hat\mu\nu})^2 - 2(\partial_z A^{\perp,a}_{\hat\mu})^2 - 2(\partial_z\partial_{\hat\mu}\phi^a)^2 \Big] \\ &+ \frac{M_A^{ab}}{2z^2}\Big[A^{\hat\mu,a}_{\perp}A^{\perp,b}_{\hat\mu} + (\partial^{\hat\mu}\pi^a - \partial^{\hat\mu}\phi^a)(\partial_{\hat\mu}\pi^b - \partial_{\hat\mu}\phi^b) - (\partial_z\pi^a)(\partial_z\pi^b) \Big] \\ &+ \partial_{\hat\mu}(\ldots) \Big\}, \end{aligned} \tag{4.78}$$

where the terms in $(\ldots)$ are surface terms that vanish after choosing periodic boundary conditions for the fields.

We stress that due to the term involving M_A^{ab} we have the possibility of mixing terms in the axial sector. In fact, as we will see, this will occur when (a,b) are $(8,15)$ or $(15,8)$. Then it is convenient to split the index $a = (\bar a, \hat a)$ where $\bar a \neq (8,15)$ and $\hat a = (8,15)$, in order to make explicit the calculations involving the mixing terms.

The action (4.78) is in a suitable form for the Kaluza-Klein expansion. This consists in expanding the 5-d fields in an infinite discrete set of modes. Each mode will be a product of a pure wave function in the radial coordinate z and a meson field depending on the Minkowski coordinates x. For more details about the Kaluza-Klein expansion and its relation with the gauge invariant operators see Ref. [5]. For the present case, the Kaluza-Klein expansion for the bulk fields $V^{a}_{\hat\mu}$, $A^{\perp,a}_{\hat\mu}$, π^a and ϕ^a take the form

$$
\begin{aligned}
V^{\perp,a}_{\hat\mu}(x,z) &= g_5\sum_{n=0}^{\infty} v^{a,n}(z)\hat V^{a,n}_{\hat\mu}(x)\,, && (4.79)\\
\tilde\pi^{a}(x,z) &= g_5\sum_{n=0}^{\infty} \tilde\pi^{a,n}(z)\hat\pi^{a,n}_{V}(x), \quad \tilde\phi^{a}(x,z) = g_5\sum_{n=0}^{\infty} \tilde\phi^{a,n}(z)\hat\pi^{a,n}_{V}(x)\,, && (4.80)\\
A^{\perp,\bar a}_{\hat\mu}(x,z) &= g_5\sum_{n=0}^{\infty} a^{\bar a,n}(z)\hat A^{\bar a,n}_{\hat\mu}(x), \quad A^{\perp,\hat a}_{\hat\mu}(x,z) = g_5\sum_{n=0}^{\infty} a^{\hat a\hat b,n}(z)\hat A^{\hat b,n}_{\hat\mu}(x)\,, && (4.81)\\
\pi^{\bar a}(x,z) &= g_5\sum_{n=0}^{\infty} \pi^{\bar a,n}(z)\hat\pi^{\bar a,n}(x), \quad \pi^{\hat a}(x,z) = g_5\sum_{n=0}^{\infty} \pi^{\hat a\hat b,n}(z)\hat\pi^{\hat b,n}(x)\,, && (4.82)\\
\phi^{\bar a}(x,z) &= g_5\sum_{n=0}^{\infty} \phi^{\bar a,n}(z)\hat\pi^{\bar a,n}(x), \quad \phi^{\hat a}(x,z) = g_5\sum_{n=0}^{\infty} \phi^{\hat a\hat b,n}(z)\hat\pi^{\hat b,n}(x)\,. && (4.83)
\end{aligned}
$$

The wave functions $\phi^{\bar a,n}(z)$ and $\pi^{\bar a,n}(z)$ are not independent. The relation between them can be obtained from the 5d field equations in Eqs. (4.67) or via an off-shell integration. The indices a and $\bar a$ are fixed whereas the index $\hat b$ is summed implicitly. Using these expansions in the action (4.78), the z and x integrals can be separated, so that S_2 takes the form

$$
\begin{aligned}
S_2 = \sum_{n,m=0}^{\infty}\int d^4x\Big\{ &-\frac{1}{4}\Delta^{a,nm}_{V}\hat v^{a,n}_{\hat\mu\hat\nu}\hat v^{\hat\mu\hat\nu}_{a,m} + \frac{1}{2}M^{a,nm}_{V}\hat V^{a,n}_{\hat\mu}\hat V^{\hat\mu}_{a,m}\\
&+ \frac{1}{2}\Delta^{a,nm}_{\pi_V}(\partial_{\hat\mu}\hat\pi^{a,n}_{V})(\partial^{\hat\mu}\pi^{a,m}_{V}) - \frac{1}{2}M^{a,nm}_{\pi_V}\hat\pi^{a,n}_{V}\hat\pi^{a,m}_{V}\\
&- \frac{1}{4}\Delta^{\bar a,nm}_{A}\hat a^{\bar a,n}_{\hat\mu\hat\nu}\hat a^{\hat\mu\hat\nu}_{\bar a,m} + \frac{1}{2}M^{\bar a,nm}_{A}\hat A^{\bar a,n}_{\hat\mu}\hat A^{\hat\mu}_{\bar a,m}\\
&+ \frac{1}{2}\Delta^{\bar a,nm}_{\pi}(\partial_{\hat\mu}\hat\pi^{\bar a,n})(\partial^{\hat\mu}\hat\pi^{\bar a,m}) - \frac{1}{2}M^{\bar a,nm}_{\pi}\hat\pi^{\bar a,n}\hat\pi^{\bar a,m}\\
&- \frac{1}{4}\Delta^{\hat a\hat b,nm}_{A}\hat a^{\hat a,n}_{\hat\mu\hat\nu}\hat a^{\hat\mu\hat\nu}_{\hat b,m} + \frac{1}{2}M^{\hat a\hat b,nm}_{A}\hat A^{\hat a,n}_{\hat\mu}\hat A^{\hat\mu}_{\hat b,m}\\
&+ \frac{1}{2}\Delta^{\hat a\hat b,nm}_{\pi}(\partial_{\hat\mu}\hat\pi^{\hat a,n})(\partial^{\hat\mu}\hat\pi^{\hat b,m}) - \frac{1}{2}M^{\hat a\hat b,nm}_{\pi}\hat\pi^{\hat a,n}\hat\pi^{\hat b,m}\Big\}\,, \qquad (4.84)
\end{aligned}
$$

with coefficients defined by the z integrals

$$
\begin{aligned}
\Delta^{a,nm}_{V} &= \int\frac{dz}{z}v^{a,n}(z)v^{a,m}(z)\,,\\
M^{a,nm}_{V} &= \int\frac{dz}{z}\Big\{[\partial_z v^{a,n}(z)][\partial_z v^{a,m}(z)] + \beta^{a}_{V}(z)v^{a,n}(z)v^{a,m}(z)\Big\}\,,\\
\Delta^{a,nm}_{\pi_V} &= \int\frac{dz}{z}\Big\{[\partial_z\tilde\phi^{a,n}(z)][\partial_z\tilde\phi^{a,m}(z)] + \beta^{a}_{V}(z)[\tilde\pi^{a,n}(z)-\tilde\phi^{a,n}(z)][\tilde\pi^{a,m}(z)-\tilde\phi^{a,m}(z)]\Big\}\,,\\
M^{a,nm}_{\pi_V} &= \int\frac{dz}{z}\beta^{a}_{V}(z)[\partial_z\tilde\pi^{a,n}][\partial_z\tilde\pi^{a,m}]\,,\\
\Delta^{\bar a,nm}_{A} &= \int\frac{dz}{z}a^{\bar a,n}(z)a^{\bar a,m}(z)\,,
\end{aligned}
$$

$$
\begin{aligned}
M_A^{\bar{a},nm} &= \int \frac{dz}{z}\Big\{[\partial_z a^{\bar{a},n}(z)][\partial_z a^{\bar{a},m}(z)] + \beta_A^{\bar{a}\bar{a}}(z)a^{\bar{a},n}(z)a^{\bar{a},m}(z)\Big\}\,, \\
\Delta_\pi^{\bar{a},nm} &= \int \frac{dz}{z}\Big\{[\partial_z \phi^{\bar{a},n}(z)][\partial_z \phi^{\bar{a},m}(z)] + \beta_A^{\bar{a}\bar{a}}(z)[\pi^{\bar{a},n}(z) - \phi^{\bar{a},n}(z)][\pi^{\bar{a},m}(z) - \phi^{\bar{a},m}(z)]\Big\}\,, \\
M_\pi^{\bar{a},nm} &= \int \frac{dz}{z}\beta_A^{\bar{a}\bar{a}}(z)[\partial_z \pi^{\bar{a},n}][\partial_z \pi^{\bar{a},m}]\,, \\
\Delta_A^{\hat{a}\hat{b},nm} &= \int \frac{dz}{z} a^{\hat{c}\hat{a},n}(z)a^{\hat{c}\hat{b},m}(z)\,, \\
M_A^{\hat{a}\hat{b},nm} &= \int \frac{dz}{z}\Big\{[\partial_z a^{\hat{c}\hat{a},n}(z)][\partial_z a^{\hat{c}\hat{b},m}(z)] + \beta_A^{\hat{c}\hat{d}}(z)a^{\hat{c}\hat{a},n}(z)a^{\hat{d}\hat{b},m}(z)\Big\}\,, \\
\Delta_\pi^{\hat{a}\hat{b},nm} &= \int \frac{dz}{z}\Big\{[\partial_z \phi^{\hat{c}\hat{a},n}(z)][\partial_z \phi^{\hat{c}\hat{b},m}(z)] + \beta_A^{\hat{c}\hat{d}}(z)[\pi^{\hat{c}\hat{a},n}(z) - \phi^{\hat{c}\hat{a},n}(z)][\pi^{\hat{d}\hat{b},m}(z) - \phi^{\hat{d}\hat{b},m}(z)]\Big\}\,, \\
M_\pi^{\hat{a}\hat{b},nm} &= \int \frac{dz}{z}\beta_A^{\hat{c}\hat{d}}(z)[\partial_z \pi^{\hat{c}\hat{a},n}][\partial_z \pi^{\hat{d}\hat{b},m}]\,.
\end{aligned} \tag{4.85}
$$

For simplicity, we have defined

$$
\beta_V^a = \frac{g_5^2}{z^2}(M_V^a)^2, \quad \beta_A^{ab} = \frac{g_5^2}{z^2}M_A^{ab}\,. \tag{4.86}
$$

In order to obtain standard kinetic terms in (4.84) we impose the following conditions under the Δ's coefficients

$$
\Delta_V^{a,nm} = \Delta_{\pi_V}^{a,nm} = \Delta_A^{\bar{a},nm} = \Delta_\pi^{\bar{a},nm} = \delta^{nm}\,, \quad \Delta_A^{\hat{a}\hat{b},nm} = \Delta_\pi^{\hat{a}\hat{b},nm} = \delta^{\hat{a}\hat{b}}\delta^{nm}\,, \tag{4.87}
$$

and the following conditions for the mass coefficients

$$
M_V^{a,nm} = m^2_{V^{a,n}}\delta^{nm}, \quad M_{\pi_V}^{a,nm} = m^2_{\pi_V^{a,n}}\delta^{nm}, \quad M_A^{\bar{a},nm} = m^2_{A^{\bar{a},n}}\delta^{nm} \tag{4.88}
$$

$$
M_\pi^{\bar{a},nm} = m^2_{\pi^{\bar{a},n}}\delta^{nm}, \quad M_A^{\hat{a}\hat{b},nm} = m^2_{A^{\hat{a},n}}\delta^{\hat{a}\hat{b}}\delta^{nm}, \quad M_\pi^{\hat{a}\hat{b},nm} = m^2_{\pi^{\hat{a},n}}\delta^{\hat{a}\hat{b}}\delta^{nm}\,. \tag{4.89}
$$

In this way, from (4.84), we arrive at the following 4d action

$$
\begin{aligned}
S_2 &= \sum_{n=0}^{\infty}\int d^4x\Big\{-\frac{1}{4}\hat{v}^{a,n}_{\hat{\mu}\hat{\nu}}\hat{v}^{\hat{\mu}\hat{\nu}}_{a,n} + \frac{1}{2}m^2_{V^{a,n}}\hat{V}^{a,n}_{\hat{\mu}}\hat{V}^{\hat{\mu}}_{a,n} + \frac{1}{2}(\partial_{\hat{\mu}}\hat{\pi}_V^{a,n})(\partial^{\hat{\mu}}\pi_V^{a,n}) - \frac{1}{2}m^2_{\pi_V^{a,n}}\hat{\pi}_V^{a,n}\hat{\pi}_V^{a,n} \\
&- \frac{1}{4}\hat{a}^{a,n}_{\hat{\mu}\hat{\nu}}\hat{a}^{\hat{\mu}\hat{\nu}}_{a,n} + \frac{1}{2}m^2_{A^{a,n}}\hat{A}^{a,n}_{\hat{\mu}}\hat{A}^{\hat{\mu}}_{a,n} + \frac{1}{2}(\partial_{\hat{\mu}}\hat{\pi}^{\bar{a},n})(\partial^{\hat{\mu}}\hat{\pi}^{\bar{a},n}) - \frac{1}{2}m^2_{\pi^{a,n}}\hat{\pi}^{a,n}\hat{\pi}^{a,n}\Big\}\,.
\end{aligned} \tag{4.90}
$$

The conditions for the Δ coefficients in (4.87) give normalization conditions for the corresponding wave functions, $v^{a,n}(z)$, $a^{a,n}(z)$, $\pi^{a,n}(z)$ and $\phi^{a,n}(z)$. On the other hand, the conditions for the masses are equivalent to the conditions for the Δ coefficients if we impose the following equations

$$
\left[-\partial_z\left(\frac{1}{z}\partial_z\right) + \frac{1}{z}\beta_V^a(z)\right]v^{a,n}(z) = \frac{m^2_{V^{a,n}}}{z}v^{a,n}(z)\,, \tag{4.91}
$$

$$
\frac{\beta_V^a(z)}{z}\left[\tilde{\pi}^{a,n}(z) - \tilde{\phi}^{a,n}(z)\right] = -\partial_z\left[\frac{1}{z}\partial_z\tilde{\phi}^{a,n}(z)\right]\,, \tag{4.92}
$$

$$\beta_V^a(z)\,\partial_z\tilde{\pi}^{a,n}(z) = m^2_{\pi_V^{a,n}}\partial_z\tilde{\phi}^{a,n}(z)\,, \tag{4.93}$$

$$\left[-\partial_z\left(\frac{1}{z}\partial_z\right)+\frac{1}{z}\beta_A^{\bar{a}\bar{a}}(z)\right]a^{\bar{a},n}(z) = \frac{m^2_{A^{\bar{a},n}}}{z}a^{\bar{a},n}(z)\,, \tag{4.94}$$

$$\frac{\beta_A^{\bar{a}\bar{a}}(z)}{z}\left[\pi^{\bar{a},n}(z)-\phi^{\bar{a},n}(z)\right] = -\partial_z\left[\frac{1}{z}\partial_z\phi^{\bar{a},n}(z)\right]\,, \tag{4.95}$$

$$\beta_A^{\bar{a}\bar{a}}(z)\,\partial_z\pi^{\bar{a},n}(z) = m^2_{\pi^{\bar{a},n}}\partial_z\phi^{\bar{a},n}(z)\,, \tag{4.96}$$

$$-\partial_z\left(\frac{1}{z}\partial_z\right)a^{\hat{a}\hat{b},n}(z)+\frac{1}{z}\beta_A^{\hat{a}\hat{c}}(z)a^{\hat{c}\hat{b},n}(z) = \frac{m^2_{A^{\hat{b},n}}}{z}a^{\hat{a}\hat{b},n}(z)\,, \tag{4.97}$$

$$\frac{\beta_A^{\hat{a}\hat{c}}(z)}{z}\left[\pi^{\hat{c}\hat{b},n}(z)-\phi^{\hat{c}\hat{b},n}(z)\right] = -\partial_z\left[\frac{1}{z}\partial_z\phi^{\hat{a}\hat{b},n}(z)\right]\,, \tag{4.98}$$

$$\beta_A^{\hat{a}\hat{c}}(z)\,\partial_z\pi^{\hat{c}\hat{b},n}(z) = m^2_{\pi^{\hat{b},n}}\partial_z\phi^{\hat{a}\hat{b},n}(z)\,. \tag{4.99}$$

These equations of motion can be interpreted as the on-shell conditions for the wave functions $v^{a,n}(z)$, $a^{a,n}(z)$, $\pi^{a,n}(z)$ and $\phi^{a,n}(z)$. It should be noted that these equations can be obtained also from the 5d field equations in Eq. (4.67) going to 4d momentum space. However, the advantage of our method is the fact that the final 4d action in (4.90) remains off-shell, a property that can be very useful when considering scattering amplitudes, which require the knowledge of Feynman rules.

To conclude this part, we mention that all the meson masses $m_{\pi^{a,n}}$, $m_{V^{a,n}}$ and $m_{A^{a,n}}$ are completely determined once we find solutions for Eqs. (4.91-4.99). Following what have been done in Ref. [9], the solutions for these equations are found by imposing Dirichlet boundary conditions at $z=\epsilon$:

$$\pi^{a,n}|_{z=\epsilon} = v^{a,n}|_{z=\epsilon} = a^{a,n}|_{z=\epsilon} = 0, \tag{4.100}$$

and Neumann boundary conditions at $z=z_0$:

$$\partial_z\pi^{a,n}|_{z=z_0} = \partial_z v^{a,n}|_{z=z_0} = \partial_z a^{a,n}|_{z=z_0} = 0. \tag{4.101}$$

The solutions obtained from these conditions are the normalized solutions whose normalization constants are obtained using the conditions (4.87).

4.4.3 Leptonic decay constants

In this section, we show how to obtain a holographic prescription for the leptonic decay constants of the mesons from the holographic QCD model. This will be useful in the next section when we derive an equivalent equation for the generalized Gell-Mann-Oakes-Renner relation in QCD.

As observed in Ref. [85], the simplest method for extracting the leptonic decay constants is to replace the fields in the dual currents prescription, (4.71)-(4.73), by their Kaluza-Klein expansions (4.79)-(4.83). This way, we can find

$$\langle J^{\hat{\mu}}_{V,a}(x)\rangle = \sum_{n=0}^{\infty}\left[\frac{1}{g_5 z}\partial_z v^{a,n}(z)\right]_{z=\epsilon}\hat{V}^{\hat{\mu}}_{a,n}(x)+\sum_{n=0}^{\infty}\left[\frac{1}{g_5 z}\partial_z\tilde{\phi}^{a,n}(z)\right]_{z=\epsilon}\partial^{\hat{\mu}}\hat{\pi}^{a,n}_{V}(x)\,, \quad (4.102)$$

$$\langle J^{\hat{\mu}}_{A,\bar{a}}(x)\rangle = \sum_{n=0}^{\infty}\left[\frac{1}{g_5 z}\partial_z a^{\bar{a},n}(z)\right]_{z=\epsilon}\hat{A}^{\hat{\mu}}_{\bar{a},n}(x)+\sum_{n=0}^{\infty}\left[\frac{1}{g_5 z}\partial_z\phi^{\bar{a},n}(z)\right]_{z=\epsilon}\partial^{\hat{\mu}}\hat{\pi}^{\bar{a},n}(x), \quad (4.103)$$

$$\langle J_{\Pi,\bar{a}}(x)\rangle = -\sum_{n=0}^{\infty}\left[\frac{\beta^{\bar{a}\bar{a}}_{A}(z)}{g_5 z}\partial_z\pi^{\bar{a},n}(z)\right]_{z=\epsilon}\hat{\pi}^{\bar{a},n}(x). \quad (4.104)$$

In the expansions (4.102)-(4.104), the 4d fields $\hat{V}^{\hat{\mu}}_{a,n}(x), A^{\hat{\mu}}_{a,n}(x), \hat{\pi}^{a,n}_{V}(x)$ and $\hat{\pi}^{\bar{a},n}(x)$ are on-shell. From these expansions we define the following coefficients

$$g_{V^{a,n}} = \left[\frac{1}{g_5 z}\partial_z v^{a,n}(z)\right]_{z=\epsilon}, \quad f_{\pi^{a,n}_{V}} = -\left[\frac{1}{g_5 z}\partial_z\tilde{\phi}^{a,n}(z)\right]_{z=\epsilon}, \quad (4.105)$$

$$g_{A^{\bar{a},n}} = \left[\frac{1}{g_5 z}\partial_z a^{\bar{a},n}(z)\right]_{z=\epsilon}, \quad f_{\pi^{\bar{a},n}} = -\left[\frac{1}{g_5 z}\partial_z\phi^{\bar{a},n}(z)\right]_{z=\epsilon}. \quad (4.106)$$

It is quite easy to identify these coefficients as being holographic prescriptions for leptonic decay constants of the mesons. This can be seen from the following identities

$$\langle 0|J^{\hat{\mu}}_{V,a}(x)|V^{b,m}(p,\lambda)\rangle = \sum_{n} g_{V^{a,n}}\langle 0|\bar{V}^{\hat{\mu}}_{a,n}(x)|V^{b,m}(p,\lambda)\rangle = g_{V^{a,m}}e^{-ip\cdot x}\epsilon^{\hat{\mu}}(p,\lambda)\delta^{ab}, \quad (4.107)$$

$$\langle 0|J^{\hat{\mu}}_{V,a}(x)|\pi^{b,m}_{V}(p)\rangle = \sum_{n} f_{\pi^{a,n}_{V}}\langle 0|\bar{V}^{\hat{\mu}}_{a,n}(x)|\pi^{a,m}_{V}(p)\rangle = f_{\pi^{a,n}_{V}}e^{-ip\cdot x}\delta^{ab}, \quad (4.108)$$

$$\langle 0|J^{\hat{\mu}}_{A,a}(x)|A^{b,m}(p,\lambda)\rangle = \sum_{n} g_{A^{a,n}}\langle 0|\bar{A}^{\hat{\mu}}_{a,n}(x)|A^{b,m}(p,\lambda)\rangle = g_{A^{a,m}}e^{-ip\cdot x}\epsilon^{\hat{\mu}}(p,\lambda)\delta^{ab}, \quad (4.109)$$

$$\langle 0|J^{\hat{\mu}}_{A,a}(x)|\pi^{b,m}(p)\rangle = \sum_{n} f_{\pi^{a,n}}\langle 0|\bar{A}^{\hat{\mu}}_{a,n}(x)|\pi^{a,m}(p)\rangle = f_{\pi^{a,m}}e^{-ip\cdot x}\delta^{ab}, \quad (4.110)$$

where the coefficients $g_{V^{a,n}}, f_{\pi^{a,n}_{V}}, g_{A^{\bar{a},n}}, f_{\pi^{\bar{a},n}}$ are the leptonic decay constants for the vector, scalars, axial-vector and pseudoscalar mesons, respectively. Once that, the above relations are the standard definitions for meson decay constants.

4.5 Exploring the Action up to third order

Next, we will find expressions for the three-meson coupling constants predicted by the model. Clearly, these must be obtained from the trilinear term of the expansion of 5d action (4.61). These terms will involve the three-meson couplings and they can be used to make connection with coupling constants and the symmetry relations in Ref. [86] at what will be discussed later on. Using the AdS_5 metric (4.24), the action (4.61) can be separated into following form

$$S_3 = S_{VVV} + S_{VAA} + S_{VA\pi} + S_{V\pi\pi}\,, \tag{4.111}$$

where each term is written as

$$\begin{aligned}
S_{VVV} &= -\frac{1}{2g_5^2} f^{abc}\int d^4x \int \frac{dz}{z}\left[v_a^{\hat\mu\hat\nu}V_{\hat\mu}^b V_{\hat\nu}^c - 2v_{z\hat\mu}^a V_z^b V_c^{\hat\mu}\right], & (4.112)\\
S_{VAA} &= \frac{1}{2g_5^2} f^{abc}\int d^4x \int \frac{dz}{z}\Big[v_a^{\hat\mu\hat\nu}A_{\hat\mu}^b A_{\hat\nu}^c - 2v_{z\hat\mu}^a A_z^b A_c^{\hat\mu} - 2a_a^{\hat\mu\hat\nu}V_{\hat\mu}^b A_{\hat\nu}^c & (4.113)\\
&+ 2a_{z\hat\mu}^a(V_z^b A_c^{\hat\mu} - V_b^{\hat\mu}A_z^c)\Big], & (4.114)\\
S_{VA\pi} &= \frac{1}{g_5^2}\int d^4x \int \frac{dz}{z}\left[\beta_V^b(z) f^{abc} - \beta_A^{ae}(z) f^{ebc}\right]\left[-A_z^a V_z^b + A_{\hat\mu}^a V_b^{\hat\mu}\right]\pi^c\,, & (4.115)\\
S_{V\pi\pi} &= \frac{1}{2g_5^2}\int d^4x \int \frac{dz}{z}\left[-\beta_V^b(z) + 2\beta_A^{ae}(z) f^{ebc}\right]\left[-(\partial_z\pi^a)V_z^b + (\partial_{\hat\mu}\pi^a)V_b^{\hat\mu}\right]\pi^c\,. & (4.116)
\end{aligned}$$

Now, using the decompositions (4.75), (4.75) and (4.77) and also the transformations allowed by the gauge symmetry (4.76), the actions (4.112-4.116) become

$$\begin{aligned}
S_{VVV} &= -\frac{1}{2g_5^2} f^{abc}\int d^4x \int \frac{dz}{z}\Big[v_{\perp,a}^{\hat\mu\hat\nu}V_{\hat\mu}^{\perp,b}V_{\hat\nu}^{\perp,c} + 2v_{\perp,a}^{\hat\mu\hat\nu}(\partial_{\hat\mu}\xi^b)V_{\hat\nu}^{\perp,c} + 2(\partial_z V_{\hat\mu}^{\perp,a})(\partial_z\tilde\pi^b)V_{\perp,c}^{\hat\mu}\\
&+ v_{\perp,a}^{\hat\mu\hat\nu}(\partial_{\hat\mu}\xi^b)(\partial_{\hat\nu}\xi^c) + 2(\partial_z V_{\hat\mu}^{\perp,a})(\partial_z\tilde\pi^b)\partial^{\hat\mu}\xi^c + 2(\partial_z\partial_{\hat\mu}\tilde\phi^a)(\partial_z\tilde\pi^b)\partial^{\hat\mu}\xi^c\Big], & (4.117)\\
S_{VAA} &= \frac{1}{2g_5^2} f^{abc}\int d^4x \int \frac{dz}{z}\Big[v_{\perp,a}^{\hat\mu\hat\nu}A_{\hat\mu}^{\perp,b}A_{\hat\nu}^{\perp,c} - 2a_{\perp,a}^{\hat\mu\hat\nu}V_{\hat\mu}^{\perp,b}A_{\hat\nu}^{\perp,c} + 2(\partial_z V_{\hat\mu}^{\perp,a})(\partial_z\phi^b)A_{\perp,c}^{\hat\mu}\\
&+ 2(\partial_z A_{\hat\mu}^{\perp,a})V_{\perp,b}^{\hat\mu}(\partial_z\phi^c) + 2(\partial_z\partial_{\hat\mu}\phi^a)V_{\perp,b}^{\hat\mu}(\partial_z\phi^c) - 2a_{\perp,a}^{\hat\mu\hat\nu}(\partial_{\hat\mu}\xi^b)A_{\hat\nu}^{\perp,c} - 2(\partial_z A_{\hat\mu}^{\perp,a})(\partial_z\tilde\pi^b)A_{\perp,c}^{\hat\mu}\\
&+ 2(\partial_z\partial_{\hat\mu}\tilde\phi^a)(\partial_z\phi^b)A_{\perp,c}^{\hat\mu} + 2(\partial_z A_{\hat\mu}^{\perp,a})\partial^{\hat\mu}\xi^b(\partial_z\phi^c) - 2(\partial_z\partial_{\hat\mu}\phi^a)(\partial_z\tilde\pi^b)A_{\perp,c}^{\hat\mu}\\
&+ 2(\partial_z\partial_{\hat\mu}\phi^a)\partial^{\hat\mu}\xi^b(\partial_z\phi^c)\Big], & (4.118)\\
S_{VA\pi} &= \frac{1}{g_5^2}\int d^4x \int \frac{dz}{z}\left[\beta_V^b(z) f^{abc} - \beta_A^{ae}(z) f^{ebc}\right]\Big[A_{\hat\mu}^{\perp,a}V_{\perp,b}^{\hat\mu}(\pi^c - \phi^c) + A_{\hat\mu}^{\perp,a}\partial^{\hat\mu}\xi^b(\pi^c - \phi^c)\\
&- (\partial_z\phi^a)(\partial_z\tilde\pi^b)(\pi^c - \phi^c)\Big], & (4.119)\\
S_{V\pi\pi} &= \frac{1}{2g_5^2}\int d^4x \int \frac{dz}{z}\left[-\beta_V^b(z) f^{abc} + 2\beta_A^{ae}(z) f^{ebc}\right]\Big[(\partial_{\hat\mu}\pi^a - \partial_{\hat\mu}\phi^a)V_{\perp,b}^{\hat\mu}(\pi^c - \phi^c)\\
&+ (\partial_{\hat\mu}\pi^a - \partial_{\hat\mu}\phi^a)\partial^{\hat\mu}\xi^b(\pi^c - \phi^c) + (\partial_z\pi^a - \partial_z\phi^a)(\partial_z\tilde\pi^b)(\pi^c - \phi^c)\Big]. & (4.120)
\end{aligned}$$

The actions written above are in a convenient form to use again the Kaluza-Klein expansion (4.79)-(4.83) and get an effective 4d action. In, doing this, we find the actions that we are interested in:

$$S_{\hat{V}\hat{V}\hat{V}} = -\sum_{\ell,m,n=0}^{\infty} g_{\hat{V}^{a,\ell}\hat{V}^{b,m}\hat{V}^{c,n}} \int d^4x\, \hat{v}^{a,\ell}_{\hat{\mu}\hat{\nu}} \hat{V}^{\hat{\mu}}_{b,m} V^{\hat{\nu}}_{c,n}\,, \tag{4.121}$$

$$S_{\hat{\pi}\hat{V}\hat{\pi}} = \sum_{\ell,m,n=0}^{\infty} g_{\hat{\pi}^{a,\ell}\hat{V}^{b,m}\hat{\pi}^{c,n}} \int d^4x (\partial_{\hat{\mu}}\hat{\pi}^{a,\ell})\hat{V}^{\hat{\mu}}_{b,m}\hat{\pi}^{c,n}\,. \tag{4.122}$$

We have found an interaction action for 3-vector mesons, $S_{\hat{V}\hat{V}\hat{V}}$ and also an interaction action for 2-pseudoscalars and a vector meson, $S_{\hat{\pi}\hat{V}\hat{\pi}}$. From these actions, the coefficients are

$$g_{\hat{V}^{a,\ell}\hat{V}^{b,m}\hat{V}^{c,n}} = \frac{g_5}{2} f^{abc} \int \frac{dz}{z} v^{a,\ell}(z) v^{b,m}(z) v^{c,n}(z)\,, \tag{4.123}$$

$$\begin{aligned} g_{\hat{\pi}^{\bar{a},\ell}\hat{V}^{b,m}\hat{\pi}^{\bar{c},n}} &= \frac{g_5}{2} f^{\bar{a}b\bar{c}} \int \frac{dz}{z} \Big\{ 2(\partial_z \phi^{\bar{a},\ell}) v^{b,m} (\partial_z \phi^{\bar{c},n}) \\ &+ \left[-\beta^b_V(z) + 2\beta^{\bar{a}\bar{a}}_A(z)\right] (\pi^{\bar{a},\ell} - \phi^{\bar{a},\ell}) v^{b,m} (\pi^{\bar{c},n} - \phi^{\bar{c},n}) \Big\}\,. \end{aligned} \tag{4.124}$$

In the interaction (4.122), as we will discuss later on, we are interested only in the cases where $a = \bar{a}$ and $c = \bar{c}$.

An important point here is that the actions for 3-vector mesons in (4.121) and for 2-pseudoscalars and one vector meson in (4.122) are not in a standard form to conclude that the couplings are the physical coupling constants. In order to find them we need to do some algebraic manipulations. Starting with the action (4.121), we use integrations by parts in the action and use the symmetry properties of the 3-vector mesons couplings (4.123), and we get

$$S_{\hat{V}\hat{V}\hat{V}} = 2 f^{abc} \sum_{\ell,m,n=0}^{\infty} \bar{g}_{\hat{V}^{a,\ell}\hat{V}^{b,m}\hat{V}^{c,n}} \int d^4x\, \hat{V}^{\hat{\mu}}_{a,\ell} \,(\partial_{\hat{\mu}} \hat{V}^{b,m}_{\hat{\nu}})\, V^{\hat{\nu}}_{c,n}\,, \tag{4.125}$$

where we have

$$\bar{g}_{\hat{V}^{a,\ell}\hat{V}^{b,m}\hat{V}^{c,n}} = \frac{g_5}{2} \int \frac{dz}{z} v^{a,\ell}(z) v^{b,m}(z) v^{c,n}(z)\,. \tag{4.126}$$

On the other hand, in the case of the action (4.122), we have noted that it should be symmetric in the indexes a and c by crossing symmetry. So, to reach this, we integrate by parts this action and we use the condition for the on-shell field, $\partial_{\hat{\mu}} V^{\hat{\mu}} = 0$ (that can be obtained from the equation of motion of the 4d action in (4.90)). Then, we rewrite the above action as

$$S_{\hat{\pi}\hat{V}\hat{\pi}} = -\frac{1}{2} \sum_{\ell,m,n=0}^{\infty} g_{\hat{\pi}^{a,\ell}\hat{V}^{b,m}\hat{\pi}^{c,n}} \int d^4x \hat{V}^{\hat{\mu}}_{b,m} [\hat{\pi}^{a,\ell}(\partial_{\hat{\mu}}\hat{\pi}^{c,n}) - (\partial_{\hat{\mu}}\hat{\pi}^{a,\ell})\hat{\pi}^{c,n}]\,. \tag{4.127}$$

Note that, the integrand above is antisymmetry in the exchange of the indices a and c; let us then consider the symmetric and antisymmetric parts of $g_{\hat{\pi}^{a,\ell}\hat{V}^{b,m}\hat{\pi}^{c,n}}$ in the indices a and c,

$$\frac{1}{2} g_{\hat{\pi}^{a,\ell}\hat{V}^{b,m}\hat{\pi}^{c,n}} = g^s_{\hat{\pi}^{a,\ell}\hat{V}^{b,m}\hat{\pi}^{c,n}} + g^a_{\hat{\pi}^{a,\ell}\hat{V}^{b,m}\hat{\pi}^{c,n}}\,, \tag{4.128}$$

where we have defined the symmetric and antisymmetric parts, respectively, as

$$
\begin{aligned}
g^{s}_{\hat{\pi}^{a,\ell}\hat{V}^{b,m}\hat{\pi}^{c,n}} &= \frac{1}{4}(g_{\hat{\pi}^{a,\ell}\hat{V}^{b,m}\hat{\pi}^{c,n}} + g_{\hat{\pi}^{c,n}\hat{V}^{b,m}\hat{\pi}^{a,\ell}}),\\
g^{a}_{\hat{\pi}^{a,\ell}\hat{V}^{b,m}\hat{\pi}^{c,n}} &= \frac{1}{4}(g_{\hat{\pi}^{a,\ell}\hat{V}^{b,m}\hat{\pi}^{c,n}} - g_{\hat{\pi}^{c,n}\hat{V}^{b,m}\hat{\pi}^{a,\ell}}).
\end{aligned} \tag{4.129}
$$

As we can easily check, just the antisymmetric part $g^{a}_{\hat{\pi}^{a,\ell}\hat{V}^{b,m}\hat{\pi}^{c,n}}$ will give a non zero action. Thus, we extract the structure constant of the antisymmetric coupling and obtain

$$
g^{a}_{\hat{\pi}^{a,\ell}\hat{V}^{b,m}\hat{\pi}^{c,n}} = \frac{1}{4}f^{abc}(\hat{g}_{\hat{\pi}^{a,\ell}\hat{V}^{b,m}\hat{\pi}^{c,n}} + \hat{g}_{\hat{\pi}^{c,\ell}\hat{V}^{b,m}\hat{\pi}^{a,n}}) = \frac{1}{4}f^{abc}\bar{g}_{\hat{\pi}^{a,\ell}\hat{V}^{b,m}\hat{\pi}^{c,n}}. \tag{4.130}
$$

Now, the action (4.127) becomes symmetric in the indices a and c and takes the form

$$
S_{\hat{\pi}\hat{V}\hat{\pi}} = f^{abc}\sum_{\ell,m,n=0}^{\infty}\bar{g}_{\hat{\pi}^{a,\ell}\hat{V}^{b,m}\hat{\pi}^{c,n}}\int d^4x\,\hat{V}^{\hat{\mu}}_{b,m}\left[(\partial_{\hat{\mu}}\hat{\pi}^{a,\ell})\hat{\pi}^{c,n} - (\partial_{\hat{\mu}}\hat{\pi}^{c,n})\hat{\pi}^{a,\ell}\right], \tag{4.131}
$$

where

$$
\begin{aligned}
\bar{g}_{\hat{\pi}^{\bar{a},\ell}\hat{V}^{b,m}\hat{\pi}^{\bar{c},n}} &= \frac{g_5}{8}\int\frac{dz}{z}v^{b,m}\Big\{4(\partial_z\phi^{\bar{a},\ell})(\partial_z\phi^{\bar{c},n})\\
&+ \left[-2\beta^{b}_{V}(z) + 2(\beta^{\bar{a}\bar{a}}_{A}(z) + \beta^{\bar{c}\bar{c}}_{A}(z))\right](\pi^{\bar{a},\ell} - \phi^{\bar{a},\ell})(\pi^{\bar{c},n} - \phi^{\bar{c},n})\Big\}.
\end{aligned} \tag{4.132}
$$

The actions we have obtained in Eqs. (4.125)-(4.131) are now in a standard form and the respective coupling constants are physical. Our results can be used to make connection with those in Ref. [86], as we will show in the chapter 6 for some cases.

5 Decay constants of the pion and its excitations in Holographic QCD

As we have anticipated, an exact result from QCD states that: the excited states of the pion have leptonic decay constant that vanish in the chiral limit when chiral symmetry is dynamically broken [13]. But, as we have discussed in chapter 2, as the masses of the u and d quarks are small compared with strong-interaction scale Λ_{QCD}, it is expected that such leptonic decay constants are dramatically suppressed in nature. There are two crucial features relevant for understanding this behavior: [1] the dynamical breaking of chiral symmetry in QCD and the (pseudo) Goldstone boson nature of the ground-state pion. This might seem surprising at first view. But, by looking at the quark model approach, it is also expected a large suppression for the leptonic decay constants for excited states. In this approach, the leptonic decay constant is proportional to the configuration-space wavefunction at the origin and, for the excited states, these wavefunctions are strongly suppressed when compared to the wavefunction for the ground state at the origin. But, unfortunately, this perspective is unable to give a physical mechanism that points for a explanation of a dramatic reduction of the decay constants for the excited states.

Also, some works in lattice QCD have reported this behavior: in 2006, came out the first lattice result [87] and reported results for the pion's first radial excitation, giving $f_{\pi^1}/f_{\pi^0} \sim 0.08$, when extrapolating to the chiral limit. Some years ago, a very small value for f_{π^1} also was reported by another lattice collaboration [88] when the authors extrapolated to the chiral limit. More recently, another lattice group has reported results for the three lowest excited states of the pion: f_{π^1} is slightly suppressed, f_{π^2} is significantly suppressed, and finally $f_{\pi^3} \simeq f_{\pi^1}$. Experimental results supporting this behavior is not easy due its enormous difficulty, but, despite this, experimental results have been reported in Ref. [89], giving $f_{\pi^1}/f_{\pi^0} < 0.064$. Some other approaches also have found strongly suppressed values for f_{π^1}, as calculations based on sum rules [90, 91, 92], calculations on effective chiral Lagrangians [93]. The chiral quark model [94] also finds strongly suppressed values for f_{π^1}. In summary, there is compelling evidence for the suppression of the leptonic decay constants of pion's excited states. This is clearly a nonperturbative effect that any model intending to describe QCD should reproduce.

Moreover, as it is an exact result from nonperturbative QCD, many nonperturbative methods as lattice QCD and hadronic models of QCD can take advantage from this feature and use it as a gauge to validate techniques and truncation schemes in approximate calculations.

In Ref. [95, 96], another interesting approach in the holographic description of QCD was proposed, named light-front holography (LFH). In this approach, the frame-independent light-front wavefunctions in Minkowski space are mapped to hadronic amplitudes moving in AdS space-time. Such a mapping is possible due to a natural identification of the Lorentz-invariant coordinate that measures the separation of the constituents within a hadron at equal light-front time with the coordinate z in AdS space-time. However, the authors used a nonstandard way to introduce the chiral symmetry [97]. Using this model, the authors reproduced very well the experimental values of the masses of the lowest radially and also orbitally excited states of the pion. But, this model does not reproduce the vanishing of the leptonic decay constants of the excited states in the chiral limit. An extension of this model, the soft-wall LFH approach [98], has reproduced the same feature of obtaining a massless pion without DCSB, in which confinement property is modelled with a soft cutoff provided by a background dilaton field in the AdS space-time.

The authors in [13], using the axial-vector Ward-Takahashi identity and exact Dyson-Schwinger equations of QCD, have found a generalized Gell-Mann-Oakes-Renner (GOR) relationship

$$f_{\pi^n}\, m_{\pi^n}^2 = \left(m_{q_1}(\xi) + m_{q_2}(\xi)\right) \rho_{\pi^n}(\xi), \tag{5.1}$$

valid for every 0^- meson. Here, ξ is the regularization mass-scale, m_{π^n} is the mass of the pion's n-th excited state and ρ_{π^n} is the gauge-invariant residue at the pole $P^2 = -m_{\pi^n}^2$ in the pseudoscalar vertex function; it is related to the matrix-valued Bethe-Salpeter wavefunction $\chi_{\pi^n}^a(P, q)$ via

$$i\rho_{\pi^n}\delta^{ab} = \int \frac{d^4k}{(2\pi)^4} \, \mathrm{Tr}\left[T^a \gamma_5 \chi_{\pi^n}^b(q, P)\right], \tag{5.2}$$

with the $SU(2)$ generators T^a, $a = 1, 2, 3$, normalized as $2\,\mathrm{Tr}\left(T^a T^b\right) = \delta^{ab}$. Note that, although m_{q_1}, m_{q_2} and ρ_{π^n} are regularization mass-scale dependents, their product is not. For simplicity, we will assume from now on the isospin symmetry $m_{q_1} = m_{q_2} = m_q$.

In this context, we note that: (1) the existence of excited states entails finite matrix-valued $\chi_{\pi^n}(P, q)$ wavefunctions; (2) the integral in eq. (5.2) is finite (this follows from the ultraviolet behavior of the QCD quark-antiquark scattering kernel); (3) then, as a consequence, we have

$$\rho_{\pi^n}^0 = \lim_{m_q \to 0} \rho_{\pi^n} < \infty, \tag{5.3}$$

that means that the ρ_{π^n}-function is finite in the chiral limit; and (4), the assumption that $m^2_{\pi^n} \neq 0$ in the chiral limit. These facts naturally leads to $f_{\pi^n} = 0$ in the chiral limit for the excited states $(n > 0)$. Still, from the holographic QCD point of view, the vanishing of the leptonic decay constants of pion's excited states in the chiral limit already could also be inferred in [99] by looking the spectral representation of the two-point function of axial-vector currents. In fact, the residues of the pole terms in the two-point function are proportional to matrix elements related to the leptonic decay constants and, in the chiral limit, the pole terms associated with the pion's excited states would be absent – see e.g. Eq. (51) in Ref. [99].

For the ground-state pion, we have that the DCSB implies in

$$\rho_{\pi^0}(\xi) = -\frac{1}{f_{\pi^0}} \langle \bar{q}q \rangle_\xi, \tag{5.4}$$

where $\langle \bar{q}q \rangle = \langle \bar{u}u \rangle = \langle \bar{d}d \rangle$ is the vacuum quark condensate. Replacing it in the Eq. (5.1), we can obtain the GOR relationship, written as

$$f^2_{\pi^0}\, m^2_{\pi^0} = 2m_q(\xi)\, |\langle \bar{q}q \rangle|_\xi. \tag{5.5}$$

This shows that the GOR relationship is a natural consequence of the general relation (5.1).

Motivated by these results and by the incapacity of LFH to reproduce this result, we will investigate the leptonic decay constants of the pion and its excitations in the five-dimensional bottom-up holographic QCD model presented in the previous chapter. The decay constants are obtained directly from the Kaluza-Klein expansion of the holographic currents. We use the model to proof numerically that the leptonic decay constants of the excited states of the pion vanish in the chiral limit. In particular, we show that these results arise from a generalized GOR relationship derived in the holographic QCD model.

In the next section, we show how to identify the pion in the model and rewrite the equations for the pseudoscalar sector in order to describe it. We also introduce some mathematical tricks to manipulate the equations that allow us to find a convenient form for the asymptotic behavior for the fields. In section 5.2, we present the most important relations for this chapter, we use the holographic currents derived from the model and we show how the PCAC and the generalized GOR arise. In section 5.3, we briefly study the ρ meson and its spectrum and we show how it is fundamental to fix an important parameter of the model, the position of the hard wall z_0. We also discuss how to fix the chiral condensate in the model. Finally, in section 5.4 we present the numerical results for the spectrum of the pion and its excitations. The results for the vanishing of the decay constant and for the finiteness of the ρ_{π^n} function are also presented and discussed.

5.1 Pions and their excitations

Here, we will identify the pion in the holographic model and extract some important hadronic properties from the model, especially the leptonic decay constants. As a pseudoscalar meson, we will just need the equations involving the pseudoscalars fields found in the previous chapter, rewritten as

$$\frac{\beta_A^{aa}(z)}{z}\left[\pi^{a,n}(z)-\phi^{a,n}(z)\right]=-\partial_z\left[\frac{1}{z}\partial_z\phi^{a,n}(z)\right], \tag{5.6}$$

$$\beta_A^{aa}(z)\,\partial_z\pi^{a,n}(z)=m^2_{\pi^{a,n}}\partial_z\phi^{a,n}(z). \tag{5.7}$$

We easily identify the pions through the flavour indexes in the adjoint representation of the SU(2)-flavor symmetry group. These indices are those in the equations for the pseudoscalars in (5.6, 5.7). The pseudoscalar matrix $P=\pi^i t^i$, in this case, is written as

$$P=\frac{1}{\sqrt{2}}\begin{pmatrix}\frac{\pi^0}{\sqrt{2}} & \pi^+\\ \pi^- & -\frac{\pi^0}{\sqrt{2}}\end{pmatrix}, \tag{5.8}$$

where the matrices t^i are those as in Eq. (2.11). For the SU(2) case, they are $t^i=1/2\tau^i$, where τ^i are the Pauli matrices

$$t^1=\frac{1}{2}\begin{pmatrix}0 & 1\\ 1 & 0\end{pmatrix},\qquad t^2=\frac{1}{2}\begin{pmatrix}0 & -i\\ i & 0\end{pmatrix},\qquad t^3=\frac{1}{2}\begin{pmatrix}1 & 0\\ 0 & -1\end{pmatrix}. \tag{5.9}$$

The charge states of the pions are written as

$$\pi^{\pm}=\frac{1}{\sqrt{2}}(\pi_1\mp i\pi_2),\qquad \pi^0=\pi_3. \tag{5.10}$$

Thus, we can identify the charged pions $\pi^{\pm}$ by the flavor indices $(a,b=1,2)$ and the neutral pion π^0 by the flavour index $a=3$. In this chapter, we will be interested in the physics involving the $\pi^{\pm}$, namely, we will focus just in the indexes $(a,b=1,2)$. This way, the function $\beta_A^{aa}(z)$ in (5.6, 5.7) and defined in (4.86) becomes

$$\beta_A^{11}(z)=\frac{g_5^2}{z^2}M_A^{11},\qquad \frac{M_A^{11}}{2}=\mathrm{Tr}(\{T^1,X_0\}\{T^1,X_0\}), \tag{5.11}$$

$$\beta_A^{22}(z)=\frac{g_5^2}{z^2}M_A^{22},\qquad \frac{M_A^{22}}{2}=\mathrm{Tr}(\{T^2,X_0\}\{T^2,X_0\}), \tag{5.12}$$

where, for the SU(2) case, $X_0(z)$ is given by

$$X_0=\frac{1}{2}\begin{pmatrix}v_u & 0\\ 0 & v_d\end{pmatrix}, \tag{5.13}$$

and where we have used the definitions

$$v_u(z) = \zeta m_u z + \frac{1}{\zeta}\sigma_u z^3, \quad v_d(z) = \zeta m_d z + \frac{1}{\zeta}\sigma_d z^3 \tag{5.14}$$

As we have discussed in chapter 2, the up and down quark masses are very close. It is then a very good approximation for the SU(2) case to consider the isospin symmetry limit for the up and down quarks: $m_u = m_d = m_q$ and $\sigma_u = \sigma_d = \sigma$. This led us to $v_u = v_d = v$ and makes X_0 proportional to identity matrix, as

$$X_0 = \frac{1}{2}v(z)\mathbb{1}_{2\times 2}. \tag{5.15}$$

Finally, this simplifies $\beta_A^{11}(z) = \beta_A^{22}(z) = \beta(z)$, which can be written as

$$\beta(z) = \frac{g_5^2}{z^2}v(z)^2 = g_5^2\Big(\zeta m_q + \frac{\sigma}{\zeta}z^2\Big)^2. \tag{5.16}$$

Having set all the above, we are almost ready to extract the spectrum of the pions in the present hard wall holographic model. We first rewrite Eqs. (5.6), (5.7) in a simple way for the normalized modes:

$$\frac{\beta(z)}{z}\left[\pi^n(z) - \phi^n(z)\right] = -\partial_z\left[\frac{1}{z}\partial_z\phi^n(z)\right], \tag{5.17}$$

$$\beta(z)\,\partial_z\pi^n(z) = m_{\pi^n}^2\partial_z\phi^n(z), \tag{5.18}$$

where we have omitted the flavors indices once we already considering the case for our interest: the pion. So, from now on, it will be omitted. In order to obtain the spectrum directly from those equations, is convenient to decouple them defining a new function $\Pi^n(z) = \partial_z\pi^n(z)$ and finding a new and independent equation for this function. This way, we have

$$(z\partial_z)^2\,\Pi^n(z) + A(z)z\partial_z\Pi^n(z) + B^n(z)\Pi^n(z) = 0\,, \tag{5.19}$$

with $A(z)$ and $B_n(z)$ given by

$$A(z) = z\partial_z\ln\beta(z) - 2, \tag{5.20}$$

$$B_n(z) = 1 + z^2\left[\partial_z^2\ln\beta(z) + m_{\pi^n}^2 - \beta(z)\right]. \tag{5.21}$$

The boundary conditions for a new function comes naturally from (4.100), (4.101) given by

$$\Pi^n(z)|_{z=\epsilon} = 0 \quad \text{and} \quad \Pi^n(z)|_{z=z_0} = 0. \tag{5.22}$$

Then, using the function $\Pi^n(z)$ we reduced the problem of finding the spectrum via a coupled equations systems to solve one differential equation. Similarly to the functions $\pi^n(z)$ and $\phi^n(z)$, the new function $\Pi^n(z)$ also obey a normalization condition, which is, easily found using Eq. (4.89). We can write the normalized function in the form $\Pi^n_N(z) = C_n \Pi^n_U(z)$, where we defined $\Pi^n_U(z)$ as the unnormalized function associated with $\Pi^n(z)$, and C_n being its normalization constant:

$$\int \frac{dz}{z}\,\beta(z)\,\Pi^n(z)\Pi^m(z) = m^2_{\pi^n}\delta^{mn}, \tag{5.23}$$

where we have chosen to C_n as

$$C_n = \frac{m_{\pi^n}}{N_{\pi^n}}, \tag{5.24}$$

which, in turn, leads to

$$N^2_{\pi^n} = \int \frac{dz}{z}\,\beta(z)\,\left[\Pi^n_U(z)\right]^2. \tag{5.25}$$

This normalization condition will be useful when we rewrite the decay constants.

5.1.1 Asymptotic expansion

Another great advantage in the definition of $\Pi^n(z)$ is that it allows us evaluate the asymptotic expansion near to the boundary $z = \epsilon$, where the gauge field theory lives. We use the Frobenius's method to find this expansion and we get

$$\begin{aligned} \Pi^n(z) &= C_n\left[-z + \frac{1}{4}\left(m^2_{\pi^n} + \frac{32\pi^2\sigma}{3m_q} - 3m_q^2\right)z^3 + \cdots\right] \\ &= C_n\,\Pi^n_U(z), \quad z \to 0, \end{aligned} \tag{5.26}$$

where the dots represent higher powers in z. In the numerical procedure we will focus on the function $\Pi^n_U(z)$. Note that the solution (5.26) naturally satisfies the Dirichlet boundary condition (4.100), showing the consistency of the approach. Using this asymptotic expansion we also obtain the asymptotic expansions for the functions $\pi^n(z)$ and $\phi^n(z)$, as

$$\begin{aligned} \pi^n(z) &= C_n\left[-\frac{z^2}{2} + \frac{1}{4}\left(m^2_{\pi^n} + \frac{32\pi^2\sigma}{3m_q} - 3m_q^2\right)\frac{z^4}{4} + \cdots\right] \\ \phi^n(z) &= -C_n\frac{g_5^2}{m^2_{\pi^n}}\left[\xi^2 m_q^2\frac{z^2}{2} + 2m_q\sigma\frac{z^4}{4} + \cdots\right], \quad z \to 0. \end{aligned} \tag{5.27}$$

5.2 Extended PCAC and Generalized GOR

Let us use again the holographic currents that we have evaluated in the previous chapter to find an important relation. First of all, we take the divergence of the axial holographic current (4.103) and use the on-shell 4d equation of motion for the $\hat{\pi}_n(x)$ obtained from the Eq. (4.90), $\partial^2\hat{\pi}^n(x) = m^2_{\pi^n}\hat{\pi}_n(x)$, to get

$$\partial_\mu\langle J_A^{\hat{\mu}}(x)\rangle = \sum_{n=0}^{\infty} f_{\pi^n} m^2_{\pi^n}\hat{\pi}^n(x). \tag{5.28}$$

This relation clearly shows that the divergence of the axial vector current (in QCD it is related to the fundamental degrees of freedom, the quarks) is completely determined by hadronic properties. We can see this in a more formal way: using the Eq. (4.96) in the expression for pseudoscalar holographic current (4.104), we obtain

$$\langle J_\Pi(x)\rangle \;\; = \;\; -\sum_{n=0}^{\infty}\left[\frac{\beta(z)}{g_5 z}\partial_z\pi^n(z)\right]_{z=\epsilon}\hat{\pi}^n(x) = \sum_{n=0}^{\infty} f_{\pi^n} m^2_{\pi^n}\hat{\pi}^n(x), \tag{5.29}$$

where we have used the holographic prescription for the pseudoscalar decay constant (4.105). From these relations, we find the relation

$$\partial_{\hat{\mu}}\langle J_A^{\hat{\mu}}(x)\rangle \;\; = \;\; \langle J_\Pi(x)\rangle. \tag{5.30}$$

That is, we see that the bottom-up holographic QCD model give us a notable relation between axial and the pseudoscalar sectors. This relation is strictly identical to partially conserved axial current (PCAC) relation derived in chapter 2 in the current algebra context, in which, the divergence of the axial vector current operator is dominated by the chiral Goldstone bosons, namely, the pions (in the present case). The relation (5.30) can be seen as the holographic version of PCAC. Finally, the expression in (5.29) still provide us the following notable relation

$$f_{\pi^n} m^2_{\pi^n} \;\; = \;\; -\left[\frac{\beta(z)}{g_5 z}\partial_z\pi^n(z)\right]_{z=\epsilon}. \tag{5.31}$$

Note that we have found a relation similar to the generalized GOR relationship (5.1) derived in the Dyson-Schwinger approach [13]. Because of this similarity, we name it as holographic generalized GOR relationship (HGOR), once that it came from an holographic approach and it is valid for the ground state of the pion, as well as, for their excitations.

Now, it straightforward to make the connection with the ρ-function introduced via Dyson-Schwinger equations and related with the condensate for the ground state. In fact, comparing

Eq. (5.31) with the Eq. (5.1) from the Dyson-Schwinger approach, we find the following holographic prescription for the ρ-function

$$\rho_{\pi^n} = -\frac{1}{2m_q}\left[\frac{\beta(z)}{g_5 z}\partial_z \pi^n(z)\right]_{z=\epsilon} . \tag{5.32}$$

A very important point here is that the generalized HGOR and the holographic ρ-functions are entirely determined by the asymptotic behavior of the field $\pi^n(z)$. This is quite different compared with the Dyson-Schwinger approach, where the ρ-function is obtained by solving a set of coupled integral equations and in general involves a painful numerical efforts.

We can still find a reduced expression for the decay constant (5.31) and for the ρ-function (5.32). Using the asymptotic behavior for the $\pi^n(z)$ given in (5.27) and the expression for the $\beta(z)$ in (5.16), we find following expression

$$f_{\pi^n} = g_5\zeta^2\frac{m_q^2}{m_{\pi^n}N_{\pi^n}}, \tag{5.33}$$

for the leptonic decay constant of the pion and its excitations, and

$$\rho_{\pi^n} = \frac{g_5\zeta^2}{2}\frac{m_q m_{\pi^n}}{N_{\pi^n}}, \tag{5.34}$$

for the ρ-function of the pion and its all excitations. In the chiral limit, the vanishing of the decay constant and the finiteness of the ρ-function depends on the behavior of the hadronic masses (m_{π^n}) and the normalization constant (N_{π^n}) with the quark masses. In section (5.4), we will show numerically these dependencies using the Mathematica code.

5.3 Fixing the free parameters

The model considered here, contains just two free parameters: the position of hard wall z_0 and the chiral condensate σ. In principle, we should also consider the quark mass as an input parameter, but we won't, instead, it will be considered a variable of the dependence of m_{π^n} and N_{π^n}. In order to fix the position of hard wall z_0, we follow the standard procedure used previously in the literature by fixing it by fitting the ρ meson mass. To do this, we use the equation for the vector field, given in Eq. (4.91):

$$\left[-\partial_z\left(\frac{1}{z}\partial_z\right)+\frac{1}{z}\beta_V^a(z)\right]v^{a,n}(z) = \frac{m_{V^{a,n}}^2}{z}v^{a,n}(z). \tag{5.35}$$

The ρ meson belongs to adjoint representation of the SU(2), where its matrix representation is given as $V = V^i t^i$, assuming form

$$V = \frac{1}{\sqrt{2}}\begin{pmatrix}\frac{\rho^0}{\sqrt{2}} & \rho^+ \\ \rho^- & -\frac{\rho^0}{\sqrt{2}}\end{pmatrix}, \tag{5.36}$$

where we have used the definition for the t^i matrices given in (5.9). The charge states of the ρ mesons are defined as

$$\rho^{\pm} = \frac{1}{\sqrt{2}}(V_1 \mp iV_2), \quad \rho^0 = V_3. \tag{5.37}$$

We will be interested in the uncharged ρ meson (ρ^0); then, setting $a = 3$, the function $\beta_V^a(z)$ takes the form

$$\beta_V^3(z) = \frac{g_5^2}{z^2}(M_V^3)^2, \quad \frac{(M_V^3)^2}{2} = -\mathrm{Tr}([T^3, X_0][T^3, X_0]). \tag{5.38}$$

By the isospin symmetry, we have seen that $2X_0 = v(z)\mathbb{1}_{2\times 2}$ and as direct consequence, we get $\beta_V^3(z) = 0$. This fact allows us to find an analytical solution for the Eq. (5.35) with the following boundary conditions $v^n(\epsilon \to 0) = \partial_z v^n(z_0) = 0$.

Using the Dirichlet condition $v^n(\epsilon \to 0) = 0$), we find

$$v^n(z) = \frac{\sqrt{2}zJ_1(zm_{\rho^n})}{z_0J_1(z_0m_{\rho^n})}, \tag{5.39}$$

where the function is normalized by the normalization condition in Eq. (4.87)

$$\int \frac{dz}{z}v^m(z)v^n(z) = \delta^{mn}. \tag{5.40}$$

Note that, for simplicity, we have omitted the index $a = 3$. The Neumann boundary condition, $\partial_z v^n(z_0) = 0$, in the IR gives the condition $J_0(z_0 m_{\rho^n}) = 0$. This naturally shows a discrete mass spectrum for the ρ meson. So, if r_n denote the n-th zero of J_0, the masses are given by

$$m_{\rho^n} = \frac{r_n}{z_0}. \tag{5.41}$$

Now, we use the mass of the ground state ($n = 0$) for the ρ meson to fix the z_0 parameter. Indeed, using $M_{\rho^0} = 775.55$ MeV we get the value

$$z_0 = \frac{1}{322.5}\mathrm{MeV}^{-1}, \tag{5.42}$$

About the chiral condensate, we first recall that from QCD, we know that the chiral condensate has a dependence in the quark mass and this behavior is not taken into account in the present model. But, probably this does not affect significantly the results once we are near to the chiral limit. As input parameter, we follow the main references [7, 8, 9] and use the value $\sigma = (213.7\ \mathrm{MeV})^3$.

5.4 Numerical results and discussions

In this section we present our numerical results for this chapter. We start obtaining the mass spectrum of the pions. The spectrum is obtained by solving Eq. (5.19) for the auxiliary wave function $\Pi^n(z) = \partial_z \pi^n(z)$ and imposing the boundary conditions $\pi^n(\epsilon) = 0$ and $\partial_z \pi^n(z_0) = 0$. Using the asymptotic solution in Eq. (5.26) we integrate numerically Eq. (5.19) from $z = \epsilon$ to $z = z_0$ with a Mathematica code. For this, we use one of the many numerical methods available in that platform, the shooting method, which consists basically in finding values in the parameter-plane m_{π^n} vs m_q until we find a solution that satisfies the IR condition $\Pi^n(z_0) = \partial_z \pi^n(z_0) = 0$.

Due to the linearity property of Eq. (5.19), it is sufficient to work with the unnormalized wave function $\Pi_U^n(z)$, defined in Eq. (5.26), to obtain the pion spectrum. This is equivalent to setting C_n to 1. This done, Fig. (5.1) displays the results for the m_q dependence of the masses, for the ground state and first three excited states of the pion.

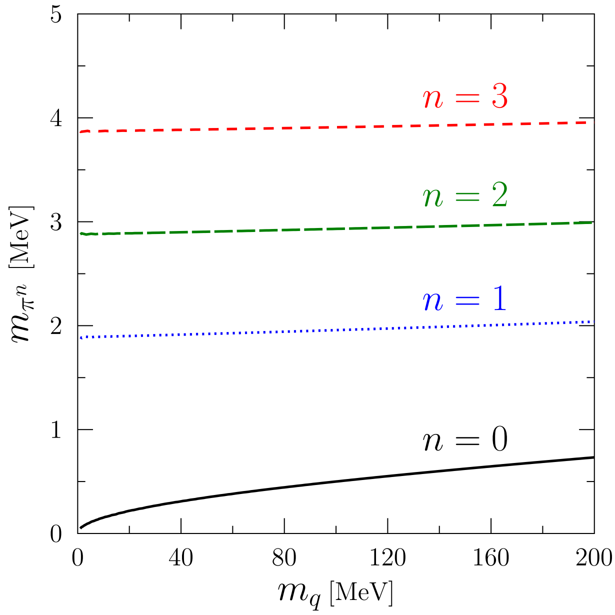

Figure 5.1: Quark mass dependence of the pion masses.

In our code, we have also generated solutions for $n > 3$ up to $n = 6$ and the m_q dependence of those solutions is quite similar to that shown in Fig. (5.1) for the three lowest excited states. Fitting the mass of the ground-state pion, we obtain that $m_{\pi^0} \sim m_q^{1/2}$ near to the chiral limit, which is the required behavior by the GOR, Eq. (5.5). On the other hand, fitting the masses of the excited states, we find a linear form as $m_{\pi^n} = m_{\pi^n}^0 + a_n m_q$, where $m_{\pi^n}^0$ are the corresponding masses in the chiral limit and a_n is slope for each linear form.

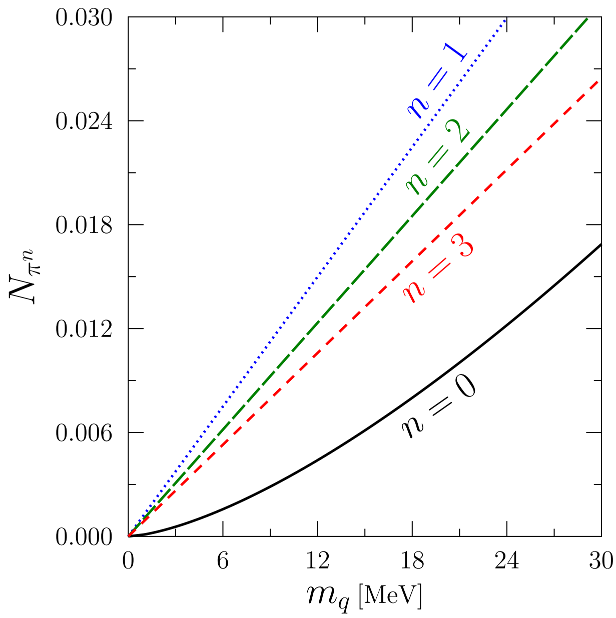

Figure 5.2: Quark mass dependence of the normalization constants.

Now, we will consider the m_q dependence of the normalization constant N_{π^n}, defined in Eq. (5.25), in order to establish the finiteness of ρ_{π^n}-function in the chiral limit. As we see, the N_{π^n} are completely determined from the knowledge of the unnormalized wave functions $\Pi_U^n(z)$, which in turn enter in the determination of the mass spectrum. We displayed the results obtained in Fig. (5.2).

Fitting the curve for the ground-state pion, we obtain that $N_{\pi^0} \sim m_q^{3/2}$, while the fitting for the excited states are done with linear function as $N_{\pi^n} \sim m_q$, $n \geq 1$. As we will show soon, these different m_q dependencies of N_{π^n} for the ground state and the excited states, when combined with the different m_q dependence of m_{π^n}, are responsible for the finiteness of f_{π^0} and the vanishing of f_{π^n} for $n \geq 1$ in the chiral limit.

Once the mass spectrum and the normalization constant N_{π^n} are known, we can readily determine the function ρ_{π^n} using its reduced formula in Eq. (5.32). We displayed our results in Fig. (5.3). In this figure, the curves show that the function ρ_{π^n} is finite as $m_q \to 0$ and m_q independent for all the values of n investigated within of range $0 \leq m_q \leq 30$ MeV. Focusing near to the chiral limit, for the ground state, as we have $m_{\pi^0} \sim m_q^{1/2}$ and $N_{\pi^0} \sim m_q^{3/2}$, the ρ_{π^n} function behaves like

$$\rho_{\pi^0} = g_5 \zeta^2 \frac{m_q m_{\pi^0}}{N_{\pi^0}} \sim g_5 \zeta^2, \tag{5.43}$$

and for the excited states, as $m_{\pi^n} \sim m_{\pi^n}^0$ and $N_{\pi^n} \sim m_q$, we obtain

$$\rho_{\pi^n} = g_5 \zeta^2 \frac{m_q m_{\pi^n}}{N_{\pi^n}} \sim m_{\pi^n}^0, \quad n \geq 1. \tag{5.44}$$

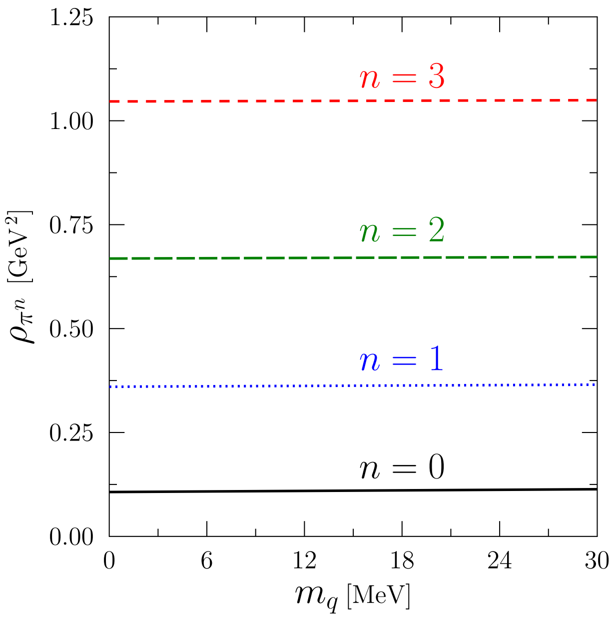

Figure 5.3: Quark mass dependence of ρ_{π^n}.

This clearly establishes the finiteness of ρ_{π^n} in the chiral limit, in complete agreement with the results obtained in the context of the Dyson-Schwinger approach in QCD. As we discuss next, it leads to the conclusion that in the chiral limit, $f_{\pi^n} = 0$ for $n \geq 1$.

At this stage we are able to present our main numerical results of the present chapter, namely the behavior of the pion decay constants f_{π^n} near to the chiral limit. We displayed our results in Fig. (5.4). As one can see from this figure, the ground-state pion possesses a finite leptonic decay constant f_{π^0} while the excited states have leptonic decay constants f_{π^n} that vanish in the chiral limit, revealing that the present holographic QCD model also reproduces the exact result in QCD. We can still obtain the m_q dependence of f_{π^0} near to the chiral limit. In fact, for the ground state we have the following behavior

$$f_{\pi^0} = g_5 \zeta^2 \frac{m_q^2}{m_{\pi^0} N_{\pi^0}} \sim g_5 \zeta^2. \tag{5.45}$$

We also note that the curves in Fig. (5.4) for the excited states can be fitted with a linear quark mass dependence. Such a linear m_q scaling of f_{π^n} for $n \geq 1$ is precisely the one predicted in QCD [13] through the generalized GOR relationship, Eq. (5.33)

$$f_{\pi^n} = g_5 \zeta^2 \frac{m_q^2}{m_{\pi^n} N_{\pi^n}} \sim m_q, \quad n \geq 1. \tag{5.46}$$

Note that, for $m_q = 8.31$ MeV, the ground-state pion decay constant is $f_{\pi^0} \approx 92.4$MeV. We show in table (5.1) some values for f_{π^n}. The results shown in table (5.1) explicitly show a big suppression for the excited states when compared with the ground state. In general, it is very

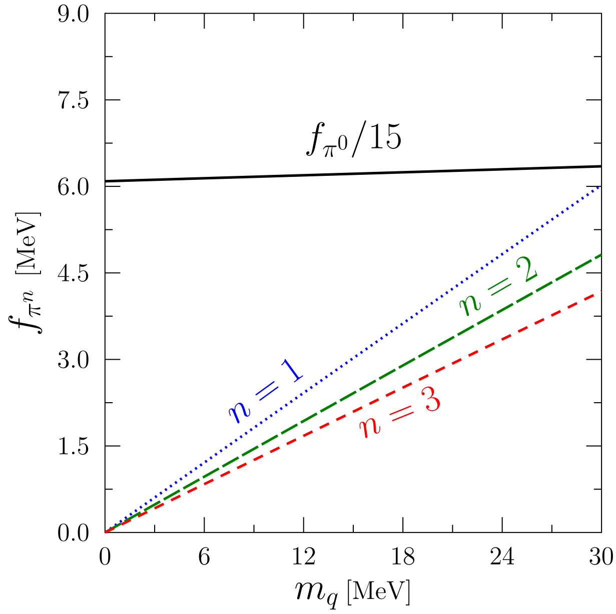

Figure 5.4: Quark mass dependence of f_{π^n}.

n	0	1	2	3
f_{π^n} (MeV)	92.4	1.68	1.34	1.16

Table 5.1: Leptonic decay constants for the ground-state and the first three excited states of the pion.

difficult the experimental extraction of the leptonic decay constants of the excited states due to the fact that the decays are dominated by strong decays. From B decays [89], it is possible to extract a bound on f_{π^1}, which is $f_{\pi^1} < 0.064\ f_{\pi^0}$. Our result in table 5.1 is in perfect agreement with this bound, however it is about five times smaller than the lattice result of Ref. [87].

Before finish our discussion, let us for completeness examine $\rho^0_{\pi^n}$, which is the chiral limit of ρ_{π^n} defined in Eq. (5.3), as a function of the pion masses of excited states in the chiral limit, $m^0_{\pi^n}$. Note that although the ρ_{π^n} are, to a good precision, m_q independent, the masses m_{π^n} are slightly dependent on m_q and this makes the m_{π^n} dependence of ρ_{π^n} nontrivial. Our results are shown in Fig. (5.5). We found that the six lowest discrete eigenvalues can be fitted as

$$\rho^0_{\pi^n} = \gamma \left(m^0_{\pi^n} \right)^{3/2}, \quad n \geq 1, \tag{5.47}$$

with $\gamma = 4.375\,\mathrm{MeV}^{1/2}$. In this way, Eq. (5.33) implies that the pion decay constant, for excited

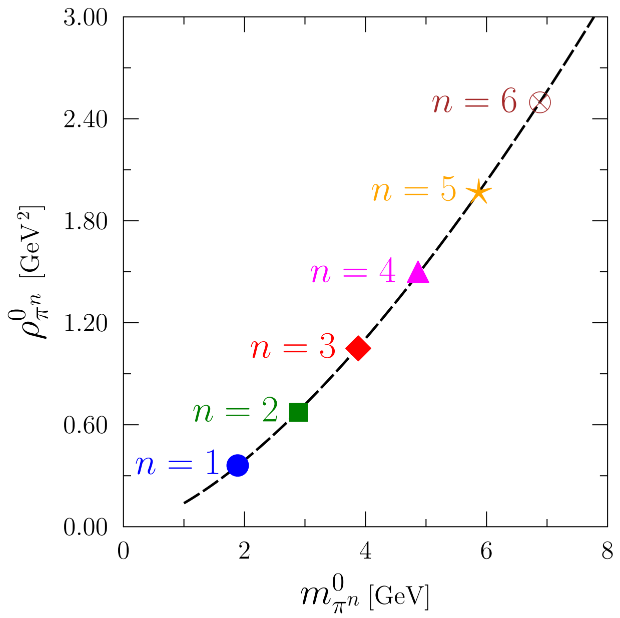

Figure 5.5: The function $\rho^0_{\pi^n}$, for the first six excited states. The dashed line is a fit to the discrete eigenvalues.

states, takes the following form

$$f^0_{\pi^n} = \lim_{m_q \to 0} f_{\pi^n} = \gamma \, \frac{2m_q}{\sqrt{m^0_{\pi^n}}}, \quad n \geq 1. \tag{5.48}$$

It is important to mention here that the present model, the hard wall holographic QCD model fails dramatically to reproduce the famous Regge trajectory of mesons. This failure is a typical feature of some holographic QCD models that are based on the supergravity approximation. The more realist soft-wall holographic QCD model, which contains an additional background dilaton field, proposed by Karch et al. [100], is capable to reproduce the correct Regge trajectory of mesons and it is also expected to emerge from string theory beyond the supergravity approximation. Besides, as pointed out in Ref. [101], in order to get a chiral condensate consistent with dynamical chiral symmetry breaking it is necessary the inclusion of higher order terms in the background scalar potential $U(X)$, as a quartic term. Despite of that, moving from a hard-wall background to a soft-wall background, the meson wave functions change, but none of the holographic prescriptions for the currents will be changed. The reason is that the soft-wall dilaton goes to zero in the ultraviolet regime. In addition, due to the fact that the background scalar X and the unnormalized pion wave function should have the same ultraviolet behavior as in the hard-wall model, the ρ function, defined in Eqs. (5.32) and (5.34), should also remain valid. As a direct consequence, this means the way we derived the GOR relation is just modified by the soft wall dilaton and potential $U(X)$

will be dictated by the normalization constants of the pion wave functions. Therefore, it is quite natural to think that the qualitative conclusion of the dramatic suppression of the leptonic decay constants of pion's excited states will therefore remain valid in the soft-wall model. Although, our results are derived in a hard wall model of holographic QCD, nevertheless, we believe that the vanishing of the leptonic decay constants of pion's excited states in the chiral limit will occur in any holographic QCD model that implements dynamical chiral symmetry breaking and gives the generalized GOR relationship. A detailed study of this will be the subject of a future work.

6 Strong couplings and form factors of charmed mesons in Holographic QCD

The important role that electromagnetic (EM) form factors play in our understanding of hadronic structure has been well established for more than fifty years. They can give important information about the internal structure of hadrons in terms of quark and gluon degrees of freedom and their shapes. A good example is the great attention given to the electromagnetic form factors of the nucleon [102, 103, 104], both experimentally and theoretically. Of particular recent interest, are the form factors of the pion and the kaon, once these pseudoscalar mesons are pseudo Goldstone bosons associated with the dynamical chiral symmetry breaking and also because they play important role in the study of the nuclear force. On the pion electromagnetic form factor, there are various works using lattice calculations [105, 106, 107] and also there is an important experimental result from the scattering of 300 GeV pions from electrons of a liquid hydrogen target [108]. On the other hand, the kaon electromagnetic form factor is poorly known experimentally, except in the region of very low momentum transfer [109]. Vector meson electromagnetic form factors have received less attention due to great experimental difficulties to access information.

Nowadays, there is widespread theoretical and experimental interest in the study of the interactions of charmed hadrons with light hadrons, in special in the properties of D mesons in nuclear matter [110]. These D mesons are also important in the context of the so-called X,Y,Z exotic hadrons, named as exotic due to the fact that they do not have the composition as predicted in the quark model of either quark anti-quark (mesons) or threequark (baryons). A good review is found in Ref. [111]. Unfortunately, a firm theoretical understanding about these new hadrons is still missing. In addition to investigations happening at existing laboratories, like the LHC and BES III, there is an extensive program [112, 113] at the forthcoming FAIR facility, aiming at the investigation of charmed hadrons and their interactions with ordinary matter.

The theoretical study of the charmed interactions with light faces big challenges due the lack of experimental information on the interactions in free space. For example, most of the present knowledge on the DN interaction arises from calculations based on effective Lagrangians that, in turn, are generalizations of light-flavor chiral Lagrangians using $SU(4)$ flavor symmetry [114, 115, 116, 117, 118] and heavy quark symmetry [119, 120]. Normally, such Lagrangians involve strong coupling constants whose values are taken from $SU(4)$ flavor and heavy-quark symmetry relations. A known example involves the coupling constants of the ρ meson to the pseudoscalar mesons (π, K, D), that invoking the $SU(4)$ flavor symmetry we have

$$g_{\rho DD} = g_{\rho KK} = \frac{g_{\rho\pi\pi}}{2}. \tag{6.1}$$

In addition, if we require the heavy-quark spin symmetry, we obtain the following relations [121]

$$g_{\rho DD} = g_{\rho D^* D} = g_{\rho D^* D^*} = g_{\pi D^* D}. \tag{6.2}$$

Other approaches have studied the symmetry breaking pattern in the strong couplings, calculations based on QCD sum rules found $SU(4)$ symmetry breaking in three-hadron couplings whose values vary from 7% to 70% [19], in another work [20], using a model which is constrained by Dyson-Schwinger equations of QCD, the authors found that the relation $g_{\rho DD} = g_{\rho\pi\pi}/2$ is violated at the level of 300% or more, in a more recent work [21], using the same model, the authors find that $SU(4)$ symmetry relations between couplings of D, D^*-mesons and π, ρ-mesons can deviate by almost an order-of-magnitude, and besides that, the corresponding form factors also exhibit different momentum dependences. As we will see soon, the results of calculations presented here will be more in line that using the $^3\mathrm{P}_0$ quark-pair creation model in the nonrelativistic quark model [17, 18].

Flavor symmetry is strongly broken in the QCD Lagrangian due to the largely different values of the quark masses. While in the light quark sector one has good $SU(2)$ flavor symmetry ($m_u \approx m_d$), in the $SU(3)$ and $SU(4)$ sector, this symmetry is badly broken ($m_c \gg m_s \gg m_u$) at the level of the QCD Lagrangian. Given the importance of effective Lagrangians in the study of a great variety of phenomena involving D-mesons, we extend the holographic QCD model presented in chapter 4 for the case of $N_f = 4$ in order to include the charm quark. With the extended model, we can investigate the implications of the widely different values of the quark masses on the effective three-meson couplings $g_{\rho DD}$ and $g_{\rho D^* D^*}$ and the electromagnetic form factors of the D and D^* mesons. The parameters of the model are the quark masses, the chiral condensates and the location of the hard wall z_0.

The organization of this chapter is as follows. In section 6.1, we identify the flavor indices for the pseudoscalar and the vector mesons and also we rewrite the equations that describe them. In section 6.2, we obtain the effective Lagrangians for the interactions involving two pseudoscalars and one vector meson, and also the interaction of three vector mesons. In section 6.3, we discuss the electromagnetic form factors (EMFF) and how it can be decomposed in terms of neutral flavor currents, as in the vector meson dominance (VMD) model. Using the effective Lagrangians, we show the expressions for the electromagnetic form factors of the pseudoscalar and vector mesons. We also discuss the high and low Q^2 limits of those form factors. In section 6.4, we present the numerical results for the strong coupling constants and the electromagnetic form factors for the pseudoscalars pion, kaon and D meson and for the vector mesons ρ, K^* and D^* mesons.

6.1 Mesonic spectrum

We start reviewing the equations that allows us to evaluate the spectrum of pseudoscalar and vector mesons. To reach this, we focus on the action of the model expanded up to second order, described in detail in chapter 4. Recalling that the pseudoscalars are described by π^a and as we are considering four flavors, we write the $SU(4)$ matrix for the pseudoscalar mesons, as

$$\pi = \pi^a t^a = \frac{1}{\sqrt{2}} \begin{pmatrix} \frac{\pi_3}{\sqrt{2}} + \frac{\pi_8}{\sqrt{6}} + \frac{\pi_{15}}{\sqrt{12}} & \frac{\pi_1 - i\pi_2}{\sqrt{2}} & \frac{\pi_4 - i\pi_5}{\sqrt{2}} & \frac{\pi_9 - i\pi_{10}}{\sqrt{2}} \\ \frac{\pi_1 + i\pi_2}{\sqrt{2}} & -\frac{\pi_3}{\sqrt{2}} + \frac{\pi_8}{\sqrt{6}} + \frac{\pi_{15}}{\sqrt{12}} & \frac{\pi_6 - i\pi_7}{\sqrt{2}} & \frac{\pi_{11} - i\pi_{12}}{\sqrt{2}} \\ \frac{\pi_4 + i\pi_5}{\sqrt{2}} & \frac{\pi_6 + i\pi_7}{\sqrt{2}} & -2\frac{\pi_8}{\sqrt{6}} + \frac{\pi_{15}}{\sqrt{12}} & \frac{\pi_{13} - i\pi_{14}}{\sqrt{2}} \\ \frac{\pi_9 + i\pi_{10}}{\sqrt{2}} & \frac{\pi_{11} + i\pi_{12}}{\sqrt{2}} & \frac{\pi_{13} + i\pi_{14}}{\sqrt{2}} & -3\frac{\pi_{15}}{\sqrt{12}} \end{pmatrix}. \tag{6.3}$$

In this way, we use this representation to identify the indices that represent the meson states. This can be done if we write the pseudoscalar matrix with the pseudoscalar mesons, as follows

$$P = \frac{1}{\sqrt{2}} \begin{pmatrix} \frac{\pi^0}{\sqrt{2}} + \frac{\eta}{\sqrt{6}} + \frac{\eta_c}{\sqrt{12}} & \pi^+ & K^+ & \bar{D}^0 \\ \pi^- & -\frac{\pi^0}{\sqrt{2}} + \frac{\eta}{\sqrt{6}} + \frac{\eta_c}{\sqrt{12}} & K^0 & D^- \\ K^- & \bar{K}^0 & -\sqrt{\frac{2}{3}}\eta + \frac{\eta_c}{\sqrt{12}} & D_s^- \\ D^0 & D^+ & D_s^+ & -\frac{3}{\sqrt{12}}\eta_c \end{pmatrix}, \tag{6.4}$$

where we have the made identifications:

$$\pi^\pm = \frac{1}{\sqrt{2}}(\pi_1 \mp i\pi_2), \qquad \pi^0 = \pi_3,$$

$$K^\pm = \frac{1}{\sqrt{2}}(\pi_4 \mp i\pi_5), \quad K^0 = \frac{1}{\sqrt{2}}(\pi_6 - i\pi_7), \quad \bar{K}^0 = \frac{1}{\sqrt{2}}(\pi_6 + i\pi_7), \quad \eta = \pi_8,$$

$$\bar{D}^0 = \frac{1}{\sqrt{2}}(\pi_9 - i\pi_{10}), \quad D^0 = \frac{1}{\sqrt{2}}(\pi_9 + i\pi_{10}), \quad D^\pm = \frac{1}{\sqrt{2}}(\pi_{11} \pm i\pi_{12}),$$

$$D_s^{\pm} = \frac{1}{\sqrt{2}}(\pi_{13} \pm i\pi_{14}), \qquad \eta_c = \pi_{15}. \tag{6.5}$$

In chapter 4 we have seen that the mass spectrum of the pseudoscalar and axial mesons are obtained by solving a set of coupled differential equations that represent the normalized modes moving in the AdS$_5$ background. These equations, defined in Eqs. (4.94), (4.95) and (4.96), are given by

$$\frac{\beta_A^{aa}(z)}{z}\left[\pi^{a,n}(z) - \phi^{a,n}(z)\right] = -\partial_z\left[\frac{1}{z}\partial_z\phi^{a,n}(z)\right], \tag{6.6}$$

$$\beta_A^{aa}(z)\,\partial_z\pi^{a,n}(z) = m^2_{\pi^{a,n}}\partial_z\phi^{a,n}(z), \tag{6.7}$$

$$\left[-\partial_z\left(\frac{1}{z}\partial_z\right) + \frac{1}{z}\beta_A^{aa}(z)\right]a^{a,n}(z) = \frac{m^2_{A^{a,n}}}{z}a^{a,n}(z), \tag{6.8}$$

where we do not have considered the mixed terms, which are relevant for the η, η_c physics.

Similarly, in the vector sector, one can also write a $SU(4)$ matrix with the vector mesons in order to incorporate them in our approach. As in the pseudoscalar case, we have $V = V^a t^a$ which has the same structure of (6.3). Then, we have that

$$V = V^a t^a = \frac{1}{\sqrt{2}}\begin{pmatrix} \frac{\rho^0}{\sqrt{2}} + \frac{\omega'}{\sqrt{6}} + \frac{\psi}{\sqrt{12}} & \rho^+ & K^{*+} & \bar{D}^{*0} \\ \rho^- & -\frac{\rho^0}{\sqrt{2}} + \frac{\omega'}{\sqrt{6}} + \frac{\psi}{\sqrt{12}} & K^{*0} & D^{*-} \\ K^{*-} & \bar{K}^{*0} & -\sqrt{\frac{2}{3}}\omega' + \frac{\psi}{\sqrt{12}} & D_s^{*-} \\ D^{*0} & D^{*+} & D_s^{*+} & -\frac{3}{\sqrt{12}}\psi \end{pmatrix}, \tag{6.9}$$

where we have the made identifications:

$$\rho^{\pm} = \frac{1}{\sqrt{2}}(V_1 \mp iV_2), \qquad \rho^0 = V_3,$$

$$K^{*\pm} = \frac{1}{\sqrt{2}}(V_4 \mp iV_5), \quad K^{*0} = \frac{1}{\sqrt{2}}(V_6 - iV_7), \quad \bar{K}^{*0} = \frac{1}{\sqrt{2}}(V_6 + iV_7), \quad \omega' = V_8,$$

$$\bar{D}^{*0} = \frac{1}{\sqrt{2}}(V_9 - iV_{10}), \qquad D^{*0} = \frac{1}{\sqrt{2}}(V_9 + iV_{10}), \qquad D^{*\pm} = \frac{1}{\sqrt{2}}(V_{11} \pm iV_{12}),$$

$$D_s^{*\pm} = \frac{1}{\sqrt{2}}(V_{13} \pm iV_{14}), \qquad \psi = V_{15}, \tag{6.10}$$

In this case, the mass spectrum of the vector and scalar mesons are found by solving a set of second order differential equations given in Eqs. (4.91), (4.92) and (4.92) that represent the normalized modes moving in AdS_5 background. We write down the equations for the vector sector

$$
\begin{aligned}
&\left[-\partial_z\left(\frac{1}{z}\partial_z\right)+\frac{1}{z}\beta_V^a(z)\right]v^{a,n}(z)=\frac{m^2_{V^{a,n}}}{z}v^{a,n}(z)\,,\\
&\frac{\beta_V^a(z)}{z}\left[\tilde{\pi}^{a,n}(z)-\tilde{\phi}^{a,n}(z)\right]=-\partial_z\left[\frac{1}{z}\partial_z\tilde{\phi}^{a,n}(z)\right]\,,\\
&\beta_V^a(z)\,\partial_z\tilde{\pi}^{a,n}(z)=m^2_{\pi_V^{a,n}}\partial_z\tilde{\phi}^{a,n}(z).
\end{aligned}
\tag{6.11}
$$

In this stage, it is important to recall that the leptonic decay constants associated with these mesons. Holographically, they are defined in terms of the normalized modes as

$$
\begin{aligned}
g_{V^{a,n}} &= \left[\frac{1}{g_5 z}\partial_z v^{a,n}(z)\right]_{z=\epsilon}, \quad f_{\pi_V^{a,n}}=-\left[\frac{1}{g_5 z}\partial_z\tilde{\phi}^{a,n}(z)\right]_{z=\epsilon},\\
g_{A^{a,n}} &= \left[\frac{1}{g_5 z}\partial_z a^{a,n}(z)\right]_{z=\epsilon}, \quad f_{\pi^{a,n}}=-\left[\frac{1}{g_5 z}\partial_z\phi^{a,n}(z)\right]_{z=\epsilon}.
\end{aligned}
\tag{6.12}
$$

As observed in the previous chapter, the divergence of the axial current is related with the pseudoscalar current, this is the PCAC relation. Similarly, taking the divergence of the vector current in Eq. (4.110) and using the on-shell 4d equation of motion for the $\hat{\pi}_V^{a,n}(x)$ obtained from the Eq. (4.90), $\partial^2\hat{\pi}_V^{a,n}(x)=m^2_{\pi_V^{a,n}}\hat{\pi}_V^{a,n}(x)$, we get

$$
\partial_{\hat{\mu}}\langle J^{\hat{\mu}}_{V,a}(x)\rangle=f_{\pi_V^{a,n}}m^2_{\pi_V^{a,n}}\hat{\pi}_V^{a,n}(x),
\tag{6.13}
$$

where $f_{\pi_V^{a,n}}$ is the leptonic decay constant of the scalar mesons (4.105). Eq. (6.13) encodes the effect of flavor symmetry breaking (FSB) in the vector current. Interestingly, the scalar mesons $\hat{\pi}_V^{a,n}(x)$ of FSB and the pseudoscalar mesons $\hat{\pi}^{a,n}(x)$ of chiral symmetry breaking appear in a similar way in Eqs. (6.13) and (5.28), respectively.

6.2 Strong Coupling Constants

As we have highlighted before, coupling constants can provide a real opportunity for studying the nature of pseudoscalar and vector mesons. In order to explore that, we use interaction actions (4.125)-(4.131) and also the expressions for the coupling constants in (4.126, 4.132). We are interested in describing strong couplings involving charmed mesons D and D^*, strange mesons K and K^* as well as light mesons π and ρ. Then, in (4.126) and (4.132) we select $a=(1,..,7)$ and $a=(9,..,12)$ for the pseudoscalar mesons π^a, whereas for the vector mesons V^a we pick $a=(1..,7)$, $a=(9,..,12)$ and $a=(8,15)$. The reason we include $a=(8,15)$ in the vector sector is because it will contribute to the electromagnetic form factors of the D and D^*, as shown below in this section. This way, using the results in (6.5)-(6.10) and evaluating the $SU(4)$ structure constants f^{abc} we arrive at the effective Lagrangians

$$\mathcal{L}_{V\pi\pi} = \mathcal{L}_{\pi D^* D} + \mathcal{L}_{\rho DD} + \mathcal{L}_{\omega' DD} + \mathcal{L}_{\psi DD} + \mathcal{L}_{\pi K^* K} + \mathcal{L}_{\rho KK} + \mathcal{L}_{\omega' KK} + \mathcal{L}_{\rho\pi\pi}, \tag{6.14}$$

$$\mathcal{L}_{\mathrm{VVV}} = \mathcal{L}_{\rho D^* D^*} + \mathcal{L}_{\omega' D^* D^*} + \mathcal{L}_{\psi D^* D^*} + \mathcal{L}_{\rho K^* K^*} + \mathcal{L}_{\omega' K^* K^*} + \mathcal{L}_{\rho\rho\rho}\ , \tag{6.15}$$

where

$$\begin{aligned}\mathcal{L}_{\pi D^* D} &= i\sqrt{2}\, g_{\pi D^* D}\left[D^{*+}_\mu\left(\bar{D}^0 \overleftrightarrow{\partial^\mu} \pi^-\right) + D^{*-}_\mu\left(\pi^+ \overleftrightarrow{\partial^\mu} D^0\right) + D^{*0}_\mu\left(D^- \overleftrightarrow{\partial^\mu} \pi^+\right) + \bar{D}^{*0}_\mu\left(\pi^- \overleftrightarrow{\partial^\mu} D^+\right)\right] \\ &+ i g_{\pi D^* D}\left[D^{*+}_\mu\left(\pi^0 \overleftrightarrow{\partial^\mu} D^-\right) + D^{*-}_\mu\left(D^+ \overleftrightarrow{\partial^\mu} \pi^0\right) + D^{*0}_\mu\left(\bar{D}^0 \overleftrightarrow{\partial^\mu} \pi^0\right) + \bar{D}^{*0}_\mu\left(\pi^0 \overleftrightarrow{\partial^\mu} D^0\right)\right],\end{aligned} \tag{6.16}$$

$$\mathcal{L}_{\rho DD} = i\sqrt{2}\, g_{\rho DD}\left[\rho^+_\mu\left(D^0 \overleftrightarrow{\partial^\mu} D^-\right) + \rho^-_\mu\left(D^+ \overleftrightarrow{\partial^\mu} \bar{D}^0\right)\right] + i g_{\rho DD}\left[\rho^0_\mu\left(D^- \overleftrightarrow{\partial^\mu} D^+\right) + \rho^0_\mu\left(D^0 \overleftrightarrow{\partial^\mu} \bar{D}^0\right)\right], \tag{6.17}$$

$$\mathcal{L}_{\omega' DD} = \frac{i}{\sqrt{3}}\, g_{\omega' DD}\left[\omega'_\mu\left(D^+ \overleftrightarrow{\partial^\mu} D^-\right) + \omega'_\mu\left(D^0 \overleftrightarrow{\partial^\mu} \bar{D}^0\right)\right], \tag{6.18}$$

$$\mathcal{L}_{\psi DD} = i\sqrt{\frac{8}{3}}\, g_{\psi DD}\left[\psi_\mu\left(D^+ \overleftrightarrow{\partial^\mu} D^-\right) + \psi_\mu\left(D^0 \overleftrightarrow{\partial^\mu} \bar{D}^0\right)\right], \tag{6.19}$$

$$\begin{aligned}\mathcal{L}_{\rho D^* D^*} &= i\sqrt{2}\, g_{\rho D^* D^*}\Big[D^{*+}_\mu\left(\rho^-_\nu \overleftrightarrow{\partial^\mu} \bar{D}^\nu_{*0}\right) + D^{*-}_\mu\left(D^{*0}_\nu \overleftrightarrow{\partial^\mu} \rho^\nu_+\right) + D^{*0}_\mu\left(\rho^+_\nu \overleftrightarrow{\partial^\mu} D^\nu_{*-}\right) + \bar{D}^{*0}_\mu\left(D^{*+}_\nu \overleftrightarrow{\partial^\mu} \rho^\nu_-\right) \\ &+ \rho^+_\mu\left(D^{*-}_\nu \overleftrightarrow{\partial^\mu} D^\nu_{*0}\right) + \rho^-_\mu\left(\bar{D}^{*0}_\nu \overleftrightarrow{\partial^\mu} D^\nu_{*+}\right)\Big] + i g_{\rho D^* D^*}\Big[D^{*+}_\mu\left(D^{*-}_\nu \overleftrightarrow{\partial^\mu} \rho^\nu_0\right) + D^{*-}_\mu\left(\rho^0_\nu \overleftrightarrow{\partial^\mu} D^\nu_{*+}\right) \\ &+ D^{*0}_\mu\left(\rho^0_\nu \overleftrightarrow{\partial^\mu} \bar{D}^\nu_{*0}\right) + \bar{D}^{*0}_\mu\left(D^{*0}_\nu \overleftrightarrow{\partial^\mu} \rho^\nu_0\right) + \rho^0_\mu\left(D^{*+}_\nu \overleftrightarrow{\partial^\mu} D^\nu_{*-}\right) + \rho^0_\mu\left(\bar{D}^{*0}_\nu \overleftrightarrow{\partial^\mu} D^\nu_{*0}\right)\Big],\end{aligned} \tag{6.20}$$

$$\begin{aligned}\mathcal{L}_{\omega' D^* D^*} &= -\frac{i}{\sqrt{3}} g_{\omega' D^* D^*}\Big[D^{*+}_\mu\left(D^{*-}_\nu \overleftrightarrow{\partial^\mu} \omega'^\nu\right) + D^{*-}_\mu\left(\omega'^\nu \overleftrightarrow{\partial^\mu} D^{*+}_\nu\right) \\ &+ D^{*0}_\mu\left(\bar{D}^{*0}_\nu \overleftrightarrow{\partial^\mu} \omega'^\nu\right) + \bar{D}^{*0}_\mu\left(\omega'^\nu \overleftrightarrow{\partial^\mu} D^{*0}_\nu\right) + \omega'_\mu\left(D^{*+}_\nu \overleftrightarrow{\partial^\mu} D^\nu_{*-}\right) + \omega'_\mu\left(D^{*0}_\nu \overleftrightarrow{\partial^\mu} \bar{D}^\nu_{*0}\right)\Big],\end{aligned} \tag{6.21}$$

$$\begin{aligned}\mathcal{L}_{\psi D^* D^*} &= -i\sqrt{\frac{8}{3}} g_{\psi D^* D^*}\Big[D^{*+}_\mu\left(D^{*-}_\nu \overleftrightarrow{\partial^\mu} \psi^\nu\right) + D^{*-}_\mu\left(\psi^\nu \overleftrightarrow{\partial^\mu} D^{*+}_\nu\right) + D^{*0}_\mu\left(\bar{D}^{*0}_\nu \overleftrightarrow{\partial^\mu} \psi^\nu\right) + \bar{D}^{*0}_\mu\left(\psi^\nu \overleftrightarrow{\partial^\mu} D^{*0}_\nu\right) \\ &+ \psi_\mu\left(D^{*+}_\nu \overleftrightarrow{\partial^\mu} D^\nu_{*-}\right) + \psi_\mu\left(D^{*0}_\nu \overleftrightarrow{\partial^\mu} \bar{D}^\nu_{*0}\right)\Big],\end{aligned} \tag{6.22}$$

$$
\begin{aligned}
\mathcal{L}_{\pi K^* K} &= i\sqrt{2}\, g_{\pi K^* K}\Big[K^{*+}_\mu \left(\pi^- \overleftrightarrow{\partial^\mu} \bar{K}^0\right) + K^{*-}_\mu \left(K^0 \overleftrightarrow{\partial^\mu} \pi^+\right) + K^{*0}_\mu \left(\pi^+ \overleftrightarrow{\partial^\mu} K^-\right) + \bar{K}^{*0}_\mu \left(K^+ \overleftrightarrow{\partial^\mu} \pi^-\right)\Big] \\
&+ i g_{\pi K^* K}\Big[K^{*+}_\mu \left(\pi^0 \overleftrightarrow{\partial^\mu} K^-\right) + K^{*-}_\mu \left(K^+ \overleftrightarrow{\partial^\mu} \pi^0\right) + K^{*0}_\mu \left(\bar{K}^0 \overleftrightarrow{\partial^\mu} \pi^0\right) + \bar{K}^{*0}_\mu \left(\pi^0 \overleftrightarrow{\partial^\mu} K^0\right)\Big],
\end{aligned} \tag{6.23}
$$

$$
\mathcal{L}_{\rho K K} = i\sqrt{2}\, g_{\rho K K}\Big[\rho^+_\mu \left(K^- \overleftrightarrow{\partial^\mu} K^0\right) + \rho^-_\mu \left(\bar{K}^0 \overleftrightarrow{\partial^\mu} K^+\right)\Big] + i g_{\rho K K}\Big[\rho^0_\mu \left(K^- \overleftrightarrow{\partial^\mu} K^+\right) + \rho^0_\mu \left(K^0 \overleftrightarrow{\partial^\mu} \bar{K}^0\right)\Big], \tag{6.24}
$$

$$
\mathcal{L}_{\omega' K K} = i\sqrt{3}\, g_{\omega' K K}\Big[\omega'_\mu \left(K^- \overleftrightarrow{\partial^\mu} K^+\right) + \omega'_\mu \left(\bar{K}^0 \overleftrightarrow{\partial^\mu} K^0\right)\Big], \tag{6.25}
$$

$$
\begin{aligned}
\mathcal{L}_{\rho K^* K^*} &= i\sqrt{2} g_{\rho K^* K^*}\Big[K^{*+}_\mu \left(\bar{K}^{*0}_\nu \overleftrightarrow{\partial^\mu} \rho^\nu_-\right) + K^{*-}_\mu \left(\rho^+_\nu \overleftrightarrow{\partial^\mu} K^{*0}_\nu\right) + K^{*0}_\mu \left(K^{*-}_\nu \overleftrightarrow{\partial^\mu} \rho^\nu_+\right) + \bar{K}^{*0}_\mu \left(\rho^-_\nu \overleftrightarrow{\partial^\mu} K^\nu_{*+}\right) \\
&+ \rho^+_\mu \left(K^{*0}_\nu \overleftrightarrow{\partial^\mu} K^\nu_{*-}\right) + \rho^-_\mu \left(K^{*+}_\nu \overleftrightarrow{\partial^\mu} \bar{K}^\nu_{*0}\right)\Big] + i g_{\rho K^* K^*}\Big[K^{*+}_\mu \left(K^{*-}_\nu \overleftrightarrow{\partial^\mu} \rho^\nu_0\right) + K^{*-}_\mu \left(\rho^0_\nu \overleftrightarrow{\partial^\mu} K^\nu_{*+}\right) \\
&+ K^{*0}_\mu \left(\rho^0_\nu \overleftrightarrow{\partial^\mu} \bar{K}^\nu_{*0}\right) + \bar{K}^{*0}_\mu \left(K^{*0}_\nu \overleftrightarrow{\partial^\mu} \rho^\nu_0\right) + \rho^0_\mu \left(K^{*+}_\nu \overleftrightarrow{\partial^\mu} K^\nu_{*-}\right) + \rho^0_\mu \left(\bar{K}^{*0}_\nu \overleftrightarrow{\partial^\mu} K^\nu_{*0}\right)\Big],
\end{aligned} \tag{6.26}
$$

$$
\begin{aligned}
\mathcal{L}_{\omega' K^* K^*} &= i\sqrt{3}\, g_{\omega' K^* K^*}\Big[K^{*+}_\mu \left(K^{*-}_\nu \overleftrightarrow{\partial^\mu} \omega'^\nu\right) + K^{*-}_\mu \left(\omega'_\nu \overleftrightarrow{\partial^\mu} K^\nu_{*+}\right) + K^{*0}_\mu \left(\bar{K}^{*0}_\nu \overleftrightarrow{\partial^\mu} \omega'^\nu\right) \\
&+ \bar{K}^{*0}_\mu \left(\omega'_\nu \overleftrightarrow{\partial^\mu} K^\nu_{*0}\right) + \omega'_\mu \left(K^{*+}_\nu \overleftrightarrow{\partial^\mu} K^\nu_{*-}\right) + \omega'_\mu \left(K^{*0}_\nu \overleftrightarrow{\partial^\mu} \bar{K}^\nu_{*0}\right)\Big],
\end{aligned} \tag{6.27}
$$

$$
\mathcal{L}_{\rho\pi\pi} = i g_{\rho\pi\pi}\Big[\rho^+_\mu \left(\pi^0 \overleftrightarrow{\partial^\mu} \pi^-\right) + \rho^-_\mu \left(\pi^+ \overleftrightarrow{\partial^\mu} \pi^0\right) + \rho^0_\mu \left(\pi^- \overleftrightarrow{\partial^\mu} \pi^+\right)\Big], \tag{6.28}
$$

$$
\mathcal{L}_{\rho\rho\rho} = i g_{\rho\rho\rho}\Big[\rho^+_\mu \left(\rho^-_\nu \overleftrightarrow{\partial^\mu} \rho^\nu_0\right) + \rho^-_\mu \left(\rho^0_\nu \overleftrightarrow{\partial^\mu} \rho^\nu_+\right) + \rho^0_\mu \left(\rho^+_\nu \overleftrightarrow{\partial^\mu} \rho^\nu_-\right)\Big]. \tag{6.29}
$$

It is important to remember that, the above Lagrangeans have the structure similar that found in Ref. [114] showing the consistence of the model used here. We have used the double arrow derivative $f\overleftrightarrow{\partial^\mu} g := f(\partial^\mu g) - (\partial^\mu f)g$ and for simplicity we have omitted the indices ℓ, m, n that distinguish the fundamental states from the corresponding resonances. In the above, the couplings are given by

$$
\begin{aligned}
g_{\pi D^* D} &= \bar{g}_{\hat{\pi}^a \hat{V}^b \hat{\pi}^c}, \quad a = (1,2,3)\ ,\ (b,c) = (9,..,12)\ , \\
g_{\rho D D} &= \bar{g}_{\hat{\pi}^a \hat{V}^b \hat{\pi}^c}, \quad (a,c) = (9,..,12)\ ,\ b = (1,2,3)\ , \\
g_{\omega' D D} &= \bar{g}_{\hat{\pi}^a \hat{V}^b \hat{\pi}^c}, \quad (a,c) = (9,..,12)\ ,\ b = 8\ , \\
g_{\psi D D} &= \bar{g}_{\hat{\pi}^a \hat{V}^b \hat{\pi}^c}, \quad (a,c) = (9,..,12)\ ,\ b = 15\ , \\
g_{\rho D^* D^*} &= \bar{g}_{\hat{V}^a \hat{V}^b \hat{V}^c}, \quad a = (1,2,3)\ ,\ (b,c) = (9,..,12)\ , \\
g_{\omega' D^* D^*} &= \bar{g}_{\hat{V}^a \hat{V}^b \hat{V}^c}, \quad a = 8\ ,\ (b,c) = (9,..,12)\ ,
\end{aligned}
$$

$$\begin{aligned}
g_{\psi D^* D^*} &= \bar{g}_{\hat{V}^a \hat{V}^b \hat{V}^c}, \quad a = 15\ ,\ (b,c) = (9,..,12)\ , \\
g_{\pi K^* K} &= \bar{g}_{\hat{\pi}^a \hat{V}^b \hat{\pi}^c}, \quad a = (1,2,3)\ ,\ (b,c) = (4,..,7)\ , \\
g_{\rho K K} &= \bar{g}_{\hat{\pi}^a \hat{V}^b \hat{\pi}^c}, \quad (a,c) = (4,..,7)\ ,\ b = (1,2,3)\ , \\
g_{\omega' K K} &= \bar{g}_{\hat{\pi}^a \hat{V}^b \hat{\pi}^c}, \quad (a,c) = (4,..,7)\ ,\ b = 8\ , \\
g_{\rho K^* K^*} &= \bar{g}_{\hat{V}^a \hat{V}^b \hat{V}^c}, \quad a = (1,2,3)\ ,\ (b,c) = (4,..,7)\ , \\
g_{\omega' K^* K^*} &= \bar{g}_{\hat{V}^a \hat{V}^b \hat{V}^c}, \quad a = 8\ ,\ (b,c) = (4,..,7)\ , \\
g_{\rho\pi\pi} &= 2\bar{g}_{\hat{\pi}^a \hat{V}^b \hat{\pi}^c}, \quad (a,b,c) = (1,2,3)\ , \\
g_{\rho\rho\rho} &= 2\bar{g}_{\hat{V}^a \hat{V}^b \hat{V}^c}, \quad (a,b,c) = (1,2,3)\ .
\end{aligned} \tag{6.30}$$

Its worth recalling the expressions for $\bar{g}_{\hat{\pi}^{\bar{a},\ell}\hat{V}^{b,m}\hat{\pi}^{\bar{c},n}}$ and $\bar{g}_{\hat{V}^a\hat{V}^b\hat{V}^c}$, obtained in chapter 4. They are

$$\begin{aligned}
\bar{g}_{\hat{\pi}^{\bar{a},\ell}\hat{V}^{b,m}\hat{\pi}^{\bar{c},n}} &= \frac{g_5}{8}\int \frac{dz}{z} v^{b,m}\Big\{4(\partial_z\phi^{\bar{a},\ell})(\partial_z\phi^{\bar{c},n}) \\
&+ \Big[-2\beta_V^b(z) + 2(\beta_A^{\bar{a}\bar{a}}(z) + \beta_A^{\bar{c}\bar{c}}(z))\Big](\pi^{\bar{a},\ell} - \phi^{\bar{a},\ell})(\pi^{\bar{c},n} - \phi^{\bar{c},n})\Big\}.
\end{aligned} \tag{6.31}$$

$$\bar{g}_{\hat{V}^{a,\ell}\hat{V}^{b,m}\hat{V}^{c,n}} = \frac{g_5}{2}\int \frac{dz}{z} v^{a,\ell}(z) v^{b,m}(z) v^{c,n}(z)\,. \tag{6.32}$$

In the limit where the quark masses and condensates are equal, $SU(4)$ flavor symmetry is recovered and the couplings satisfy the relations:

$$g_{\pi D^* D} = g_{\rho DD} = g_{\omega' DD} = g_{\psi DD} = g_{\pi K^* K} = g_{\rho KK} = g_{\omega' KK} = \frac{1}{2} g_{\rho\pi\pi} = \frac{g}{4}\,, \tag{6.33}$$

$$g_{\rho D^* D^*} = g_{\omega' D^* D^*} = g_{\psi D^* D^*} = g_{\rho K^* K^*} = g_{\omega' K^* K^*} = \frac{1}{2} g_{\rho\rho\rho} = \frac{\tilde{g}}{4}\,. \tag{6.34}$$

In this case all the couplings can be obtained from the interaction terms $ig\mathrm{Tr}(\partial^\mu\pi[\pi, V_\mu])$ and $i\tilde{g}\mathrm{Tr}(\partial^\mu V^\nu[V_\mu, V_\nu])$—see e.g. Ref. [114]. One of our main purposes in this chapter is determine the deviations from Eqs. (6.33) and (6.34) are implied by the different values of quark masses and condensates. But, before, we will analyse an important characteristic in hadronic physics, the electromagnetic form factors.

6.3 Electromagnetic Form Factors

As we have discussed, a form factor is related to the substructure of a particle and appears for example in elastic electron scattering. In fact, e.g. nucleons do have an internal structure was discovered in 1950's. At the time, experiments at SLAC found that the corresponding form factors were not constant with respect to the probing momentum transfer, as they should be point-like particles. In the case of the electromagnetic form factor, it represents the interaction of a particle, an hadron in our case, with an external photon and provides information on the charge and magnetization distribution of hadron. We start this study pointed a very nice observation: in the absence of baryonic number the EM current is obtained from a linear combination of flavor currents

$$J^{\mu}_{EM}(x) = \sum_{a=(3,8,15)} c_a J^{\mu}_{a}(x)\,, \tag{6.35}$$

where the flavor indexes $a = 3, 8, 15$ correspond to the ρ^0, ω' and J/ψ mesons, respectively. The coefficients c_a depend of the species of quarks that will be considered in the EM current. In the present case, where we are considering the EM form factors of the heavy-light D and D^* charmed mesons, the strange quark does not participate in the process and the EM current is given as

$$J^{\mu}_{EM} = \frac{2}{3}\bar{u}\gamma^{\mu}u - \frac{1}{3}\bar{d}\gamma^{\mu}d + \frac{2}{3}\bar{c}\gamma^{\mu}c. \tag{6.36}$$

Then the EM current can be decomposed as (6.35) with coefficients $c_3 = 1$, $c_8 = 7/(3\sqrt{3})$ and $c_{15} = -8/(3\sqrt{6})$, up to the strangeness current which do not contribute when evaluating the current at the external states. On the other hand, the EM form factors for the strange K and K^* are obtained from the EM current

$$J^{\mu}_{EM} = \frac{2}{3}\bar{u}\gamma^{\mu}u - \frac{1}{3}\bar{d}\gamma^{\mu}d - \frac{1}{3}\bar{s}\gamma^{\mu}s, \tag{6.37}$$

In the case of pion and ρ meson, the EM current is the same without the strangeness part in the above. This allows us to replace the photon by a sum of neutral vector mesons $\rho^{0,n}$, ω'^{n} and ψ^n. As we shall see, these currents in a holographic realization provide a generalized vector meson dominance (GVMD) [122], in that also the resonances are included and not only the fundamental states, as occurs in its original formulation, the vector meson dominance (VMD). It was firstly proposed in a seminal work by J. J. Sakurai [123] in the 1960's, before the consolidation of quantum chromodynamics as the correct theory to describe interactions between energetic photons and hadronic matter. In the VMD model, interactions between photons and hadronic matter occur by the exchange of vector mesons between the dressed photon and the hadronic target, as depicted in Fig. 6.1

For the pion and ρ meson only the states $\rho^{0,n}$ contribute to the EM form factors. In the case of strange mesons K and K^*, from Eq. (6.37), we have that the states $\rho^{0,n}$ and ω'^{n} contribute to the EM form factors whereas, from Eq. (6.36), the EM form factors for the charmed D and D^* mesons receive only contributions from $\rho^{0,n}$, ω'^{n} and ψ^n. It turns out that, in our model, we have that

$$\beta^{3}_{V}(z) = \beta^{8}_{V}(z) = \beta^{15}_{V}(z), \tag{6.38}$$

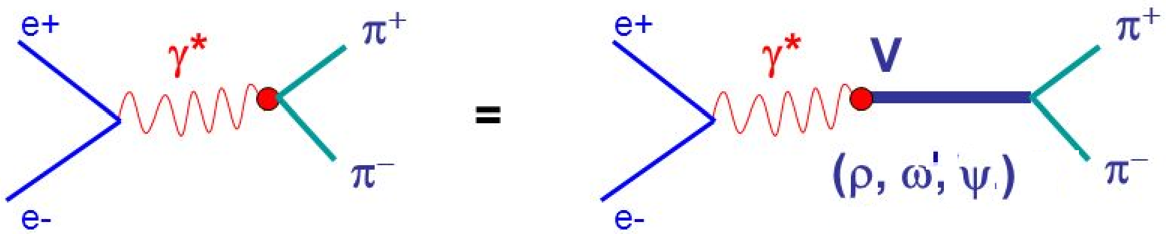

Figure 6.1: Interaction between photons and hadronic matter via neutral vector mesons.

and, as consequence, the equation of the vector meson states that the mesons ω'^n and ψ^n are identical to the mesons $\rho^{0,n}$ as well as their couplings to external states. Although this leads to an unrealistic spectrum for the ψ^n mesons, as we will see below, its contribution to the EM form factors is not only required by consistency but also leads to reasonable results, consistent either with experimental data or lattice QCD data.

The effective Lagrangian in Eq. (6.14) describes the interaction between a vector meson and two pseudoscalar mesons. If the vector meson is off-shell and the pseudoscalar mesons are on-shell, we can use Eq. (6.14) to investigate the electromagnetic (EM) form factors of pseudoscalar mesons. Similarly, using the effective Lagrangian in Eq. (6.15) and taking one of the vector mesons off shell, we can investigate the EM form factors of vector mesons. The most general structure for the on-shell pseudoscalar-pseudoscalar-vector vertex, consistent with Lorentz invariance, has the form

$$\langle \pi^a(p+q)|J^\mu_{EM}(0)|\pi^a(p)\rangle = (2p+q)^\mu F_{\pi^a}(q^2)\,, \tag{6.39}$$

where $F_{\pi^a}(q^2)$ is the pseudoscalar form factor associated with the pseudoscalar meson π^a. Using the Feynman rules for the vector meson propagator and the triple vertex as well as the EM current decomposition (6.35), with the suitable coefficients, we extract the (elastic) EM form factors for the pion, kaon and D meson, as follows

$$\begin{aligned}
F_\pi(Q^2) &= \sum_n \frac{g_{\rho^n} g_{\rho^n\pi\pi}}{m^2_{\rho^n}+Q^2}\,, &(6.40)\\
F_K(Q^2) &= \sum_n \Big[\frac{g_{\rho^n} g_{\rho^n KK}}{m^2_{\rho^n}+Q^2} + \frac{g_{\omega'^n} g_{\omega'^n KK}}{m^2_{\omega'^n}+Q^2}\Big] = 2\sum_n \frac{g_{\rho^n} g_{\rho^n KK}}{m^2_{\rho^n}+Q^2}\,, &(6.41)\\
F_D(Q^2) &= \sum_n \Big[\frac{g_{\rho^n} g_{\rho^n DD}}{m^2_{\rho^n}+Q^2} - \frac{7}{9}\frac{g_{\omega'^n} g_{\omega'^n DD}}{m^2_{\omega'^n}+Q^2} + \frac{16}{9}\frac{g_{\psi^n} g_{\psi^n DD}}{m^2_{\psi^n}+Q^2}\Big] = 2\sum_n \frac{g_{\rho^n} g_{\rho^n DD}}{m^2_{\rho^n}+Q^2}\,, &(6.42)
\end{aligned}$$

where $Q^2 = -q^2$. The two last equalities in Eqs. (6.41) and (6.42) come from the identification of the states ω'^n and ψ^n with the states $\rho^{0,n}$.

For the vector meson sector, due to the vector nature of the mesons we have a more complicated form for the on-shell vector-vector-vector matrix element. We write down the general expression for the EM vertex of a spin-1 particle of mass M can be written (assuming P and T invariance) in terms of three form factors [124]

$$\begin{aligned}\langle v^a(p'),\epsilon'|J^{\mu,em}(0)|v^a(p),\epsilon\rangle &= (\epsilon'\cdot\epsilon)(2p+q)^\mu F^1_{v^a}(q^2) + [\epsilon'^\mu(\epsilon\cdot q) - \epsilon^\mu(\epsilon'\cdot q)][F^1_{v^a}(q^2) \\ &\quad + F^2_{v^a}(q^2)] + \frac{1}{M^2_{v^a}}(q\cdot\epsilon')(q\cdot\epsilon)(2p+q)^\mu F^3_{v^a}(q^2),\end{aligned} \tag{6.43}$$

where we have used transversality $\epsilon'\cdot p' = \epsilon\cdot p = 0$, and $2p\cdot q + q^2 = 0$ valid for the elastic case. Note also that this matrix element satisfies the tranversality condition $q_\mu\langle v^a|J^{\mu,em}(0)|v^a\rangle = 0$.

Linear combinations of the form factors in Eq. (6.43) define the so called electric, magnetic and quadrupole form factors as

$$\begin{aligned}F^E_{v^a} &= F_1^{(v^a)} + \frac{q^2}{6M^2_{v^a}}\Big[F_2^{(v^a)} - \Big(1 - \frac{q^2}{4M^2_{v^a}}\Big)F_3^{(v^a)}\Big], \qquad F^M_{v^a} = F_1^{(v^a)} + F_2^{(v^a)} \\ F^Q_{v^a} &= -F_2^{(v^a)} + \Big(1 - \frac{q^2}{4M^2_{v^a}}\Big)F_3^{(v^a)}.\end{aligned} \tag{6.44}$$

The matrix element in Eq. (6.43) can be calculated from the corresponding Feynman diagram shown in Fig. 6.2. From the effective Lagrangian in Eq. (4.78), together with the interaction terms in Eq. (4.125), we find for the elastic case that

$$\langle v^a(p'),\epsilon'|J^{\mu,em}(0)|v^a(p),\epsilon\rangle = \{(\epsilon'\cdot\epsilon)(2p+q)^\mu + 2[\epsilon'^\mu(\epsilon\cdot q) - \epsilon^\mu(\epsilon'\cdot q)]\}F_{v^a}(q^2), \tag{6.45}$$

where $F_{v^a}(q^2)$ is the elastic form factor, given by

$$F_{v^a}(q^2) = \sum_{n=0}^{\infty}\frac{g_{v^n}g_{v^a v^n v^a}}{Q^2 + M^2_{v^n}}. \tag{6.46}$$

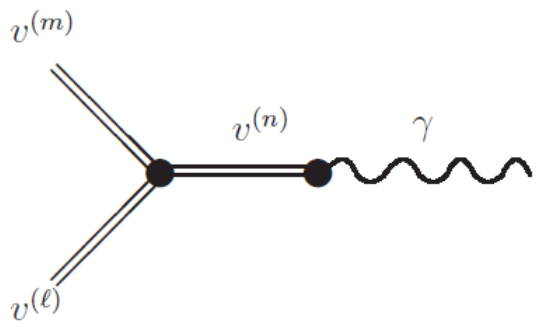

Figure 6.2: Feynman diagram for vector meson form factor.

By comparing Eq. (6.43) with Eq. (6.45) we easily find that

$$F^1_{v^a} = F^2_{v^a} = F_{v^a}, \quad F^3_{v^a} = 0. \tag{6.47}$$

Therefore, the electric, magnetic and quadrupole form factors predicted by the model for vector mesons are

$$F^{E}_{v^a} = \Big(1 + \frac{Q^2}{6M^2_{v^a}}\Big)F_{v^a}\,, \quad F^{M}_{v^a} = 2F_{v^a}\,, \quad F^{Q}_{v^a} = -F_{v^a}\,. \tag{6.48}$$

Similarly to the pseudoscalar case, we also can extract the (elastic) EM form factors for the vector meson: ρ, K^* and D^*, as follows

$$F^1_{\rho} = F^2_{\rho} = F_{\rho}(Q^2) = \sum_n \frac{g_{\rho^n} g_{\rho^n \rho\rho}}{m^2_{\rho^n} + Q^2}; \quad F^1_{K^*} = F^2_{K^*} = F_{K^*}(Q^2) = 2\sum_n \frac{g_{\rho^n} g_{\rho^n K^* K^*}}{m^2_{\rho^n} + Q^2}\,, \tag{6.49}$$

$$F^1_{D^*} = F^2_{D^*} = F_{D^*}(Q^2) = 2\sum_n \frac{g_{\rho^n} g_{\rho^n D^* D^*}}{m^2_{\rho^n} + Q^2}; \quad F^3_{\rho} = F^3_{K^*} = F^3_{D^*} = 0\,. \tag{6.50}$$

6.3.1 Low and high Q^2 behaviors

Here we will explore the high and low Q^2 behavior of the form factors. In the regime when $Q^2 \approx 0$, the electromagnetic form factor can be expanded as

$$F_{\pi^a}(Q^2) = F_{\pi^a}(0) + \frac{1}{6}\left\langle r^2_{\pi^a}\right\rangle Q^2 + ... \tag{6.51}$$

where we should have $F_{\pi^a}(0) = 1$, by charge conservation. In fact, the relation $F_{\pi^a}(0) = 1$ follows nicely from the sum rules

$$\sum_n \frac{g_{\rho^n} g_{\rho^n \pi\pi}}{m^2_{\rho^n}} = 2\sum_n \frac{g_{\rho^n} g_{\rho^n KK}}{m^2_{\rho^n}} = 2\sum_n \frac{g_{\rho^n} g_{\rho^n DD}}{m^2_{\rho^n}} = 1\,. \tag{6.52}$$

These sum rules can also be proven using the equations of motion and completeness relations for vector mesons as well as the normalization of the external states. The second term defines the charge radius of the pseudoscalar mesons. It this related with the form factor as

$$\left\langle r^2_{\pi^a}\right\rangle = -6\, \frac{dF_{\pi^a}(Q^2)}{dQ^2}\bigg|_{Q^2=0} = 6\sum_{n=1} \frac{g_{v^n} g_{\pi^a v^n \pi^a}}{M^4_{v^n}}. \tag{6.53}$$

Note that, the expansion (6.51) reveals a quadratic behavior of the form factor, in agreement with several results in the literature.

For the vector mesons, the expansion for the electromagnetic form factor is similar to Eq. (6.51), and their charge is

$$\left\langle r^2_{v^a}\right\rangle = -6\, \frac{dF^E_{v^a}(Q^2)}{dQ^2}\bigg|_{Q^2=0}. \tag{6.54}$$

The magnetic μ and quadrupole D moments of the vector mesons in the present model take the canonical values

$$\begin{aligned} \mu &= F^M_{V^a}(0) = 2\,, \\ D &= \frac{1}{M^2_{V^a}} F^Q_{V^a}(0) = -\frac{1}{M^2_{V^a}}\,, \end{aligned} \tag{6.55}$$

where we have used the relation $F_{V^a}(0) = 1$ which follows from the sum rules

$$\sum_n \frac{g_{\rho^n} g_{\rho^n \rho\rho}}{m^2_{\rho^n}} = 2\sum_n \frac{g_{\rho^n} g_{\rho^n K^* K^*}}{m^2_{\rho^n}} = 2\sum_n \frac{g_{\rho^n} g_{\rho^n D^* D^*}}{m^2_{\rho^n}} = 1\,. \tag{6.56}$$

It is important to mention that such sum rules follow from the equations of motion and completeness of the ρ^n states and also the normalization of the external states. In fact, the sum rules given in Eqs. (6.52) and (6.56) are universal rules in bottom up and top-down holographic models for QCD. The reader interested on this, can see a detailed discussion in Ref. [125].

On the other hand, in the regime of large Q^2, the EM form factors of pseudoscalar mesons can be expanded as

$$\begin{aligned} F_\pi(Q^2) &= \frac{1}{Q^2}\sum_{n=0}^{\infty} g_{\rho^n} g_{\rho^n \pi\pi}\Big[1 - \frac{m^2_{\rho^n}}{Q^2} + \dots\Big]\,, \\ F_K(Q^2) &= \frac{2}{Q^2}\sum_{n=0}^{\infty} g_{\rho^n} g_{\rho^n KK}\Big[1 - \frac{m^2_{\rho^n}}{Q^2} + \dots\Big]\,, \\ F_D(Q^2) &= \frac{2}{Q^2}\sum_{n=0}^{\infty} g_{\rho^n} g_{\rho^n DD}\Big[1 - \frac{m^2_{\rho^n}}{Q^2} + \dots\Big]. \end{aligned} \tag{6.57}$$

A similar expansion holds for the EM form factors of vector mesons

$$\begin{aligned} F_\rho(Q^2) &= \frac{1}{Q^2}\sum_{n=0}^{\infty} g_{\rho^n} g_{\rho^n \rho\rho}\Big[1 - \frac{m^2_{\rho^n}}{Q^2} + \dots\Big]\,, \\ F_{K^*}(Q^2) &= \frac{2}{Q^2}\sum_{n=0}^{\infty} g_{\rho^n} g_{\rho^n K^* K^*}\Big[1 - \frac{m^2_{\rho^n}}{Q^2} + \dots\Big]\,, \\ F_{D^*}(Q^2) &= \frac{2}{Q^2}\sum_{n=0}^{\infty} g_{\rho^n} g_{\rho^n D^* D^*}\Big[1 - \frac{m^2_{\rho^n}}{Q^2} + \dots\Big]. \end{aligned} \tag{6.58}$$

Now, we are ready to present our numerical predictions for the strong coupling constants and the EM form factors for the pions, kaons, ρ mesons, K^* and the charmed mesons: D and D^*. Due to the lack of experimental information, we will compare our results for the D and D^* EM form factors with the recent lattice QCD results. Using Eqs. (6.53) and (6.54), we will also extract the charge radii of all those mesons and compare against experimental data or lattice QCD data. Last but not least, the high-Q^2 behavior of the form factors in Eqs. (6.57)-(6.58) will be compared with perturbative QCD calculations.

6.4 Results and comparison with experimental and lattice QCD

In this section we present our numerical results for the spectrum, decay constants, coupling constants and EM form factors involving the charmed mesons. It is convenient to define unnormalized wave functions for the scalar mesons ($\tilde{\phi}_U^{a,n}$ and $\tilde{\pi}_U^{a,n}$), pseudoscalar mesons ($\phi_U^{a,n}$ and $\pi_U^{a,n}$), vector mesons ($v_U^{a,n}$) and axial vector mesons ($a_U^{a,n}$) so that the first coefficient near the boundary is fixed arbitrarily (due to the linearity of the differential equations). Eqs. (6.8) and (6.11) dictate the near boundary behaviour of the unnormalized wave functions

$$\begin{aligned} \tilde{\phi}_U^{a,n}(z) &= -z^2+\ldots, \quad \tilde{\pi}_U^{a,n}(z) = -\frac{m^2_{\pi_V^{a,n}}}{\beta_V^a(0)}z^2+\ldots\,, &(6.59)\\ \phi_U^{a,n}(z) &= -z^2+\ldots, \quad \pi_U^{a,n}(z) = -\frac{m^2_{\pi^{a,n}}}{\beta_A^a(0)}z^2+\ldots\,, &(6.60)\\ v_U^{a,n}(z) &= z^2+\ldots, \quad a_U^{a,n}(z) = z^2+\ldots\,. &(6.61)\end{aligned}$$

In Eq. (6.61), the first coefficients were fixed to 1 or -1 to guarantee a positive sign for the decay constants in Eqs. (6.12) and positive normalization constants. The normalized wave functions assume the following form

$$\begin{aligned} \tilde{\phi}^{a,n}(z) &= N_{\pi_V^{a,n}}\tilde{\phi}_U^{a,n}(z), \quad \tilde{\pi}^{a,n}(z) = N_{\pi_V^{a,n}}\tilde{\pi}_U^{a,n}(z)\,,\\ \phi^{a,n}(z) &= N_{\pi^{a,n}}\phi_U^{a,n}(z), \quad \pi^{a,n}(z) = N_{\pi^{a,n}}\pi_U^{a,n}(z)\,,\\ v^{n,a}(z) &= N_{V^{a,n}}v_U^{a,n}(z), \quad a^{n,a}(z) = N_{A^{a,n}}a_U^{a,n}(z), \qquad (6.62)\end{aligned}$$

with the normalization constants defined by the integrals

$$\begin{aligned} N^{-2}_{\pi_V^{a,n}} &= \int\frac{dz}{z}\Big\{(\partial_z\tilde{\phi}_U^{a,n}(z))^2+\beta_V^a(z)(\tilde{\pi}_U^{a,n}(z)-\tilde{\phi}_U^{a,n}(z))^2\Big\}\,,\\ N^{-2}_{\pi^{a,n}} &= \int\frac{dz}{z}\Big\{(\partial_z\phi_U^{a,n}(z))^2+\beta_V^a(z)(\pi_U^{a,n}(z)-\phi_U^{a,n}(z))^2\Big\}\,,\\ N^{-2}_{V^{a,n}} &= \int\frac{dz}{z}(v_U^{a,n}(z))^2, \quad N^{-2}_{A^{a,n}} = \int\frac{dz}{z}(a_U^{a,n}(z))^2\,. \qquad (6.63)\end{aligned}$$

This way, using Eqs. (6.61) and (6.62) we find that the meson decay constants, written in Eqs. (6.12), can be determined by the normalization constants through the following relations

$$\begin{aligned} f_{\pi_V^{a,n}} &= \frac{2}{g_5}N_{\pi_V^{a,n}}, \quad f_{\pi^{a,n}} = \frac{2}{g_5}N_{\pi^{a,n}}\,,\\ g_{V^{a,n}} &= \frac{2}{g_5}N_{V^{a,n}}, \quad g_{A^{a,n}} = \frac{2}{g_5}N_{A^{a,n}}\,. \qquad (6.64)\end{aligned}$$

So far, we have described the procedure for finding the meson spectrum and decay constants. Now, we are ready to fit the parameters of the model, namely the quark masses m_u, m_s, m_c, quark condensates $\sigma_u, \sigma_s, \sigma_c$ and the position of the hard wall z_0. Following the procedure in the previous chapter, we choose to fit the parameter z_0 using only the mass of the ρ meson, once that observable does not depend on any other parameter: $z_0^{-1} = 322.5\text{MeV}$. Then, we proceed with a global fit using 10 observables to fix the quark masses and quark condensates, they are: the light meson masses (m_π, m_{a_1}), the strange meson masses $(m_K, m_{K^*}, m_{K_1}, m_{K_0^*})$ and the charmed meson masses $(m_D, m_{D^*}, m_{D_s}, m_{D_s^*})$. Note that we have included the scalar meson K_0^*.

In order to find the best values of the parameters of the model, we compare the experimental results for the masses and decay constants with that obtained in the numerical procedure. To do so, we define a following function

$$\chi^2 = \frac{1}{N}\sum_{i,j,k,l}\Big(\frac{(M_{\text{exp}} - M_{\text{o}}[i,j,k,l])^2}{M_{\text{exp}}} + \frac{(F_{\text{exp}} - F_{\text{o}}[i,j,k,l])^2}{F_{\text{exp}}}\Big), \tag{6.65}$$

where M_{exp} and F_{exp} are the experimental values for the masses and decay constants, and M_{o} and F_{o} are the numerical values obtained with the model. The indexes i, j, k, l are the of values used in our fit and N is the number of data points used. Using general minimization, we find the parameters listed in Table 6.1

quarks	up	down	strange	charm
masses	9.00 MeV	9.00 MeV	190 MeV	1560 MeV
condensates	(198 MeV)^3	(198 MeV)^3	(205 MeV)^3	(280 MeV)^3

Table 6.1: Quark masses and condensates fitted using the formal in Eq. (6.65)

We use the Mathematica code with Neumann boundary conditions at the hard wall $z = z_0$ and the asymptotic behavior in Eq. (6.61) to solve the Eqs. (6.8)-(6.11). In Tab. (6.2) we compare the fit to the values in the particle data group.

Note that our fitting provides very good results for the isospin and strange sectors, as we already expected from previous works. The extension of the model to the charm sector also allows to obtain a reasonably good fit of properties of heavy-light D and D^* mesons.

Once we have completed our fitting of the parameters, we are able to make predictions. In Tab. (6.3) we show a set of predictions for masses and decay constants. In the cases where experimental or lattice data are available, the measured values are also presented, for comparison. Concerning the masses $m_{D_0^*}$ and $m_{D_{0s}^*}$, the large difference between the model prediction and the experimental values [126] may be associated with the not clear distinction between the ground and excited states.

Mass	Model (MeV)	Measured (MeV)
m_ρ	775.6	775.3 ± 0.3 [126]
m_π	142.5	139.6 [126]
m_{a_1}	1232	1230 ± 40 [126]
m_K	489.2	493.7 [126]
m_{K^*}	803.7	891.7 ± 0.3 [126]
m_{K_1}	1359	1272 ± 7 [126]
$m_{K_0^*}$	674.9	682 ± 29 [126]
m_D	1831	1870 [126]
m_{D_s}	1987	1968 [126]
m_{D^*}	2161	2010 [126]
$m_{D_s^*}$	2006	2112 [126]

Table 6.2: Global fit to masses of eleven selected mesons. The mass of the ρ meson was fit separately using z_0.

Now, let us move on and present the numerical results for the triple meson couplings defined in the effective Lagrangians (6.14) and (6.15). To do so, we use the expressions in Eqs. (6.32) and (6.31) and the relations in Eq. (6.30) to find the couplings $g_{\rho^n\pi\pi}$, $g_{\rho^n\rho\rho}$, $g_{\rho^n KK}$, $g_{\rho^n K^*K^*}$, $g_{\rho^n DD}$ and $g_{\rho^n D^*D^*}$. Our results are shown in Tab. (6.4) where we can notice that an interesting shows up. The triple coupling $g_{\rho^n DD}$, involving the heavy-light pseudoscalar charmed mesons, does not decrease with n as occurs in the case of the triple couplings $g_{\rho^n\pi\pi}$ and $g_{\rho^n KK}$, involving light and strange pseudoscalar mesons respectively. The same behavior appears in the triple coupling $g_{\rho^n D^*D^*}$, involving vector charmed mesons, when compared to the triple couplings $g_{\rho^n\rho\rho}$ and $g_{\rho^n K^*K^*}$, involving vector light and strange mesons respectively. For example, in the case of $g_{\rho^n DD}$, we see that actually the first resonance $\rho^{n=1}$ couples stronger than the fundamental $\rho^{n=0}$ state.

Due to flavor symmetry breaking, given by the different values for the quark masses and condensates, we expect a violation of $SU(4)$ relations given in Eqs. (6.33)-(6.34). In Table (6.5), we compare our results with the values when $SU(4)$ flavor symmetry is exact. We note that our results show the trend $g_{\rho DD} < g_{\rho KK} < g_{\rho\pi\pi}/2$ for the pseudoscalar mesons, which in turn is opposite to that found with the QCD sum rules [19] and also Dyson-Schwinger calculations in Ref. [20], but it agrees with calculations based on ${}^3P_0$ quark-pair creation model in the nonrelativistic quark mo-

Observable	Model (MeV)	Measured (MeV)
f_π	84.41	92.07 ± 1.2 [126]
$g_\rho^{1/2}$	329.3	345 ± 8 [127]
$g_{a_1}^{1/2}$	440.9	420 ± 40 [128]
f_K	98.14	110 ± 0.3 [126]
$g_{K^*}^{1/2}$	331	-
$g_{K_1}^{1/2}$	478.3	-
$f_{K_0^*}$	33.48	-
m_{D_1}	2500	2423 ± 2 [126]
$m_{D_0^*}$	1704	2318 ± 29 [126]
$m_{D_{0s}^*}$	1547	2318 ± 1 [126]
f_D	186.7	149.8 ± 0.8 [126]
f_{D_s}	195	176.1 ± 0.8 [126]
$g_{D^*}^{1/2}$	572.7	-
$g_{D_s^*}^{1/2}$	546.4	-
$g_{D_1}^{1/2}$	722	-
$f_{D_0^*}$	159	-
$f_{D_{0s}^*}$	150.5	-

Table 6.3: Set of predictions for masses and decay constants, compared to experimental or lattice data. The measured value for f_D and f_{D_s}, taken from Ref. [126], are averages from lattice QCD results. The other measured values are taken from experimental data.

del [17]. For the case of vector mesons, we find a similar trend $g_{\rho D^* D^*} < g_{\rho K^* K^*} < g_{\rho\rho\rho}/2$. Note, however, that the coupling $g_{\rho K^* K^*}$ is quite close to $g_{\rho\rho\rho}/2$. The reason behind this proximity is that the vector meson spectrum, found from the first equation in Eq. (6.11), depends more significantly on the condensate difference than the mass difference appearing in $\beta_V^a(z)$. Since the strange and light condensates σ_s and σ_u are very close to each other, the masses and wave functions of the ρ and K^* are also very similar.

Finally, after we have shown our results for the coupling constants, we show our results for the meson (elastic) EM form factors defined in the previous section. Using the couplings obtained in Table (6.4) and evaluating the expressions in Eqs. (6.40) and (6.42), we obtain a series expansion

n	0	1	2	3	4
$g_{\rho^n\pi\pi}$	4.9144	1.6019	-0.8511	0.0325	0.0231
$g_{\rho^n\rho\rho}$	6.8634	-1.9971	0.022	-0.0025	0.0005
$g_{\rho^n KK}$	2.2163	1.1512	-0.377	-0.0241	0.0103
$g_{\rho^n K^*K^*}$	3.4246	-0.981	0.0013	0.0003	-0.0002
$g_{\rho^n DD}$	1.103	1.8591	0.8386	0.0327	-0.0564
$g_{\rho^n D^*D^*}$	2.1431	1.5691	-0.4344	-0.3573	-0.0467

Table 6.4: Couplings for the pseudoscalars mesons with the ρ meson and their excitations

Ratios	$SU(4)$ symmetry	Model
$\frac{2g_{\rho KK}}{g_{\rho\pi\pi}}$	1	0.902
$\frac{2g_{\rho K^*K^*}}{g_{\rho\rho\rho}}$	1	0.998
$\frac{2g_{\rho DD}}{g_{\rho\pi\pi}}$	1	0.449
$\frac{2g_{\rho D^*D^*}}{g_{\rho\rho\rho}}$	1	0.625

Table 6.5: SU(4) flavor symmetry breaking in the holographic QCD model

n	0	1	2	3	4
$\frac{g_{\rho^n}}{m^2_{\rho^n}} g_{\rho^n\pi\pi}$	0.886	0.192	-0.082	0.003	0.002
$\frac{g_{\rho^n}}{m^2_{\rho^n}} g_{\rho^n\rho\rho}$	1.237	-0.239	0.002	0.000	0.000
$2\frac{g_{\rho^n}}{m^2_{\rho^n}} g_{\rho^n KK}$	0.799	0.276	-0.072	-0.004	0.002
$2\frac{g_{\rho^n}}{m^2_{\rho^n}} g_{\rho^n K^*K^*}$	1.235	-0.235	0.000	0.000	0.000
$2\frac{g_{\rho^n}}{m^2_{\rho^n}} g_{\rho^n DD}$	0.398	0.446	0.161	0.005	-0.008
$2\frac{g_{\rho^n}}{m^2_{\rho^n}} g_{\rho^n D^*D^*}$	0.773	0.376	-0.083	-0.059	-0.007

Table 6.6: Contributions of the five first states to the EM form factors of mesons at $Q^2 = 0$.

for the EM form factors of the pion, kaon and D meson. Following the same procedure, we take the coupling in Table (6.4) and evaluate the expressions in Eqs. (6.49-6.50) to obtain a series expansion for the EM form factors of the ρ, K^* and D^* mesons. In both cases, we have obtained excellent convergence after considering 5 states (4 resonances ρ^n and, of course, the fundamental $\rho^{n=0}$). This is explicitly shown in Tab. (6.6) for the case $Q^2 = 0$.

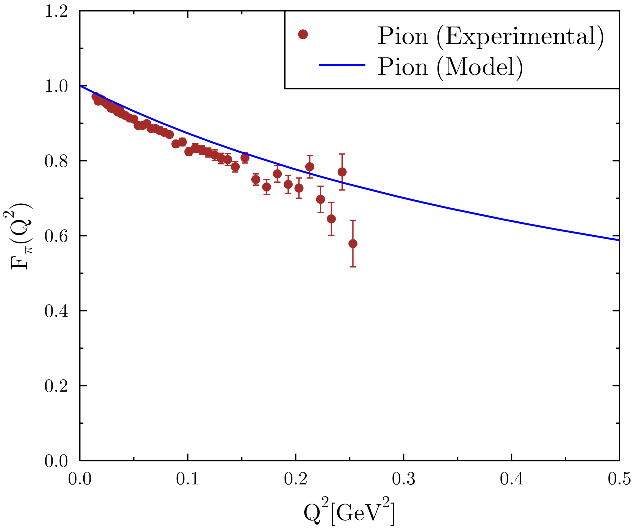

Figure 6.3: Electromagnetic form factor of the pion (solid line) compared to experimental data [108] (points with error bars).

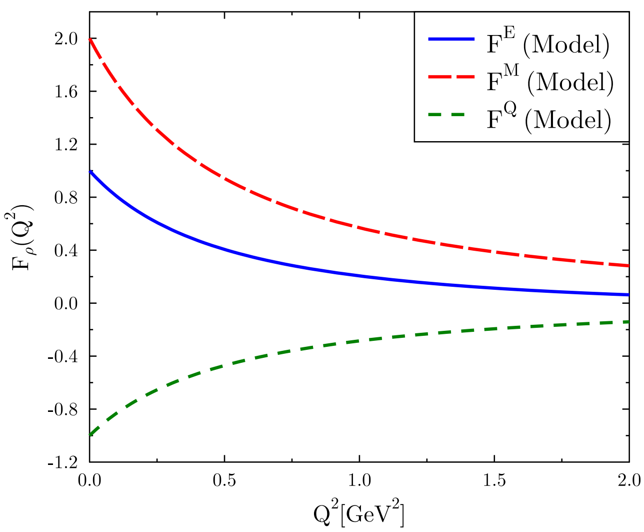

Figure 6.4: The electric (blue), magnetic (red) and quadrupole (green) EM form factors of the ρ meson.

Table (6.6) shows again a clear distinction between the light mesons and charmed mesons. On the top of the table, we have that vector meson dominance (VMD) is a good approximation, whereas on the bottom, the EM form factors receive significant contribution from the first ρ resonance. This is a clear example of generalized vector meson dominance (GVMD) acting on EM form factors. This is consistent with the results discussed in Ref. [129], where the authors claimed that the radial excitations of the ρ meson are important for the EM form factors of non-zero spin hadrons, as nucleons.

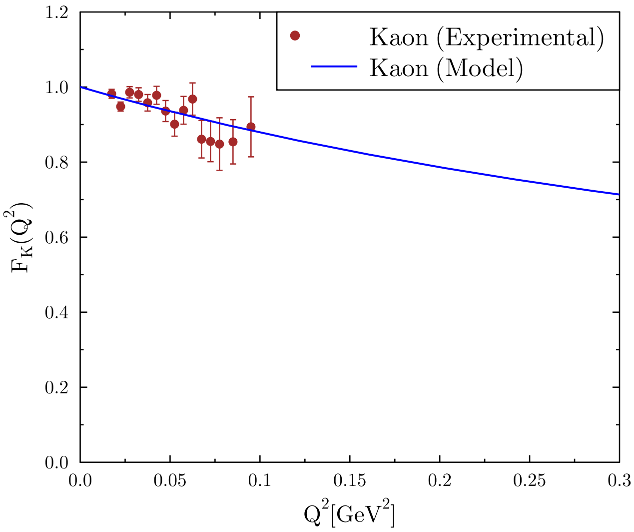

Figure 6.5: Electromagnetic form factor of the kaon (solid line) compared with experimental data [109] (points with error bars).

We show our numerical results for the EM form factors of the π, ρ, K and K^* mesons in Figs. 6.3, 6.4, 6.5 and 6.6. We compared the pion and kaon EM form factors with experimental data. Previous works in holographic QCD have reported results for the pion and the kaon EM form factors, they can be found in Refs. [96, 130] for pion case, and in Ref. [131] for kaon. Also, results for the EM form factor of the ρ meson has been reported in Ref. [132]. Finally, we show our predictions for the D meson and D^* meson EM form factors. They are shown in figures 6.7 and 6.8 and are compared with data from lattice QCD. As we promised, we find good agreement with the lattice results.

At the low Q^2 regime, we use the relations given in Eqs. (6.53) and (6.54) and extract the charge radii of pseudoscalar and vector mesons. They are displayed in Tab. (6.7). For the light mesons, we compare our results with available experimental data and those for the charmed mesons we

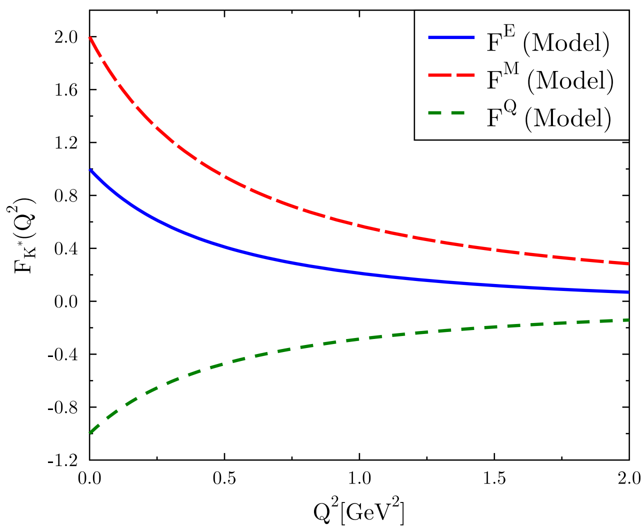

Figure 6.6: The electric (blue), magnetic (red) and quadrupole (green) EM form factors of the K^* meson.

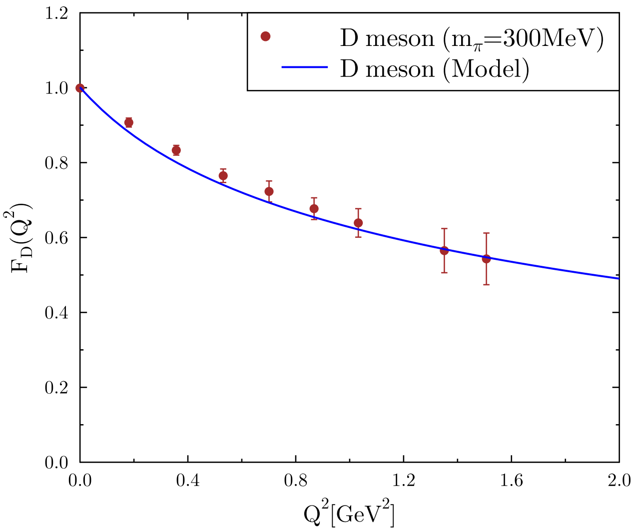

Figure 6.7: Electromagnetic form factor of the D meson (solid line) compared to lattice QCD data [22] (points with error bars).

compare with lattice QCD data.

At the high Q^2 regime, we use the expansions in Eqs. (6.57) and (6.58) to obtain the Q^2 depen-

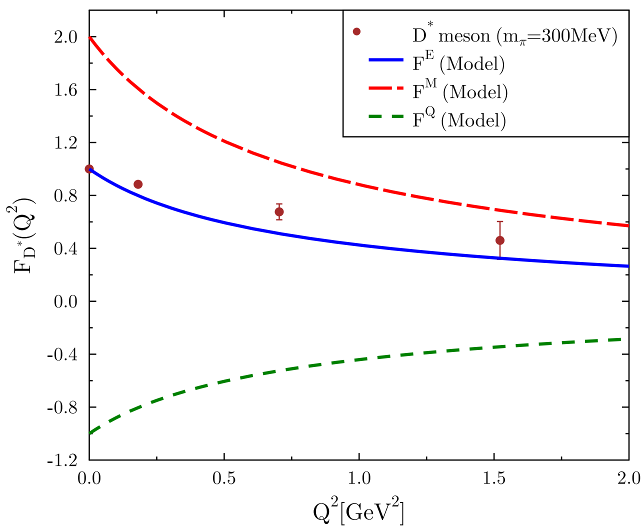

Figure 6.8: The electric (blue), magnetic (red) and quadrupole (green) EM form factors of the D^* meson. The electric form factor $F^E_{D^*}(Q^2)$ (solid blue line) is compared to lattice QCD data [22] (points with error bars).

$\langle r^2\rangle$ (fm^2)	Model	Experiment	Lattice QCD
π^+	0.35	0.45 ± 0.01 [126]	-
ρ^+	0.53	0.56 ± 0.04 [133]	-
K^+	0.33	0.31 ± 0.03 [126]	-
K^{*+}	0.52	-	-
D^+	0.19	-	0.14 ± 0.01 [22]
D^{*+}	0.33	-	0.19 ± 0.02 [22]

Table 6.7: The charge radii of π, ρ, K, K^*, D and D^* meson compared to experiment and lattice QCD.

dence of the EM form factors, the results are displayed in Figs. 6.9 and 6.10. We note that, for the case of pseudoscalar mesons, we find that EM form factor behave like $F_{\pi^a}(Q^2) \sim Q^{-2}$ and EM form factors of the vector mesons behave like $F_{V^a}(Q^2) \sim Q^{-4}$. Both results are consistent with perturbative QCD expectations and conformal symmetry in the UV.

As seen in Table 6.5, the coupling constants obtained involving the ground-state ρ meson and the

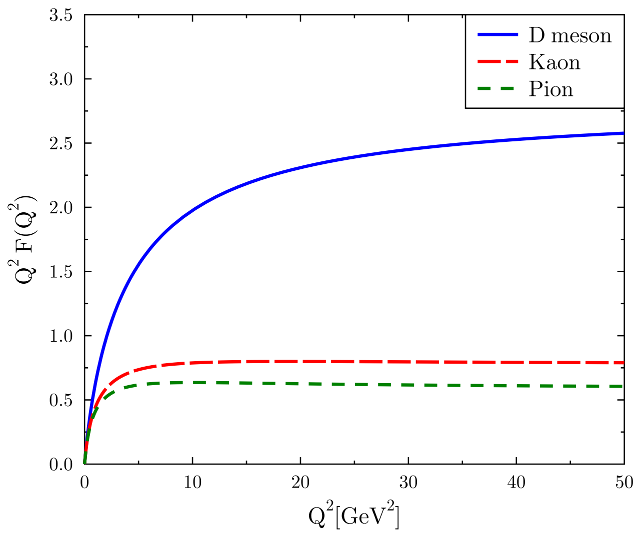

Figure 6.9: Plots of the large Q^2 behavior for the pseudoscalars: pion, kaon and D meson

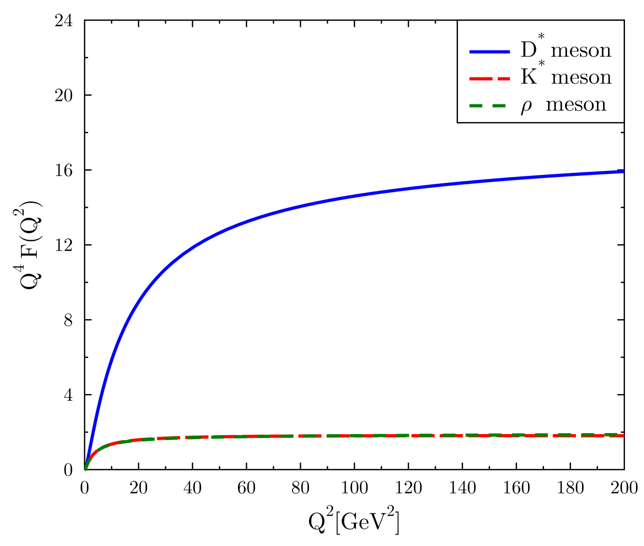

Figure 6.10: Large Q^2 behavior for the D^*-meson, K^*-meson and ρ-meson electromagnetic form factor.

charmed mesons, namely $g_{\rho DD}$ and $g_{\rho D^* D^*}$, are much smaller than the values obtained from $SU(4)$ flavor symmetry. Predictions based on the vector meson dominance model have given $g_{\rho DD} = 2.52 - 2.8$ that are bigger than our result $g_{\rho DD} = 1.103$. Furthermore, our result also shows the behavior $g_{\rho DD} < g_{\rho\pi\pi}/2$, which in turn, reveals a opposite trend to the predictions based on QCD sum rules [19] and Dyson-Schwinger equations of QCD [20], but it is in line that results obtained with the $^3\mathrm{P}_0$ pair-creation model in the nonrelativistic quark model in Ref. [17]. A reasonable explanation for the disparity for the small values of the couplings is that the electromagnetic form factor of the D meson is a great and dramatic example where the contribution of the resonances ρ^n can not be neglected, as occurs in the VMD approximation.

We finish this chapter making considerations on the applicability of the model used here. As discussed in chapter 4, this bottom-up holographic QCD model is based on light-flavor chiral Lagrangian, which we stress it in order to describe heavy-light mesons, once that the internal structure of these mesons is dictated by essentially the same nonperturbative physics governing the internal structure of light meson, which occurs at the scale Λ_{QCD}. But, in contrast, the internal structure of heavy-heavy mesons, as e.g. the ψ and η_c mesons, is governed by short-distance physics at the scale of the heavy quark mass. From the holographic point of view, an adequate description of these mesons requires the inclusion of long open strings. In this picture, it should be possible to describe the non-relativistic limit of heavy quarks where a spin-flavor symmetry takes place [134]. Although there have been some proposals using top-down models [135, 136, 137, 138] and others bottom-up models [139, 140], a realistic model for heavy-heavy mesons remains a challenge in holographic QCD.

7 Inverse Magnetic Catalysis in Dynamic Holographic QCD

In heavy-ion collision experiments intense magnetic fields can be created and influence the thermodynamics of the matter produced in the collisions [141]. For a long time the common understanding was that at any value of temperature the magnetic field should enhance the chiral condensate, an effect named as "magnetic catalysis"- a good review is found in Ref. [142]. This scenario received enormous support from the first lattice QCD results in the quenched approximation [143], performed using heavier quarks, instead physical quarks and without a proper continuum extrapolation [144, 145]. Recently, another lattice QCD study, where it has been used physical quark masses and performed an extrapolation to the continuum limit, reached a new and interesting conclusion [146]: the enhancement of the chiral condensate by the magnetic field (magnetic catalysis) at low temperature and a suppression of the chiral condensate by the magnetic field at high temperatures, revealing an inverse magnetic catalysis. In fact, around the crossover temperature T_c, the system reacts in a more complicated way to a external magnetic field, as consequence, the chiral condensate is a non-monotonic function of the external magnetic field and when this external magnetic field is large enough, it acts to suppresses the chiral condensate rather than enhancing it. This behavior is illustrated in Fig. 7.1, where it is shown the behavior of the chiral condensate as a function of the magnetic field at various temperatures around T_c.

Among attempts to explain such phenomenon, a promising one suggests a competition between the "valence" and the "sea" quark contributions in the QCD path integral, which in turn, has been observed on the lattice [147, 148]. We mean by valence quarks, ones that correspondent to the quarks in the $\bar{q}q$ operator inside the path integral and the magnetic effects, through this contribution, always work to catalyze the chiral condensate. We mean by sea quark contributions, ones that arise from the quark determinant that are related with the fluctuations around the path integral of the gluon part. In general terms, it is really difficult to find the B and T dependence of this contribution, but it end up suppressing the chiral condensate near to chiral transition

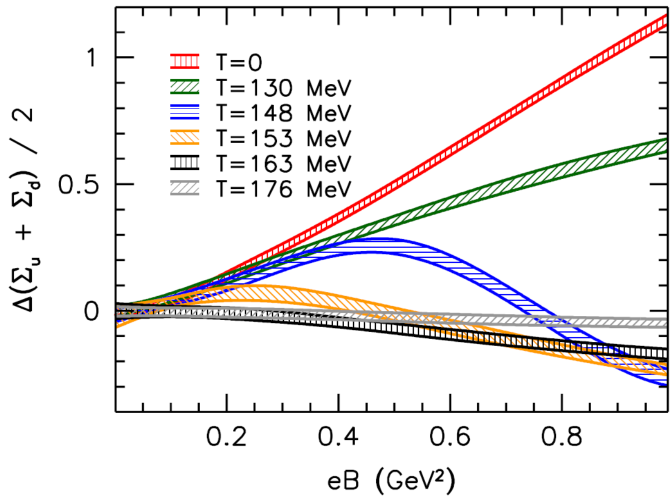

Figure 7.1: Lattice results for the change in the quark condensate as a function of magnetic field strength over a range of temperatures - figure taken from [24].

temperature. Despite this, is more fair to mention that a correct explanation of the mystery of the inverse magnetic catalysis still missing.

Holographically, there are several efforts trying to reproduce this interesting behavior. In recent AdS/QCD papers [149, 150], the inverse magnetic catalysis has been studied, but concentrated in the deconfinement temperature. The chiral physics was not directly included in such papers. More recently, some papers have studied the inverse magnetic catalysis using a model that includes the chiral physics [151, 152]. Interestingly, the authors in Ref. [153] claim that they do not have observed inverse magnetic catalysis in hard and soft wall holographic QCD models in the corresponding chiral transition, but they do have only for the deconfinement transition.

Motivated by these findings, in the present chapter we investigate the presence of the inverse magnetic catalysis in the chiral transition. As mentioned above, in Ref. [153] was found that the hard wall holographic QCD model, considered in the chapters 4, 5 and 6, does not support the inverse magnetic catalysis, because of this we will consider a different model based on the D3/D7 brane configuration. As we will see soon, the great advantage of the model is to turn on the chiral physics dynamically, namely, the chiral condensate is not an input but it is dynamically generated. Due to this feature, it is named as Dynamic Holographic QCD or Dynamic AdS/QCD. This situation is different compared with the hard wall holographic QCD model where the chiral condensate is an input. In other words, the Dynamic Holographic QCD model can be seen as an extension of the hard wall holographic QCD model.

This chapter is organized as follows: in the next section, we review the D3/D7 brane configuration and show how the inclusion of the dilaton changes the anomalous dimension and turns on the chiral condensate; in section 7.2, we present the Dynamic Holographic QCD model by imposing a specific form for the anomalous dimension, besides we show how this leads to a natural IR cutoff scale; in section 7.3, we include a black hole in the background to simulate the thermal effects and study the chiral phase transition in the model; in section 7.4, we implement the magnetic field terms in the model with two phenomenological parameters and identify regions where there are magnetic catalysis (MC) and inverse magnetic catalysis (IMC). We focus in the IMC region and show the decrease of the chiral transition temperature with the magnetic field, the behavior of the second order chiral transition and the decrease of the chiral condensate for large magnetic field, showing that our results are consistent with Fig. 7.1.

7.1 D3/D7 Brane Configuration - Review

As we have discussed in chapter 3, the simplest way to include quark bilinear operators in the gauge/gravity duality is to add N_f Dp-branes. As discussed there, the N_f D7 branes can be added in such a way that they extend in space-time, as summarized in Table 7.1, where 0 is the time direction. A good review on this subject is found in Refs. [154, 155]. We consider a stack of N_c coincident D3-branes (along 0123) which are embedded into the world volume of N_f D7 branes, along 01234567. In this way, the matter fields living in the fundamental representation of the $SU(N_c)$ group are generated through open strings ending in the D7-brane (flavor brane) and the other located in the D3-brane (color brane)

	0	1	2	3	4	5	6	7	8	9
D3	X	X	X	X						
D7	X	X	X	X	X	X	X	X		

Table 7.1: The D3/D7-brane intersection in 9 + 1 dimensional space.

In Fig. 7.2, we show the intersection between the D3 and D7 brane configurations and their separation L in the 89-directions, in a Minkowski space. However, as we have discussed in chapter 3, this distance is directly related to minimum energy of a string straining between D3-branes and D7-branes and also the lightest modes of such 3-7 strings gives rise to the quarks, whose bare mass

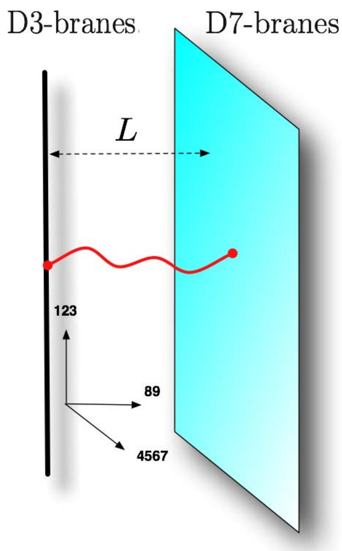

Figure 7.2: Intersection between the D3 and D7 brane configurations

is

$$m_q = \frac{L}{2\pi\alpha'} \tag{7.1}$$

In general, this system is hard to study but it can be tractable if we consider it in the limit where the N_f D7 brane configurations are treated as probes, namely, $N_c/N_f \to \infty$. In this limit, the N_c D3-branes dominate and give rise to the AdS$_5 \times S^5$ space-time, and then, we neglect completely the backreaction of the N_f D7 branes on the AdS$_5 \times S^5$ geometry. Thus, the metric generated is that given in Eq. (3.100), written as

$$ds = r^2(-dt^2 + dx_i^2) + \frac{1}{r^2}(dr^2 + r^2 d\Omega_5^2), \tag{7.2}$$

where we can still interpret that the second term in parentheses represents a $\mathbb{R}^6$ space. It is a transverse space to the N_c D3-branes, given by the 456789-directions. Then, we can write the radial coordinate r in terms of these transverse coordinates as

$$r^2 = x_4^2 + ... + x_9^2. \tag{7.3}$$

It is worth to remember that, once that just the gravitational effect of the D3-branes is taken into account, the 6-dimensional space transverse to them is not a flat space, so the Cartesian coordinates are not suitable. Despite this, they are still useful to label the different directions in this space.

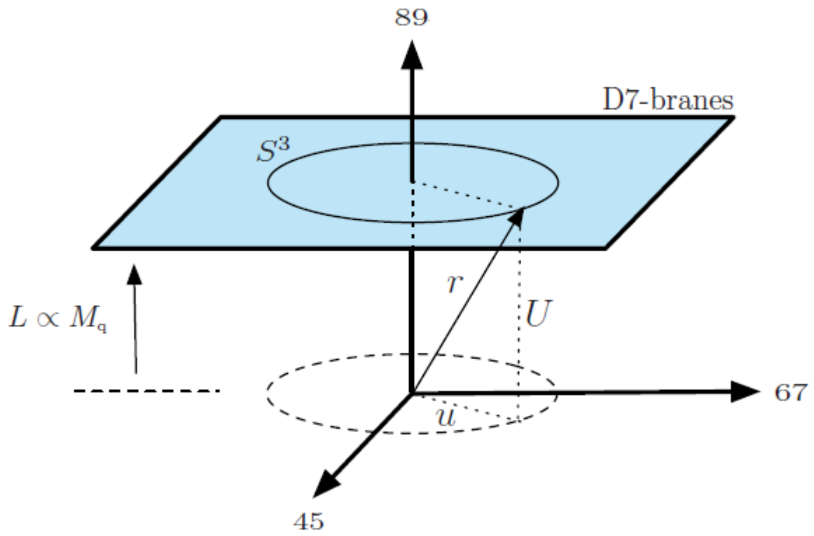

Figure 7.3: We present the coordinates in the 6-dimensional space transverse to the D3-branes. Each axis actually represents two directions, i.e, a plane (or, equivalently, the radial direction in that plane)

Before we write the action for the N_f D7-branes, let us first rewrite the metric element, in Eq. (7.2), of the background in a convenient form for our purposes by writing the six dimensional space as $\mathbb{R}^6 = \mathbb{R}^4 \times \mathbb{R}^2$. Then, in the $\mathbb{R}^4$ space we can define the following radial coordinate $\rho^2 = x_4^2 + ... + x_7^2$. This allows us to write the differentials as

$$dx_4^2 + ... + dx_7^2 = d\rho^2 + \rho^2 d\Omega_3^2, \tag{7.4}$$

where Ω_3 collects three spherical coordinates which parameterize an S^3-sphere, that we called by θ_1, θ_2 and θ_3. Similarly, in the $\mathbb{R}^2$ space we can also define another radial coordinate as $U^2 = x_8^2 + x_9^2$, and so, the differential

$$dx_8^2 + dx_9^2 = dU^2 + U^2 d\phi^2, \tag{7.5}$$

where ϕ is a polar angle in the plane $\mathbb{R}^2$. With such definitions, we have the overall radial coordinate r takes the form $r^2 = \rho^2 + U^2$ and we can also write

$$dx_4^2 + ... + dx_9^2 = d\rho^2 + \rho^2 d\Omega_3^2 + dU^2 + U^2 d\phi^2. \tag{7.6}$$

Our analysis is shown in Fig. 7.3, where have omitted the four first coordinates. It is showed a geometric view of the position of the D7 brane, ignoring the curvature generated by D3-branes, for simplification. It is worth to remember that our analysis remains valid if we take into account this curvature. Then, the metric of the $\mathrm{AdS}_5 \times S^5$ space in Eq. (7.2) assumes the following form

$$ds = r^2(-dt^2 + dx_i^2) + \frac{1}{r^2}(d\rho^2 + \rho^2 d\Omega_3^2 + dU^2 + U^2 d\phi^2). \tag{7.7}$$

Now we include the D7-brane in this scenario as a probe. A convenient way to write the probe D7-brane action is to choose a physical embedding where seven of the local coordinates on the D7-brane worldvolume are directly identified with the space-time coordinates $\mathrm{AdS}_5 \times S^5$. Since the D7-branes only span in the 4567-directions, they only wrap an S^3 inside the S^5, i.e, the D7-brane will wrap the three-sphere Ω_3. The position of the brane is therefore a point in the remaining two directions (U, ϕ). Then, we choose the following physical embedding

$$(\xi^0, \xi^1, \xi^2, \xi^3) = (x^0, x^1, x^2, x^3), \quad \xi^4 = \rho, \quad (\xi^5, \xi^6, \xi^7) = (\theta_1, \theta_2, \theta_3). \tag{7.8}$$

Thus, the D7-brane worldvolume may be parametrized by the coordinates $\{t, x_i, \rho, \Omega_3\}$. In order to locate the D7-branes one must then specify the remaining space-time coordinates, U and ϕ, as functions of all the worldvolume coordinates. However, the translational symmetry in the $\{t, x_i\}$-directions and rotational symmetry in the Ω_3-directions make U and ϕ depending only on ρ coordinate.

Thus, as discussed in chapter 3, the dynamics of the D7-brane configuration is described by the Dirac-Born-Infeld action given in Eq. (3.92), that we rewrite below

$$S_{DBI} = -T_7 \int d^8\xi \lambda(r) \sqrt{-\det(P[G_{ab}] + 2\pi\alpha' F_{ab})}, \tag{7.9}$$

where $T_7 = \left[(2\pi)^7 g_s \alpha'^4\right]^{-1}$ is the D7-brane tension and P denotes the pullback of the bulk field to the worldvolume of the brane. The dilation field is represented by $\lambda(r)$ in the action. F_{ab} is the world-volume field strength. For the moment, we will ignore the strength field $F_{ab} = 0$, but we will return to it later. It is worth to mention that the D7-brane action also contains a fermionic term S^f_{D7} [156], that naturally describes the spectrum of fermionic fluctuations of the D7-brane and, holographically, describes the baryonic system [75]. In this chapter, will not consider this fermionic sector.

The pullback of the metric $P[G_{ab}]$ given by

$$P[G_{ab}] = G_{MN} \frac{dx^M}{d\xi^a} \frac{dx^N}{d\xi^b}, \tag{7.10}$$

is evaluated using the relation in Eq. (7.8) and the metric in Eq. (7.7), so that

$$P[G_{00}] = -r^2, \quad P[G_{ii}] = r^2 \delta_{ii}, \quad P[G_{\rho\rho}] = \frac{1}{r^2}(1 + (\partial_\rho U)^2 + U^2(\partial_\rho \phi)^2), \tag{7.11}$$

$$P[G_{\theta_1\theta_1}] = P[G_{\theta_2\theta_2}] = P[G_{\theta_3\theta_3}] = \frac{\rho^2}{r^2}. \tag{7.12}$$

Initially, we will ignore the dilation effects in our description, which means we set $\lambda(r) = 0$, and so the DBI action in Eq. (7.9) becomes

$$S_{DBI} = -T_7 \mathrm{Vol}_{S^3} \mathrm{Vol}_{\mathbb{R}^{3,1}} \int d\rho\rho^3 \sqrt{1 + (\partial_\rho U)^2 + U^2(\partial_\rho \phi)^2}. \tag{7.13}$$

Recalling the D7-branes lie at $U = L$ and using the rotational symmetry in the 89-plane, that means we set $\phi = 0$, the above action is reduced to following form

$$S_{DBI} = -T_7 \mathrm{Vol}_{S^3} \mathrm{Vol}_{\mathbb{R}^{3,1}} \int d\rho\rho^3 \sqrt{1 + (\partial_\rho L)^2}. \tag{7.14}$$

This action can be still simplified if we take small configurations around $L = 0$. Then, linearizing the above action and keeping only the finite part, we get

$$S = \int d\rho\rho^3 (\partial_\rho L(\rho))^2, \tag{7.15}$$

where we have absorbed the volume factors into in S. We can rewrite the action in a standard form for a scalar in AdS_5 with mass squared equal to -3. This is done using the rescaling $L = \rho X$ and integrating by parts, which leads to

$$S = \int d\rho \frac{1}{2}\Big(\rho^5 (\partial_\rho X)^2 - 3\rho^3 X^2\Big). \tag{7.16}$$

This is the canonical form for a scalar field in AdS_5. Note that, the action in Eq. (7.16) has the same form of Eq. (4.32), with the identification $\rho = 1/z$. Therefore, the solution of the equation of motion that comes from the action in Eq. (7.16) is also that given in Eq. (4.34). In terms of the L field, we have

$$L(\rho) = m + \frac{\sigma}{\rho^2}, \tag{7.17}$$

where, following the holographic dictionary described in chapter 3, the L field is related to a field theory operator of dimension 3 and its dimension 1 source, where the coefficients m and σ are interpreted, respectively, as the bare quark mass and the quark condensate. Based on the top-down D3/D7 system, we use the IR condition $\partial_\rho L(0) = 0$ as a regularity condition in the IR regime. This IR condition leads to the condition $\sigma = 0$. That means that we do not have spontaneous chiral symmetry breaking (SCSB).

In order to turn on SCSB, we have to modify the behavior of the field configuration in the IR region. To do so, we consider the dilaton effects, incorporated via $\lambda(r)$, in the linearization process.

Thus, expanding again the action in Eq. (7.14) for small L, we have the following leading order terms

$$S = \int d\rho \Big[\frac{1}{2}\,\lambda(r)|_{L=0}\,\rho^3 L'(\rho)^2 + \rho^3\,\lambda''(r)|_{L=0}\,L(\rho)^2\Big], \tag{7.18}$$

where $L'(\rho) = \partial_\rho L(\rho)$. In order to find the canonical kinetic term we can use the following transformation

$$\lambda(\rho)\rho^3 \frac{d}{d\rho} = \tilde{\rho}^3 \frac{d}{d\tilde{\rho}}. \tag{7.19}$$

The first term in Eq. (7.18) can be rewritten by setting $L = \tilde{\rho} X$ as

$$S = \int d\rho \frac{1}{2}\tilde{\rho}^3 L'^2 = \int d\rho \frac{1}{2}\Big(\tilde{\rho}^5 X'^2 - 3\tilde{\rho}^3 X^2\Big), \tag{7.20}$$

where $L'(\tilde{\rho}) = \partial_{\tilde{\rho}} L(\tilde{\rho})$. This is precisely the action obtained before for a canonical scalar field in AdS_5 given in Eq. (7.16). The remaining term in Eq. (7.18) becomes

$$S = \int d\tilde{\rho} \frac{1}{2}\lambda \frac{\rho^5}{\tilde{\rho}}\frac{d\lambda}{d\rho} X^2. \tag{7.21}$$

Then, we see that the mass of the scalar field acquires a ρ dependent mass squared, given by

$$m^2 = -3 + \Delta m, \quad \Delta m = -\lambda \frac{\rho^5}{\tilde{\rho}^4}\frac{d\lambda}{d\rho}. \tag{7.22}$$

Going back to the L field, the action (7.18) is rewritten as

$$S = \int d\rho \frac{1}{2}\Big(\rho^3 (\partial_\rho L(\rho))^2 + \rho \Delta m L(\rho)^2\Big). \tag{7.23}$$

Note that the term Δm involves all the leading order dilaton effects and acts to change the mass of the scalar field. Using the relation between the scalar mass squared and the dimension of the field theory operator, $m^2 = \Delta(\Delta - 4)$, obtained in chapter 3, we conclude that the change in the mass implies in a running in the dimension of the operator $\bar{q}q$. Thus, in the UV regime we have $\Delta m = 0$, and the scalar field describes a dimension 3 operator and dimension 1 source as it is required for it to represent $\bar{q}q$ and the quark mass m.

Now, we can find the Euler-Lagrange equation for determine of L field, we have

$$\partial\rho[\rho^3 \partial_\rho L] - \rho\Delta m L = 0, \tag{7.24}$$

where we point out that: in the UV regime, the solution remains that in Eq. (7.17) but the profile of the field configuration L is modified in the IR due to presence of the Δm. This leads to the realization of the spontaneous chiral symmetry breaking, $\sigma \neq 0$. In other words, the running of the dimension of $\bar{q}q$ turns on the chiral dynamics.

7.2 The Dynamic Holographic QCD model

In the previous section, we have obtained a linearized action (7.23) of a scalar field from the D3/D7(probe) configuration. We also have observed that the dilaton introduced a running in the mass of the scalar field and this generated a chiral condensate in the model. These two facts motivate us to propose a model living in AdS_5 where Δm is chosen via QCD running coupling. Thus, action of the model is exactly the action in Eq. (7.23) (dropping the overall constant)

$$S = \int d\rho\Big(\rho^3(\partial_\rho L(\rho))^2 + \rho\Delta m(r)L(\rho)\Big), \tag{7.25}$$

living in the five dimensional background AdS_5 with the metric given by

$$ds^2 = r^2(-dt^2 + dx_1^2 + dx_2^2 + dx_3^2) + \frac{1}{r^2}d\rho^2, \tag{7.26}$$

where the coordinate $r = \sqrt{\rho^2 + L^2}$ is identified with the energy scale $r = \mu$, using the holographic identification. Note that, if $L = 0$ the quarks are massless and the above metric is pure AdS_5, making the dual field theory conformal. But, if $L \neq 0$ the metric just becomes AdS_5 asymptotically in UV regime, i.e, when $\rho \gg L$. This shows that L breaks the conformal symmetry and so an IR cutoff is generated. This is illustrated in Fig. 7.4

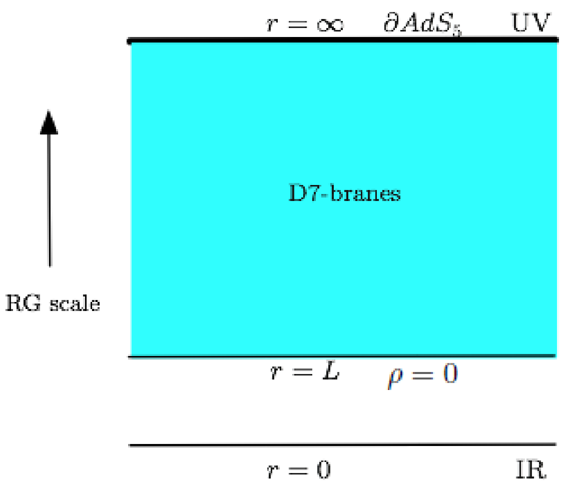

Figure 7.4: The radial coordinate r, holographically identified as the energy scale μ. Note that, interestingly, the IR cutoff is generated by the value of the $L(0)$.

In general, the dynamic holographic QCD model consists in imposing a specific form for Δm and we do so using the anomalous dimension of $\bar{q}q$ that comes from perturbative QCD at two loops. It is important to point out that this is an mere ansatz for the model. Then, the $\bar{q}q$ operator dimension, written as $\Delta = 3 - \gamma(\mu)$ can be used to rewrite the mass-dimension relation as $m^2 = -3 - 2\gamma(\mu)$. Now, using relation (7.22), we easily identify that $\Delta m = -2\gamma(\mu)$, whose explicit form is

$$\Delta m = -2\gamma = -\frac{3(N_c^2 - 1)}{2N_c\pi}\alpha(\mu), \tag{7.27}$$

where the two-loop running result for $\alpha(\mu)$ is

$$\mu\frac{d\alpha}{d\mu} = -b_0\alpha^2 - b_1\alpha^3, \tag{7.28}$$

where

$$b_0 = \frac{1}{6\pi}(11N_c - 2N_f), \quad b_1 = \frac{1}{24\pi^2}\left(34N_c^2 - 10N_cN_f - 3\frac{N_c^2-1}{N_c}N_f\right). \tag{7.29}$$

As we mentioned before, the perturbative ansatz used for the running coupling is only valid near to the UV regime of the theory but it provides a sensible guess as to the form of the running in QCD. In fact for $N_c = N_f = 3$, the case studied here, the two loop contribution has only a small effect on the deep IR. Going to two loops does allow the study of walking and conformal window dynamics as done in Refs. [157, 158]. [1]

Given a specific choice of the running of γ, we can solve numerically the Euler-Lagrange equation which gives the dynamics of L field. Besides, the simplest way to identify the spontaneous chiral symmetry breaking is to look for solutions that start with $\partial_\rho L(0) = 0$ in the IR regime and shoot out the behavior in the UV regime to match with $L(\rho \to \infty) = 0$. So, spontaneous chiral symmetry breaking can be signalized by the value of $L(0)$, that is naively identified as the IR quark mass, once that for $L(0) = 0$ the solution vanishes and there is no chiral condensate and for $L(0) \neq 0$ the solution reaches the UV with a curvature, implying in the occurrence of a chiral condensate. Still, as have been pointed out in Ref. [159], the chiral breaking is realized when the mass of the scalar field L can run below the Breitenlohner-Freedman (BF) bound [160], $m^2 \leq -4$ or $\Delta m \leq -1$, making it unstable (see Fig. 7.5). In fact, above this bound the flat solution $L = 0$ is more energetically favorable and leads to a vanishing condensate. Otherwise, if the mass crosses the BF bound, the solution obtained from $L(0) \neq 0$ is energetically favorable than the flat solution $L = 0$ and as consequently, the chiral condensate is dynamically generated. This condition is very important to obtain the chiral physics in the model.

Another important observation is that, as have shown in Ref. [159], it is possible to show that a change in the number of flavors also leads to mass crossing the Breitenlohner-Freedman (BF) bound,

[1] We also have explored larger N_f, N_c parameter space with B field but the behaviours we find are very like those reported here for the $N_c = N_f = 3$ QCD case so we do not present them here.

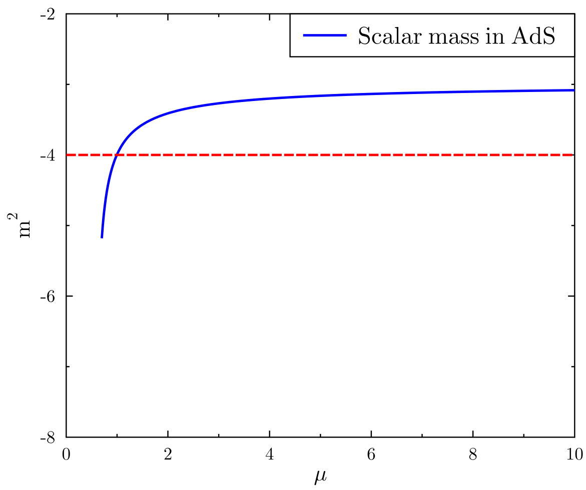

Figure 7.5: The mass of the scalar field $L(\rho)$ crossing the BF bound $m \leq -4$ triggering the spontaneous symmetry breaking ($\sigma \neq 0$).

suggesting a dependence of the chiral condensate with the number of flavors and consequently their vanishing. As we have said in the introduction of this chapter, this scenario is quite different when compared with the hard wall holographic QCD model, when the condensate is introduced by hand.

We highlight an important point here: in the IR regime, we should consider a natural cut off $\mu \sim \Lambda_{QCD}$ and we will take this into account when we solve the equation of motion that comes from Eq. (7.25). Then, we choose to impose the IR condition ($\partial_\rho L = 0$) at the scale where $L = \rho$, corresponding to the "on mass shell" condition for the quark. If we were to consider the theory below this scale, we would have to include the decoupling of the quarks from the QCD running below that scale, but this is not necessary for our purposes that is to study the chiral condensation. We show in Fig. 7.6 the solutions for Eq. (7.24)

7.3 Dynamic Holographic QCD at finite temperature

We now turn our attention to the case of nonzero temperature, $T \neq 0$. As discussed in chapter 3, finite temperature can be included in the model by introducing a black hole in the background [5]. We have

$$ds^2 = \rho^2(-f dt^2 + d\vec{x}^2) + \frac{d\rho^2}{f\rho^2}, \quad f = 1 - \frac{r_H^4}{r^4}, \tag{7.30}$$

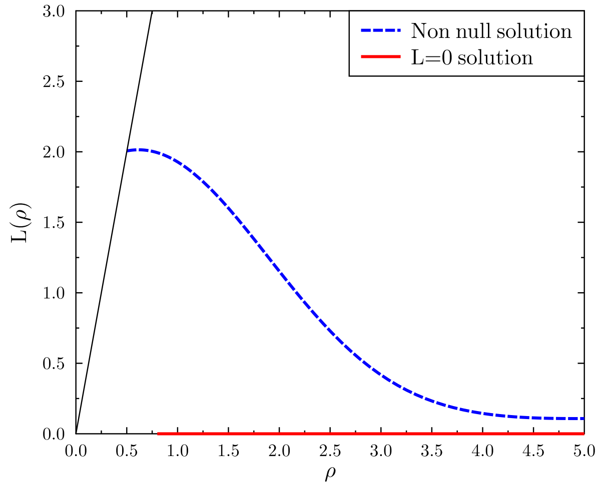

Figure 7.6: The red curve shows the vanishing solution for $\partial_\rho L(0) = 0$ and the blue curve shows the nonvanishing solution for $\partial_\rho L(0) \neq 0$.

where r_H is the event horizon and it is proportional to the temperature ($T = r_H/\pi$). Thus, the action in Eq. (7.25) for L becomes

$$S = \int d^4x d\rho \, \left(\rho^3 f (\partial_\rho L)^2 + \rho \Delta m^2(r) L^2\right). \tag{7.31}$$

The study we must perform here is very analogous to that of the last section, but the equations are more complicated due to thermal terms. Now, for the radial coordinate r we adopt the following prescription

$$r = \sqrt{\rho^2 + \kappa L^2}. \tag{7.32}$$

Most simply one would set $\kappa = 1$. Note that, the parameter κ can deform the black hole in the ρ-L plane. One again seeks numerical solutions of the Euler-Lagrange equations subject to $L \to 0$ as $\rho \to \infty$ to describe massless quarks. In the IR one chooses either $\partial_\rho L = 0$ at the "on-mass" shell condition or for the end point of the flow to lie on the black hole. In the presence of the black hole, we have the possibility of three solutions. The first one is that does not touch the black hole, the non black hole solution (nbh). The second one touches the black hole, the black hole solution (bh). The last one is already known as the flat solution ($L = 0$). The true solution will be given by one that minimizes the free energy, holographically defined as $F = -S$.

The general idea here is to get the chiral condensate as a function of the temperature. For $\kappa = 1$ case: the bh solution is not energetically favorable ever and increasing the temperature, the nbh

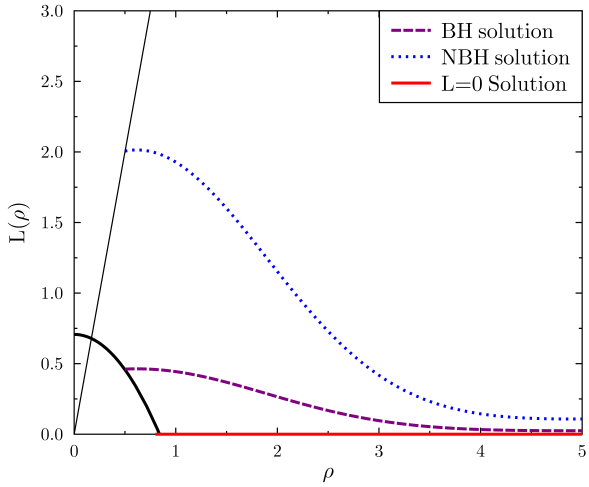

Figure 7.7: Three possible solutions at finite temperature: non black hole solution, the black hole solution and the flat solution.

solution is energetically favorable until a critical temperature T_c. Above this critical temperature the flat solution ($L = 0$) starts being favorable, abruptly. This behavior signalizes a first order transition for the condensate in terms of the temperature at T_c. This can be checked in the black curve in Fig. 7.8.

As pointed out in Ref. [161], lower values of κ turn on the transition to second order. In fact, decreasing the values of κ, we note that the bh solution plays an important role. This way, at low temperatures, the nbh solution is more favorable than the others. Decreasing the value of κ, the nbh solutions move to the bh solutions. As the value of κ is decreased the bh solution approaches the flat solution ($L = 0$), at higher temperatures, reaching thus at a second order transition at some critical temperature T_c. In the second order case there is again an horizon ending solution for L but it now emerges at low T from the chiral symmetry breaking solution and then moves to merge with the $L = 0$ embedding at higher temperature. In Fig. 7.8, we plot these results in terms of the chiral condensate, σ, against T and we see that it is possible to move from the first order to second order transitions when we move from the $\kappa = 1$ for $\kappa = 0.05$. In Fig. 7.9, we show the explicit second-order behaviour at $\kappa = 0.05$ by plotting the embeddings of the scalar L in the chiral limit (i.e. $L(\rho \to \infty) = 0$) as the temperature is increased towards the critical value. At $\rho \approx 2$ it is already evident that the value of the condensate, proportional to the gradient of the embedding $\partial_\rho L|_{\rho\to\infty}$, decreases with increasing temperature. Moreover, as we approach the critical

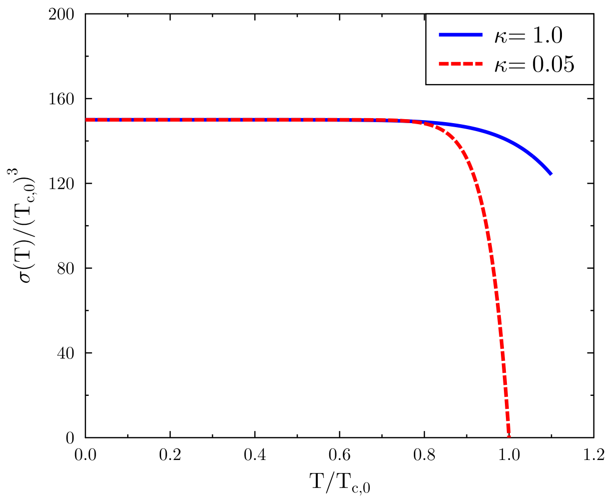

Figure 7.8: Thermal phase transitions in the holographic model with $N_c = N_f = 3$. For values of the parameter κ close to $\kappa = 1$, a first order chiral transition is present. As the value of κ is reduced and the black hole is deformed along the L-axis, the phase transition switches to second order.

temperature, the angle subtended by the arc of the black-hole horizon between $L(\rho)$ and $L = 0$ decreases smoothly to zero at $T = T_{c,0}$. Above this value only the flat, chirally symmetric $L = 0$ embedding exists.

It is also important to explain the physics that involves the two continuous transitions shown in Fig. 7.9. At low temperatures the solution lies off the black hole horizon and those small fluctuations around this solution will correspond to the mesonic modes [162]. In this phase, they are completely stable. However, when the solution moves on to the black hole the correspondent mesonic fluctuations become quasi-normal modes that describe unstable plasma fluctuations, as discussed in Ref. [163], namely, the mesons of the theory have melted. The solution continues to evolve with T until it reaches the vanishing solution (flat solution) and chiral symmetry is finally restored.

In this effective description, we take κ as a parameter to be adjusted to reproduce correctly the expected chiral phase structure at a given N_c, N_f. To represent QCD we choose the second order behaviour and, as seen, we set $\kappa = 0.05$. We will use the value of r_H at which the transition occurs at $B = 0$ to set the scale of the radial energy direction, ρ, in the holographic model. Thus, we set $T_{c,0} = 160$ MeV.

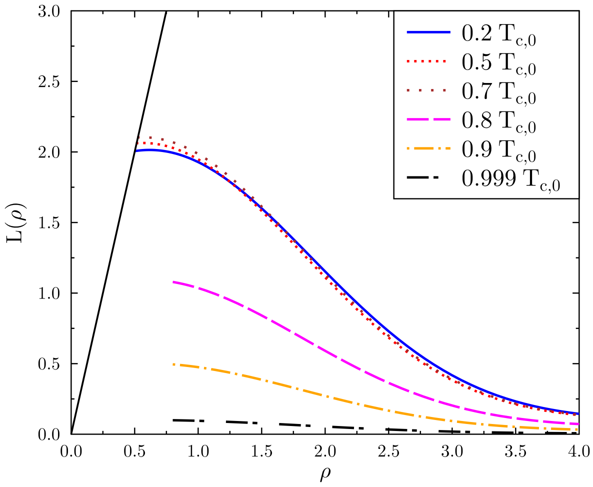

Figure 7.9: Plot showing the chiral embeddings for a range of temperatures. Each embedding is colored to match the black hole horizon (not illustrated) pertaining to the relevant temperature. The second order nature of the transition is evident; the embedding smoothly transforms into the flat $L = 0$ embedding at the critical temperature, $T_{c,0}$.

7.4 Magnetic Field in Dynamic Holographic QCD

Next we complete our description by introducing a magnetic field in the model to study how it affects the behavior of the chiral condensate. As anticipated in section 7.1, the magnetic field comes from the massless $U(1)$ gauge field that appears in the DBI action in Eq. (7.9). Following the same procedure adopted in section 7.1 and taking just the leading order terms in the expansion in L, we obtain interaction terms like products between the field L and its derivative $\partial_\rho L$ and F^2. As before, these two terms allow us to propose an additional action that involves the $U(1)$ gauge field, as follows

$$\Delta S = \int d^4x d\rho \, \left(a\rho F^2 L^2 + b\rho^3 f(r) F^2 (\partial_\rho L)^2 \right), \tag{7.33}$$

where we have already included in the second term the black hole factor to take into account temperature effects. Now, for the case where the magnetic field is fixed and including the metric factors, we have that $F^2 = B^2/\rho^4$. Furthermore, in the present case, we will treat a and b as phenomenological parameters that will be fixed. Note that the term involving the a parameter gives a direct B dependent contribution for the running of the L mass, and consequently, for the anomalous dimension of the quark-antiquark operator. The choice of the sign of a can favor or disfavor chiral condensation by affecting where the BF bound is violated. On the other hand, the term involving the b parameter, also depending on its sign, changes the curvature of the L profile which, in turn, also can favor or disfavor chiral condensation. We note that the magnetic field now enters into the action in the combinations aB^2 and bB^2 so it is possible by choice of the magnitude of a and b to move the scale of effects in B.

Note that only the second term in Eq. (7.33) has temperature dependence when one naively inserts the metric factors (from the ρ index contraction in $(\partial_\rho L)^2$). As one approaches the black hole horizon, this term decreases. One can play with these two terms against each other. This way, at zero temperature the second term might dominate and favor chiral condensation. Though, at finite temperature it will be less favored and the first term might take over suppressing chiral condensation. This is our first strategy to realize the observed pattern of catalysis and inverse catalysis with temperature.

Our numerical procedure is again to find the solutions for L for each value of T and B and for given values of the phenomenological parameters a, b and κ; here we will set $N_f = N_c = 3$. As we have seen, for κ of order one the thermal transition is first order. The embedding profile for L jumps from a solution off the black hole to the flat embedding ending on the horizon. Thus, the transition is driven by the black hole "eating" the $L = 0$ configuration until its energy becomes smaller than energy of the solution off the black hole. For this reason, the chirally symmetric low T phase is fairly insensitive to the temperature and it is very hard to engineer T dependent behaviour. The only shifts from magnetic catalysis to inverse catalysis that we can find occur when the a and b terms are so finely tuned that they have negligible net effect at $T = 0$. The catalysis effect is well below a percent. We conclude that the QCD behaviour with B, T is a result of the second order transition behaviour.

We next turn to $\kappa = 0.05$ as an example of a model with a second order transition. In Fig. 7.10 we show the structure predicted by the model in terms of the phenomenological parameters a and b. This $a - b$ phase space comprises four different sectors; a region in which the chiral condensate, σ, is *always* enhanced relative to the external magnetic field, a region in which σ is *always* suppressed relative to the external magnetic field and two regions where it is either enhanced at low temperatures and suppressed at high temperatures (IMC) or vice versa.

For each point in the a, b plane we can plot the condensate against T at non-zero B. In all cases the chiral transitions are second order. Before showing our main result, we need to make a good choice for the parameters of the model, a, b. We will choose them in order to get the best

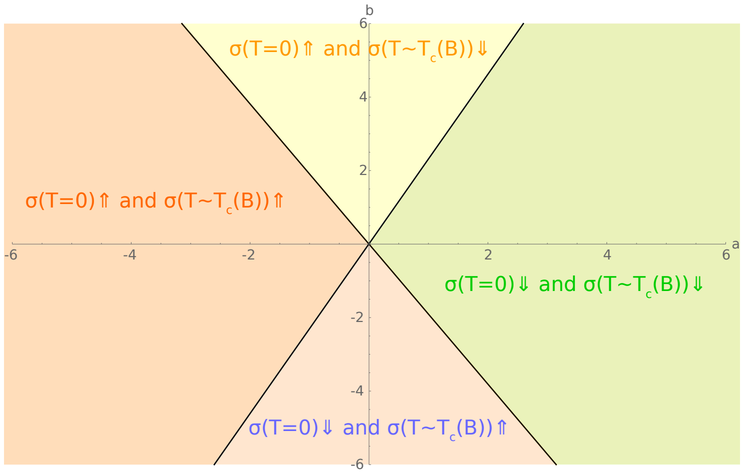

Figure 7.10: The phase-structure of the holographic model in terms of the phenomenological parameters a and b. The $a-b$ plane can be dissected into four sectors wherein the condensate is affected differently with temperature and an external magnetic field.

fit to the QCD behaviour. As we already discussed, the inverse magnetic catalysis (IMC) is also characterized by a reduction of the critical temperature with the magnetic field. Focusing in the case in which $a = 0, b = 0.037$, we show the consistency of the model showing the decrease of the critical temperature in Fig. 7.11.

We have found a good fit to the QCD behaviour when we take $\kappa = 0.05$ and $a = 0$. To fit b we use the lattice fit in Ref. [164] for the temperature dependence of the critical temperature. In that work, the authors fit the result with a function of the form

$$\frac{T_c(eB)}{T_{c,0}} = \frac{1+\alpha(eB)^2}{1+\beta(eB)^2}, \tag{7.34}$$

where $e^2/4\pi = 1/137$. The lattice results find central values, from fitting to the light quark condensate, $\alpha = 0.54$ and $\beta = 0.82$. In Fig. 7.11 we show our fit to this data for b - the lattice and holographic models can be made to lie very close to each other when $b = 0.037$ - the holographic QCD model best fits the functional form with $\alpha = 0.78$ and $\beta = 1.08$.

As we mentioned in the introduction of this chapter, the lattice QCD result shown in Fig. 7.1 indicates a non-trivial relationship between the chiral condensate and the strength of the external magnetic field. As seen, at low temperatures, the magnetic catalysis of the condensate is apparent and at temperatures approaching the critical value, there is a suppression of the condensate with B, revealing the inverse magnetic catalysis phenomenon. This, first of all, points us to the top centre quadrant of the $a-b$ plane in Fig. 7.10. It is encouraging that the holographic QCD model can incorporate the QCD behaviour although the freedom of the a, b parameter space suggested

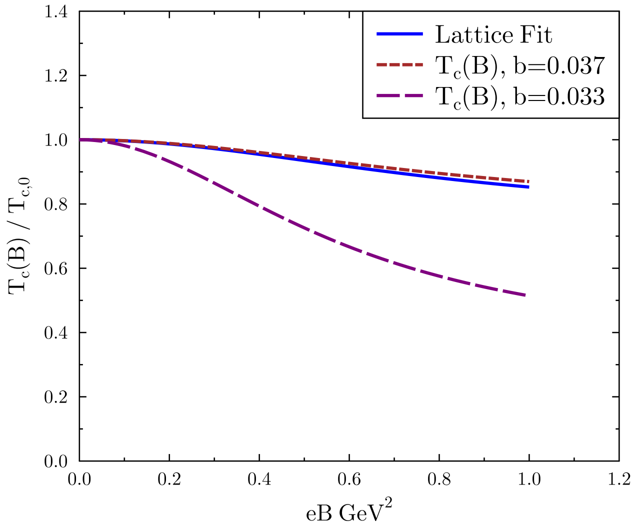

Figure 7.11: The critical temperature against eB, $T_{c,0} = 160$MeV. We show the best fit lattice data taken from [164] and the holographic model best fit to that data ($\kappa = 0.05, a = 0, b = 0.037$). We also show the holographic model prediction for another value of $b = 0.33$ - the model depends on the quantity bB^2 so the eB axis is simply rescaled by this change.

it should be possible. We show the dependence of the condensate on the temperature in Fig. 7.12 where one sees that the chiral condensate is enhanced at small T but suppressed at $T \approx T_{c,0}$. The value of the critical temperature of the chiral phase transition, of course, is dependent on how the external magnetic field affects the value of the condensate.

A further interesting feature of the lattice plot is that for a narrow range of temperatures approaching the critical value, $\sigma(B)$ behaves non-monotonically, indicating magnetic catalysis for small values of the magnetic field but as the strength of the external B-field is increased, the field catalyses a suppression - we will refer to this intermediate behaviour as the 'cross-over' regime. One question we could ask of our model is whether or not this cross-over behaviour can be obtained if one were to select values of the phenomenological parameters a and b to be inside the appropriate sector of the $a - b$ plane.

The appropriate quadrant shown in Fig. 7.10 that contains the b axis where $a = 0$ is the key point that allows us to achieve the cross-over behaviour in the holographic QCD model discussed here. Intriguingly, just the b term contribution is able to generate magnetic catalysis at low temperatures

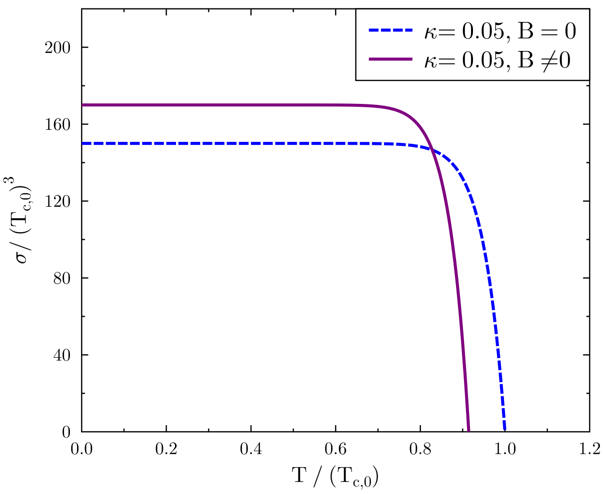

Figure 7.12: The introduction of a magnetic field affects the value of the transition order parameter, σ. We show an example with magnetic catalysis at low temperature and inverse magnetic catalysis at higher temperatures, a phenomenon which reduces the critical temperature, $T_c(B) < T_{c,0}$. This is plotted using the choices $a = 0, b = 0.037$

and inverse magnetic catalysis at higher temperatures. A detailed investigation shows that the reason behind this is that term acts differently on solutions that touch the black hole and that do not touch it. In Fig. 7.13, we show the effect of the magnetic field on the solutions (embeddings) at an intermediate temperature $T = 0.75T_{c,0}$. At zero magnetic field we see the phase before the mesons have melted. Increasing the magnetic field in the theory keeping only the b interaction term, derivatives are stimulated in the UV regime but not close to the horizon where the b term vanishes due to its T dependence. As a consequence, in the IR regime the magnetic field moves the solution towards a melted phase whilst the UV condensate grows. Once the embedding is brought onto the black hole, the magnetic field moves the solution down the horizon and then the UV condensate decreases. We did not deliberately engineer this behaviour but it does match the observed lattice results.

With all parameters fixed, we are able to plot the fractional change in the condensate against eB at different T values. We show these results in Fig. 7.14. We see the enhancement of the chiral condensate at zero temperature but a suppression near the critical value. Of course, it should be reiterated that without the lattice data already in place, we do not know *a priori* which values of a and b should be chosen to best fit QCD. Once chosen these appropriate values for

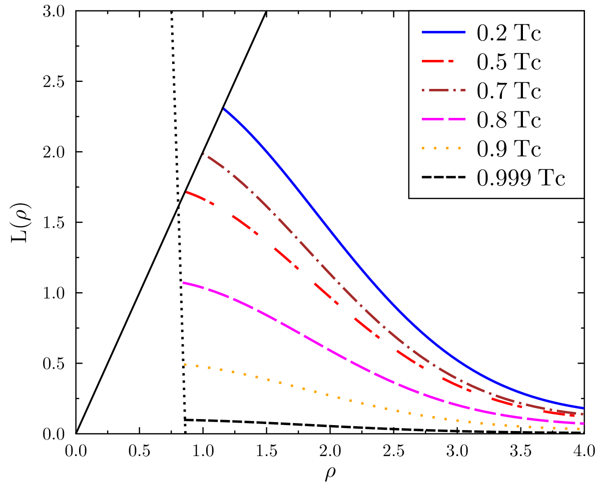

Figure 7.13: The chiral embeddings at $T = 0.75T_{c,0}$ for a range of values of magnetic field. Increasing B moves the embedding towards to the horizon but initially also increases the condensate value.

the phenomenological parameters a and b, it is no surprise that we can reproduce the expected enhancement and suppression of σ at low and high temperatures, respectively. More remarkable, however, we also find the cross-over regime needed by Fig. 7.1. For intermediate temperatures, a transition occurs at some value of B at which the condensate changes from increasing to decreasing with an increasing magnetic field strength. The turn over point of this transition can be identified in the holographic QCD model as the value of the magnetic field at which the non black solution moves to the black hole solution, i.e. the meson melting phase transition. The match between Fig. 7.1 and Fig. 7.14 is not exact once the holographic QCD model gives less catalysis at low T and too much inverse catalysis at higher T but the general structure is similar. We hope that we have learnt from the holographic QCD model that the meson melting behaviour is key to the structure of the transitions seen with B.

We conclude by remarking that the dynamic holographic QCD model seems to provide an excellent extension of the hard wall holographic QCD model because all the chiral physics emerges naturally from the running of the anomalous dimension of the $\bar{q}q$ operator. We have fitted the κ parameter to turn on the second order chiral phase transition. Magnetic field enters the holographic model through two terms linking the condensate and a bulk baryon number gauge field. Finally, we have shown that, for the zero quark mass theory, magnetic catalysis at low T and inverse catalysis

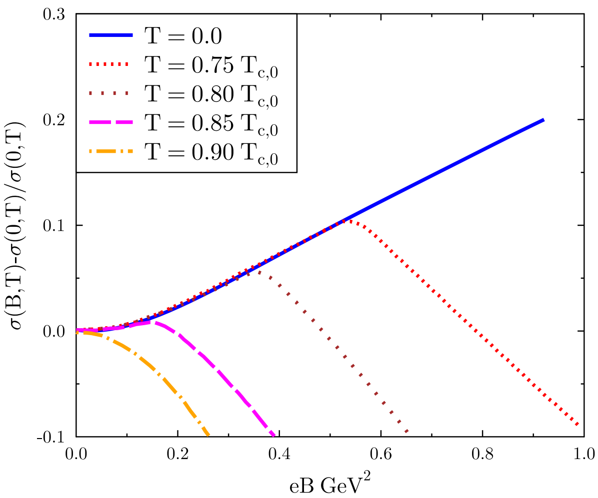

Figure 7.14: Results predicted by the holographic model for the change in the condensate of light quarks as a function of magnetic field strength over a range of temperatures for $N_c = N_f = 3$. $T_{c,0}$ is the thermal transition temperature at $B = 0$ which is used to set our holographic energy scale (which is approximately 160 MeV according to the lattice simulations). For this plot the model parameters are taken as $\kappa = 0.05$ and $b = 0.037$.

at high T can be achieved in the parameter space of the model. In Ref. [165], we have included the quark mass in the model in order to investigate its effects on the inverse magnetic catalysis, as argued there, the scale in B at which inverse catalysis sets in grows with the quark mass. Since the model is not valid at too large values of B this suggests the physics of large quark masses is dominated by catalysis rather than inverse catalysis. This behaviour may be useful for understanding the observed lattice QCD data.

8 Conclusions

In this thesis we studied three problems relevant for the hadron physics, in special involving chiral and flavor physics: the vanishing of the leptonic decay constants of pion's excited states, the SU(4) flavor symmetry breaking on the strong coupling constants and the inverse magnetic catalysis. We have used holographic QCD models that are motivated in the gauge/gravity duality, originally proposed in Refs. [5, 3]. Since then, the duality has been used for study nonperturbative phenomena in several area of research.

In chapter 2 we revising important aspects of QCD; we presented the chiral symmetry as a good approximation for QCD as we consider the light quarks. We also discussed the dynamical chiral symmetry breaking and how it is related to existence of the pseudo-Goldstone bosons (pion and kaons). The partially conserved axial-vector current (PCAC) was derived and it was used to obtain the Gell-Mann-Oakes-Renner relation (GOR) for the pion, showing the behavior $m_\pi \sim m_q^{1/2}$. We finished the chapter discussing the color-confinement hypothesis, by introducing the Wilson loop as a criterium to indicate whether or not a certain gauge system is confining. As the Wilson loop is related with the quark-antiquark potential, in the quenched approximation, the confinement is signalized when the potential is linear. As mentioned in this chapter, there are other quantities that can indicate confinement as the Polyakov loop, the 't Hooft loop, vortex free energy.

In chapter 3 we introduced the basis of the gauge/gravity duality using a geometrized version of the renormalization group and, based on this, we obtained the AdS_5 space-time as result of a conformal invariance in four dimensions. We presented how fields in 5d are related with currents in 4d via holographic dictionary and we presented the GKPW prescription that identifies the generating functional of the gravity side in 5d with that of the 4d gauge field theory and allow to evaluate the correlation functions of the field theory. To clarify this prescription we evaluated correlations functions of a conformal field theory using a scalar field in AdS_5 space-time. In addition, we showed that the temperature is introduced in the duality inserting a black hole in AdS_5 space-time. We finished this chapter revising shortly the gauge/gravity duality from string theory perspective, we discussed the low energy limit of a N_c branes system in two approaches that lead to conjecture

SUSY theory as equivalent to supergravity theory. This makes clear the limit of validity of the classical approximation, $N_c \to \infty$. Finally, we discussed the inclusion of the N_f flavors in the duality via a N_f probe brane in the transverse direction of the N_c branes.

In chapter 4 we started explaining how the duality is addressed to QCD and we presented two approaches in which holographic QCD models can be constructed: top down and bottom-up approaches. Next, we discussed the holographic version of the Wilson loop, a string moving in the background space-time, and showed the criterium that the background must satisfy to be confining. This way, we used the simplest confining background, the hard wall. We introduced the bottom-up holographic QCD model that implements dynamical chiral symmetry breaking via the X field and the vacuum structure is given in terms of the quark masses and condensates. We used the action expanded up to second order and the Kaluza-Klein expansion to find the equations, whose eigenvalues are the masses of the mesons, and find the decay constants of mesons via the definition of holographic currents. We used also the action expanded up to third order and the Kaluza-Klein expansion we found a direct prescription for the coupling constants involving 2 pseudoscalar and 1 vector meson and coupling constants involving 3 vector mesons.

In chapter 5 we used the holographic QCD model for 2 flavors to include the pion and study the vanishing of the leptonic decay constants of their excited states in the chiral limit, as predicted in QCD. We wrote the equations that give the mass spectrum for the $SU(2)$ case and considered the isospin limit. This way, we obtained the asymptotic expansion for the fields near to the boundary. Next, we used the holographic currents to derive the partial conserved axial current (PCAC) and generalized Gell-Mann-Oakes-Renner relationship. We have fitted the position of the hard wall using the ground state of ρ meson. Then, we used the Mathematica to find, as function of quark mass, the mass, the normalization constant and the decay constant, for the ground and excited states. This way, we have found leptonic decay constants of excited states vanish in the chiral limit. Despite of our results have been derived in a hard wall background, we believe that them will happen in any holographic model that implements dynamical chiral symmetry breaking and reproduces the Gell-Mann-Oakes-Renner relationship relationship. Such aspects should be investigated in sophisticated holographic QCD models.

In chapter 6 we extended the model to include 4 flavors and study the $SU(4)$ flavor symmetry breaking in the strong coupling constants. We used the equations that give the mass spectrum and used them for the $SU(4)$ case and using the holographic currents for vector and scalar sectors, we found an equivalent PCAC for this sector. Next, we used the interaction actions and the matrix representation for pseudoscalar and vector mesons, and found effective Lagrangians involving 2 pseudoscalar and 1 vector meson and effective Lagrangians involving 3 vector mesons, as well as, the coupling constants. We showed the expressions for the electromagnetic form factors for the pseudoscalar and vector mesons by taking the photon as a sum of neutral vector mesons, vector meson dominance, and we studied their low and high Q^2 limits. In the numerical part, we fitted all parameters of the model via a global fit using the masses of 11 mesons given in Particle Data Group. This way, we obtained predictions for others masses and decay constants. Using the expressions for the coupling constants we obtained the values for couplings involving 2 pseudoscalar and 1 vector meson $g_{\rho^n\pi\pi}$, g_{ρ^nKK} and g_{ρ^nDD} and involving 3 vector mesons $g_{\rho^n\rho\rho}$, $g_{\rho^nK^*K^*}$ and $g_{\rho^nD^*D^*}$. Our results showed the trend $g_{\rho^0\pi\pi} < g_{\rho^0KK} < g_{\rho^0DD}$ in the line of the calculations based $^3P_0$ pair-creation model in the nonrelativistic quark model. In the case of D and D^* mesons, we also showed that the first excitation of the ρ meson couples with these mesons stronger than ground state. Finally, we showed our results for the electromagnetic form factors of the pseudoscalar and vector mesons. Those of pion and kaon are in good agreement with the experimental results and that for D meson agrees with the prediction from the lattice. The form factors for the vector mesons are showed and that of the D^* meson agrees with the result from the lattice. We also compared the charge radii of the mesons with the experimental and lattice.

In chapter 7 we studied the inverse magnetic catalysis in a holographic QCD model that implements the chiral dynamics dynamically through of the dilaton effect. We started revising the D3/D7 brane system and showed that the presence of the dilaton lead to existence of chiral condensate, as well, an anomalous dimension Δm for the operator $\bar{q}q$. This way, we introduced the dynamic holographic QCD model by choosing Δm via QCD running coupling. We also discussed that another characteristic to turn on the chiral dynamics is that the Breitenlohner-Freedman bound is violated. We introduced temperature via a black hole in the background and the κ is chosen to be consistent with the second order chiral phase transition. Then, we introduced the magnetic field via a massless $U(1)$ gauge field living in the background and, in addition, two phenomenological parameters a and b. By looking the $a-b$ parameter space we showed regions when occur magnetic and inverse magnetic catalysis. This way, choosing $a = 0,\ b = 0.037$, we showed that critical temperature decreases with magnetic field in agreement with the lattice. Finally, we showed the condensate versus the magnetic field for different values of temperature; our analysis showed that catalysis magnetic is related with solutions of $L(\rho)$ that do not touch the black hole and the inverse magnetic catalysis is related to solutions of $L(\rho)$ that touches the black hole. The results agree with that from lattice.

Holographic QCD models can also be useful in the study of the quark-gluon plasma physics. This has been strongly supported by the experimental data in RHIC and indicate that the quark-gluon plasma is a coupled strongly system and would be described by the non-perturbative QCD regime. Others phenomena like the evolution of jets and quarkonium can be studied in a simple way using the holographic QCD models due to possibility of including the real-time formalism. Future projects can include the study of some transport coefficients relevant for quark-gluon plasma out the equilibrium and under magnetic field effects.

9 Appendix

9.1 Some algebra

We show below some calculations relevant for understanding of the chapter 4. As follows

$$\begin{aligned}\tilde{D}_m X_H &= \tilde{D}_m X_0 - \frac{1}{2}\tilde{D}_m\{\Pi,\{\Pi,X_0\}\} + \mathcal{O}(\Pi^4)\,,\\ \tilde{D}_m X_A &= i\tilde{D}_m\{\Pi,X_0\} + \mathcal{O}(\Pi^3)\,.\end{aligned} \tag{9.1}$$

Then we find

$$\begin{aligned}\mathrm{Tr}(\tilde{D}^m X_H \tilde{D}_m X_H &- \tilde{D}^m X_A \tilde{D}_m X_A)\\ &= \mathrm{Tr}(\tilde{D}^m X_0 \tilde{D}_m X_0 + \{\tilde{D}^m\Pi, X_0\}\{\tilde{D}_m\Pi, X_0\}\\ &+ \{\tilde{D}^m\Pi, X_0\}\{\Pi, \tilde{D}_m X_0\} - \{X_0,\Pi\}\{\tilde{D}^m\Pi, \tilde{D}_m X_0\})\,,\\ &+ \mathcal{O}(\Pi^4)\end{aligned} \tag{9.2}$$

where we have used $\mathrm{Tr}(A\{B,C\}) = \mathrm{Tr}(\{A,B\}C)$. Now, using the identity

$$\mathrm{Tr}(\{A,B\}\{C,D\} - \{B,C\}\{A,D\} + [A,C][B,D]) = 0\,, \tag{9.3}$$

we can rewrite (9.2) as

$$\begin{aligned}\mathrm{Tr}(\tilde{D}^m X_H \tilde{D}_m X_H &- \tilde{D}^m X_A \tilde{D}_m X_A)\\ &= \mathrm{Tr}(\tilde{D}^m X_0 \tilde{D}_m X_0 + \{\tilde{D}^m\Pi, X_0\}\{\tilde{D}_m\Pi, X_0\} + [\tilde{D}^m\Pi, \Pi][\tilde{D}_m X_0, X_0])\\ &+ \mathcal{O}(\Pi^4).\end{aligned} \tag{9.4}$$

Similarly we can find that

$$\begin{aligned}\mathrm{Tr}(2i\{A^m, X_H\}\tilde{D}_m X_A &- 2i\{A^m, X_A\}\tilde{D}_m X_H)\\ &= \mathrm{Tr}(-2\{A^m, X_0\}\{\tilde{D}_m\Pi, X_0\} - 2\{A^m, X_0\}\{\Pi, \tilde{D}_m X_0\}\\ &+ 2\{\tilde{D}_m X_0, A^m\}\{\Pi, X_0\}) + \mathcal{O}(A\Pi^3)\\ &= \mathrm{Tr}(-2\{A^m, X_0\}\{\tilde{D}_m\Pi, X_0\} - 2[A^m, \Pi][\tilde{D}_m X_0, X_0])\\ &+ \mathcal{O}(A\Pi^3)\end{aligned} \tag{9.5}$$

9.2 Kaluza-Klein Reduction

As we have seen in this thesis, in the original gauge/gravity duality, the background obtained is the $\mathrm{AdS}_5 \times S^5$ from the N_c D3-branes configurations. In the bottom-up approaches, we never investigate what happens to the dependence of the fields on the location of the sphere. In fact, there is a standard energetic and intuitive explanation that we can make use to neglected it: the space defined by the sphere is a compact space, thus the momentum along these space is quantised and this leads to the excitation of the finite-momentum modes in the compact directions have an energy gap. In others words, any momentum along the sphere would cost extra energy. This is the basic reason for separate the dynamics along compact directions and it is quit known as a Kaluza-Klein (KK) expansion and is very useful in holographic QCD models. Originally, this proposal came in 1921 in the works of Theodor Kaluza in the attempt of unifying the gravity force with the electromagnetic force. For this, it assumed that the gravity theory lives in a five-dimensional space-time with one extra spatial dimension in addition to the observed world. Some years later, precisely in 1926, Oscar Klein provided the important element in this idea that one can ignore all the dynamics in this extra direction if it is a compact circle with a small radius.

Now, let us look this Kaluza-Klein expansion in more detail by considering an arbitrary space-time defined as $M_D = M_4 \times K_n$, where K_n is a necessary compact space, for example a sphere S^n or torus $T^n = S^1 \times ... \times S^1$. If we consider that every point in space-time x^μ we have a space K_n that can depend on x^μ, so K_n with coordinates y^m. As an example, in the simplest case of a compactification S^1 (circle), with the extra dimension denoted as $y \approx y + 2\pi R$, we can write the scalar functions as $\phi(x^\mu, y^m)$ and its Fourier expansions are given by

$$\phi(x^\mu, y^m) = \sum_{n \geq 0} e^{iny/R} \phi_n(x^\mu), \tag{9.6}$$

where n is an integer for periodic boundary conditions, or a half-integer for antiperiodic ones. We have clearly sum over discrete indexes of fields $\phi_n(x)$. The KK theory is just a generalization of this analysis.

In a general case, we can write this expansion in terms of general functions as

$$\phi(x^\mu, y^m) = \sum_{n \geq 0} \phi_n(x^\mu) Y_n(y^m), \tag{9.7}$$

where the $Y_n(y^m)$ presents the function in the compact coordinates y^m of the space. Its important to mention that the KK expansion should be consistent of the equations of motion that will govern the dynamical of the fields.

As we have discussed in the chapter 4, this has important consequences in holography once it enables us to find a 4d effective action for the mesons.

Bibliography

[1] H. David Politzer. “Reliable Perturbative Results for Strong Interactions?” *Phys. Rev. Lett.* 30 (1973), pp. 1346–1349.

[2] David J. Gross and Frank Wilczek. “Ultraviolet Behavior of Nonabelian Gauge Theories”. *Phys. Rev. Lett.* 30 (1973), pp. 1343–1346.

[3] Juan Martin Maldacena. “The Large N limit of superconformal field theories and supergravity”. *Int. J. Theor. Phys.* 38 (1999). [Adv. Theor. Math. Phys.2,231(1998)], pp. 1113–1133. arXiv: hep-th/9711200 [hep-th].

[4] S. S. Gubser, Igor R. Klebanov, and Alexander M. Polyakov. “Gauge theory correlators from noncritical string theory”. *Phys. Lett.* B428 (1998), pp. 105–114. arXiv: hep-th/9802109 [hep-th].

[5] Edward Witten. “Anti-de Sitter space and holography”. *Adv. Theor. Math. Phys.* 2 (1998), pp. 253–291. arXiv: hep-th/9802150 [hep-th].

[6] Ofer Aharony et al. “Large N field theories, string theory and gravity”. *Phys. Rept.* 323 (2000), pp. 183–386. arXiv: hep-th/9905111 [hep-th].

[7] Joshua Erlich et al. “QCD and a holographic model of hadrons”. *Phys. Rev. Lett.* 95 (2005), p. 261602. arXiv: hep-ph/0501128 [hep-ph].

[8] Leandro Da Rold and Alex Pomarol. “Chiral symmetry breaking from five dimensional spaces”. *Nucl. Phys.* B721 (2005), pp. 79–97. arXiv: hep-ph/0501218 [hep-ph].

[9] Zainul Abidin and Carl E. Carlson. “Strange hadrons and kaon-to-pion transition form factors from holography”. *Phys. Rev.* D80 (2009), p. 115010. arXiv: 0908.2452 [hep-ph].

[10] Henrique Boschi-Filho and Nelson R. F. Braga. “Gauge / string duality and scalar glueball mass ratios”. *JHEP* 05 (2003), p. 009. arXiv: hep-th/0212207 [hep-th].

[11] Alex Pomarol and Andrea Wulzer. “Baryon Physics in Holographic QCD”. *Nucl. Phys.* B809 (2009), pp. 347–361. arXiv: 0807.0316 [hep-ph].

[12] Sean A. Hartnoll. "Lectures on holographic methods for condensed matter physics". *Class. Quant. Grav.* 26 (2009), p. 224002. arXiv: 0903.3246 [hep-th].

[13] A. Holl, A. Krassnigg, and C. D. Roberts. "Pseudoscalar meson radial excitations". *Phys. Rev.* C70 (2004), p. 042203. arXiv: nucl-th/0406030 [nucl-th].

[14] Gastão Krein. "Review of hadrons in medium". *AIP Conf. Proc.* 1701 (2016), p. 020012.

[15] R. A. Briceño et al. "Issues and Opportunities in Exotic Hadrons". *Chin. Phys.* C40.4 (2016), p. 042001. arXiv: 1511.06779 [hep-ph].

[16] Atsushi Hosaka et al. "Heavy Hadrons in Nuclear Matter" (2016). arXiv: 1606.08685 [hep-ph].

[17] Gastão Krein. "SU(4)-flavor symmetry breaking in hadron couplings". *PoS* ConfinementX (2012), p. 144.

[18] C. E. Fontoura, J. Haidenbauer, and G. Krein. "SU(4) flavor symmetry breaking in D-meson couplings to light hadrons". *Eur. Phys. J.* A53.5 (2017), p. 92. arXiv: 1705.09408 [nucl-th].

[19] M. E. Bracco et al. "Charm couplings and form factors in QCD sum rules". *Prog. Part. Nucl. Phys.* 67 (2012), pp. 1019–1052. arXiv: 1104.2864 [hep-ph].

[20] Bruno El-Bennich et al. "Flavor SU(4) breaking between effective couplings". *Phys. Rev.* D85 (2012), p. 031502. arXiv: 1111.3647 [nucl-th].

[21] Bruno El-Bennich et al. "Couplings between the ρ and D- and D^*-mesons". *Phys. Rev.* D95.3 (2017), p. 034037. arXiv: 1604.01861 [nucl-th].

[22] K. U. Can et al. "Vector and axial-vector couplings of D and D* mesons in 2+1 flavor Lattice QCD". *Phys. Lett.* B719 (2013), pp. 103–109. arXiv: 1210.0869 [hep-lat].

[23] Vladimir A. Miransky and Igor A. Shovkovy. "Quantum field theory in a magnetic field: From quantum chromodynamics to graphene and Dirac semimetals". *Phys. Rept.* 576 (2015), pp. 1–209. arXiv: 1503.00732 [hep-ph].

[24] G. S. Bali et al. "QCD quark condensate in external magnetic fields". *Phys. Rev.* D86 (2012), p. 071502. arXiv: 1206.4205 [hep-lat].

[25] E. Fermi and Chen-Ning Yang. "ARE MESONS ELEMENTARY PARTICLES?" *Phys. Rev.* 76 (1949), pp. 1739–1743.

[26] Shoichi Sakata. “On a Composite Model for the New Particles”. *Prog. Theor. Phys.* 16 (1956), pp. 686–688.

[27] Murray Gell-Mann. “The Eightfold Way: A Theory of strong interaction symmetry” (1961).

[28] Yuval Ne’eman. “Derivation of strong interactions from a gauge invariance”. *Nucl. Phys.* 26 (1961), pp. 222–229.

[29] Murray Gell-Mann. “A Schematic Model of Baryons and Mesons”. *Phys. Lett.* 8 (1964), pp. 214–215.

[30] G. Zweig. “An SU(3) model for strong interaction symmetry and its breaking. Version 1” (1964).

[31] Kaoru Hagiwara et al. “Review of particle physics. Particle Data Group”. *Phys. Rev.* D66 (2002), p. 010001.

[32] O. W. Greenberg. “Spin and Unitary Spin Independence in a Paraquark Model of Baryons and Mesons”. *Phys. Rev. Lett.* 13 (1964), pp. 598–602.

[33] M. Y. Han and Yoichiro Nambu. “Three Triplet Model with Double SU(3) Symmetry”. *Phys. Rev.* 139 (1965), B1006–B1010.

[34] J. D. Bjorken and Emmanuel A. Paschos. “Inelastic Electron Proton and gamma Proton Scattering, and the Structure of the Nucleon”. *Phys. Rev.* 185 (1969), pp. 1975–1982.

[35] Chen-Ning Yang and Robert L. Mills. “Conservation of Isotopic Spin and Isotopic Gauge Invariance”. *Phys. Rev.* 96 (1954), pp. 191–195.

[36] A. H. Mueller. “Perturbative Quantum Chromodynamics”. *World Scientific* Singapore (1989).

[37] U. Aglietti. “Introduction to perturbative QCD”. *1st School on Field Theory and Gravitation Vitoria, Brazil, April 15-19, 1997.* 1997. arXiv: hep-ph/9705277 [hep-ph].

[38] Davison E. Soper. “Basics of QCD perturbation theory”. *The Strong interaction, from hadrons to partons: Proceedings, 24th SLAC Summer Institute on Particle Physics (SSI 96), Stanford, Calif., 19-30 Aug 1996.* 1996, pp. 15–42. arXiv: hep-ph/9702203 [hep-ph].

[39] Craig D. Roberts. “Strong QCD and Dyson-Schwinger Equations” (2012). arXiv: 1203.5341 [nucl-th].

[40] Sidney R. Coleman, J. Wess, and Bruno Zumino. “Structure of phenomenological Lagrangians. 1.” *Phys. Rev.* 177 (1969), pp. 2239–2247.

[41] Curtis G. Callan Jr. et al. "Structure of phenomenological Lagrangians. 2." *Phys. Rev.* 177 (1969), pp. 2247–2250.

[42] Nathan Isgur and Mark B. Wise. "Weak Decays of Heavy Mesons in the Static Quark Approximation". *Phys. Lett.* B232 (1989), pp. 113–117.

[43] Benjamin Grinstein. "Light quark, heavy quark systems". *Ann. Rev. Nucl. Part. Sci.* 42 (1992), pp. 101–145.

[44] Geoffrey T. Bodwin, Eric Braaten, and G. Peter Lepage. "Rigorous QCD predictions for decays of p wave quarkonia". *The Fermilab Meeting DPF 92. Proceedings, 7th Meeting of the American Physical Society, Division of Particles and Fields, Batavia, USA, November 10-14, 1992. Vol. 1, 2.* 1992, pp. 1063–1066. arXiv: hep-ph/9211253 [hep-ph].

[45] Christian W. Bauer, Sean Fleming, and Michael E. Luke. "Summing Sudakov logarithms in B —> X(s gamma) in effective field theory". *Phys. Rev.* D63 (2000), p. 014006. arXiv: hep-ph/0005275 [hep-ph].

[46] Edward Witten. "Anti-de Sitter space, thermal phase transition, and confinement in gauge theories". *Adv. Theor. Math. Phys.* 2 (1998), pp. 505–532. arXiv: hep-th/9803131 [hep-th].

[47] Igor R. Klebanov and Edward Witten. "Superconformal field theory on three-branes at a Calabi-Yau singularity". *Nucl. Phys.* B536 (1998), pp. 199–218. arXiv: hep-th/9807080 [hep-th].

[48] Joseph Polchinski and Matthew J. Strassler. "The String dual of a confining four-dimensional gauge theory" (2000). arXiv: hep-th/0003136 [hep-th].

[49] Igor R. Klebanov and Matthew J. Strassler. "Supergravity and a confining gauge theory: Duality cascades and chi SB resolution of naked singularities". *JHEP* 08 (2000), p. 052. arXiv: hep-th/0007191 [hep-th].

[50] William A. Bardeen et al. "Deep Inelastic Scattering Beyond the Leading Order in Asymptotically Free Gauge Theories". *Phys. Rev.* D18 (1978), p. 3998.

[51] Fred L. Wilson. "Fermi's Theory of Beta Decay". *Am. J. Phys.* 36.12 (1968), pp. 1150–1160.

[52] Gunnar S. Bali. "QCD forces and heavy quark bound states". *Phys. Rept.* 343 (2001), pp. 1–136. arXiv: hep-ph/0001312 [hep-ph].

[53] Jeff Greensite. "An introduction to the confinement problem". *Lect. Notes Phys.* 821 (2011), pp. 1–211.

[54] J. Greensite. "The Confinement problem in lattice gauge theory". *Prog. Part. Nucl. Phys.* 51 (2003), p. 1. arXiv: hep-lat/0301023 [hep-lat].

[55] A. Bashir, A. Raya, and J. Rodriguez-Quintero. "QCD: Restoration of Chiral Symmetry and Deconfinement for Large Nf ". *Phys. Rev.* D88 (2013), p. 054003. arXiv: 1302.5829 [hep-ph].

[56] C. E. Fontoura, G. Krein, and V. E. Vizcarra. "$\bar{D}$N interaction in a color-confining chiral quark model". *Phys. Rev.* C87.2 (2013), p. 025206. arXiv: 1208.4058 [nucl-th].

[57] John M. Cornwall. "Entropy, confinement, and chiral symmetry breaking". *Phys. Rev.* D83 (2011), p. 076001. arXiv: 1011.3524 [hep-ph].

[58] A. Doff, F. A. Machado, and A. A. Natale. "Chiral symmetry breaking in QCD-like gauge theories with a confining propagator and dynamical gauge boson mass generation". *Annals Phys.* 327 (2012), pp. 1030–1049. arXiv: 1106.2860 [hep-ph].

[59] Tina Katharina Herbst, Jan M. Pawlowski, and Bernd-Jochen Schaefer. "The phase structure of the PolyakovŰquarkŰmeson model beyond mean field". *Phys. Lett.* B696 (2011), pp. 58–67. arXiv: 1008.0081 [hep-ph].

[60] Kenji Fukushima. "Chiral effective model with the Polyakov loop". *Phys. Lett.* B591 (2004), pp. 277–284. arXiv: hep-ph/0310121 [hep-ph].

[61] Agnes Mocsy, Francesco Sannino, and Kimmo Tuominen. "Effective Lagrangians for QCD: Deconfinement and chiral symmetry restoration". *KIAS-APCTP International Symposium in Astro-Hadron Physics: Compact Stars: Quest for New States of Dense Matter Seoul, Korea, November 10-14, 2003*. 2004. arXiv: hep-ph/0401149 [hep-ph].

[62] Bernd-Jochen Schaefer, Jan M. Pawlowski, and Jochen Wambach. "The Phase Structure of the Polyakov–Quark-Meson Model". *Phys. Rev.* D76 (2007), p. 074023. arXiv: 0704.3234 [hep-ph].

[63] E. Megias, E. Ruiz Arriola, and L. L. Salcedo. "Polyakov loop in chiral quark models at finite temperature". *Phys. Rev.* D74 (2006), p. 065005. arXiv: hep-ph/0412308 [hep-ph].

[64] Kei-Ichi Kondo. "Toward a first-principle derivation of confinement and chiral-symmetry-breaking crossover transitions in QCD". *Phys. Rev.* D82 (2010), p. 065024. arXiv: 1005.0314 [hep-th].

[65] Gerard 't Hooft. "A Planar Diagram Theory for Strong Interactions". *Nucl. Phys.* B72 (1974), p. 461.

[66] Yuri V. Kovchegov. "AdS/CFT applications to relativistic heavy ion collisions: a brief review". *Rept. Prog. Phys.* 75 (2012), p. 124301. arXiv: 1112.5403 [hep-ph].

[67] Samir D. Mathur. "Black holes and holography". *J. Phys. Conf. Ser.* 405 (2012), p. 012005. arXiv: 1207.5431 [hep-th].

[68] Bernard S. Kay. "Entropy and quantum gravity". *Entropy* 17 (2015), p. 8174. arXiv: 1504.00882 [gr-qc].

[69] Kostas Skenderis. "Lecture notes on holographic renormalization". *Class. Quant. Grav.* 19 (2002), pp. 5849–5876. arXiv: hep-th/0209067 [hep-th].

[70] Sergej Moroz. "Below the Breitenlohner-Freedman bound in the nonrelativistic AdS/CFT correspondence". *Phys. Rev.* D81 (2010), p. 066002. arXiv: 0911.4060 [hep-th].

[71] S. W. Hawking. "Particle Creation by Black Holes". *Commun. Math. Phys.* 43 (1975). [,167(1975)], pp. 199–220.

[72] S. S. Gubser, Igor R. Klebanov, and A. W. Peet. "Entropy and temperature of black 3-branes". *Phys. Rev.* D54 (1996), pp. 3915–3919. arXiv: hep-th/9602135 [hep-th].

[73] Joseph Polchinski. "Dirichlet Branes and Ramond-Ramond charges". *Phys. Rev. Lett.* 75 (1995), pp. 4724–4727. arXiv: hep-th/9510017 [hep-th].

[74] David Garfinkle, Gary T. Horowitz, and Andrew Strominger. "Charged black holes in string theory". *Phys. Rev.* D43 (1991). [Erratum: Phys. Rev.D45,3888(1992)], p. 3140.

[75] Andreas Karch and Emanuel Katz. "Adding flavor to AdS / CFT". *JHEP* 06 (2002), p. 043. arXiv: hep-th/0205236 [hep-th].

[76] Igor R. Klebanov. "QCD and string theory". *Int. J. Mod. Phys.* A21 (2006), pp. 1831–1843. arXiv: hep-ph/0509087 [hep-ph].

[77] Steven S. Gubser and Andreas Karch. "From gauge-string duality to strong interactions: A Pedestrian's Guide". *Ann. Rev. Nucl. Part. Sci.* 59 (2009), pp. 145–168. arXiv: 0901.0935 [hep-th].

[78] J. Babington et al. "Chiral symmetry breaking and pions in nonsupersymmetric gauge / gravity duals". *Phys. Rev.* D69 (2004), p. 066007. arXiv: hep-th/0306018 [hep-th].

[79] Martin Kruczenski et al. "Towards a holographic dual of large N(c) QCD". *JHEP* 05 (2004), p. 041. arXiv: hep-th/0311270 [hep-th].

[80] Tadakatsu Sakai and Shigeki Sugimoto. "Low energy hadron physics in holographic QCD". *Prog. Theor. Phys.* 113 (2005), pp. 843–882. arXiv: hep-th/0412141 [hep-th].

[81] Tadakatsu Sakai and Shigeki Sugimoto. "More on a holographic dual of QCD". *Prog. Theor. Phys.* 114 (2005), pp. 1083–1118. arXiv: hep-th/0507073 [hep-th].

[82] Soo-Jong Rey and Jung-Tay Yee. "Macroscopic strings as heavy quarks in large N gauge theory and anti-de Sitter supergravity". *Eur. Phys. J.* C22 (2001), pp. 379–394. arXiv: hep-th/9803001 [hep-th].

[83] Y. Kinar, E. Schreiber, and J. Sonnenschein. "Q anti-Q potential from strings in curved space-time: Classical results". *Nucl. Phys.* B566 (2000), pp. 103–125. arXiv: hep-th/9811192 [hep-th].

[84] Aleksey Cherman, Thomas D. Cohen, and Elizabeth S. Werbos. "The Chiral condensate in holographic models of QCD". *Phys. Rev.* C79 (2009), p. 045203. arXiv: 0804.1096 [hep-ph].

[85] Alfonso Ballon-Bayona, Gastão Krein, and Carlisson Miller. "Decay constants of the pion and its excitations in holographic QCD". *Phys. Rev.* D91 (2015), p. 065024. arXiv: 1412.7505 [hep-ph].

[86] Zi-wei Lin and C. M. Ko. "A Model for J / psi absorption in hadronic matter". *Phys. Rev.* C62 (2000), p. 034903. arXiv: nucl-th/9912046 [nucl-th].

[87] C. McNeile and Christopher Michael. "The Decay constant of the first excited pion from lattice QCD". *Phys. Lett.* B642 (2006), pp. 244–247. arXiv: hep-lat/0607032 [hep-lat].

[88] Koichi Hashimoto and Taku Izubuchi. "eta-prime meson from two flavor dynamical domain wall fermions". *Prog. Theor. Phys.* 119 (2008), pp. 599–641. arXiv: 0803.0186 [hep-lat].

[89] M. Diehl and G. Hiller. "New ways to explore factorization in b decays". *JHEP* 06 (2001), p. 067. arXiv: hep-ph/0105194 [hep-ph].

[90] A. L. Kataev, N. V. Krasnikov, and A. A. Pivovarov. "The Use of the Finite Energetic Sum Rules for the Calculation of the Light Quark Masses". *Phys. Lett.* B123 (1983), p. 93.

[91] Victor Elias et al. "Beyond the narrow resonance approximation: Decay constant and width of the first pion excitation state". *Phys. Lett.* B412 (1997), pp. 131–136. arXiv: hep-ph/9706472 [hep-ph].

[92] Kim Maltman and Joachim Kambor. "Decay constants, light quark masses and quark mass bounds from light quark pseudoscalar sum rules". *Phys. Rev.* D65 (2002), p. 074013. arXiv: hep-ph/0108227 [hep-ph].

[93] M. K. Volkov and C. Weiss. "A Chiral Lagrangian for excited pions". *Phys. Rev.* D56 (1997), pp. 221–229. arXiv: hep-ph/9608347 [hep-ph].

[94] Alexander A. Andrianov, D. Espriu, and R. Tarrach. "The Extended chiral quark model and QCD". *Nucl. Phys.* B533 (1998), pp. 429–472. arXiv: hep-ph/9803232 [hep-ph].

[95] Stanley J. Brodsky and Guy F. de Teramond. "Hadronic spectra and light-front wavefunctions in holographic QCD". *Phys. Rev. Lett.* 96 (2006), p. 201601. arXiv: hep-ph/0602252 [hep-ph].

[96] Stanley J. Brodsky and Guy F. de Teramond. "Light-Front Dynamics and AdS/QCD Correspondence: The Pion Form Factor in the Space- and Time-Like Regions". *Phys. Rev.* D77 (2008), p. 056007. arXiv: 0707.3859 [hep-ph].

[97] Stanley J. Brodsky, Guy F. De Téramond, and Hans Günter Dosch. "Threefold Complementary Approach to Holographic QCD". *Phys. Lett.* B729 (2014), pp. 3–8. arXiv: 1302.4105 [hep-th].

[98] Tanja Branz et al. "Light and heavy mesons in a soft-wall holographic approach". *Phys. Rev.* D82 (2010), p. 074022. arXiv: 1008.0268 [hep-ph].

[99] Hovhannes R. Grigoryan and Anatoly V. Radyushkin. "Pion in the Holographic Model with 5D Yang-Mills Fields". *Phys. Rev.* D78 (2008), p. 115008. arXiv: 0808.1243 [hep-ph].

[100] Andreas Karch et al. "Linear confinement and AdS/QCD". *Phys. Rev.* D74 (2006), p. 015005. arXiv: hep-ph/0602229 [hep-ph].

[101] Tony Gherghetta, Joseph I. Kapusta, and Thomas M. Kelley. "Chiral symmetry breaking in the soft-wall AdS/QCD model". *Phys. Rev.* D79 (2009), p. 076003. arXiv: 0902.1998 [hep-ph].

[102] C. F. Perdrisat, V. Punjabi, and M. Vanderhaeghen. "Nucleon Electromagnetic Form Factors". *Prog. Part. Nucl. Phys.* 59 (2007), pp. 694–764. arXiv: hep-ph/0612014 [hep-ph].

[103] J. Arrington, C. D. Roberts, and J. M. Zanotti. "Nucleon electromagnetic form-factors". *J. Phys.* G34 (2007), S23–S52. arXiv: nucl-th/0611050 [nucl-th].

[104] Kees de Jager. “Nucleon Form Factor Experiments and the Pion Cloud”. *AIP Conf. Proc.* 904 (2007). [,95(2006)], pp. 95–103. arXiv: nucl-ex/0612026 [nucl-ex].

[105] R. M. Woloshyn and A. M. Kobos. “Numerical Study of the Lattice Meson Form-factor”. *Phys. Rev.* D33 (1986), p. 222.

[106] W. Wilcox and R. M. Woloshyn. “Meson Electric Form-factor on the Lattice”. *Phys. Rev.* D32 (1985). [Erratum: Phys. Rev.D35,773(1987)], p. 3282.

[107] Terrence Draper et al. “Electromagnetic Form-factors of Hadrons”. *Nucl. Phys. Proc. Suppl.* 9 (1989), pp. 175–180.

[108] S. R. Amendolia et al. “A Measurement of the Space - Like Pion Electromagnetic Form-Factor”. *Nucl. Phys.* B277 (1986), p. 168.

[109] S. R. Amendolia et al. “A Measurement of the Kaon Charge Radius”. *Phys. Lett.* B178 (1986), pp. 435–440.

[110] Laura Tolos. “Charming mesons with baryons and nuclei”. *Int. J. Mod. Phys.* E22 (2013), p. 1330027. arXiv: 1309.7305 [nucl-th].

[111] Ahmed Ali, Jens Sören Lange, and Sheldon Stone. “Exotics: Heavy Pentaquarks and Tetraquarks” (2017). arXiv: 1706.00610 [hep-ph].

[112] M. F. M. Lutz et al. “Physics Performance Report for PANDA: Strong Interaction Studies with Antiprotons” (2009). arXiv: 0903.3905 [hep-ex].

[113] Elisabetta Prencipe, Jens Soeren Lange, and Alexander Blinov. “New spectroscopy with $\bar{P}ANDA$ at FAIR: X, Y, Z and the F-wave charmonium states”. *AIP Conf. Proc.* 1735 (2016), p. 060011. arXiv: 1512.05496 [hep-ex].

[114] Zi-wei Lin, C. M. Ko, and Bin Zhang. “Hadronic scattering of charm mesons”. *Phys. Rev.* C61 (2000), p. 024904. arXiv: nucl-th/9905003 [nucl-th].

[115] T. Mizutani and A. Ramos. “D mesons in nuclear matter: A DN coupled-channel equations approach”. *Phys. Rev.* C74 (2006), p. 065201. arXiv: hep-ph/0607257 [hep-ph].

[116] J. Haidenbauer et al. “Anti-D N interaction from meson-exchange and quark-gluon dynamics”. *Eur. Phys. J.* A33 (2007), pp. 107–117. arXiv: 0704.3668 [nucl-th].

[117] J. Haidenbauer et al. “Charmed meson rescattering in the reaction anti-p d —> anti-D N”. *Eur. Phys. J.* A37 (2008), pp. 55–67. arXiv: 0803.3752 [hep-ph].

[118] J. Haidenbauer et al. "DN interaction from meson exchange". *Eur. Phys. J.* A47 (2011), p. 18. arXiv: 1008.3794 [nucl-th].

[119] Shigehiro Yasui and Kazutaka Sudoh. "Exotic nuclei with open heavy flavor mesons". *Phys. Rev.* D80 (2009), p. 034008. arXiv: 0906.1452 [hep-ph].

[120] C. Garcia-Recio et al. "The s-wave charmed baryon resonances from a coupled-channel approach with heavy quark symmetry". *Phys. Rev.* D79 (2009), p. 054004. arXiv: 0807.2969 [hep-ph].

[121] R. Casalbuoni et al. "Phenomenology of heavy meson chiral Lagrangians". *Phys. Rept.* 281 (1997), pp. 145–238. arXiv: hep-ph/9605342 [hep-ph].

[122] J. J. Sakurai and D. Schildknecht. "Generalized vector dominance and inelastic electron - proton scattering". *Phys. Lett.* B40 (1972), pp. 121–126.

[123] J. J. Sakurai. "Theory of strong interactions". *Annals Phys.* 11 (1960), pp. 1–48.

[124] R. G. Arnold, Carl E. Carlson, and Franz Gross. "Elastic electron-Deuteron Scattering at High-Energy". *Phys. Rev.* C21 (1980), p. 1426.

[125] C. A. Ballon Bayona et al. "Pion and Vector Meson Form Factors in the Kuperstein-Sonnenschein holographic model". *JHEP* 08 (2010), p. 122. arXiv: 1006.2363 [hep-th].

[126] C. Patrignani et al. "Review of Particle Physics". *Chin. Phys.* C40.10 (2016), p. 100001.

[127] J. F. Donoghue, E. Golowich, and Barry R. Holstein. "Dynamics of the standard model". *Camb. Monogr. Part. Phys. Nucl. Phys. Cosmol.* 2 (1992). [Camb. Monogr. Part. Phys. Nucl. Phys. Cosmol.35(2014)], pp. 1–540.

[128] Nathan Isgur, Colin Morningstar, and Cathy Reader. "The a1 in tau Decay". *Phys. Rev.* D39 (1989), p. 1357.

[129] A. Bramon, E. Etim, and Mario Greco. "A Vector meson dominance approach to scale invariance". *Phys. Lett.* B41 (1972), pp. 609–612.

[130] Herry J. Kwee and Richard F. Lebed. "Pion form-factors in holographic QCD". *JHEP* 01 (2008), p. 027. arXiv: 0708.4054 [hep-ph].

[131] H. Z. Sang and Xiao-Hong Wu. "Strange Meson Form Factors in Holographic QCD" (2010). arXiv: 1004.4392 [hep-ph].

[132] Hovhannes R. Grigoryan and Anatoly V. Radyushkin. "Form Factors and Wave Functions of Vector Mesons in Holographic QCD". *Phys. Lett.* B650 (2007), pp. 421–427. arXiv: hep-ph/0703069 [hep-ph].

[133] A. F. Krutov, R. G. Polezhaev, and V. E. Troitsky. "The radius of the rho meson determined from its decay constant". *Phys. Rev.* D93.3 (2016), p. 036007. arXiv: 1602.00907 [hep-ph].

[134] Aneesh V. Manohar and Mark B. Wise. "Heavy quark physics". *Camb. Monogr. Part. Phys. Nucl. Phys. Cosmol.* 10 (2000), pp. 1–191.

[135] Johanna Erdmenger, Nick Evans, and Johannes Grosse. "Heavy-light mesons from the AdS/CFT correspondence". *JHEP* 01 (2007), p. 098. arXiv: hep-th/0605241 [hep-th].

[136] Johanna Erdmenger, Kazuo Ghoroku, and Ingo Kirsch. "Holographic heavy-light mesons from non-Abelian DBI". *JHEP* 09 (2007), p. 111. arXiv: 0706.3978 [hep-th].

[137] Koji Hashimoto, Noriaki Ogawa, and Yasuhiro Yamaguchi. "Holographic Heavy Quark Symmetry". *JHEP* 06 (2015), p. 040. arXiv: 1412.5590 [hep-th].

[138] Yizhuang Liu and Ismail Zahed. "Holographic Heavy-Light Chiral Effective Action". *Phys. Rev.* D95.5 (2017), p. 056022. arXiv: 1611.03757 [hep-ph].

[139] Nelson R. F. Braga, M. A. Martin Contreras, and Saulo Diles. "Holographic model for heavy-vector-meson masses". *Europhys. Lett.* 115.3 (2016), p. 31002. arXiv: 1511.06373 [hep-th].

[140] Yizhuang Liu and Ismail Zahed. "Heavy-Light Mesons in Chiral AdS/QCD" (2016). arXiv: 1611.04400 [hep-ph].

[141] V. Skokov, A. Yu. Illarionov, and V. Toneev. "Estimate of the magnetic field strength in heavy-ion collisions". *Int. J. Mod. Phys.* A24 (2009), pp. 5925–5932. arXiv: 0907.1396 [nucl-th].

[142] Igor A. Shovkovy. "Magnetic Catalysis: A Review". *Lect. Notes Phys.* 871 (2013), pp. 13–49. arXiv: 1207.5081 [hep-ph].

[143] E. M. Ilgenfritz et al. "Two-color QCD with staggered fermions at finite temperature under the influence of a magnetic field". *Phys. Rev.* D85 (2012), p. 114504. arXiv: 1203.3360 [hep-lat].

[144] Massimo D'Elia, Swagato Mukherjee, and Francesco Sanfilippo. "QCD Phase Transition in a Strong Magnetic Background". *Phys. Rev.* D82 (2010), p. 051501. arXiv: 1005.5365 [hep-lat].

[145] Massimo D'Elia and Francesco Negro. "Chiral Properties of Strong Interactions in a Magnetic Background". *Phys. Rev.* D83 (2011), p. 114028. arXiv: 1103.2080 [hep-lat].

[146] G. S. Bali et al. "The QCD phase diagram for external magnetic fields". *JHEP* 02 (2012), p. 044. arXiv: 1111.4956 [hep-lat].

[147] Falk Bruckmann, Gergely Endrodi, and Tamas G. Kovacs. "Inverse magnetic catalysis and the Polyakov loop". *JHEP* 04 (2013), p. 112. arXiv: 1303.3972 [hep-lat].

[148] Falk Bruckmann, Gergely Endrodi, and Tamas G. Kovacs. "Inverse magnetic catalysis in QCD" (2013). arXiv: 1311.3178 [hep-lat].

[149] Kiminad A. Mamo. "Inverse magnetic catalysis in holographic models of QCD". *JHEP* 05 (2015), p. 121. arXiv: 1501.03262 [hep-th].

[150] Romulo Rougemont, Renato Critelli, and Jorge Noronha. "Holographic calculation of the QCD crossover temperature in a magnetic field". *Phys. Rev.* D93.4 (2016), p. 045013. arXiv: 1505.07894 [hep-th].

[151] Umut Gürsoy et al. "Inverse Magnetic Catalysis from improved Holographic QCD in the Veneziano limit". *JHEP* 03 (2017), p. 053. arXiv: 1611.06339 [hep-th].

[152] Florian Preis, Anton Rebhan, and Andreas Schmitt. "Inverse magnetic catalysis in dense holographic matter". *JHEP* 03 (2011), p. 033. arXiv: 1012.4785 [hep-th].

[153] D. Dudal, Diego R. Granado, and Thomas G. Mertens. "No inverse magnetic catalysis in the QCD hard and soft wall models". *Phys. Rev.* D93.12 (2016), p. 125004. arXiv: 1511.04042 [hep-th].

[154] Mariana Grana and Joseph Polchinski. "Gauge / gravity duals with holomorphic dilaton". *Phys. Rev.* D65 (2002), p. 126005. arXiv: hep-th/0106014 [hep-th].

[155] M. Bertolini et al. "N=2 gauge theories on systems of fractional D3/D7 branes". *Nucl. Phys.* B621 (2002), pp. 157–178. arXiv: hep-th/0107057 [hep-th].

[156] Johanna Erdmenger et al. "Mesons in Gauge/Gravity Duals - A Review". *Eur. Phys. J.* A35 (2008), pp. 81–133. arXiv: 0711.4467 [hep-th].

[157] Nick Evans and Marc Scott. "Hyper-Scaling Relations in the Conformal Window from Dynamic AdS/QCD". *Phys. Rev.* D90.6 (2014), p. 065025. arXiv: 1405.5373 [hep-ph].

[158] Johanna Erdmenger, Nick Evans, and Marc Scott. "Meson spectra of asymptotically free gauge theories from holography". *Phys. Rev.* D91.8 (2015), p. 085004. arXiv: 1412.3165 [hep-ph].

[159] Raul Alvares, Nick Evans, and Keun-Young Kim. "Holography of the Conformal Window". *Phys. Rev.* D86 (2012), p. 026008. arXiv: 1204.2474 [hep-ph].

[160] Peter Breitenlohner and Daniel Z. Freedman. "Stability in Gauged Extended Supergravity". *Annals Phys.* 144 (1982), p. 249.

[161] Nick Evans et al. "Towards a Holographic Model of the QCD Phase Diagram". *J. Phys.* G39 (2012), p. 054005. arXiv: 1109.2633 [hep-th].

[162] Martin Kruczenski et al. "Meson spectroscopy in AdS / CFT with flavor". *JHEP* 07 (2003), p. 049. arXiv: hep-th/0304032 [hep-th].

[163] Carlos Hoyos-Badajoz, Karl Landsteiner, and Sergio Montero. "Holographic meson melting". *JHEP* 04 (2007), p. 031. arXiv: hep-th/0612169 [hep-th].

[164] Gergely Endrodi. "Critical point in the QCD phase diagram for extremely strong background magnetic fields". *JHEP* 07 (2015), p. 173. arXiv: 1504.08280 [hep-lat].

[165] Nick Evans, Carlisson Miller, and Marc Scott. "Inverse Magnetic Catalysis in Bottom-Up Holographic QCD". *Phys. Rev.* D94.7 (2016), p. 074034. arXiv: 1604.06307 [hep-ph].